



Institut de Física Interdisciplinària i Sistemes Complexos

TESI DOCTORAL

Collective phenomena in social dynamics: consensus problems, ordering dynamics and language competition

Tesi presentada per Xavier Castelló Llobet, al Departament de Física de la Universitat de les Illes Balears, per optar al grau de Doctor en Física

Xavier Castelló Llobet

Palma de Mallorca, Febrer del 2010

Collective phenomena in social dynamics: consensus problems, ordering dynamics and language competition

Xavier Castelló Llobet
Institut de Física Interdisciplinària i Sistemes Complexos
IFISC (UIB-CSIC)

PhD Thesis

Directors: Prof. Maxi San Miguel and Dr. Víctor M. Eguíluz

Copyright 2010, Xavier Castelló Llobet
Universitat de les Illes Balears
Palma de Mallorca

This document was typeset with $\text{\LaTeX}2_{\epsilon}$

Maxi San Miguel, Catedràtic de la Universitat de les Illes Balears, i Víctor M. Eguíluz, Científico Titular del CSIC (Consejo Superior de Investigaciones Científicas)

CERTIFIQUEN

que aquesta tesi doctoral ha estat realitzada pel Sr. *Xavier Castelló Llobet* sota la seva direcció a l'Institut de Física Interdisciplinària i Sistemes Complexos; IFISC (UIB-CSIC) i, per a donar-ne constància, firmen la mateixa.

Palma de Mallorca, 22 de febrer del 2010

Maxi San Miguel

Víctor M. Eguíluz

Als meus pares

*“to the answer already contained in a question...one should answer with questions
from another answer.” — Deleuze and Guattari, 1987*

Acknowledgments

En primer lloc vull agrair als meus directors de tesi, el Prof. Maxi San Miguel i el Dr. Víctor M. Eguíluz, que hagin confiat en mi per a dur a terme aquesta tesi, tot apostant per donar un impuls decidit a una nova línia de recerca a l'IFISC. Agrair així mateix motivar-me amb noves idees, fomentar un tracte de tu a tu, i donar-me l'oportunitat de visitar altres universitats i centres de recerca per a formar-me i aprendre més enllà dels seus consells. Sense ells aquesta tesi no hauria estat possible. Voldria fer un èmfasi especial en el teu esforç, Maxi, per seguir tant de prop com t'ha sigut possible la meva recerca malgrat les situacions difícils; especialment en la recta final de la tesi. Gràcies.

I also acknowledge Prof. Vittorio Loreto (Università di Roma, "la Sapienza"), Prof. Kimmo Kaski and Dr. Jari Saramäki (Helsinki University of Technology) and Dr. Damon Centola (MIT, Massachusetts Institute of Technology) for giving me the opportunity to visit their corresponding research groups during my PhD and to learn from them. My acknowledgements also to the other scientists I have had the pleasure to collaborate with: Dr. Riitta Toivonen, Dr. Federico Vázquez, Dr. Lucía Loreiro-Porto, Prof. Dietrich Stauffer, Dr. Andrea Baronchelli, Prof. Guillaume Deffuant, Dr. Laetitia Chapel. Vull agrair especialment a en Federico les llargues i profitoses discussions, el seu temps (que sempre sabia trobar), i tot allò que he après durant la seva llarga estada a l'IFISC. Vull agrair també especialment a la Lucía la seva aportació sociolingüística a aquesta tesi, i haver-se llençat a la piscina de la col·laboració interdisciplinària amb nosaltres.

I want to acknowledge as well Prof. Steven Strogatz and Dr. Daniel Abrams for the time they dedicated to me in Copenhagen when I met them in 2005, being still an undergraduate student. They presented a model on language competition that extremely caught my attention and which finally focused my

research interests, ultimately leading me to IFISC to start my PhD thesis. It is nice when you are at the right place at the right time: I feel lucky to have met personally the ones who made the first step from where I have indeed started my research.

Vull agrair als investigadors i membres de l'IFISC l'haver fet possible un ambient de treball excel·lent, i en particular l'ajuda i el caliu dels meus companys (molts d'ells, bons amics), sense els quals segur que hauria sigut més feixuc el camí. L'ambient horitzontal de la "Efe" és un luxe en tots els sentits, professionalment i personalment, i ha fet d'aquests anys una experiència inoblidable. La llista és llarga (tots sabeu que penso en vosaltres!), però sí voldria mencionar aquí especialment: n'Adrian, pel seu temps i incomptables cops de mà; en Juan Carlos, amb qui he compartit camí des del començament (línia de recerca, directors, congressos); i sobretot n'Alejandro, perquè sempre m'ha fet pensar i gaudir pensant; més enllà dels precipicis... També vull agrair a la Lucía el seu cop de mà amb la correcció de la introducció de la tesi, a n'Alejandro i en Samer els seus comentaris sempre motivadors, a la Sònia estar sempre a prop, i a la Cati el seu temps i ajuda en el disseny de la portada.

Unes línies per a en Dani, company de viatge durant l'aventura a Mallorca des del primer dia. Gràcies amic, per compartir el "curro infinit", les alegries i les penes, i per haver-me fet sentir, en una terra que primer era estranya, *a casa*. També agrair aquí especialment a la Laura haver cregut en mi durant un camí tant llarg i ple, haver-me donat l'empenta necessària en moments de dubte. Perquè sense la teva energia, potser no hagués començat mai aquesta tesi.

Amics i família tots, d'una i altra banda d'aquest mar que vull que uneixi; gràcies per ser-hi!!

Per últim, i per això d'una especial importància, donar les gràcies als meus pares. Sempre heu estat al meu costat, incondicionalment, confiant en mi i recolzant-me. Perquè m'heu fet un regal que sempre duc allà on vaig: les ganes i la possibilitat d'aprendre amb il·lusió, de meravellar-me davant la sorpresa. Iaia, també vull agrair-te des d'aquí tot el temps que hem pogut passar junts, que malauradament no ha sigut prou aquests últims anys. També va per a tu, guapa! Recordant-te, et sento viva.

Mariabel, vull acabar aquestes línies agraint-te el teu recolzament durant aquest temps, tot l'amor i tota l'atenció, el teu somriure i els teus ulls que sempre brillen; sobretot en aquest final del viatge, que sempre fa pujada. Content de poder gaudir fent camí junts. Gràcies, Mariabel!

*Xavier Castelló Llobet
Palma de Mallorca, Febrer del 2010*

Resum

L'objectiu principal de la Física Estadística és entendre el comportament col·lectiu de sistemes formats per moltes partícules en termes d'una descripció microscòpica basada en la interacció entre aquestes. En bona part degut a l'èxit d'aquesta disciplina en establir una connexió entre el comportament a nivell *micro* i *macro*, els fenòmens col·lectius en sistemes socials s'estan començant a estudiar cada cop més a partir de models microscòpics d'agents en interacció. En problemes de dinàmica social, els agents es consideren com nodes integrants d'una xarxa que canvien el seu estat (opció social) en funció d'unes regles d'interacció amb els seus veïns de la xarxa. Aquest tipus de problemes inclouen des de dinàmiques d'opinió i dilemes socials fins a dinàmiques de difusió cultural i competició entre llengües.

Els estudis de competició entre llengües analitzen les dinàmiques de competència lingüística i d'ús d'una llengua degudes a les interaccions socials, i recentment han estat considerats des de l'òptica de la física estadística i els sistemes complexos. En aquesta tesi i motivats per estudis de competició entre llengües, estudiem problemes de consens social. Els problemes de consens social són problemes de caràcter general, estudiats recentment per la física estadística: es tracta d'establir quan una dinàmica d'interacció entre un conjunt d'agents que poden escollir entre diverses opcions, dóna lloc a un escenari de consens en una d'aquestes opcions (domini/extinció d'una llengua), o bé quan s'arriba a un estat final on diverses opcions socials coexisteixen (coexistència entre llengües).

La competició entre llengües és un exemple particular d'un tipus de problemes de consens en els quals les opcions són no-excloents, és a dir, un agent pot compartir les dues opcions en competició a nivell individual (agents bilingües). Des d'aquest punt de vista, i partint del model d'Abrams-Strogatz per a la

competició entre dues llengües, estudiem i comparem aquest model de consens de dos estats amb un model de dos opcions no-excloents, que definim com una extensió del primer en el qual els agents poden estar en un dels dos estats oposats (A o B) o en un tercer estat (AB, agents bilingües) que inclou les dues opcions (*Model Bilingüe*). Els models es basen en les probabilitats de transició entre els possibles estats dels agents, que depenen essencialment de les densitats d'agents en cadascun dels estats (A, B, AB), comptabilitzades a partir dels nodes veïns de la xarxa. A més, aquests models depenen de dos paràmetres. Per una banda, el paràmetre de *prestigi*, que captura la diferència d'estatus entre les dues opcions (llengües) en competició i que, matemàticament, és un paràmetre de trencament de simetria. Per altra banda, el paràmetre de *volatilitat*, que dona una mesura de la resistència dels agents a canviar d'opció i que, matemàticament, modela la forma funcional de les probabilitats de transició entre els possibles estats dels agents. En aquest context, estem especialment interessats en el paper dinàmic que desenvolupen l'estat AB i els paràmetres dels models, així com en els efectes de la xarxa social d'interacció.

En primer lloc, presentem i analitzem en detall un model de dues opcions no-excloents, el model-AB, que correspon al Model Bilingüe per al cas d'opcions socialment equivalents (d'igual prestigi) i de volatilitat neutra, és a dir, quan les probabilitats de transició depenen linealment de les densitats d'agents veïns. Al mateix temps, aquest model pot ésser interpretat com una extensió del model del votant (model prototípic de dinàmica fora de l'equilibri amb dos estats absorbents), cosa que el fa especialment rellevant. Estem interessats en els processos de creixement de dominis en aquests dos models, i analitzem els mecanismes d'agregament (*coarsening*) en xarxes regulars, on demostrem que la dinàmica està governada per moviment interfacial. De fet, mostrem com l'addició de l'estat AB canvia la dinàmica interfacial governada per soroll del model del votant, a una governada per curvatura. En comparació amb les xarxes regulars, i per tal de discernir el paper que desenvolupen les interaccions de llarg abast en una xarxa, estudiem l'efecte de xarxes de *petit-món* en la dinàmica. Essencialment, els agents AB juntament amb les interaccions de llarg abast aconseguen que la dinàmica arribi a una situació de consens molt més ràpidament.

A part del fenomen de petit-món, l'estructura mesoescalar o de comunitats és una de les característiques principals de les xarxes socials reals. Per aquest motiu, considerem a continuació el paper de l'estructura de comunitats en el model del votant i el model-AB, així com el tipus de metaestabilitat que s'hi manifesta. En el model-AB, trobem estats metaestables atrapats (*trapped*) de llarga durada en els que la distribució dels estats dels agents a la xarxa es correlaciona amb l'estructura de comunitats, i dona lloc a estats metaestables a qualsevol escala temporal. En aquest context, estudiem les condicions sota les quals no existeix

una escala de temps característica de la dinàmica d'ordenament cap a un dels dos estats absorbents. Per tal d'aconseguir-ho, estudiem xarxes aleatòries i xarxes amb estructura mesoescalar construïdes a partir de subestructures completament connectades (*cliques*) enllaçades aleatòriament. També comparem el model-AB amb un altre model amb dues opcions no-excloents introduït en el context de dinàmica semiòtica (el *Naming Game*), en el qual els agents interactuen d'un en un per tal de negociar convencions, és a dir, associacions entre formes i significats.

Per últim, estudiem el model d'Abrams-Strogatz i el Model Bilingüe en tot l'espai de paràmetres (prestigi-volatilitat). Ens interessa l'estudi d'aquests problemes de consens com a transicions ordre-desordre. Es tracta d'establir en quines regions de l'espai de paràmetres el sistema acaba eventualment homogeneïtzat en una de les opcions (ordre o consens) o bé si al contrari, s'arriba a una configuració de coexistència entre les dues opcions (desordre o coexistència). Deduïm descripcions macroscòpiques en xarxes completament connectades, xarxes aleatòries sense correlacions i xarxes regulars bidimensionals, per tal d'estudiar les transicions ordre-desordre tant analíticament com numèricament. El resultat principal consisteix en una transició de primer ordre a l'espai de paràmetres: a grans trets, consens en qualsevol de les dues opcions per a un règim de volatilitat baixa i coexistència per a un règim de volatilitat alta. A més, cal destacar que els agents-AB, així com el fet de tenir xarxes d'interacció amb pocs veïns, redueixen l'escenari de coexistència i introdueixen efectes no trivials del paràmetre de prestigi: l'emergència de zones en l'espai de paràmetres de domini només de l'opció més prestigiosa.

Aquesta tesi vol contribuir a la comprensió dels mecanismes subjacents en problemes de consens social en els quals dues opcions poden ser no-excloents, tot estudiant els fenòmens col·lectius emergents en models d'agents en interacció en els que les dinàmiques d'ordenament, la naturalesa de la xarxa i la metaestabilitat són analitzades en detall.

Preface

A deep understanding of collective phenomena in Statistical Physics is well established in terms of microscopic models based on the interaction rules among the particles in the system. Partly inspired by this success in linking micro and macro behavior, collective social phenomena are being currently studied in terms of microscopic models of interacting agents. In problems of social dynamics, agents sit in the nodes of a network and change their state (social option) according to specified dynamical rules of interaction with their neighbors in the network. These problems range from opinion dynamics and social dilemmas to cultural dissemination and language competition.

Language competition studies the dynamics of language use and competence due to social interactions, and has been recently addressed from the point of view of statistical physics and complex systems. In this thesis, and motivated by studies of language competition dynamics, we study problems of social consensus. The consensus problem is a general one of broad interest, recently addressed by statistical physics: the question is to establish when the dynamics of a set of interacting agents that can choose among several options leads to a consensus in one of these options (dominance/extinction of a language), or alternatively, when a state with several coexisting social options prevails (language coexistence).

In particular, language competition is a prominent example of a class of consensus problems in which options are non-excluding, that is, an agent can share the two options at play at the individual level (bilingual agents). In this direction, and building upon the Abrams-Strogatz model for two competing languages, we study two-state consensus models in comparison with models with two non-excluding options, which are defined as extensions in which agents can be in either of two opposite states (A and B) or in a third mixed state of coexisting

options (AB, bilingual). We are specially interested in the role of the AB-state and the parameters of the models in the dynamics, together with the effects of the network structure.

We first present and analyze in detail the AB-model, a model of two non-excluding and socially equivalent options, which can be interpreted as an extension of the voter model, a prototype spin-model of nonequilibrium dynamics with two equivalent absorbing states. We are interested in the processes of domain growth in these two models, so we analyze the coarsening mechanisms in lattices, where dynamics is shown to be dominated by interface motion. In comparison to these topologies and in order to elucidate the role of long range interactions in the network, we study the effect of small world networks in the dynamics. Beyond the small world phenomena, mesoscale or community structure has been shown to appear as one of the main complex features of real social networks. In this direction, we also address the role of community structure in the voter and the AB-model, as well as associated forms of metastability. In this scenario, we search for conditions under which a characteristic time scale for ordering dynamics towards either of two absorbing states in a finite complex network does not exist. For this, we study random networks and networks with mesoscale structure built up from randomly connected cliques. The thesis also addresses the comparison of the AB-model with another model with two non-excluding options introduced in the context of semiotic dynamics (the Naming Game), in which agents interact pairwise in order to negotiate conventions, i.e., associations between forms and meanings. Finally, we tackle the consensus problem as reminiscent of order-disorder transitions. Following this direction, in the last part of the thesis we study the Abrams-Strogatz model and its extension to account for the AB-state in the full range of parameters of the models. The aim is to establish regions in the parameter space for which the system is eventually dominated by one option (order or consensus) or, on the contrary, when a configuration of global coexistence is reached (disorder or coexistence). We derive macroscopic descriptions in fully connected networks, uncorrelated random networks and two-dimensional lattices, in order to study the order-disorder transitions both analytically and numerically.

This work aims to be a contribution towards the understanding of the mechanisms underlying in social consensus problems in which options can be non-excluding; studying the collective emerging phenomena in models of interacting agents in which the ordering dynamics, the nature of the network structure and the metastability in the models are analyzed in detail.

Contents

Titlepage	i
Acknowledgments	ix
Contents	xvii
1 Introduction	1
1.1 Collective phenomena: physics, complexity and social sciences . . .	1
1.2 Complex networks	6
1.2.1 Brief History: from networks in social sciences to the sta- tistical physics approach	7
1.2.2 Basic concepts	12
1.2.3 Standard models of complex networks	14
1.2.4 Networks with mesoscale structure	21
1.3 The consensus problem. Mechanisms and models	24
1.4 Paradigmatic two-state models in consensus problems	25
1.4.1 Coarsening processes. Absorbing, metastable and trapped states	27
1.4.2 The voter model	28
1.4.3 The zero-temperature spin-flip kinetic Ising (SFKI) model	37
1.5 Language competition	44
1.6 Ordering dynamics: from two-state models to models with two non-excluding options	48
1.7 Outline	52
	xvii

2	The models	53
2.1	The Abrams-Strogatz model	53
2.2	The Bilinguals model	55
2.3	The voter model and the AB-model	57
2.4	Phenomenology of the models: qualitative exploration of the <i>volatility-prestige</i> parameter space	59
2.5	Analysis of the models. General concepts	64
3	The AB-model (I): from regular lattices to small world networks	67
3.1	Fully connected networks	68
3.2	Two-dimensional lattices	70
3.3	Small world networks	80
3.4	From random imitation to majority rule dynamics: the ϵ -model .	85
3.5	Concluding remarks	87
4	The AB-model (II): networks with mesoscale structure	91
4.1	Anomalous lifetime distributions and topological traps in order- ing dynamics	92
4.1.1	The network model: a class of social networks	92
4.1.2	Trapped metastable states and lifetime distributions	94
4.2	Sufficient conditions for broad lifetime distributions in complex networks	102
4.2.1	Random networks	103
4.2.2	The role of communities	106
4.3	Concluding remarks	114
5	Comparing models with two non-excluding options	117
5.1	The Naming Game <i>vs</i> the AB-model: generalized models	118
5.2	Macroscopic description	121
5.3	Order-disorder transition	122
5.4	Interface dynamics: 1-d and 2-d lattices	125
5.5	Concluding remarks	129
6	Macroscopic descriptions and order-disorder transitions	131
6.1	Abrams-Strogatz model	132
6.1.1	Fully connected networks	133
6.1.2	Complex networks	140
6.2	Bilinguals model	148
6.2.1	Fully connected networks	148
6.2.2	Complex networks	151

<i>CONTENTS</i>	xix
6.3 Two-dimensional lattices	152
6.4 Concluding remarks	158
7 Conclusions	161
7.1 General conclusions	161
7.2 Specific conclusions	168
7.3 Outlook and final remarks	174
8 List of publications	179
Appendices	181
A Equation for the spin field ϕ_r in the Abrams-Strogatz model	183
B Viability and Resilience of Languages in Competition	185
B.1 Theoretical bounds of the Abrams-Strogatz model (I)	206
B.2 Theoretical bounds of the Abrams-Strogatz model (II)	208
List of Tables	211
List of Figures	213
References	218

Introduction

1.1

Collective phenomena: physics, complexity and social sciences

Understanding the complex collective behavior of many particle systems in terms of a microscopic description based on the interaction rules among the particles is the well established purpose of Statistical Physics. This micro-macro paradigm [1] is also shared by Social Science studies based on agent interactions. In many cases, parallel research in both disciplines goes far beyond superficial analogies. For example, Schelling's model [2] of residential segregation is mathematically equivalent to the zero-temperature spin-exchange Kinetic Ising model with vacancies. Cross-fertilization between these research fields opens interesting new topics of research [3, 4].

On the one hand, the concepts, formalism and methods from statistical physics and complex systems theory, such as emergence of collective phenomena, nonequilibrium dynamics, coarsening or phase transitions, are becoming a powerful framework so as to model and understand social systems. These systems are indeed of high complexity, and social phenomena appear to be of increasing interest for the physicists community, as indicated by the large and increasing number of publications on the statistical physics approach to social dynamics (see the review by Castellano et al. [5]). On the other hand, interactions in complex networks is a relatively recent paradigm in statistical physics and complex systems [6]. The works at the end of the 1990s by Watts and Strogatz [7], and Barabási and Albert [8] opened a novel approach to the modeling and under-

CHAPTER 1. INTRODUCTION

standing of complex networks from the point of view of statistical physics. Since then, many systems beyond physics are modeled and studied through network theory, ranging from biology to economy and the social sciences. In particular, network theory applied to complex social networks makes possible an analysis of the effect of the network structure on nonequilibrium dynamics proposed in order to model social behavior*.

In this way, the micro-macro paradigm in the study of social systems is reinforced, extended and renewed by statistical physics and complex systems theory. The microscopic interaction rules include two main ingredients: (i) structure: a set of interacting agents, which can account for individuals, groups of individuals, organizations, institutions, etc., which are embedded in a framework of interaction modeled by a network; and (ii) dynamics: the interaction mechanism between agents which defines the nonequilibrium dynamics mentioned above. These dynamics have been proposed in parallel to the explosion of the complex networks research field, and deal with problems such as opinion dynamics [9], cooperation [10], culture dissemination [11], epidemics [12], language dynamics [13], dynamics of financial markets [14], social dilemmas [15] etc. This micro-macro approach is generally known as Agent-Based Modeling (ABM) in computational and social sciences [16].

The idea of modeling mathematically social systems has a long history. As reviewed by Ball [17], a statistical view of social phenomena inspired the raise and success of statistical physics in the natural sciences. Already in the 17th century, Hobbes made the first attempt to develop a political theory that does not assume an a priori shaped society but one arising from few assumptions and a mechanistic view of the way humans behave. Later, it was the interest in quantifying aspects of societies such as the death and birth rates or crime what since the 17th century and specially during the 18th century gave birth to the early stages of *statistics*. At the time, Hume was arguing for the access to the first principles in human nature through empiricism. Already in the 19th century, Quetelet was among the first who attempted to systematically apply the new science of probability and statistics to social science, planning what he called a *social physics* [18]. He applied the law of large numbers to human demography which, in a few words, can be described as the way a pure random process gives rise to deterministic probabilities when the number of events is large enough. In fact, Comte had used the term social physics before, although he did not share Quetelet's enthusiasm for quantification. It was later that Comte coined the term *sociology* [19], and he is considered one of the fathers of this discipline. Other philosophers who in different lines of thought aimed to create a scientific

*Due to the central role played by network structure on social dynamics, we devote the whole next Section to present the field of complex networks in detail.

1.1. COLLECTIVE PHENOMENA: PHYSICS AND SOCIAL SCIENCES

political theory range from Locke, Bentham and Stuart Mill to Marx. For instance, Marx used statistical laws by Quetelet to develop the labor theory of value. It was in this scenario that contemporary 19th century physicists looked at the social sciences in order to move beyond Newtonian physics towards statistical mechanics. Maxwell was among the first ones to use statistical laws of society as analogies in natural sciences, which finally gave rise to the kinetic theory of gases. Order at the macroscopic level was shown to be possible from microscopic uncertainty. In the second half of the 20th century, statistical physics research focused in the study of interacting spin models (triggered by the Ising model), critical phenomena or pattern formation in extended systems, moving towards the understanding of collective emergent phenomena.

It is now interesting to notice that at the beginning of the 21st century, the increasing computational power, the new social phenomena related to new technologies from which real data can be obtained systematically (e-mails, mobile phone calls, on-line communities, collaborative tagging systems), and an increasing collaboration between physicists and social scientists, led a critical mass of physicists to look at social sciences back again [5]. Building upon the theories, tools and methods developed by statistical physics, which at the beginning were in part inspired by studies in social sciences, they face collective phenomena in social dynamics from this new standing point.

Of course, the development of social sciences embraces a much wider spectrum of thought than the naturalist point of view we have briefly presented above, but an exhaustive analysis is out of the scope of this introduction. However, it is worth mentioning that in social sciences, there does not exist a general agreement on the questions to be addressed and the methods to apply. In this sense, there is not a common paradigm among all social scientists. For this reason, social systems have historically been studied from essentially two different philosophical points of view [20]: (i) the naturalist, which as we mentioned above has looked at the concepts, formalism, methods and tools from natural sciences in order to develop a theory of social science (also referred as empiricism, behaviorism or positivism); and (ii) the interpretativist (or anti-naturalist), which argues that natural sciences methods are not appropriate for the analysis of human behavior and for the development of a theory of social science (which contains many philosophical lines of thought: idealism, structuralism, postmodernism, deconstructionism,...). In general, the first one argues for the need to look at natural sciences methods to profit from the progress these sciences have reached since the 17th century, and in order to gain prediction on the systems studied. On the contrary, the second argues that such methods are not appropriate for the study of human behavior, as they usually tend to oversimplify the meanings associated to the system of study, and argues for the need to focus on the understanding

CHAPTER 1. INTRODUCTION

and intelligibility of the system*. In some way and focusing now on classical sociology, Durkheim and Weber belong to these two main lines of thought [21]. On the one hand, Durkheim looks at the natural sciences methods, and argues for social pressure mechanisms and external influences as driving forces of human action, conceiving society as an objective reality. On the other hand, Weber is interested in the intention beyond social actions and the associated subjective meanings.

We think that both approaches should listen to each another if there is some possibility to trace a path together. In fact, from our point of view, *sociophysics*[†], and in particular the work we present in this thesis, aims to contribute to the understanding of mechanisms of social interaction and their consequences, rather than to its prediction, which is today in most of the social issues out of the aim (and out of scope) of the present models: the goal is to move beyond the observation of correlations, in order to establish cause-effect relations between mechanisms and its consequences. It is in this sense that we cannot talk about a *theory of social physics*, but about the *first bricks in the wall* towards its modeling and understanding. One of the main reasons concerns the fact that in many social systems there is a lack of accurate, broad and high frequency data (in comparison to natural sciences standards) to account for a dynamical fitting of the time evolution of the systems studied. This is of course related to the large amount of individuals one needs to study in order to have significant data sets, the difficulty (if not impossibility in many cases) to move beyond observation and make social experiments, and the time scales involved in the dynamics[‡]. This hinders today the path towards such possible theory, as it is difficult to discriminate between the large amount of models appearing in the last years. However, and specially regarding the promising sort of social data obtained from the new technologies (Internet, mobile phones, etc), question-driven data can be extremely helpful in this direction, that is, data collection with the aim to answer clear questions of interest defined *a priori*.

Regarding contemporary studies coming from the social sciences, we find Social Impact Theory [22], which is very close to the statistical physics approach.

*Qualitative research is the method of inquiry generally applied in this approach to social sciences. The aim is to gather an in-depth understanding of human behavior and the reasons that govern such behavior. In comparison to quantitative methods, the qualitative method focuses its investigation in the *why* and *how* of decision making and human action. Hence, smaller but complete and focused samples are often studied, rather than large samples. However, conclusions derived from qualitative methods are usually more difficult to be generalized.

[†]To our knowledge, the International Conference *SocioPhysics* held in Bielefeld (Germany) in 2002 is the first time in which the concept has been formally employed, referring to the work of statistical physicists who study problems of social dynamics.

[‡]For instance, in order to have relevant data to account for language competition dynamics, at least data regarding several generations are needed.

1.1. COLLECTIVE PHENOMENA: PHYSICS AND SOCIAL SCIENCES

Modeled through cellular automata, it considers the social impact on a subject in terms of the number of agents in the social group, its relative power, and the distance from the subject, which can be spatial or relative to an abstract space of individual relationships. Other models from social scientists which would fall into this line of thought are the works by Granovetter on the role of weak ties in social networks [23], Schelling on residential segregation [2] and Axelrod on cultural dissemination [11].

It is in these common interests and approaches where the collaboration between social and physical sciences is giving rise to new and promising lines of research. Today, researchers working with Agent-Based Models come from very different backgrounds (physics, mathematics, engineering, computer science, economics, sociology or cognitive science) and start to share a common formalism which is both theoretical and experimental. It is theoretical because the micro-macro paradigm inherited from complex systems is underlying the conceptual modeling; and it is experimental in the sense that computer simulations make it possible to generate the data needed by scientists in order to study the models proposed, which can be statistically analyzed [24]. As we mentioned above regarding real data analysis, the recent explosion of the information and communication technologies has been crucial, as it has increased enormously the amount of real data available to study social systems. Although scientists from different disciplines think and develop models in a different way according to their own background, agent-based modeling is currently giving a common framework and enhancing interdisciplinary research in many areas of science.

In this thesis, we are interested in the class of social processes in which agents are considered adaptive rather than rational, and where the emphasis is in the social influence they feel from the other agents in the network (see Section 1.2), in the line of social impact theory [22], instead of their strategies or goals, which would correspond to other approaches such as game theory [25]. Two of the main mechanisms of this class of social interactions concern consensus problems* (see Section 1.3) driven by imitation and social pressure, which correspond to the voter model [27] and the zero-temperature spin-flip kinetic Ising model ($T = 0$ SFKI) [28], respectively. As we refer to them throughout the thesis, in Section 1.4 we make a detailed review of the main results for these models in different complex networks. Our work is motivated by scenarios of language competition [29], which concern the dynamics of language use and competence due to social interactions (see Section 1.5). Language competition belongs to the general class of consensus problems in which options are non-excluding, that is, an agent

*A consensus problem is defined as the dynamics of a set of interacting agents that can choose among several options, which leads to a consensus in one of these options or, alternatively, to a state in which several coexisting social options prevail [26].

CHAPTER 1. INTRODUCTION

can share the two options at play at the individual level (bilingual agents). In Section 1.6 we present the aim of this thesis in detail, which focuses on a detailed study of this type of consensus problems, comparing two-state models with three-state models with two non-excluding options.

1.2

Complex networks

In this Section we present a brief review of the history, basic concepts and models in the active field of complex networks theory. Networks have become a widely used framework to analyze complex systems, in which there exists a set of interacting units that can be modeled as nodes (representing the units) connected through links or edges (representing the interactions among them) and which display collective emergent phenomena. In this way, complex networks can be seen as the skeleton of complex systems. We find complex networks in very different scientific disciplines: biology and biochemistry (ecological networks, metabolic networks), economics (networks of firms), social sciences (social networks), or technological architectures (Internet, power grids). In the social sciences, networks naturally model individuals (nodes) which have social ties between them (links); and in this way, they become a key ingredient in order to model social dynamics.

In the work presented in this thesis, we are interested in the topological effects of different complex networks on nonequilibrium dynamics which, motivated by language competition processes, model social consensus problems among a set of interacting agents. In this way, this Section is a presentation of the main concepts and model networks we use throughout the thesis, including Erdős-Rényi random networks [30], Watts-Strogatz small world networks [7] and Barabási-Albert scale free networks [8], together with networks with mesoscale structure [31].

The field of complex networks has been growing extremely fast during this last decade, and an exhaustive analysis is out of the scope of the present study. A complete review of complex networks has been provided by Albert and Barabási [6]. Other interesting reviews are the ones by Dorogovtsev and Mendes [32] and Newman [33]. More recent reviews by Boccaletti et al. [34] and Dorogovtsev et al. [35] include also results on different dynamics on complex networks.

1.2. COMPLEX NETWORKS

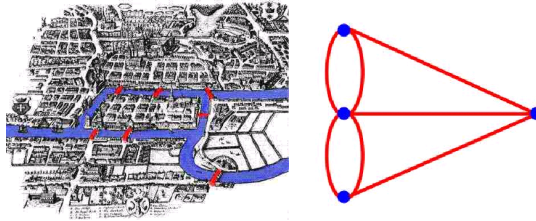


Figure 1.1: Left: In the Königsberg bridge problem, one wants to know if it is possible to go for a walk in this city, crossing all the seven bridges which link several parts of the city, once and only once. Right: By mapping the problem into a graph, Euler showed in 1736 that this was not possible. This is believed to be the first time in which networks were used to solve a problem.

1.2.1 Brief History: from networks in social sciences to the statistical physics approach

Complex networks or graphs* have been essentially studied during the 20th century by both mathematicians and social scientists, with different focus and purposes. The mathematical approach to graph theory can be traced back to the 18th century, when Euler published the solution to the famous Königsberg bridge problem (Figure 1.1). Initially, mathematicians focused on the properties of regular (non-random) networks. However, in the 1950s the work by Erdős-Rényi [30] triggered a detailed study of random networks, reviewed by Bollobás in [36]. As the thesis is motivated by social dynamics problems, we give now a special emphasis on the social science roots of the field. Then, we briefly explain how statistical physics and complex systems theory have come into play in the last decade.

Social Sciences

One of the most powerful ideas in the social sciences has been the notion that individuals form a network of social relationships and interactions which at the same time influences their individual behavior. Borgatti et al. [37] have

*Graph is the term generally used in mathematics to refer to networks.

CHAPTER 1. INTRODUCTION

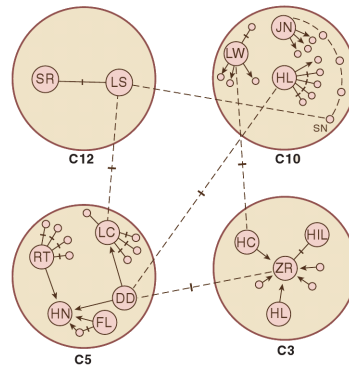


Figure 1.2: The network of runaways constructed by Moreno. The four colored circles represent cottages in which the girls lived. Each of the circles within the cottages represents an individual girl, with the 14 girls who runaway identified by initials (e.g., SR). All non-directed lines between a pair of individuals represent feelings of mutual attraction; directed lines represent one-way feelings of attraction; and dashed lines represent mutual repulsion. From *Borgatti et al.* [37].

presented an interesting brief review of the historical development of social network theory during the 20th century. Already in the 1930s, we can find the network analysis carried out by Moreno [38] to understand a sociological problem regarding an epidemic of runaways in a School for Girls in New York. He used a technique called *sociometry*, to represent graphically the subjective feelings among the girls in the study, reflecting that the importance of the position in the network of social relations was a key factor determining their probability to runaway from the school (see Figure 1.2).

In 1969 Travers and Milgram published their experiment on the small world phenomena [39], giving rise to the popular idea of six degrees of separation. They performed an experiment in the USA in which randomly selected individuals were asked to direct letters to a certain target person. Each of them should forward his or her letter to a single acquaintance whom they judged to be closer than themselves to the target, who in turn was asked to perform the same operation. Analyzing the letters that eventually reached the target (18 out of 96), they found that on average the length of the resulting acquaintance chains was

1.2. COMPLEX NETWORKS

six, giving in this way the first evidence of the small world phenomena, which has been widely studied in the last years [40]*. Another important contribution to the field comes from the theory on the strength of weak ties by Granovetter [23]. The strength of a social tie is defined as the intensity of the relationship; and in this way, social ties among close friends are strong, while acquaintances between people who rarely talk to each other are weak. He argued how strong social ties tend to be redundant, as they are embedded in clusterized parts of the network or communities. On the contrary, weak ties tend to connect different communities, i.e., connecting individuals to others which are usually unconnected to the rest of one's neighborhood. In this way, he showed the key role played by weak ties as bridges between communities, through which information and social behavior can flow along different parts of the network.

During the 1980s, social network analysis becomes an established field within the social sciences, and since then social scientists have applied social network theory to a wide spectra of fields, such as sociology, anthropology, management and consulting, public health, or national security [37]. The works by Wasserman and Faust [42] and Scott [43] have become standard literature on social network analysis, and display a complete review of the field for the newcomer.

Physical Sciences

The studies of networks by social scientists were generally focused on specific problems and considering relatively small networks, from which a fundamental understanding of the universal properties of social networks was hard to obtain. In the last decade, and since the seminal papers by Watts and Strogatz [7] and Barabási-Albert [8] on small world and scale free networks respectively, statistical physicists have come into the research field of complex networks. The appearance of these simple models to account for some of the basic features observed in real networks, together with the increasing computational power and the access to large databases (mainly due to the rise of the new technologies: Internet, mobile telephones, etc) triggered a revolution in the field of statistical physics, with the number of contributions to the field constantly increasing until today. Physicists become interested in the formation, structure and evolution of complex networks, as well as in the topological effects these may produce on social interaction problems, such as opinion dynamics, cultural diffusion or

*Recently, Dodds et al. [41] have performed an on-line experiment in which more than 60,000 e-mail users attempted to reach 18 different targets in 13 different countries (384 out of 24,163 chains reached their targets). They have obtained chain lengths of a median between five and seven, depending on the geographical separation of source and target. In this way, these results support the claims by Travers and Milgram. Notice the different scale of the experiment compared to the one in 1969, specially enhanced by the possibility of performing on-line experiments.

CHAPTER 1. INTRODUCTION

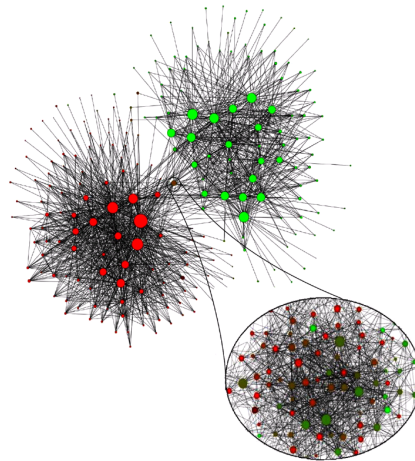


Figure 1.3: Network with community structure extracted from a Belgian mobile phone network of about 2 million customers. The size of a node is proportional to the number of individuals in the corresponding community. Color on a red–green scale represents the main language used in the community (red for French and green for Dutch). Notice the intermediate community of mixed colors between the two main language clusters: a zoom at higher resolution reveals that it is made of several subcommunities in which language use is very heterogeneous. From *Blondel et al.* [46].

language competition [5]. The study of complex networks has obtained the attention of the general public during these years, and several popular science books have been published on the topic [44, 45].

Current network analysis in statistical physics: some relevant examples

The analysis of real complex networks in different fields of science such as biology or technology can be found in [6, 47, 48]. However, due to the social motivation of the thesis, we concentrate here in some of the works on social networks done during the last years, in order to illustrate the current studies regarding the analysis of real social networks.

1.2. COMPLEX NETWORKS

Onnela et al. [49] studied a mobile telephone network with more than 4 million users. They constructed social links between two users when they found a reciprocal call between two agents, and the strength of the social tie was defined as the aggregated duration of calls they shared. It is important to stress that they could confirm Granovetter's theory of the strength of weak ties: they show the coupling between the strength of the ties and their structural position in the network (strong ties are found within communities, while weak ones tend to connect different clusters), finding that a successive removal of the weak ties results in a phase transition-like network collapse, while the same removal process starting by the strong ties has little impact in the overall structure of the network.

In another paper, Blondel et al. studied a Belgian mobile phone network of 2 million customers in which they tested a community detection algorithm based on modularity optimization [46]. Beyond the algorithm and as shown in Figure 1.3, the most interesting result for us is the correlation found between community structure and the language of the customer, which they inferred by the language in which the user signs the contract: a French and a Dutch large domains are found, joined together by a much smaller bilingual community*. Notice that both studies presented above deal with very large networks, which include up to millions of nodes. This is a change by several orders of magnitude compared to the social science studies before the 1990s (for example, the network by Moreno [38] previously presented in Figure 1.2, or the famous Zachary's karate club network [50], with only 34 members), and therefore it provides good statistics in order to uncover structural properties and features that increase our understanding of real social networks.

Regarding the connectivity or degree (number of links adjacent to a node) distribution, Amaral et al [51] studied different real social networks (the movie-actor network [52], the acquaintance network of Mormons [53], and a friendship network in a High School [54]). They observed different types of networks: (i) scale-free networks, characterized by a node connectivity distribution that decays as a power law; (ii) broad-scale networks, characterized by a connectivity distribution that has a power law regime followed by a sharp cutoff; and (iii) single-scale networks, characterized by a connectivity distribution with a fast decaying tail. They claim that in most complex networks different degree connectivities might be related to the nature of the constraints when adding a new link. In social systems, this is related to the definition of a social tie used to construct the network, from a mere acquaintance (an individual can have a high number of them) to a tight friendship that needs spending time together

*We come back to these results regarding language use in networks with community structure in Chapter 4, when we present our results for language competition models in modular networks.

CHAPTER 1. INTRODUCTION

rather often (the number of close friends of an individual is then limited by time constraints).

Other studies of real social networks deal with social phenomena such as author collaboration networks [55], sexual contacts [56] or citation networks [57].

1.2.2 Basic concepts

A network (or graph) is a pair of sets, $G = \{P, E\}$, where P is a set of N nodes (or vertices), and E is a set of links (or edges) in which each link connects a couple of nodes. Networks can be directed or undirected. In directed networks [58, 59], the interaction from node i to node j does not necessarily imply an interaction from j to i . On the contrary, when the interactions are symmetrical, we say that the network is undirected. Moreover, a network can also be weighted [60, 61]. A weight is defined as a scalar that represents the strength of the interaction between two nodes. In an unweighted network, instead, all the edges have the same weight (generally set to 1).

Besides, networks can evolve in time. When we model dynamics on networks (opinion formation, cultural diffusion, language competition, etc.) there exist essentially three cases depending on the relative time scales between the network evolution and the dynamics: (i) the characteristic time corresponding to the dynamics is much larger than the one corresponding to the network, $\tau_{dyn} \gg \tau_{net}$, which corresponds to an evolving network in which dynamics can be neglected; (ii) the characteristic time corresponding to the dynamics is much smaller than the one corresponding to the network, $\tau_{dyn} \ll \tau_{net}$, in which the network evolution can be ignored, and therefore corresponds to the case of a dynamics taking place in a fixed network; (iii) the characteristic time corresponding to the dynamics is of the same order than the one corresponding to the network, $\tau_{dyn} \sim \tau_{net}$, which corresponds to a coevolution of the dynamics and the network structure [62, 63]*. The networks we study in the present thesis are undirected, unweighted and fixed (we consider $\tau_{dyn} \ll \tau_{net}$). This corresponds to the simplest case but, as a first step, it is important to keep the modeling as simple as possible in order to capture the basic mechanisms which explain a given phenomenon. Later, one should start adding new ingredients that increase the complexity of the problem of study.

In this Section, we define basic concepts that characterize complex networks and which we use throughout the thesis. Given an undirected, unweighted and fixed network with N nodes and n links (or edges):

*A recent review on coevolutionary networks has been provided by Gross and Blasius [64].

1.2. COMPLEX NETWORKS

Degree

The number of links adjacent to a node i is defined as the degree of the node, k_i .

Degree distribution

The degree distribution $P(k)$, which gives the probability that a randomly selected node has exactly k links, characterizes a network by giving a measure of its heterogeneity in terms of the number of connections per node. Some networks might be degree-homogeneous, with an equal number of connections (regular lattices), others might have certain degree of heterogeneity in which the average degree, $\langle k \rangle = 2n/N$, characterizes the network (random networks), while others can have no typical scale, i.e., $P(k) \sim k^{-\gamma}$ (scale-free networks). Among these last networks, the most interesting case appears in those which have a diverging second moment of the degree distribution ($\gamma \leq 3$). In this case, if $\langle k \rangle$ exists (that is, for $2 < \gamma \leq 3$), it is not representative of the network and the topology is characterized by the importance of hubs.

Degree-degree correlations

Degree-degree correlations are related to the concept that the probability that a node of degree k is connected to another node of degree k' might depend on the value of k or, in other words, the degrees of two adjacent nodes are not independent. This fact can be described by the conditional probability $P(k'|k)$, which represents the probability that a node of degree k is connected to a node of degree k' . In uncorrelated networks, $P(k'|k)$ can be simply estimated as the probability that any link points to a node of degree k' , leading to $P(k'|k) = k'P(k')/\langle k \rangle$, independent of k .

As we will see, random uncorrelated networks (like Erdős-Rényi networks) have no degree-degree correlations, but many real networks do. The network is said to exhibit *assortative* mixing if there exists a positive degree-degree correlation, and *disassortative* mixing if it is negative.

Clustering coefficient

The clustering coefficient for a node i , C_i , quantifies the local cliquishness of its immediate (nearest) neighborhood, defined as $C_i = \frac{2E_i}{k_i(k_i-1)}$, where k_i is its degree and E_i is the number of links between its k_i neighbors. It is therefore a scalar normalized between 0 and 1. In other words, the clustering coefficient is the number of existing connections between the k_i neighbors of i out of the maximum possible number of connections that could exist between them. The clustering coefficient of the whole network is naturally defined as the average of all individual C_i , $C \equiv \frac{1}{N} \sum_{i=1}^N C_i$. An alternative definition is given by the proportion of triangles attached to the node i from all the possible ones that

CHAPTER 1. INTRODUCTION

can be built by linking any pair of its neighbors. The concept of clustering has its roots in the social sciences, where it appeared as the *fraction of transitive triples* [42]. In social networks, it can be easily interpreted as a measure of the probability that the friends of a given agent are at the same time friends of each other.

Average path length

The distance between two nodes is defined as the number of links along the shortest path connecting them. An important measure characterizing a network is the average path length, l , defined as the mean distance among any two randomly chosen nodes. Regular d -dimensional lattices display an average path length which scales with system size as $l \sim N^{1/d}$. However, complex networks are characterized by much shorter path lengths which, as we shall see, typically scale as $l \sim \ln(N)$.

Community

While there is not a common agreed definition of a community [31], an extended one is the following: a set of nodes is a community if the sum of all degrees within the set is larger than the sum of all degrees toward the rest of the network. Several other definitions, possibly more appropriate in some cases, can be found in [42]. In Section 1.2.4 we give an introduction to networks with mesoscale structure, where we analyze the implications of the existence of communities in complex networks in detail.

1.2.3 Standard models of complex networks

In this Section, we present a brief introduction to the paradigmatic models for complex networks that we use on the course of the present thesis: Erdős-Rényi random networks [30], Watts-Strogatz small world networks [7] and Barabási-Albert scale free networks [8].

The most important features of real social networks are known to be: (i) short average path length and (ii) large clustering coefficient [65], (iii) broad degree distribution [51], (iv) mesoscale structure [49], and (v) assortativity [66]. As we shall see, the simple models mentioned above capture some of these properties and their generating mechanisms, but fail in reproducing others. More sophisticated models are needed to recover all of these properties at the same time, as we show in the last part of our introduction when introducing models for networks including mesoscale structure.

1.2. COMPLEX NETWORKS

Erdős-Rényi random networks

The first contribution to random networks dates from the 1950s when Erdős and Rényi published their classical seminal paper [30]. In their model they define a random network* as N labeled nodes connected by n edges, which are chosen randomly from the $N(N-1)/2$ possible edges. An alternative and equivalent definition of a random network, widely used in the physics literature, is the binomial model in which starting with N nodes, every pair of them is connected with probability p . Consequently, the expected total number of edges is $pN(N-1)/2$. In the limit $n \rightarrow N(N-1)/2$ (corresponding to $p \rightarrow 1$) a complete graph topology is recovered. A complete graph (or fully connected network) is defined as a network in which every node is connected to any other node.

One of the most important results regarding random networks is that many important properties appear quite suddenly. Among many other properties (appearance of trees, cycles and other subgraphs) it can be shown that at $p_c = 1/N$ (corresponding to $\langle k \rangle \simeq 1$) the random graph changes its topology abruptly from a loose collection of small clusters to a system dominated by a single giant component. In this region the largest cluster clearly separates from the rest of the clusters, its size S increasing proportionally with the separation from the critical probability, $S \sim (p - p_c)$. This dependence is analogous to the scaling of S with the percolation probability in infinite-dimensional percolation [67]†.

With good approximation the degree distribution of a random graph is a binomial distribution, $P(k) = C_{N-1}^k p^k (1-p)^{N-1-k}$, which for large N converges to a Poisson distribution, $P(k) \simeq e^{-pN} \frac{(pN)^k}{k!} \simeq e^{-\langle k \rangle} \frac{\langle k \rangle^k}{k!}$, where the average degree is $\langle k \rangle = p(N-1)$. A random graph is likely to be sparse, and locally can be seen essentially as a tree: with large probability, the number of nodes at a distance l from a given node is approximately k^l . Equating then k^l with N , it can be obtained that the average path length scales as $l_{rand} \simeq \frac{\ln(N)}{\ln(\langle k \rangle)}$ ‡. Therefore, random networks display a small l , growing slowly (logarithmically) with system size. This is in agreement with what is found in most real networks.

Regarding the clustering coefficient, in a random network the probability that two neighbors of a given node are connected (or what is the same, the proportion of triangles among all possible ones) is the probability that there exists a link

*Notation for this Section: for convenience, we refer to Erdős-Rényi random networks simply as *random networks*.

†As mentioned in the brief historical section, a detailed review of random graphs is available in the classic book of Bollobás [36].

‡Notice that it is in this sense that complex networks are infinite dimensional: for a given node, the number of neighbors at a distance l , n_l , scales faster than a power of l ($n_l \sim l^d$), characteristic of topologies of finite dimension d .

CHAPTER 1. INTRODUCTION

between these two nodes, that is: p . Therefore, $C_{rand} = p \simeq \frac{\langle k \rangle}{N}$. It is important to notice that real social networks always have a much larger clustering compared to the one of a random network. In this way, the result for C_{rand} does not capture the very large clustering coefficient found in real social networks, which is in general independent on the system size.

Notice that beyond the Erdős-Rényi model for random networks, one can construct random uncorrelated networks* with an arbitrary degree distribution (exponential, power law, etc.). The degree of the nodes is selected from the distribution, and then their links are randomly paired (configuration model [68, 69]). As there are no correlations, the conditional probability $P(k'|k)$ is independent of k , $P(k'|k) = k'P(k')/\langle k \rangle$. A special case of random uncorrelated networks is that one of a degree-regular random network. This model, in which all nodes have exactly the same degree k_0 , is very practical for analytical calculations: the degree distribution is a Kronecker delta centered at degree k_0 , $P(k) = \delta_{k,k_0}$.

Watts-Strogatz small world networks

As we mentioned above, real social networks are characterized by a short average path length (like random networks), but with a large clustering coefficient compared to random networks. This is known as the *small-world* character[†] and describes structures which are neither completely ordered nor completely random. The social experiments performed in the 70s that we described in Section 1.2.1 by Travers and Milgram [39] already pointed to this central property of social networks.

Watts and Strogatz came with a very simple one-parameter model which interpolates between a regular lattice and a random network, in order to generate complex networks with small-world character [7], which are known now simply as Small-World networks (SW). The algorithm is as follows: start with a ring lattice with N nodes in which every node is connected to its first k_0 neighbors ($k_0/2$ on either side). In order to have a sparse but connected network during the whole rewiring process, consider $N \gg k_0 \gg 1$. Then, randomly rewire each link of the lattice with probability p such that self-connections and duplicate links are excluded[‡]. This process introduces on average $pNk_0/2$ long-range connections

*Notice that the Erdős-Rényi random network is the prototypical example of random uncorrelated networks.

[†]Notice that some of the literature considers the small world character to be only the existence of a short average path length [6].

[‡]Instead of this rewiring process, Newman and Watts [70] introduced a variant in which links are added between randomly chosen pairs of sites, but no links are removed from the regular lattice. This model is somewhat easier to analyze than the original Watts-Strogatz model; however, it does

1.2. COMPLEX NETWORKS

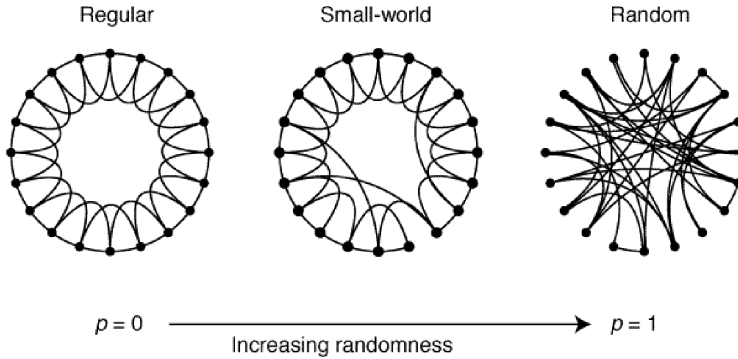


Figure 1.4: The Watts-Strogatz random rewiring procedure, which interpolates between a regular ring lattice and a random network keeping the number of nodes and links constant. $N = 20$ nodes, with four initial nearest neighbors. For $p = 0$ the original ring is unchanged; as p increases the network becomes increasingly disordered until for $p = 1$ a random network is recovered. From *Watts and Strogatz 1998* [7].

throughout the network*. In this way, by tuning p one observes a transition between order ($p = 0$) and randomness ($p = 1$) (see Figure 1.4).

On the one hand, for $p = 0$ the model keeps the initial ring lattice topology, where the average path length is $l(p = 0) \simeq N/2k_0 \gg 1$ and the clustering coefficient $C(p = 0) \simeq 3/4$; thus l scales linearly with the system size, and the clustering coefficient is large. On the other hand, for $p \rightarrow 1$ the model converges to a random graph for which $l(p = 1) \sim \ln(N)/\ln(k_0)$; and $C(p = 1) \sim k_0/N$; thus l scales logarithmically with N , and the clustering coefficient decreases with N . When analyzing the dependence on the rewiring probability p for both, the average path length and the clustering coefficient, Watts and Strogatz succeeded in uncovering a broad p -regime for which the small world phenomenon arises [7]: a short path length together with a high clustering coefficient (see Figure 1.5).

not preserve the degree distribution. For sufficiently small p and large N this model is equivalent to the Watts-Strogatz model.

*Notice that from a social network point of view, the model accounts for the fact that an individual has most of their relationships in their immediate neighborhood (neighbors, colleagues, friends in groups physically close), while having some friends who are long way away, modeled through long range connections (old acquaintances, friends abroad).

CHAPTER 1. INTRODUCTION

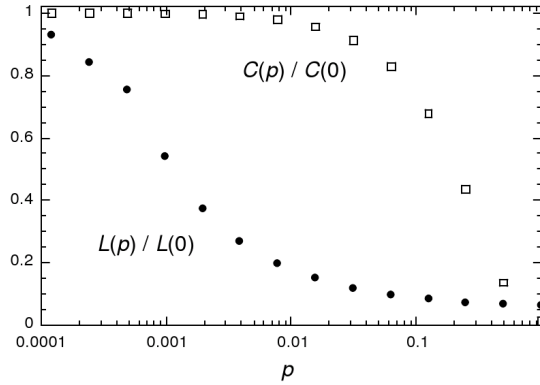


Figure 1.5: Characteristic path length $l(p)$ and clustering coefficient $C(p)$ for the Watts-Strogatz model. The data are normalized by the values $l(0)$ and $C(0)$ for a regular lattice. Averages over 20 random realizations of the rewiring process; $N = 1000$ nodes, and an average degree $\langle k \rangle = 10$. From *Watts and Strogatz 1998* [7].

The rapid drop observed in $l(p)$, corresponds to the onset of the small-world phenomenon. During this drop $C(p)$ remains almost constant, indicating that the transition to a small world is almost undetectable at the local level.

An important result concerns the dependence on the system size for the onset of the small-world behavior. The average path length, l , does not begin to decrease until $p \geq 2/Nk_0$, which ensures the existence of at least one shortcut [52]. This implies that the transition in p depends on the system size. The small-world phenomenon has been shown to appear when p is larger than $p^* \sim (1/N)^d$ [71], where d is the dimension of the original lattice: if $p < p^*$, $l \sim N^{1/d}$ (as in regular lattices), but if $p > p^*$, $l \sim \ln(N)$ (as in random networks). Trivially, for the original Watts-Strogatz model one obtains $p^* \sim (1/N)$.

Finally, the degree distribution in Watts-Strogatz small world networks is similar to that of a random graph: it has a pronounced peak at $k = k_0$ and decays exponentially for large k . Thus the topology of the network is relatively homogeneous, with all nodes having approximately the same number of links [6].

Barabási-Albert scale free networks

Another important feature of real networks besides the small-world character concerns the fact that degree distributions deviate significantly from a Poisson distribution (characteristic of random networks) and many large networks are scale free, that is, their degree distribution follows a power law for large k^* . As we have seen, this feature is not recovered in the Watts-Strogatz model; so there was a need for different approaches.

In this direction, Barabási and Albert proposed a model [8] that not only characterizes the network topology, but also accounts for the question of which mechanism might be responsible for the emergence of scale free networks. They propose a model with two ingredients: growth and preferential attachment, with the following algorithm: (i) *Growth*: starting with a small number of nodes, m_0 , at every time step, a new node is added with $m \leq m_0$ links that connect the new node to m different nodes already present in the network (ii) *Preferential attachment*: when choosing the nodes to which the new node connects, it is assumed that the probability P that a new node will be connected to node i depends on the degree k_i of node i , such that: $P = \frac{k_i}{\sum_j k_j}$. After t time steps, the network obtained has $N = m_0 + t$ nodes and mt links. As shown in Figure 1.6 (a), numerical simulations indicate a stationary scale free distribution, $P(k) \sim Ak^{-\gamma}$, with $\gamma \simeq 3^\dagger$. The second moment of the distribution diverges, and therefore there is not a characteristic scale in the network: in this sense it is *scale-free*. Moreover, the scaling exponent is independent of the only parameter in the model, m , which only affects the coefficient A of the power law distribution, $A = 2m^2$ (see inset of Figure 1.6 (a)).

Several analytical approaches have studied the dynamical properties of the Barabási-Albert network (BA-network), confirming the power law degree distribution: the continuum theory [72], the master-equation approach [73] and the rate-equation approach [74]. All these approaches are summarized in the review from Albert and Barabási [6]. An interesting result refers to the fact that the time evolution of the degree of all nodes follows a power law with an exponent 1/2 (see Figure 1.6 (b)).

*Contrary to other complex networks, social networks have the restriction that an agent can not have an arbitrary number of social contacts (the number of contacts depends crucially on how you define a social tie, from a mere acquaintance to a tight friendship). Therefore, many social networks display a broad tail followed by a cut-off [51].

†It has been shown that the fact of considering growth and preferential attachment independently does not lead to this result [8, 72]: this indicates that both mechanisms are needed simultaneously in order to generate a power law degree distribution.

CHAPTER 1. INTRODUCTION

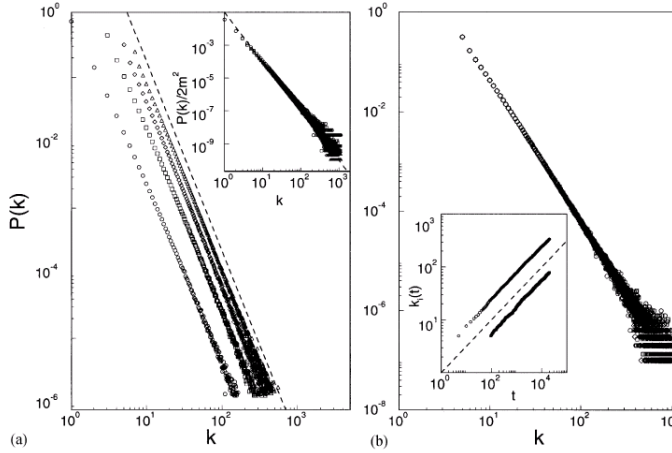


Figure 1.6: (a) Degree distribution for the BA-network. $N = m_0 + t = 3 \times 10^5$; with $m_0 = m = 1$ (circle), $m_0 = m = 3$ (square), $m_0 = m = 5$ (diamond), $m_0 = m = 7$ (triangle). The slope of the dashed line is $\gamma = 2,9$. Inset: rescaled distribution with m , $P(k)/2m^2$ for the same parameter values. The slope of the dashed line is $\gamma = 3$. (b) $P(k)$ for $m_0 = m = 5$ and system sizes $N = 10^5$ (circle), $N = 1,5 \times 10^5$ (squares), and $N = 2 \times 10^5$ (diamonds). Inset: time-evolution for the degree of two nodes added at time $t_1 = 5$ and $t_2 = 95$. Notice the same power law growth with exponent $1/2$. From *Barabási et al.* 1999 [72].

Regarding the average path length, and in contrast to random or small-world networks (where $l \sim \ln N$), it has been shown by analytical arguments [77] that random scale-free networks* with an exponent $2 < \gamma < 3$ have a much smaller path length, scaling as $l \sim \ln \ln N$ (ultrasmall networks). For $\gamma = 3$, it turns to scale as $l \sim \ln N / \ln \ln N$ [†], while for $\gamma > 3$ the behavior observed in random networks is recovered, $l \sim \ln N$ [77]. Moreover, in random scale free networks the node degrees are uncorrelated while in BA-networks correlations develop spontaneously between the degrees of connected nodes [79].

*These networks are constructed with random-graph models with arbitrary degree distribution (configuration model [69]).

[†]Although this result, obtained in [78], is for the largest distance between two nodes, their derivation makes it clear that the average path length also behaves similarly. This holds also for BA-networks with $m \geq 2$; while $l \sim \ln N$ is obtained when $m = 1$ [77].

1.2. COMPLEX NETWORKS

Regarding the clustering coefficient, it has been shown analytically to scale with the system size as $C \sim (\ln N)^2/N$ [80]. This is a slower decay compared to the random network case, $C_{rand} \sim \langle k \rangle / N$, but far from the behavior of small-world networks, where the clustering coefficient is high and independent of N .

1.2.4 Networks with mesoscale structure

We present in this Section a brief introduction to another class of complex networks that include another very important feature of complex topologies, and specially of social networks: its modular or community structure. Complex social networks are generally structured into cohesive groups within which the internal links are dense, and which are sparsely interconnected [42]. These clustered nodes are known as *communities* and are the structural elements in a mesoscale level of description. Historically, the notion of community and the first network formalizations of the concept have been proposed in the social sciences [81, 82]. As we have seen in Section 1.2.2, a community can be defined as a set of nodes in which the sum of all degrees within the set is larger than the sum of all degrees toward the rest of the network. Figure 1.7 illustrates several examples of networks with community structure.

In the first place, communities are important for the properties we can infer from their structure [31]: groups of nodes belonging to the same community probably share common properties and/or play similar roles within the network (see Figure 1.7(b) and 1.7(c)); the distribution of communities allows for a classification of nodes, according to their structural position in the modules; and by identifying them in different levels, a hierarchical structure can be uncovered.

Therefore, when analyzing network topology the detection of communities has become fundamental in network science. It is a very hard computing problem and has triggered the efforts of lots of scientists during the last years. Still, due to its complexity, it is nowadays an active open field of research. Statistical physics became involved in the problem of detection of communities after the seminal paper that appeared in 2002, by Girvan and Newman [76]. They proposed a new algorithm, aiming at the identification of links lying between communities and their successive removal according to its betweenness*, a procedure leading to the isolation of the communities, and thus its detection (see Figure 1.7(c)). This work triggered the interest of many physicists [83–90], which proposed models for community detection using spin models, percolation, random walks, optimization, synchronization, etc. Algorithms which use the modularity quality

*The betweenness of a link is a centrality measure defined as the number of shortest paths between pairs of other nodes passing through the link. It expresses the role of the link in processes where signals are transmitted across the network following the shortest paths.

CHAPTER 1. INTRODUCTION

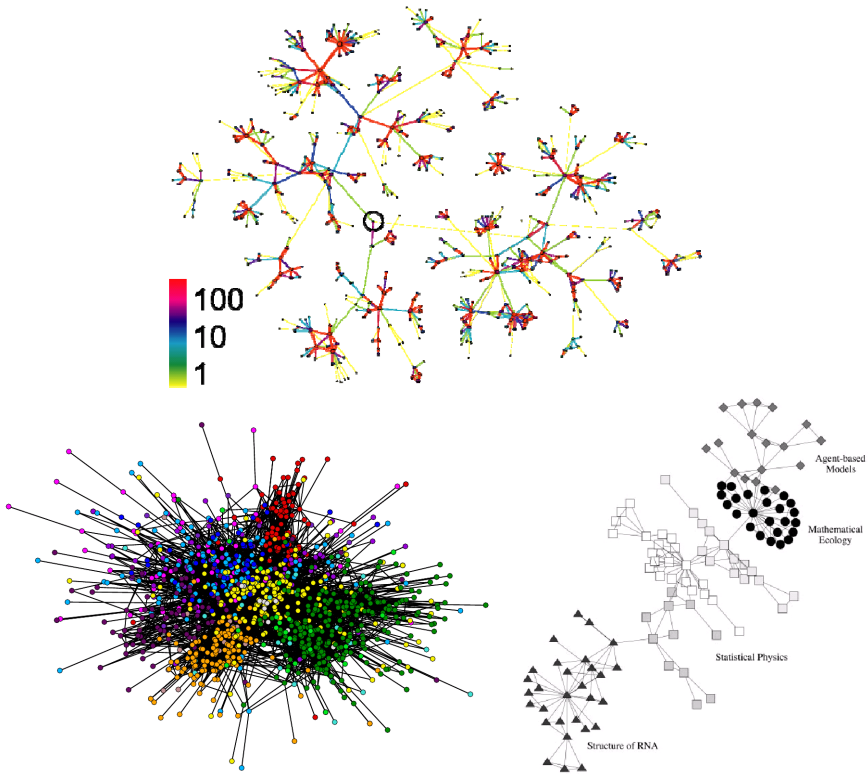


Figure 1.7: Top: Community structure of a mobile call network around a randomly chosen individual. Each link represents mutual calls between two users, and the tie strengths are defined as the aggregate call duration in minutes (see color bar). All the nodes shown are at distance less than six from a selected user, marked by a circle in the center. From *Onnela et al.* [49]. Bottom-left: Community structure of the e-mail network of URV (Universitat Rovira i Virgili). Two individuals (A and B) are connected if A sends an e-mail to B and B replies, or vice versa. Each color corresponds to the affiliation of the individual to a specific center within the university. Only e-mails within the university are shown. From *Guimerà et al.* [75]. Bottom-right: The largest component of the Santa Fe Institute collaboration network in which two nodes are connected if they have written a paper together. The Figure shows the community structure of the network. The algorithm of Girvan and Newman detects the primary divisions of the Institute, indicated by different vertex shapes. From *Girvan and Newman* [76].

1.2. COMPLEX NETWORKS

function proposed by Newman and Girvan [91] are nowadays broadly used. In the present thesis we study the effect of networks with community structure on nonequilibrium dynamics rather than analyzing its topological properties. Therefore, a review of these models is out of the scope of this introduction. Indeed, it is a huge field of research which in another context would deserve a whole chapter. The last review on the topic has been recently provided by Fortunato [31]. Lancichinetti and Fortunato [92] have also provided a comparative study of the different models and their performances in different benchmarks. Previous comparative studies can be found in the work by Danon et al. [93].

In the second place, communities are known to have a deep impact on the dynamics taking place in the network. For example, for oscillators coupled via a complex network, synchronization takes place first within highly interconnected local structures, and synchronized domains expand via intercommunity connections [94–99]. Similarly, information has been shown to spread rapidly within communities, but slowly across the network, particularly if intercommunity links are weak [49]. Communities may also promote the emergence and survival of cooperation [100], while for a two-spin system following the majority rule [101], network topologies with communities can be constructed in which no consensus takes place [102].

For these reasons, in order to foster theoretical studies of collective behavior taking place on social networks, it is important to have social network models that show the essential characteristics of real social networks, including its modular structure*. In this direction, several models have been proposed [62, 65, 66, 103–108]. Among them, we present here the one proposed by Toivonen et al. [109], which we use in the present thesis. This model mimics most of the basic features of real social networks: high clustering, short average path length, broad degree distribution, assortative mixing, and specially the existence of community structure. This is a growing network model, with two basic processes: (i) attachment to random selected nodes; and (ii) attachment to nodes belonging to the neighborhood of the first selected nodes, which gives rise to an implicit preferential attachment. The model is introduced in detail in Chapter 4, where we analyze the effect of networks with community structure on the models of social consensus studied in the present thesis.



*Notice that the network models previously presented recover some of the properties observed in real social networks, such as the small world character or scale free distributions. However, as we have seen, these simple models fail to include different features together, and do not display mesoscalar structure.

CHAPTER 1. INTRODUCTION

In summary, we have defined the basic concepts that characterize complex networks, and we have presented the main network models which recover some of the properties observed in real social networks: small world character, scale free distributions, community structure. As we have mentioned, we use these models throughout the thesis in order to analyze the effects of social structure on consensus dynamics, which are essentially motivated by language competition processes.

1.3

The consensus problem. Mechanisms and models

The consensus problem is a general one of broad interest, recently addressed by statistical physics: the question is to establish when the dynamics of a set of interacting agents that can choose among several options leads to a consensus in one of these options, or alternatively, when a state with several coexisting social options prevails [26]. For an equilibrium system the analogy would be with an order-disorder transition. For nonequilibrium dynamics we rely on ideas of studies of domain growth and coarsening in the kinetics of phase transitions [110], where dynamics is dominated by interface motion. In some cases, consensus problems give rise to coexisting social options during finite large times, after which a whole consensus might be reached. The concept of metastable state in statistical physics appears then naturally, and metastability becomes a central issue in the analysis of the dynamics.

In general, in these problems the drive towards consensus is provided by the tendency of interacting agents to become more alike. This effect is often termed *social influence* in the social science literature [111]. Another social mechanism takes place when agents tend to adopt an option different from the one of their neighbors. The approach from statistical physics has built upon the study of ferromagnetic and antiferromagnetic interactions respectively as a first step for the modeling of such mechanisms, in order to explore the qualitative behavior of the corresponding social dynamics. Moreover, the presence of individual free will, independent decision or individual learning, is often modeled by adding noise to the corresponding consensus dynamics.

In particular, several models have been proposed to account for different mechanisms of social interaction in the dynamics of social consensus. The idea is to capture the essence of different social behaviors by simple interaction rules: following the idea of universality classes [112], in collective emergent phenomena details might not matter. There are several examples of these mechanisms

1.4. PARADIGMATIC TWO-STATE MODELS IN CONSENSUS PROBLEMS

that have given fruitful results in the last years: (i) imitation (voter model [27]), (ii) social pressure (Spin Flip Kinetic Ising models, SFKI [28]), (iii) homophily (Axelrod model for cultural dissemination [11]), (iv) majority convinces (Sznajd model [113]), (v) interactions depending on a threshold (Granovetter model [114]) or complex contagions [115], (vi) bounded confidence (Deffuant model [9]), (vii) semiotic dynamics (Naming Game for the emergence of a shared language [116]), (viii) interaction through small groups (Galam model [117]), (ix) cost-benefit optimization in the framework of game theory [25]. Of course many of these mechanisms might take place at the same time in social interactions. In this direction, several models combine some of the mechanisms defined above. For example, individual learning together with imitation [118], or imitation together with homophily [119]. Castellano et al. [5] have recently reviewed the main contributions to the study of social collective phenomena by statistical physics during the last years, which include the mechanisms and models listed above.

The models for language competition, which motivate the models for social consensus studied in the present thesis, contain imitation and effective social pressure mechanisms. For this reason, in the following Section we analyze in detail the models corresponding to the first two mechanisms listed above: the voter model [27] (imitation) and the SFKI model [28] (social pressure).

1.4

Paradigmatic two-state models in consensus problems

In this Section, we present a brief review of the main dynamical results regarding two paradigmatic nonequilibrium two-state models in statistical physics: the voter model [27], and the zero-temperature spin-flip kinetic Ising ($T = 0$ SFKI) model [28]. As pointed out in Section 1.3, when considering the dynamics of social systems, these two models become an important starting point, as they capture two basic mechanisms of social interaction: *imitation* (voter model) and *social pressure* (SFKI*); see Figure 1.8. In the present thesis, we are interested in consensus problems motivated by language competition which behave as these two models for certain values of their parameter space. Therefore, it is important to have a full picture of the main results concerning these models and the mechanisms they represent, as we constantly refer to them during the

*Notation: for convenience, from now on we refer to the zero-temperature spin-flip kinetic Ising model ($T = 0$ SFKI) simply as *SFKI*.

CHAPTER 1. INTRODUCTION

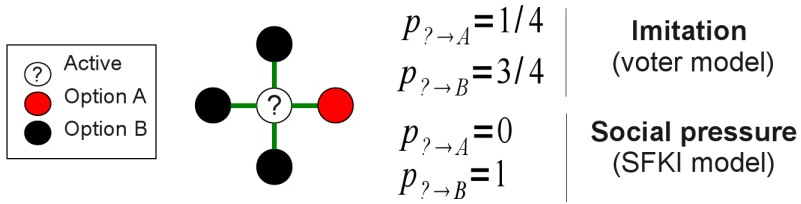


Figure 1.8: Probabilities of transition for an active node to each of the two possible states, A (red) or B (black), illustrating the two basic mechanisms of social interaction: imitation (voter model) and social pressure (SFKI model). Notice that when an agent is surrounded by a majority in one option (B in the Figure), in the voter model there is still a non-zero probability to change to the minority option (in the Figure, by imitation of the node in the minority option, A), while in the SFKI the future state of the agent is fully determined by the state of the majority.

presentation of our work, and we build up key arguments from the knowledge of the behavior of these models in different topologies.

As we have shown in Section 1.2, there has been an increasing interest on complex networks, specially on how they originate and on how to characterize them. But the most important question for the purposes of the present thesis is in which way network structure might affect nonequilibrium dynamics models; some of them already studied in regular lattices in the past. In this context, the voter model and the SFKI model have been extensively studied in complex networks during the last years, with new results appearing during the course of the present thesis.

In this Section, we first introduce the concepts of coarsening processes, and absorbing, metastable and trapped states. Then, we define each of the models and present the main findings in regular lattices, together with a brief review of the results obtained in the paradigmatic complex networks: complete graphs, Erdős-Rényi random networks [30], Watts-Strogatz small world networks [7] and Barabási-Albert scale free networks [8].

1.4. PARADIGMATIC TWO-STATE MODELS

1.4.1 Coarsening processes. Absorbing, metastable and trapped states

The voter model and the SFKI model have two equivalent absorbing states corresponding to complete consensus in one or the other option*. Absorbing states are characteristic of nonequilibrium dynamics and are defined as configurations from which the system cannot escape, i.e., the dynamics completely stops. An initially disordered system can eventually reach one of these absorbing states. In order to characterize the way this might happen, it is fundamental to study the formation and growth of coherent domains in each of the possible states of the system. These growth processes, characteristic in collective emergent phenomena, are known in statistical physics as *coarsening*. A relevant quantity in coarsening processes is the average domain size, $\xi(t)$, whose time evolution gives a characteristic growth law.

In a consensus problem, the existence of coarsening gives information about the path to consensus of the system: how fast domains in each of the two competing options are formed and grow in time. If the coarsening is not interrupted, the system eventually reaches one of the two equivalent absorbing states. In contrast, when coarsening stops, we can infer that the system does not evolve further towards ordering. In this case, a metastable state is reached, which we define as a long-lived state in which the two options are present†. In our context, metastable states are generally *dynamical* or *active*: although coarsening has stopped, agents continue flipping and the system visits a set of configurations which are macroscopically equivalent in terms of ordering. In the thermodynamic limit, the system may get stuck forever in such states. However, in finite size systems, they have a finite survival time and they finally leave such configuration due to finite size fluctuations which eventually lead them to an absorbing state. An interesting type of metastability occurs in situations in which different realizations of the dynamics are of different type‡: while some of them follow a coarsening process until finite size effects drive them to an absorbing state, others get stuck in topological traps. The existence of different topological structures in the network acting as traps (for instance, communities, hierarchical levels) leads to different metastable states with different degrees of ordering in the system. We call this special type of metastable states *trapped metastable states*. When in a finite system the dynamics gets stuck for an infinite lifetime in such configura-

*Notice that in the literature, *consensus* is considered as equivalent to reach an absorbing state with complete order, i.e., a configuration in which only one state is present in the system.

†In this way, reaching a metastable state can be interpreted as equivalent to a scenario of coexistence during a finite long time.

‡Notice that, in general, metastable states are characterized by the fact that all realizations of the dynamics are of the same class (qualitatively similar). See the voter model in Section 1.4.2.

CHAPTER 1. INTRODUCTION

tions, we call these states simply *trapped states*. These can be *frozen*, if there is no change in the system (that is, if they are absorbing); or *active*.

The voter model and the SFKI model are of special interest in this thesis, as they define two well known coarsening processes to which we refer throughout the thesis. SFKI dynamics leads to the formation of ordered domains and their coarsening as a consequence of the existence of surface tension and the drive provided by energy minimization [110]: *curvature driven* interface dynamics. In the voter dynamics, instead, no surface tension exists and the tendency towards order is the effect of the annihilation of freely diffusing interfaces between domains [120]: *interfacial noise* dynamics. Comparative studies of the consequences of these two mechanisms in different interaction networks have been reported in [121]. In consensus problems, and in particular in the models studied in this thesis, the appearance of scenarios of coexistence (which, when they take place for finite time, correspond to metastable states) is of special interest. In this way, in this Section we pay a special attention to how the different type of coarsening determines the nature of the metastable and trapped states appearing for each of the models in different topologies.

1.4.2 The voter model

The voter model is a prototype spin-model of nonequilibrium dynamics with two equivalent absorbing states (Z_2 -symmetry). The voter dynamics was first introduced by Clifford and Sudbury [122] as a model for the competition between species, and named voter model by Holley and Liggett [27]. It has become one of the most studied interacting particle systems motivated for studies in fields such as heterogeneous catalysis [123], species competition [124, 125] or opinion formation [5, 26].

The dynamics of the model is defined as follows*: given N nodes in a network, each of the sites holds one of two possible states: $s_i = +1$ or $s_i = -1$. At each time step, a site in the network is randomly chosen, and adopts the state of a randomly chosen neighbor (asynchronous update). In this way, from the point of view of interaction mechanisms, the voter model is one of random imitation of a state of a neighbor. Therefore, the probability that a node in state s_i flips can be written as:

*An applet for the voter model in regular lattices and complex networks (ER, SW and BA networks) can be found at the IFISC website [126], where it is possible to visualize simulations in real time. In this way, an intuitive understanding of the dynamics is easily achieved.

1.4. PARADIGMATIC TWO-STATE MODELS

$$P(s_i \rightarrow -s_i) = \frac{1}{2} \left(1 - \frac{s_i}{k_i} \sum_{j \in v_i} s_j \right) \quad (1.1)$$

where k_i is the degree of node i , i.e., the number of its nearest neighbors, and v_i is the neighborhood of node i , i.e., the set of nearest neighboring nodes of node i .

Conservation laws play an important role in the characterization and classification of different nonequilibrium processes of ordering dynamics. A special type of conservation law is the one referring to an ensemble average. In the voter model, we find such a law: the conservation of the average global magnetization, $\langle m \rangle^*$ [127–129], where $m \equiv \frac{1}{N} \sum_{i=1}^N s_i$. Notice that the existence of an ensemble conservation law does not imply an elementary step conservation such as the one imposed in the Ising model with Kawasaki dynamics [110]. The conservation of $\langle m \rangle$ implies that the probability to reach each of the two absorbing states is exactly given by the initial density of nodes in each state (or what is the same, by the initial magnetization, m_0).

However, in networks with an arbitrary distribution of the degree of the nodes, and for the usual node-update dynamics defined above, the average magnetization is not conserved, while an average magnetization weighted by the degree of the node, $\langle m' \rangle$, is conserved [129]. This magnetization is defined as:

$$m' \equiv \frac{\sum_{i=1}^N k_i s_i}{\sum_{i=1}^N k_i} \quad (1.2)$$

Another possible update rule is *link-update* dynamics, defined as randomly choosing a pair of nearest-neighbors, i.e., a link, and randomly assigning to both the same opinion when they are in an opposite state (+1 or –1 with equal probability), and leaving them unchanged otherwise. In this case, the average magnetization is still conserved[†] [129].

For these reasons, the magnetization is not a useful order parameter to study the ordering dynamics of the voter model. Instead, it is commonly used in the physics literature as an order parameter the density of interfaces:

*The $\langle \dots \rangle$ indicates average over different realizations of the dynamics with different random initial conditions conserving the same initial magnetization, m_0 .

[†]Notice that choosing a link (instead of a node) update process, already gives implicitly weights to the degree of the nodes.

CHAPTER 1. INTRODUCTION

$$\rho \equiv \frac{1}{\sum_{i=1}^N k_i} \left(\sum_{\langle ij \rangle} \frac{1 - s_i s_j}{2} \right) \quad (1.3)$$

where $\langle ij \rangle$ reads for summing over neighboring nodes. That is, ρ is the fraction of links connecting neighbors with opposite state. Notice that when the system reaches one of the two absorbing states, $\rho = 0$; as all nodes are in the same state. The average interface density, $\langle \rho \rangle$ is the order parameter we use throughout the thesis when analyzing the ordering dynamics of the models studied in finite systems.

Regular lattices

The voter model was first studied in lattices, where $d = 2$ is a critical dimension [120]. Full order is reached in the thermodynamic limit ($N \rightarrow \infty$) for dimension $d \leq 2$: in one dimension, an ordered state is reached with ρ^* decaying as $\rho \sim t^{-1/2}$; while in two dimensions the coarsening process takes place with $\rho \sim (\ln t)^{-1}$. The average domain size, ξ , relates to the interface density in the following way: $\xi(t) \sim 1/\rho(t)^\dagger$. Therefore, from the dependence of $\rho(t)$ with time, it follows that the coarsening growth laws for the average domain size in regular lattices are: $\xi(t) \sim t^{1/2}$ in $d = 1$, and $\xi(t) \sim (\ln t)$ in $d = 2$.

In finite systems, the coarsening is the same as in the thermodynamic limit, but in the last stage of the dynamics the system does order by finite size fluctuations. The time to reach the absorbing state scales as $\tau \sim N^2$ ($d = 1$) [130] and $\tau \sim N \ln(N)$ ($d = 2$) [123]. In Figure 1.9 we can observe the characteristic interfacial dynamics of the voter model in a two-dimensional lattice, in which the coarsening ordering dynamics takes place by *interfacial noise*, i.e., by an annihilation of freely diffusing interfaces between domains [120]. For $d > 2$ instead, the density of interfaces behaves as $\rho \sim a - bt^{-d/2}$ [131] (with $a, b \in \mathfrak{R}$ and d the dimension of the lattice),

*The same coarsening laws for $\rho(t)$ in the thermodynamic limit (no fluctuations) are valid for the average interface density $\langle \rho(t) \rangle$ in finite systems, where the time evolution for ρ in a single realization deviates from the $N \rightarrow \infty$ case due to the existence of fluctuations.

[†]*Argument:* given a d -dimensional lattice of $N = L^d$ sites (L is the one-dimensional length of the lattice) in which a coarsening process takes place, growing domains form and grow in size with a characteristic one-dimensional length ξ (thus domains are of size ξ^d). In such a lattice, interfaces define hypersurfaces of dimension $d - 1$ which are the outlines of the growing domains (walls in $d = 1$, perimeters in $d = 2$, closed surfaces in $d = 3$, etc.). Therefore, assuming there exist n growing domains, we can infer that ρ can be written as $\rho \sim n\xi^{d-1}/L^d$; where $n\xi^{d-1}$ is the number of interfaces, and the total number of links scales with the system size, L^d . As the number of domains is $n \simeq L^d/\xi^d$, from the previous expression it is straightforward to obtain that $\xi \sim 1/\rho$.

1.4. PARADIGMATIC TWO-STATE MODELS

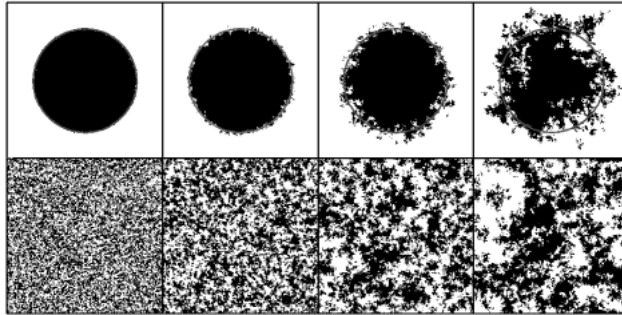


Figure 1.9: Illustration of the domain growth in the $d = 2$ voter model ($N = 256^2$). Top: Snapshots at times $t = 4, 16, 64, 256$ during the evolution of a bubble of initial radius $r_0 = 180$ (thin circle). Bottom: same from symmetric random initial conditions. From *Dornic et al. 2001* [120].

reaching a long-lived metastable state with continuously flipping nodes: order is never reached in the thermodynamic limit. Notice that in finite systems, the system gets trapped in a metastable state which does order due to finite size fluctuations (Figure 1.10), with a time to reach an absorbing state that scales with the system size as $\tau \sim N$. The degree of order in metastable states can also be quantified by the two-spin correlation function between spins i and j , $C_{ij} \equiv \langle S_i S_j \rangle$: for $d > 2$, C_{ij} decays with the spatial separation between spins $r = |i - j|$, as $C(r) \sim r^{2-d}$ [132]: therefore, distant spins become uncorrelated.

Qualitatively, the same general phenomenon occurs in complex networks of interaction of effective large dimensionality where a finite system gets trapped in long-lived metastable states.

Fully connected networks

Here we present the results for the voter model in a fully connected network (or complete graph). In the thermodynamic limit, the time evolution for the magnetization is trivially found to be:

CHAPTER 1. INTRODUCTION

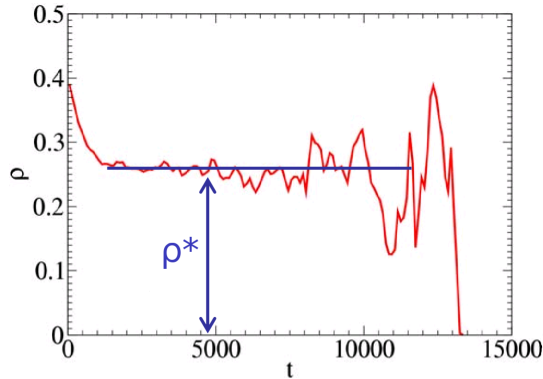


Figure 1.10: Typical metastable state in the voter model in a finite size system that reaches the absorbing state due to a finite size fluctuation. The size of the domain, ξ , can be inferred from the plateau height, as it scales as $\xi \sim 1/\rho^*$.

$$\frac{dm}{dt} = 0 \quad (1.4)$$

indicating that any initial condition for the magnetization, m_0 , is a marginal stable solution of the dynamics*. As mentioned, the magnetization is not an appropriate order parameter to study the time evolution of the system. The time evolution for ρ instead, obtained from a link mean field analysis of the interfaces, reads [133]:

$$\frac{d\rho}{dt} = 2\rho \left(1 - \frac{\rho}{2\sigma_+(1-\sigma_+)} \right) \quad (1.5)$$

where σ_+ is the initial density of nodes in state +1. The system reaches asymptotically a disordered state which depends on the initial condition, with ρ getting

*The same conservation law for $m(t)$ in the thermodynamic limit (no fluctuations) is valid for $\langle m(t) \rangle$ in finite systems, where the time evolution of the magnetization in a single realization deviates from the $N \rightarrow \infty$ case due to the existence of fluctuations.

1.4. PARADIGMATIC TWO-STATE MODELS

stuck at a plateau $\rho^* = 2\sigma_+(1 - \sigma_+)$. In a finite system instead, a single realization $\rho(t)$ fluctuates grossly until a finite size fluctuation drives it to a complete order. However, the time evolution of the average interface density is:

$$\langle \rho(t) \rangle = 2\sigma_+(1 - \sigma_+)e^{-2t/\tau(N)} \quad (1.6)$$

giving an exponential decay depending on system size. This is related to the fact that the survival time, i.e., the probability that a simulation reaches consensus at time t , decays as $S(t) \sim e^{-t/\tau(N)}$ [133]. The time to reach an absorbing state, τ , is found to scale with the system size as $\tau(N) \sim N$ [131]. Notice that the plateau ρ^* is recovered in the thermodynamic limit, as τ diverges with system size.

Random uncorrelated networks

Vázquez and Eguíluz [133] studied the dynamics of the voter model in random networks without degree correlations in great detail, deriving a complete analytical description. The time evolution of ρ is found to be,

$$\frac{d\rho}{dt} = \frac{2\rho}{\mu} \left[(\mu - 1) \left(1 - \frac{\rho}{2\sigma_+(1 - \sigma_+)} \right) - 1 \right] \quad (1.7)$$

where $\mu \equiv \frac{1}{N} \sum_{k=1}^N P_k k$ is the average degree (P_k being the probability to find a node with degree k). It is straightforward to derive from this equation the exact value of the plateau that depends only on μ , but it is independent of the particular topology (i.e., independent of the specific degree distribution; see Figure 1.11): $\rho^* = 2\zeta(\mu)\sigma_+(1 - \sigma_+)$, with

$$\zeta(\mu) = \frac{\mu - 2}{\mu - 1} \quad (1.8)$$

Notice that the plateau becomes smaller for decreasing average degree, and the complete graph case is recovered in the limit $\mu \rightarrow \infty$. Moreover, in finite systems the time evolution of the interface density is found to be [133]:

$$\langle \rho(t) \rangle = \frac{(\mu - 2)}{(\mu - 1)} 2\sigma_+(1 - \sigma_+)e^{-2t/\tau(N)} \quad (1.9)$$

CHAPTER 1. INTRODUCTION

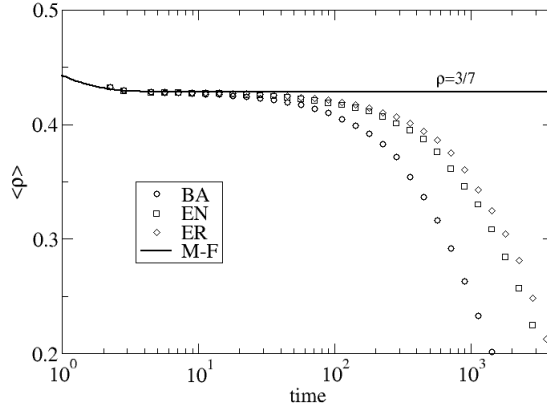


Figure 1.11: Average interface density $\langle \rho(t) \rangle$ in different topologies with $N = 10^4$ and $\mu = 8$. From left to right: BA, EN (exponential network) and ER networks. The plateau is independent of the degree distribution and equal to the mean field prediction, $\rho^* = 3/7$ (solid line). Numerical simulations depart from the plateau due to finite size effects. From Vázquez *et al.* 2009 [134]

The time for a metastable state to reach an absorbing state, τ , is also derived exactly, with a prefactor depending on the first μ , and second $\mu_2 \equiv \frac{1}{N} \sum_{k=1}^N P_k k^2$, moments of the degree distribution:

$$\tau = \frac{(\mu - 1)\mu^2 N}{(\mu - 2)\mu_2} \quad (1.10)$$

In summary, a random uncorrelated network topology does not change the qualitative picture compared to the complete graph case: ordering is not reached in the thermodynamic limit, and in finite systems, τ still depends linearly on the system size. However, the average degree affects quantitatively the height of the plateau and the prefactors for the time to reach consensus (these depend

1.4. PARADIGMATIC TWO-STATE MODELS

also on the second moment, μ_2). These results were applied successfully to degree-regular, Erdős-Rényi and Exponential networks [133].

Other complex networks

The voter model in Barabási-Albert scale free networks [8] presents essentially the same behavior described above for random networks (see Figure 1.11), but with a time to reach consensus that deviates from the linear scaling: $\tau \sim N/\log(N)$ [133, 135]. Numerically, the scaling found is $\tau \sim N^\gamma$, with $\gamma \sim 0.88 \pm 0.01$ [129] (also found in [121])^{*}.

The model has also been studied in Watts-Strogatz small world networks [7], built up by rewiring with probability p each of the links of a one-dimensional regular lattice with k neighbors. It has been shown that, contrary to what happens in a one-dimensional lattice, the presence of long-range connections inhibit the ordering process taking place in the network in the thermodynamic limit, and a metastable state with coexisting options is also found [136]. There exist two different time scales. When the average size of a growing domain, which has a size $\xi \sim 1/\rho$, is much smaller than the characteristic length between two shortcuts, $l^* = 1/(kp)$ [137], the coarsening process is practically $\rho \sim t^{-1/2}$; the system behaving still as in a one-dimensional lattice. When $\xi \sim l^*$, the long range interactions start to play a role, and the coarsening stops: ρ reaches a plateau [136] and in the thermodynamic limit the absorbing state is never reached. This is different in finite size systems: once more, finite size effects eventually drive the system to an absorbing state, and the time to reach it scales also as $\tau \sim N$ (see the time evolution for $\langle \rho(t) \rangle$ in Figure 1.12 for a SW network with $p = 0.05$).

Suchecki et al. [138] studied in great detail the effect of different characteristics of heterogeneous networks on the plateau heights of the metastable states and the survival times. They included in their discussion random networks, together with the small world and the scale free phenomena. They found that when there is no ordering in the dynamics, the average survival time of metastable states in finite networks decreases with network disorder (measured by the parameter of rewiring[†]), and degree heterogeneity (single scale VS scale free network), as fluctuations appear to be more efficient with the existence of hubs. Moreover, the

^{*}However, τ scales linearly with system size when the updating rule respects the conservation law of the average magnetization, that is, when link-update is considered [129]. Therefore, this scaling identifies a universal or generic property of the voter model dynamics associated with the conservation law of the magnetization.

[†]Network disorder refers to high rewiring in the network, which is measured by a parameter p analogous to the one defined in the Watts-Strogatz model for small world networks [7], in which rewiring starts from a ring lattice.

CHAPTER 1. INTRODUCTION

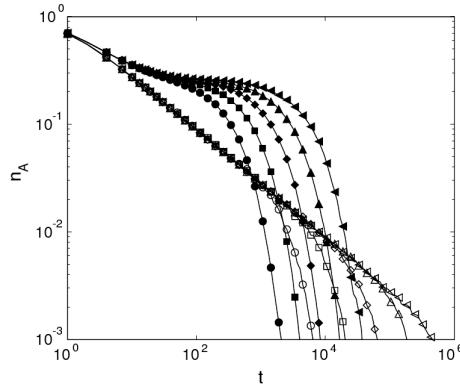


Figure 1.12: Time evolution for the average interface density (labeled n_A in the Figure). Values are averaged over 1000 runs. Time is measured in Monte Carlo steps per site. Empty symbols are for the one-dimensional case ($p = 0$). Filled symbols are for rewiring probability $p = 0.05$. From left to right: $N = 200$ (circles), $N = 400$ (squares), $N = 800$ (diamonds), $N = 1600$ (triangles up) and $N = 3200$ (triangles left). From *Castellano et al. 2003* [136].

size of an ordered domain is found to be sensitive to the network disorder and the average degree, decreasing with both; however, it is not found to depend on network size or on the heterogeneity of the degree distribution.

The results presented come to support the claim that whether the voter dynamics orders the system depends on the effective dimensionality of the interaction network [138]: in any complex network, which in general has an effective infinite dimension* (obviously larger than the critical dimension of the model, $d = 2$), the dynamics gets trapped in metastable states, which in finite systems finally reach the absorbing state by finite size fluctuations.

In this thesis we concentrate in the study of static networks, that is, networks which are fixed in time, and we analyze the effect of the topology on the dynamics. In particular, the study of the voter model in networks with community

*Suchecki et al. [138] have shown that a scale-free topology with an effective dimension equal to one [139] does indeed coarsen as a one-dimensional regular lattice.

1.4. PARADIGMATIC TWO-STATE MODELS

structure is part of the present thesis and is analyzed in Chapter 4, where we address the question of metastability in detail. We note however that the voter model has also been studied in coevolving networks by Vázquez et al. [140], predicting a fragmentation transition as a consequence of the competition between the voter and the rewiring dynamics. The networks we study are undirected, but the voter model has also been recently addressed in random directed networks [141], studying analytically the conservation laws for the model when performing both node and link updates.

1.4.3 The zero-temperature spin-flip kinetic Ising (SFKI) model

The zero-temperature spin-flip kinetic Ising model (SFKI; also known as *Glauber dynamics* [28] at zero temperature) is another prototype spin-model with two equivalent absorbing states (Z_2 -symmetry). The Glauber dynamics at finite temperature reaches asymptotically the state dictated by thermodynamic equilibrium (there are no absorbing states), which is well known also for some complex networks (random networks with arbitrary degree distribution [142], small world networks [143, 144]). Because the general interest in the present thesis does not reside in the phase transition occurring at finite temperature but on the coarsening processes taking place below the critical temperature, we present in this Section the $T = 0$ case, which, due to the lack of fluctuations, presents two equivalent absorbing states, just like the voter model. Moreover, the zero temperature SFKI does not necessarily relax to the state of minimum energy (its natural equilibrium; the absorbing state) but can get stuck in many different trapped states (which can be frozen or active) and gives an additional richness for the study of metastability.

The dynamics of the SFKI model is defined as follows*: given N nodes in a network, each of the sites holds one of two possible states: $s_i = 1$ or $s_i = -1$. At each time step, a site in the network is randomly chosen, and minimizes its energy according to the Ising Hamiltonian:

$$H = - \sum_{\langle ij \rangle} J_{ij} s_i s_j, \quad (1.11)$$

*An applet for for the SFKI in a two dimensional lattice can be found at the IFISC website [145], where it is possible to visualize simulations in real time and get easily an intuitive understanding of the dynamics.

CHAPTER 1. INTRODUCTION

where the sum is performed over all possible pairs of nodes. $J_{ij} = 1$ if node i and j are connected and $J_{ij} = 0$ otherwise. At each time step, a randomly chosen node i , which is in the state s_i , is flipped with the following transition probabilities:

$$P(s_i \rightarrow -s_i) = 1 \iff \sigma_{-s_i} > 1/2 \quad (1.12)$$

$$P(s_i \rightarrow -s_i) = 0 \iff \sigma_{-s_i} < 1/2 \quad (1.13)$$

$$P(s_i \rightarrow -s_i) = 1/2 \iff \sigma_{-s_i} = 1/2 \quad (1.14)$$

where, σ_{-s_i} is the density of nodes in the neighborhood of node i which are in state $-s_i$. In this way, from the point of view of interaction mechanisms, the SFKI model is one of majority pressure*. It is straightforward from these transition probabilities that the SFKI is equivalent to the voter model in one-dimensional lattices with two neighbors: in this special case, the mechanisms of imitation and social pressure become indistinguishable.

Regular lattices

In regular lattices, the SFKI model presents a coarsening process[†] independent of the dimensionality [110]: $\rho \sim t^{-1/2}$. Therefore, $\xi(t) \sim t^{1/2}$, where $\xi(t)$ is the characteristic length of a growing domain. The domain structure is universal in the sense that it is independent of the random initial conditions, as long as $\xi(t)$ is large compared to any length scale characterizing the initial conditions. As we mentioned, in one-dimensional lattices the coarsening law is exactly equivalent to the voter model. In dimensions $d > 2$, the energy minimization drives the ordering process, leading to a coarsening process by curvature reduction as a consequence of the existence of surface tension (see Figure 1.13).

The relaxation of homogeneous Ising ferromagnets on finite regular lattices with SFKI dynamics has been carefully studied by Spirin et al. [148], where the existence of metastable and trapped states gives a very rich behavior that is analyzed in detail. Contrary to the voter model, in the SFKI there exist trapped states: in the thermodynamic limit and in finite systems these behave in the same way, in the sense that finite size fluctuations do not order the system when it gets stuck in such state.

*A different majority rule based in group interaction is considered in [101, 146].

[†]The same coarsening laws for $\rho(t)$ in the thermodynamic limit (no fluctuations) are valid for the average interface density $\langle \rho(t) \rangle$ in finite systems, where the time evolution for ρ in a single realization deviates from the $N \rightarrow \infty$ case due to the existence of fluctuations.

1.4. PARADIGMATIC TWO-STATE MODELS

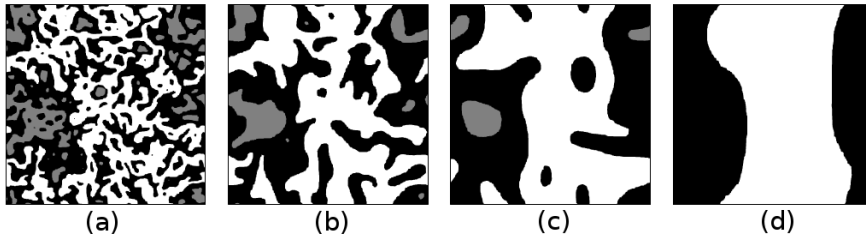


Figure 1.13: Coarsening in the SFKI model on a $N = 1024^2$ square lattice with periodic boundary conditions at times (a) 200, (b) 1000, (c) 5000, and (d) $2.5 \cdot 10^4$. Domains are regions of either state +1 (gray/white) or -1 (black). (i) Curvature driven dynamics can be specially observed in the +1 domains which fade away (highlighted in gray). (ii) A spanning +1 domain that eventually coarsens into a vertical stripe, is highlighted in white. From *Barros et al. 2009 [147]*.

In $d = 1$ a fully ordered state is always reached, while in higher dimensions the system may get stuck in a frozen state with coexisting domains of opposite magnetization. In $d = 2$ this occurs with a probability around $1/3$ for large systems: applying results from percolation theory [67], Barros et al. have analytically shown that this happens with probability 0.3390 for periodic boundary conditions [147]. The trapped states in $d = 2$ consist of vertical or horizontal stripes whose widths are all larger or equal to 2, which eventually become frozen straight stripes (see Figure 1.13). These arise because in zero-temperature Glauber dynamics a straight boundary between domains is stable; a change of state of any node along the boundary would raise the energy of the system. However, a stripe of width 1 is unstable because it can be cut in two at no energy cost by flipping one of the nodes in the stripe*.

In $d > 2$ the probability of reaching the ground state vanishes rapidly as the system size grows and the system ends up wandering forever within an isoenergy

*Long-lived diagonal stripes are also possible, but in finite systems they finally reach the absorbing state. For simulations leading to consensus, they give rise to two time scales; one for the simulations that reach directly the ground state, and another characterizing the lifetime of such diagonal-stripe trapped metastable states [148].

CHAPTER 1. INTRODUCTION

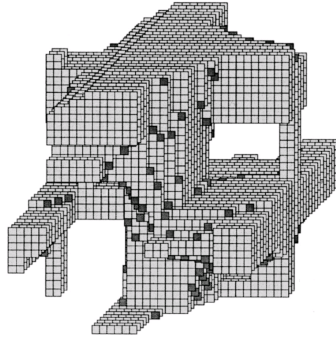


Figure 1.14: Typical trapped state on a $N = 32^3$ cubic regular lattice with periodic boundary conditions. Nodes in one of the states are indicated by small blocks. The dark shaded nodes can flip freely and are part of blinker states. From *Spirin et al. 2001 [149]*.

set of metastable states*. Another striking feature is that many metastable states in three dimensions form connected isoenergy sets, while metastable states are all isolated in two dimensions. Thus a three-dimensional system can end up wandering forever on one of these connected sets, with blinkers active at the boundaries (see Figure 1.14).

As a general feature, notice that at $T = 0$ metastable states become trapped states, which have an infinite lifetime, that can prevent the equilibrium ground state from being reached. This is the basic reason why dynamics at $T = 0$ is different from that of small positive temperature.

Fully connected networks

In a complete graph and in the thermodynamic limit, the time evolution of ρ can be obtained analytically from the analysis of the corresponding master equation [121][†]:

*In cubic lattices of linear dimension $L = 10$ and $L = 20$, the probability to reach an absorbing state has been found to be only 0.04 and 0.003 respectively. For larger lattices, the ground state has not been reached in any of the simulations [148].

[†]In all the results concerning this paper [121], when $\sigma_{-s_i} = 1/2$, $P(s_i \rightarrow -s_i) = 1$ (while generally this probability is set to $1/2$). This is to facilitate the analytical derivation of a master equation for the

1.4. PARADIGMATIC TWO-STATE MODELS

$$\rho(t) = 2[1 - (1 - \sigma_+)e^{-t}](1 - \sigma_+)e^{-t} \quad (1.15)$$

In simulations in finite size systems, the interface density for surviving runs is found to decay exponentially and then reaches a plateau, but the height of the plateau depends on N and goes to zero as $N \rightarrow \infty$. Therefore, the SFKI model is effective in reaching an ordered state on a complete graph.

Complex networks

The effect of different complex networks has also been analyzed by Castellano et al. [121]. In finite ER networks [30], numerical simulations have shown that while for large $\langle k \rangle$ the decay of the survival time $S(t)$ (the probability that a simulation reaches consensus at time t) is exponential, for smaller values of $\langle k \rangle$ a plateau appears, indicating that not all realizations of the dynamics end up in an ordered state. In such runs, the system remains trapped forever in configurations with part of the nodes with $s_i = 1$ and the rest with $s_i = -1$ (Figure 1.15)*. The magnetization in these trapped states is always very close to zero and the number of domains present is always equal to two. Moreover, for large times, the interface density in surviving runs indicates that a very high fraction of the links connects sites with different states. Therefore, the system remains stuck in configurations with two highly intertwined domains of roughly the same size. Such configurations are not frozen, but active trapped states with some nodes flipping, while keeping the energy constant. The qualitative picture is then the same holding on regular lattices for $d \geq 3$: the system wanders forever in an isoenergy set of states.

The SFKI model in BA scale free networks [8] has also been studied [121, 152]. The global behavior is qualitatively the same that for ER networks: a fraction of the simulations gets trapped in disordered active stationary states with two domains in opposite states where nodes keep flipping but the energy does not decrease further †.

model in a complete graph. Different zero temperature Glauber dynamics can be defined depending on the rate at which moves leaving energy unchanged are accepted. Provided this rate is nonzero, the behavior of the model is expected to be qualitatively the same, its precise value affecting only a

CHAPTER 1. INTRODUCTION

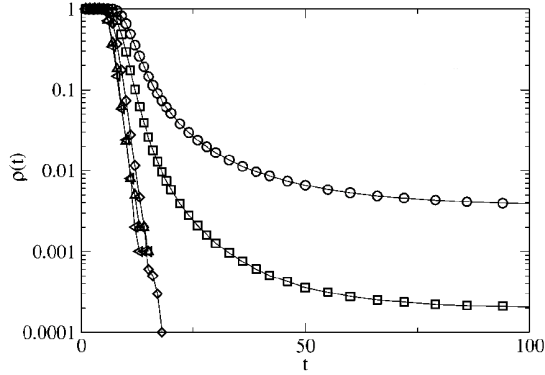


Figure 1.15: Survival probability (labeled as ρ in the Figure) for SFKI dynamics on an Erdős-Rényi random network with $N = 1000$ for different values of the average degree $\langle k \rangle$ of nodes. From right to left: $\langle k \rangle = 7, 10, 20, 200, 1000$. From *Castellano et al. 2005* [121].

The SFKI dynamics has been studied by Boyer and Miramontes [154] on SW networks, obtained from one and two-dimensional regular lattices by adding* links between randomly selected nodes with a probability p . It is found that ordering is hindered by the presence of long range interactions leading to a pinned state with a finite size of ordered domains.

On the one hand, in SW networks built up from an initial one-dimensional lattice, there exists the characteristic coarsening stage $\xi(t) \sim t^{1/2}$, but domain size saturates to a finite value. As in the voter model, this domain length scales with p , for the range of values corresponding to a SW network, as $\xi(t \rightarrow \infty) \sim 1/p$.

rescaling of the temporal scales. When such rate is zero the dynamics is said to be constrained and the behavior may be very different [150].

*A frozen trapped state for Glauber dynamics on a random graph has been found analytically in [151], where it is shown that, in the limit $N \rightarrow \infty$, the dynamics fails to reach the ordered state for any $\langle k \rangle > 0$.

†It is interesting to notice that mean field approaches to the study of these networks with arbitrary power law degree distribution, $P(k) \sim k^{-\gamma}$, which predicted a transition at $\gamma = 5/2$ between ordering and metastability [153], failed to reproduce the corresponding numerical results, as shown in [152]. In their paper, there is a call for analytical approaches, beyond the mean-field one, able to capture the observed phenomenology in BA networks.

*In contrast to the common rewiring process defined in Watts & Strogatz algorithm [7].

1.4. PARADIGMATIC TWO-STATE MODELS

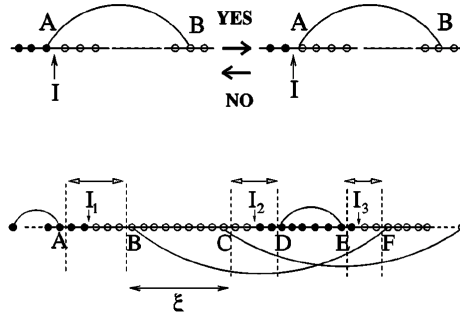


Figure 1.16: Active trapped states in a one-dimensional SW network: the interfaces I_n become localized, performing a random walk within the intervals marked in the Figure, delimited by nodes in the same state connected by a shortcut. From *Boyer and Miramontes 2003* [154].

Moreover, it is observed that nodes having a shortcut tend to be connected to nodes in the same state, blocking in this way the motion of interfaces and thus the possibility of further growth of the domains (Figure 1.16). In this way, $1/p$ represents the characteristic domain size, i.e., the average distance between such kind of nodes. It is straightforward to show that the crossover from the coarsening stage to these active trapped states*, where ordering stops, happens at $\tau \sim (1/p)^2$. On the other hand, in SW networks built up from an initial two-dimensional lattices, active trapped states are also found. Here, the finite domain size can be interpreted as the result of competing effects between surface tension (the mechanism driving the coarsening process) and the energy barriers created by nodes in the same state which are connected by a shortcut. The characteristic domain size is found to scale as $\xi(t \rightarrow \infty) \sim p^{-0.64}$.

A similar work by Herrero [155] considers a SW network built from a two dimensional lattice with a rewiring algorithm instead, which has the advantage of keeping the degree distribution constant. In this work, the same qualitative behavior is observed, with just minor quantitative differences in the scaling of the characteristic domain size with the rewiring parameter: $\xi(t \rightarrow \infty) \sim p^{-0.73}$. The larger exponent is due to the fact that, compared to the case of addition of

*Notice that in contrast to the voter model, where the metastable states have a finite lifetime, in the SFKI they are trapped states, that is, they are infinite long-lived.

CHAPTER 1. INTRODUCTION

new links, the rewiring process decreases the correlations between nodes in the lattice giving place to smaller domain sizes.

In this thesis, we study consensus models with a *curvature driven* interface dynamics. Therefore, the review presented for the SFKI model is of special relevance to us, as it provides a background from which to argue and compare our own results.



In summary, we have presented and compared the coarsening processes, and the metastable and trapped states appearing in the voter model and the SFKI model. In two dimensions, we have illustrated the two different mechanisms of domain growth and their different interface dynamics: *interfacial noise* dynamics (voter model) and *curvature driven* interface dynamics (SFKI); corresponding to mechanisms of random imitation and majority social pressure respectively.

In finite size systems, the different type of coarsening processes generates a different nature for the long-lived states appearing for large dimensional lattices and complex networks: while in the voter model these are metastable states, i.e., long-lived but reaching an absorbing state of full ordering due to finite size fluctuations; in the SFKI model their lifetime is infinite*, as the system cannot escape from the trapped configurations which can be active or frozen depending on the topology.

1.5

Language competition

In this Section, we introduce the research field of language competition, which motivates the present thesis, and we make a brief overview of the current statistical physics approach to the subject. Language competition (or language shift) studies the dynamics of language use and competence due to social interactions. It belongs to the general class of processes that can be modeled by the interaction of heterogeneous agents, as examples of collective phenomena in problems of social consensus.

*Except for the diagonal metastable states in two dimensional lattices, which as mentioned are a special case of trapped metastable states with a finite lifetime.

1.5. LANGUAGE COMPETITION

Language competition occurs today worldwide. Different languages coexist within many societies and the fate of a high number of them in the future is worrying: most of the 6000 languages spoken today are in danger, with around 50% of them facing extinction in the current century [156]. Even more striking is the distribution of speakers, since 4% of the languages are spoken by 96% of the world population, while around 25% have fewer than 1000 speakers. New pidgins and creoles are also emerging, but their number is relatively small compared with the language loss rate [157]. Language shift has caught the attention of numerous linguists interested in language contact and evolution [158–161], and it has also been subject of study of UNESCO [162], who created an Ad Hoc Expert Group on Endangered Languages so as to identify them. In order to characterize a language as endangered, there are several crucial aspects to take into account. Among them, (i) the total fraction of speakers within the population speaking the language, (ii) the point at which children no longer learn the language as their mother tongue (vertical transmission), as well as (iii) the increase of the average age of speakers (in an endangered language, eventually only older generations speak the language) [163]. In this scenario, and beyond Weinreich's *Languages in Contact* [164], numerous sociolinguistic studies have been published in order to: (1) reveal the level of endangerment of specific languages [165]; (2) find a common pattern that might relate language choice to ethnicity, community identity or the like [166]; (3) identify and study the factors that may determine the survival or disappearance of an endangered language as well as the mechanisms that could be implemented so as to revitalize it [167]; and (4) claim the role played by social networks in the dynamics of language competition, which has given rise to the monographic issue [168].

The need to provide a formal analysis in the field of sociolinguistics is getting an increasing attention [169]. Indeed, in recent years, language competition has also been addressed from a statistical physics and complex systems approach, in which the aim is to move beyond the observation of correlations in order to isolate mechanisms of social interaction and to establish cause-effect relations between these mechanisms and their consequences. In this direction, the Abrams and Strogatz model [13] for the dynamics of endangered languages has triggered a coherent effort to understand the mechanisms of language dynamics outside the traditional linguistic research. Their study considers a two-state society, that is, one in which there are speakers of either a language A or a language B, and accounts for data of extinction of endangered languages such as Quechua (in competition with Spanish), Scottish Gaelic and Welsh (both in competition with English). Although linguistics has introduced the notion of language (or dialect) continuum, which blurs the distinction between language and dialect and studies linguistic varieties from a variationist point of view [170, 171], the definition of a language in this model is restricted to the assumption that two languages

CHAPTER 1. INTRODUCTION

are clearly delimited and in this way there is no linguistic continuum. This is because the aim is to study language shift, rather than language variation and change*. The model is based on probabilities to switch languages determined by the fraction of speakers of the opposite language, and by two parameters that we call *prestige* (s) and *volatility* (a)[†]. Indeed, the prestige of a language has been considered as one of the main factors affecting language competition since Labov's Sociolinguistic Patterns [170]. It measures the status associated to a language due to individual and social advantages related to the use of that language, being higher according to its presence in education, religion, administration and the media. Besides, the volatility parameter determines the functional form of the switching probabilities. It characterizes a property of the social dynamics associated to the propensity of an agent to change its current language. It is interesting to notice that these two parameters correspond, in a way, to two of the main factors that have usually been identified as determinant in the vitality of a language by UNESCO [162]. These are (i) the governmental and institutional language attitudes and policies, including official status and use, and (ii) the community members attitudes toward their own language; which would relate to the prestige and the volatility parameter, respectively.

Abrams and Strogatz seminal work, as well as others along the same line [172, 173], belongs to the general class of studies of population dynamics based on nonlinear ordinary differential equations for the populations of speakers of two languages. Several modifications and extensions of the Abrams-Strogatz model have investigated deeper the problem of language competition: (i) introducing geographical dependencies in terms of a reaction-diffusion equation, which allow the survival of the two languages, with speakers of different languages mostly located in different geographical areas [174]; (ii) implementing Lotka-Volterra type modifications to the original model which can lead to a scenario of coexistence of the two languages in the same geographical area [175]. In addition, other models study the competition between many languages in order to reproduce the distribution of language sizes in the world in terms of the number of speakers [176, 177]. For a review of most of these models, see [178, 179].

Our first contribution to extend the seminal work of Abrams-Strogatz consists of developing agent-based models in order to study the behavior of the model in regular networks [180]. Beyond this preliminary study, we become interested in considering the effect of bilingual agents in the model, which have been claimed

*Notice that a given community exhibits a wide range of possible linguistic systems that may differ phonologically, grammatically or lexically and which oscillate between two extreme varieties. These are the ones considered as *language A* and *language B*.

[†]In the original paper [13], Abrams and Strogatz use the concept *status* (parameter s), and they do not give a specific name to the parameter a .

1.5. LANGUAGE COMPETITION

to play a relevant role in the evolution of multilingual societies [173, 181]. Indeed, a specific feature of language competition is that agents can share two of the social options that are chosen by the agents in the consensus dynamics. These are the bilingual agents, that is, agents that use both languages A and B. Inspired in the proposals by Minett and Wang [182, 183], in this work we study an extension of the Abrams and Strogatz model for the dynamics of two languages in competition [13] in which bilingualism is taken into account: the *Bilinguals model*^{*}. We are interested in comparing both models, and in analyzing the effects of considering bilingualism in the dynamics of language use[†]. Following Milroy [184], we expect that also social structure might be an important factor in language competition, and therefore, we are interested in the study of these models in social networks of interaction. The role given by Milroy to social networks for the maintenance and survival of languages was revolutionary in sociolinguistics [185]. At the time, other phenomena such as institutional, socio-political or economical factors occupied the most prominent place in the study of language shift. However, in general only small networks and case studies have been addressed in the traditional linguistics literature [186, 187]. It is in this direction that models coming from statistical physics and complex systems aim to contribute, implementing more systematic and statistically relevant studies of the role of complex social networks, and studying the general mechanisms and collective phenomena emerging in the dynamics of language competition.

Finally, other different problems of language dynamics in which statistical physics can play a relevant role are those regarding language evolution (or how the structure of language evolves) and language cognition (language learning processes). These include evolution of universal grammar [188, 189], utterance selection models [190], and social impact theory applied to language change [191]. Among these, *semiotic dynamics*, considered in the context of language games such as the *Naming Game* [116, 192], is another relevant example of the consensus problem[‡]. In the Naming Game, a shared lexicon among agents emerges from peer interaction. It has been studied in regular lattices [193] and in complex networks [194–196], and the special case of competition between only two words [197] has

^{*}Notice that the model we study (Bilinguals model) was essentially proposed by Minett and Wang in a working paper in 2005, based on their own remarks in [182]. However, during the development of this thesis, they implemented a more complicated model for bilingualism, in which they consider horizontal (social influence) and vertical transmission (inter-generational transmission). Compared to the Bilinguals model, which has two parameters (prestige and volatility) their final published version [183] leads to a model with seven parameters, which, although more detailed, makes it more difficult for the understanding of the mechanisms involved in language competition dynamics.

[†]A full description of the Abrams and Strogatz model and the Bilinguals model is addressed in Chapter 2. Notice that we model language use rather than competence.

[‡]A full description of the Naming Game is addressed in Chapter 5.

CHAPTER 1. INTRODUCTION

similarities with the AB-model [198], a particular case of the Bilinguals model mentioned above. We are also interested in comparing these two models, as they describe two general mechanisms of social interaction with two non-excluding options.

In summary, this work aims to contribute to the understanding of the mechanisms underlying processes of social interaction at work in the dynamics of language competition, as well as their consequences for language survival or extinction and for the viability of language coexistence.

1.6

Ordering dynamics: from two-state models to models with two non-excluding options

The minimal models of consensus dynamics consider that agents can choose only among two possible options. Several models, which correspond to different social interaction mechanisms (see Section 1.3 for details), belong to this class of *two-state models*, like the voter model (imitation) and the SFKI (social pressure) presented in Section 1.4. As presented in the previous Section, in the context of language contact problems, the first model considering two languages in competition is the Abrams-Strogatz model [13], which also belongs to this class of two-state models. The microscopic version [180] of this model for two equivalent languages and marginal volatility (presented in detail in Chapter 2) is equivalent to the voter model [27]. In this way, it recovers a mechanism of imitation of the language of a randomly selected neighbor.

Regarding models with a higher number of options at play, we find kinetics of multi-option models like Potts or clock models which were addressed long ago [199, 200]. Also the voter model [27] can be trivially generalized to a multi-option model. More recently, the multi-state model proposed by Axelrod [11] on cultural dynamics has been studied in some detail [201–203]. This is a multi-option model but, in general, its nonequilibrium dynamics does not minimize a potential leading to a thermodynamic equilibrium state like in traditional statistical physics [204]. In particular, the kinetics of the simplest three-options models [205–207] can be studied in more detail.

We are here interested in the class of three-state models with two opposite states (spin ± 1 , state A or B) and a third intermediate state (spin 0, state AB). Motivated by studies of language competition as mentioned in the previous Section, we consider an extension of the the Abrams and Strogatz model [13]

1.6. TOWARDS MODELS WITH TWO NON-EXCLUDING OPTIONS

inspired in the proposal by Minett and Wang [182, 183], in which bilingual agents are considered: the *Bilinguals model*. In this model, which is presented in detail in Chapter 2, the possible state of the agents is speaking either of these languages (A or B) or a third non-equivalent bilingual state (AB). In the context of consensus problems, this introduces a special ingredient in the sense that the options are not excluding: there is a possible state of the agents (bilinguals or AB agents) in which the two options at play coexist at the individual level. In a more general framework, the problem addressed here is that of competition or emergence of social norms [208] in the case where two norms can coexist at the individual level. In other words: we are concerned with the general problem of ordering dynamics with two non-excluding options*. In this way, language competition problems motivate our research from a hot topic in social sciences (see Section 1.5), but throughout the thesis we address the more general framework of models with two non-excluding options, as we believe our work might be of a broader interest from the perspective of general consensus problems. In our conclusions, we come back to the particular implications of our results for situations of language contact among two languages in competition.

In this thesis, we address the problem of three-state models with two non-excluding options in the following directions:

In the first block of results (Chapters 3 and 4) and as a first step within this general framework, we study in detail the *AB-model*, which corresponds to the Bilinguals model in the case of two socially equivalent options (equal prestige) and neutral volatility. At the same time, this model reduces to the voter model when AB agents are not considered [198][†]. As we presented in Section 1.4.2, the voter model is a prototype spin-model of nonequilibrium dynamics with two equivalent absorbing states, so in this way, understanding the extension of the voter model represented by the AB-model is a question of broad interest in the field of general spin-models of interaction, as shown by several recent publications [210–212][‡]. To this end, we study and compare the AB and the voter models in network topologies of increasing complexity (see Section 1.2), from fully connected networks and regular lattices to small world networks and networks with community structure, studying the effects of the network

*Notice that beyond language use, problems regarding the adoption of new competing technologies [209] or the practice of leisure time activities or hobbies are examples of non-excluding options. Instead, other social features such as religion, political ideas, or opinions are generally excluding.

[†]Notice that the AB-model is different from the three-state voter model, in which all the options are equivalent. In the AB-model (see Section 2.3 for details), there are two opposite equivalent states (A and B) and a third non-equivalent state of coexisting options (AB).

[‡]Other studies associated to perturbations of the voter model dynamics have also been addressed, including memory effects [210], inertia to change the current state of the agents [213], or a two-parameter family of models which includes the voter model [214].

CHAPTER 1. INTRODUCTION

topology on the collective phenomena emerging from the interactions among the agents. We analyze possible mechanisms which lead to a stable coexistence between the two options, metastable states and the role played by the AB-agents (bilinguals) in the dynamics.

Firstly, in regular lattices we are interested in the formation and growth of A or B spatial domains, the interface dynamics of the models and the times to reach consensus. A main result is that allowing for the third state (AB-state, bilinguals) modifies the nature of the interface dynamics: agents in the AB-state define thin interfaces around single-option domains and coarsening processes change from voter-like dynamics to curvature driven dynamics. This result is shown to have further implications in the behavior of the AB-model in complex networks. This change of behavior in the interface dynamics is also shown for a class of perturbations of the voter dynamics in which there is a reinforcement of the influence of the local majority surrounding an agent. A regular lattice structure captures a topology where interactions are local, that is, based on geographical proximity. However, it has been shown in Section 1.2 that social networks are far from being regular, and they are not totally random either [52]. In this direction, we study the voter model and the AB-model in Watts-Strogatz small world networks [7], addressing the effect of long range social interactions among the agents in the dynamics (publication in Ref. [198]).

Secondly, regarding the main characteristics of real complex social networks, we are specially interested in the dynamical effects of their mesoscalar or community structure. Indeed, a particular feature of networks of social interaction is that they are structured into cohesive groups within which the internal links are dense, and which are sparsely interconnected [43] (communities), and an increased knowledge of this structure has sparked the creation of new network models (see Section 1.2.4). In particular, we study the dynamics of the voter and the AB-model in the network model with mesoscalar structure presented by Toivonen et al. [109]. In the AB-model and for this class of networks with community structure, we find broad lifetime distributions with an absence of a characteristic time until consensus is reached, which seems to be associated with trapped metastable states caused by community structure (publication in Ref. [215]). In order to understand this striking result, we present a minimal model for community structure based on connected cliques. For the AB-model, we derive sufficient conditions for the existence of lifetime distributions without a characteristic time, which are shown to be related to a structural heterogeneity at the mesoscale level. Such network architecture produces trapped metastable states that survive at any time scale (publication in Ref. [216]).

In the second block of results (Chapter 5), we compare the AB-model with another three-state model with two non-excluding options, proposed in the context

1.6. TOWARDS MODELS WITH TWO NON-EXCLUDING OPTIONS

of semiotic dynamics: the Naming Game restricted to two conventions [197]*. We are interested in extending the AB-model in analogy to the Naming Game through a parameter which can be interpreted as a measure of inertia or reinforcement of the status of being in the AB-state. In this wider framework, we study and compare both models in the mean field limit including the study of order-disorder transitions (consensus-coexistence). While there exists a transition in the Naming Game restricted to two conventions, this is shown to be absent in the AB-model. Moreover, we also compare the interface dynamics in regular lattices for the original models, where both present curvature driven interface dynamics (publication in Ref. [217]).

Finally, in the last block of results (Chapter 6) and coming back to the general models on language competition, we aim to analyze the Abrams-Strogatz and the Bilinguals models beyond the symmetrical case of socially equivalent options and neutral volatility (linear dependence on the state densities of agents) on which we have concentrated until this point. In this way, we move a step further in our study and comparison between two-state models and models with two non-excluding options, studying these models analytically and numerically in the whole volatility-prestige parameter space (a,s) . We are mainly interested in the order-disorder transitions (consensus-coexistence) occurring in fully connected networks, complex random networks and two dimensional regular lattices. To this end, we derive a macroscopic description of the dynamics of the models. Beyond the mean field analysis in fully connected networks, in complex random networks we use a pair approximation method, in which correlations to second neighbors in the network can be neglected. In two-dimensional lattices instead, we derive partial differential equations for the magnetization field that depend on space and time. A stability analysis reveals that the introduction of the AB-agents generally reduces the scenario of coexistence. In the case of asymmetrical options, the coexistence is more unlikely to happen in poorly-connected than in fully connected networks, and consensus is enhanced as the connectivity decreases. This dominance effect is even stronger in two-dimensional regular lattices, where domain coarsening tends to drive the system to consensus (publication in Ref. [218]).

In summary, beyond the two-state models inspired in ferromagnetic interactions for social dynamics recently studied in statistical physics [5] and motivated by language competition problems, we study consensus problems in which the options at play can be non-excluding. This thesis presents a detailed analysis of two-state models in comparison to models with two non-excluding options,

*For a detailed description of the Naming Game and its particular case of restriction to two conventions, see Chapter 5.

CHAPTER 1. INTRODUCTION

addressing the role of a third AB-state of coexisting options at the individual level, together with the effects of the underlying network structure.

1.7

Outline

The outline of the thesis is the following:

Chapter 2 presents the microscopic models studied: the Abrams-Strogatz model and the Bilinguals model; together with the voter model and the AB-model. It includes a qualitative description of the models by using a two-dimensional Applet, showing the broad phenomenology of the dynamics throughout the parameter space. We also include a brief explanation on the nature of the numerical simulations and the general concepts we use throughout the thesis. In Chapter 3, we present the results obtained in the analysis of numerical simulations of the voter model and the AB-model in fully connected networks, two-dimensional lattices and small world networks; while Chapter 4 addresses the role of networks with mesoscale structure in the same models. In Chapter 5, we compare two consensus models with two non-excluding options: the AB-model and the Naming Game restricted to two conventions. In Chapter 6, we study the Abrams-Strogatz model and the Bilinguals model by analytical and numerical methods in fully connected and complex random networks, as well as in regular lattices. Finally, in Chapter 7 we expose our conclusions, together with an outlook and final remarks.

We also include in Appendix B a copy of our paper on the viability and resilience of two languages in competition using the Abrams-Strogatz model (publication in Ref. [219]). It is included as an appendix because this study is a more technical one, lying in the field of *control theory* and far from the collective emergent phenomena which define our general focus in the thesis.

The models

In this Chapter we present the models we study throughout the main body of the thesis: the Abrams-Strogatz model and the Bilinguals model; together with the voter model and the AB-model, which correspond to a particular setting in the parameter space of the former models, respectively. The other model studied in this work, the Naming-Game [192], is introduced in Chapter 5.

The Abrams-Strogatz model

In this Section we present the microscopic version (publication in Ref. [180]) of the Abrams-Strogatz model [13] (from now on, AS-model), a two-state model proposed for the competition between two languages. In this model, an agent i sits in a node within a network of N individuals and has k_i neighbors. Neighbors are here understood as agents sitting in nodes directly connected by a link. The agent can be in the following states: A , agent using language A (monolingual A); or B , agent using language B (monolingual B)*.

The state of an agent evolves according to the following rules: starting from a given initial condition, at each iteration we choose one agent i at random and we compute the local densities for each of the states in the neighborhood of node i , $\sigma_{i,l}$ ($l=A, B$). The agent changes its state according to the following transition probabilities:

*Notice that we consider *use* of a language rather than *competence*. In this way, learning processes are out of reach of the present model. Effectively, the situation is such as if all agents were competent in both languages.

CHAPTER 2. THE MODELS

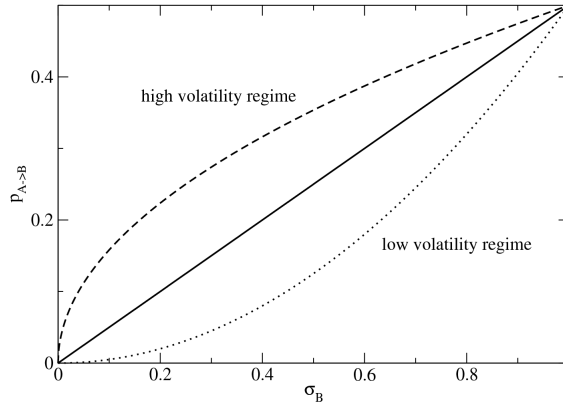


Figure 2.1: Volatility parameter, a : neutral case ($a = 1$, solid line), high volatility regime ($a < 1$, dashed line) and low volatility regime ($a > 1$, dotted line).

$$p_{i,A \rightarrow B} = (1 - s)(\sigma_{i,B})^a \quad , \quad p_{i,B \rightarrow A} = s(\sigma_{i,A})^a \quad (2.1)$$

Equations (2.1) give the probabilities for an agent i to change from state A to B, or vice-versa. They depend on the local densities ($\sigma_{i,A}$, $\sigma_{i,B}$) and on two free parameters: the *prestige* of language A, $0 \leq s \leq 1$ (the one of language B is $1 - s$); and the *volatility* parameter, $a \geq 0$. On the one hand, prestige is modeled as a scalar which aggregates the multiple factors affecting the prestige of a language. In this way, s gives a measure of the different status between the two languages, that is, which is the language that gives an agent more possibilities in the social and personal spheres. Mathematically, it is a symmetry breaking parameter. The case of socially equivalent languages corresponds to $s = 0.5$. On the other hand, the volatility parameter gives shape to the functional form of the transition probabilities (see Figure 2.1). The case $a=1$ is the neutral situation, where the transition probabilities depend linearly on the local densities. A high volatility regime exists for $a < 1$, with a probability of changing language state above the neutral case, and therefore agents change its state rather frequently. A low volatility regime exists for $a > 1$ with a probability of changing language state below the neutral case, and thus agents have a larger resistance to change its

2.2. THE BILINGUALS MODEL

state. In this way, the volatility parameter gives a measure of the propensity (or resistance) of the agents to change their language use.

In the thermodynamic limit, the model can be described by a differential equation for the total population density of agents Σ_A ($\Sigma_B = 1 - \Sigma_A$):

$$d\Sigma_A/dt = \Sigma_A(1 - \Sigma_A)[s(\Sigma_A)^{a-1} - (1-s)(1 - \Sigma_A)^{a-1}] \quad (2.2)$$

This population dynamics approach was the initial proposal by Abrams-Strogatz* in [13].

When $a \neq 1$, Equation (2.2) has three fixed points: $\Sigma_A^{(1)} = 1$ and $\Sigma_A^{(2)} = 0$, which correspond to consensus in the state A or B respectively; and $\Sigma_A^{(3)} = [(s/(1-s))^{1/a} + 1]^{-1}$. For $a > 1$, the two first fixed points are stable, and the third one is not, leading to stable consensus. For $a < 1$ instead, the stability changes via a transcritical bifurcation, and consensus becomes unstable giving rise to stable coexistence of the two states.

In the neutral case $a = 1$, Equation (2.2) becomes the logistic-Verhulst equation [180]:

$$d\Sigma_A/dt = (2s - 1)\Sigma_A(1 - \Sigma_A) \quad (2.3)$$

In this case, there exist just two fixed points: $\Sigma_A^{(1)} = 1$ and $\Sigma_A^{(2)} = 0$. For $s > 0.5$ (1) is stable and (2) unstable; while for $s < 0.5$ it happens the opposite. For the case $s = 0.5$, we obtain a null system with a degenerate line of fixed points, and therefore, any initial condition is a fixed point of the dynamics (this corresponds to the voter model; see Section 2.3).

2.2

The Bilinguals model

We present here the Bilinguals model (from now on, Bilg-model), inspired in the modifications of the AS-model proposed by Minett and Wang [182, 183] (see

*Abrams and Strogatz found an exponent $a=1.31$ when fitting to real data from the competition between Quechua-Spanish, Scottish Gaelic-English and Welsh-English. They considered only this case. Moreover, they also inferred the corresponding value of s in each of the linguistic situations.

CHAPTER 2. THE MODELS

Section 1.5), which takes into account the presence of a third possible state: the bilingual agents.

In this model, the agents can also be in a third possible state, AB , bilingual agent using both languages, A and B ; and there are three local densities to compute for each node i : $\sigma_{i,l}$ ($l = A, B, AB$). The agent changes its state according to the following transition probabilities:

$$p_{i,A \rightarrow AB} = (1-s)(\sigma_{i,B})^a, \quad p_{i,B \rightarrow AB} = s(\sigma_{i,A})^a \quad (2.4)$$

$$p_{i,AB \rightarrow B} = (1-s)(1-\sigma_{i,A})^a, \quad p_{i,AB \rightarrow A} = s(1-\sigma_{i,B})^a \quad (2.5)$$

which depend on the same two parameters of the AS-model: prestige (s) and volatility (a). Equations (2.4) give the probabilities for changing from a monolingual state, A or B , to the bilingual state AB , while equations (2.5) give the probabilities for an agent to move from the AB -state towards the A or B states. Notice that the latter depend on the local density of agents using the language to be adopted, including bilinguals ($1 - \sigma_{i,l} = \sigma_{i,j} + \sigma_{i,AB}$, $l, j = A, B$; $l \neq j$). It is important to stress that a change from state A to state B or vice-versa, always implies an intermediate step through the AB -state.

In the mean field limit, the model can as well be described by differential equations for the total population densities of agents Σ_A, Σ_B ($\Sigma_{AB} = 1 - \Sigma_A - \Sigma_B$),

$$d\Sigma_A/dt = s(1 - \Sigma_A - \Sigma_B)(1 - \Sigma_B)^a - (1-s)\Sigma_A(\Sigma_B)^a \quad (2.6)$$

$$d\Sigma_B/dt = (1-s)(1 - \Sigma_A - \Sigma_B)(1 - \Sigma_A)^a - s(\Sigma_A)^a \Sigma_B \quad (2.7)$$

Equations (2.6)-(2.7) have three fixed points: $(\Sigma_A, \Sigma_B, \Sigma_{AB}) = (1, 0, 0), (0, 1, 0)$, which correspond to consensus in the state A or B respectively; and $(\Sigma_A^*, \Sigma_B^*, \Sigma_{AB}^*)$, with $\Sigma_l^* \neq 0$ ($l = A, B, AB$). There are no closed expressions for Σ_l^* ($l = A, B, AB$) but numerical analysis is needed. A detailed stability analysis of this model is given in Chapter 6. A main result is that for $a \geq 0.63$, the two first fixed points are stable, and the third one is not, leading to stable consensus. For $a < 0.63$ instead, the stability is reversed, consensus becomes unstable and a stable state of coexistence of the three states becomes possible.

◇ ◇ ◇

The models presented above can account for the more general framework of a consensus problem (see Section 1.3), where there exists a competition between

2.3. THE VOTER MODEL AND THE AB-MODEL

two social norms or options. In this way, the AB-state represents the case when two options can coexist at the individual level (an agent using two languages in the case of language competition), the prestige parameter can be considered as a bias or preference towards one of the two options, and the volatility parameter can be interpreted as the inertia of the agent to change its current social option.

2.3

The voter model and the AB-model

In Chapters 3, 4 and 5, we concentrate in analyzing in detail the AS-model and the Bilg-model for the case of two socially equivalent norms or options (languages), $s = 0.5$, and neutral volatility, $a = 1$ [198] (both fall into the class of models with Z_2 -symmetry). Therefore, we consider exhaustively this case in this Section.

On the one hand, the transition probabilities of the microscopic AS-model for the agent i reduce to:

$$p_{i,A \rightarrow B} = \frac{1}{2} \sigma_{i,B} \quad , \quad p_{i,B \rightarrow A} = \frac{1}{2} \sigma_{i,A} \quad (2.8)$$

Equations (2.8) give probabilities for an agent to change between the two states, which are proportional to the local density of agents in the opposite option. Except for a time scale coming from the prefactor $1/2$, the AS-model becomes the voter model, which we have already extensively presented in the Introduction (see Section 1.4.2). Notice that the voter model rules are equivalent to the adoption by the agents of the option of a randomly chosen neighbor.

In the mean field approximation, the voter model reduces to the equation:

$$d\Sigma_A/dt = 0, \quad (2.9)$$

predicting that any given initial density of agents in state A would persist forever*.

On the other hand, the Bilg-model becomes:

*As we have shown in the Introduction (Section 1.4.2), notice that in terms of the magnetization, $m \equiv \Sigma_A - \Sigma_B$, Equation 2.9 can be written as $dm/dt = 0$.

CHAPTER 2. THE MODELS

$$p_{i,A \rightarrow AB} = \frac{1}{2}\sigma_{i,B} \quad , \quad p_{i,B \rightarrow AB} = \frac{1}{2}\sigma_{i,A} \quad (2.10)$$

$$p_{i,AB \rightarrow B} = \frac{1}{2}(1 - \sigma_{i,A}) \quad , \quad p_{i,AB \rightarrow A} = \frac{1}{2}(1 - \sigma_{i,B}) \quad (2.11)$$

Equations (2.10) give the probabilities for an agent i to move away from a single-option state, A or B, to the AB-state. They are proportional to the density of agents in the opposed single-option state in the neighborhood of i . On the other hand, equations (2.11) give the probabilities for an agent to move from the AB-state towards the A or B states. They are proportional to the local density of agents with the option to be adopted, including those in the AB-state ($1 - \sigma_{i,l} = \sigma_{i,j} + \sigma_{i,AB}$, $l, j=A,B; l \neq j$). It is important to remind that a change from state A to state B or vice-versa, always implies an intermediate step through the AB-state. The dynamical rules (2.10) and (2.11) are fully symmetric under the exchange of A and B, so that states A and B are equivalent with no preference for any of the two options. Reaching consensus in either of these two states is a symmetry breaking process. These dynamical rules, which define a modification of the two-state voter model to account for a third mixed AB-state, reflect the special character of this state as one of coexisting options. We refer to the model defined by (2.10) and (2.11) as the *AB-model* [198].

In a fully connected network and in the limit of infinite population size, the AB-model can be described by coupled mean field differential equations for the total population densities Σ_A, Σ_B ($\Sigma_{AB} = 1 - \Sigma_A - \Sigma_B$):

$$d\Sigma_A/dt = 1/2[1 - \Sigma_A + (\Sigma_B)^2 - 2\Sigma_B] \quad (2.12)$$

$$d\Sigma_B/dt = 1/2[1 - \Sigma_B + (\Sigma_A)^2 - 2\Sigma_A] \quad (2.13)$$

The analysis of these equations shows the existence of three fixed points: two of them stable and equivalent, corresponding to consensus in the state A or B: $(\Sigma_A, \Sigma_B, \Sigma_{AB}) = (1, 0, 0), (0, 1, 0)$; and another one unstable (saddle point), with non-vanishing values for the global densities of agents in the three states: $(\Sigma_A, \Sigma_B, \Sigma_{AB}) = ((3 - \sqrt{5})/2, (3 - \sqrt{5})/2, \sqrt{5} - 2)$. Figure 2.2 shows the phase portrait of the system, i.e., the trajectories of the system in the (Σ_A, Σ_B) space. We can observe the location of the fixed points of the system and the two basins of attraction corresponding to the stable fixed points, which are separated by the line $\Sigma_A = \Sigma_B$, the stable manifold of the saddle.

2.4. PHENOMENOLOGY OF THE MODELS: QUALITATIVE EXPLORATION OF THE VOLATILITY-PRESTIGE PARAMETER SPACE

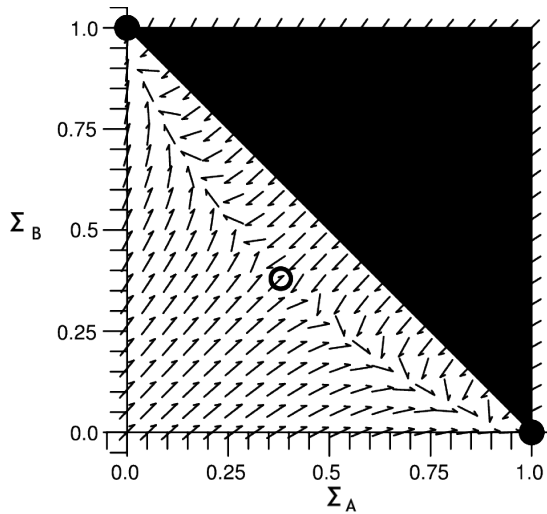


Figure 2.2: Phase portrait: trajectories in the (Σ_A, Σ_B) space for the AB-model. Each arrow shows the direction of change of the system departing from each corresponding state, allowing trajectories and fixed points to be inferred. Stable fixed points are marked by filled circles; unstable ones are marked by unfilled circles. The points such that $\Sigma_A + \Sigma_B > 1$ are not shown (black area), as they are not physical; remember that $\Sigma_A + \Sigma_B + \Sigma_{AB} = 1$.

2.4

Phenomenology of the models: qualitative exploration of the *volatility-prestige* parameter space

In this Section, we aim to present a qualitative description of the agent based models (ABMs) for the Abrams-Strogatz and Bilinguals dynamics, showing the broad phenomenology of the models throughout the parameter space (a, s) . Observations made here, are addressed from a formal and theoretical point of view in the following Chapters.

We have implemented these two models in a two-dimensional lattice by designing a Java Applet [220] in which one can tune the parameters of the models

CHAPTER 2. THE MODELS

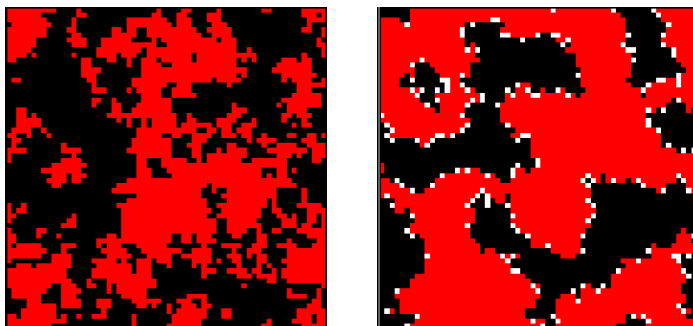


Figure 2.3: Snapshots showing the formation of domains in the voter model (Left) and the AB-model (Right) starting from an initial random distribution of states of the agents. Neutral volatility ($a = 1$) and socially equivalent options ($s = 0.5$). $N = 64^2$ agents; $t = 200$. Notice that in the AB-model, AB-agents do not form domains, but they place themselves at the interfaces between single-option domains. Red: option A; black: option B; white: AB-agents.

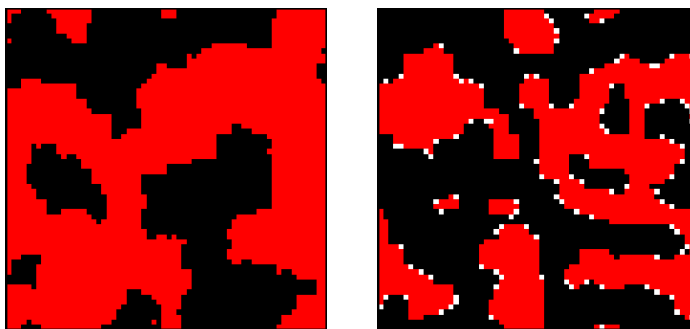


Figure 2.4: Snapshots showing the formation of domains in the AS-model (Left) and the Bilg-model (Right). Low volatility ($a = 3$) and socially equivalent options ($s = 0.5$). $N = 64^2$ agents; $t = 350$. Notice that the boundaries are flatter, due to the increase of curvature driving. Red: option A; black: option B; white: AB-agents.

2.4. PHENOMENOLOGY OF THE MODELS

(prestige s , and volatility a), set different initial conditions, and see the simulations in real time*. An interactive exploration of the parameter space (a,s) can be performed using the Applet. The following qualitative exploration of the phenomenology of the models in different parameter settings gives insights on the emergent complex behavior of these models, including issues of domain growth, interface dynamics, consensus-coexistence scenarios, and the role of AB-agents.

- Neutral volatility ($a = 1$)

In the case of socially equivalent options ($s = 0.5$), the models correspond to the voter model and the AB-model. We observe in both cases a formation and growth of single-option domains (see Figure 2.3)[†]. Notice that the AB-agents never form domains, but instead, they place themselves at the boundaries between single-option ones. Finally, one of the two options takes over the system. Due to the equivalent prestige, this happens for each of the options with equal probability.

The general role of prestige is made clear when $s \neq 0.5$: the more prestigious option dominates, causing the extinction of the other. One can also observe that changing the value of s in real time when an option is in its way to extinction can lead to its recovery.

- Low volatility regime ($a > 1$)

When volatility is low, i.e., agents have larger inertia to change its current option, both models display a similar domain growth (see Figure 2.4). Domains evolve smoothly and slowly (curvature-driven like), and the times for extinction increase. For socially asymmetric options, low volatility delays the effect of prestige difference so that the less prestigious option can persist for longer times. In comparison to the AS-model, it is interesting to notice that AB-agents slow down further the extinction of the less prestigious option (see Figure 2.5).

- High volatility regime ($a < 1$)

In the case in which volatility is high, and for socially equivalent options ($s = 0.5$), domains cease to form and agents in different states are mixed throughout the population: this scenario leads to a long lived dynamical coexistence of the two options in both models, with the two options having

*The applet can be found at: http://ifisc.uib.es/eng/lines/complex/APPLET_LANGDYN.html.

[†]The growth of these domains and their interface dynamics are addressed in Chapter 3, where it is shown that domains grow by interfacial noise in the voter model, while in the AB-model they are driven by curvature reduction. These two mechanisms can be observed intuitively in the applet through simulations in real time.

CHAPTER 2. THE MODELS

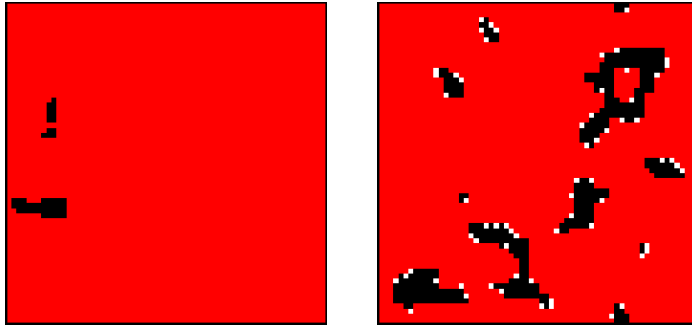


Figure 2.5: Snapshots of the AS-model (Left) and the Bilg-model (Right). High volatility ($a = 3$) and socially non-equivalent options ($s = 0.6$). $N = 64^2$ agents; $t = 225$. Notice that in the AS-model, the less prestigious option is just about to get extinct (around 1% of the population), while in the Bilg-model the minority option represents still more than 10% of the population. Red: option A; black: option B; white: AB-agents.

the same fraction of the total population, together with the survival of a large number of AB-agents in the Bilg-model* (see Figure 2.6).

The situation is different when options with different prestige are considered in a situation of high volatility ($s \neq 0.5$; see Figure 2.7). For a relatively small difference in prestige between the two options ($s = 0.6$), AB-agents in the Bilg-model cause a fast extinction of the less prestigious option, while in the absence of AB-agents (AS-model) both options coexist for long times (although the majority is in the more prestigious option, around 70% of the population). When the prestige difference becomes larger ($s \geq 0.7$), the less prestigious option dies out in both models rather fast (but still it takes more time when there are no AB-agents (AS-model)).

In summary, numerical simulations of the AS-model and the Bilg-model show that depending on the volatility of individuals and the relative difference on prestige between both options, the population can either remain indefinitely in a *coexistence* state with a finite fraction of agents in each of the two options, or it can reach a *dominance/extinction*[†] state in which one of the two options takes over

*The high frequency of changes in the option of the agents leads to a system in which both options are effectively shared by all the agents.

[†]Notice that the concept of *consensus* we have introduced in Section 1.3, broadly used in the literature, corresponds indeed to a scenario of *dominance/extinction*.

2.4. PHENOMENOLOGY OF THE MODELS

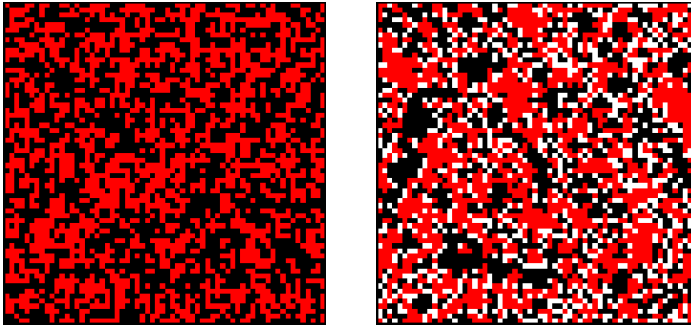


Figure 2.6: Snapshots showing the coexistence regime in the AS-model (Left) and the Bilg-model (Right). Low volatility ($a = 0.1$) and socially equivalent options ($s = 0.5$). $N = 64^2$ agents; $t = 200$. Notice that agents do not form linguistic domains, but they are completely mixed. Red: option A; black: option B; white: AB-agents.

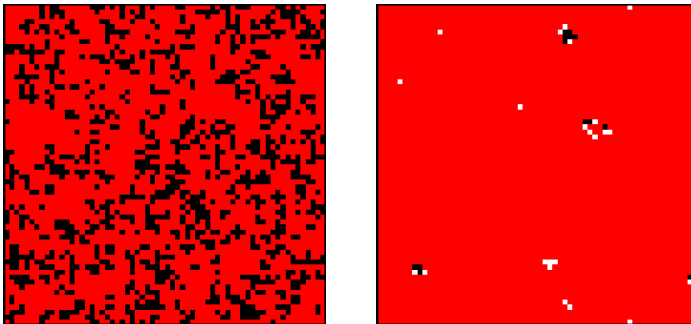


Figure 2.7: Snapshots of the AS-model (Left) and the Bilg-model (Right). Low volatility ($a = 0.1$) and socially non-equivalent options ($s = 0.6$). $N = 64^2$ agents; $t = 40$. Notice that in the Bilg-model, the less prestigious option is just about to disappear, while in the AS-model coexistence is still possible. However, in the AS-model this option becomes only the one of the minority. Red: option A; black: option B; white: AB-agents.

CHAPTER 2. THE MODELS

the whole population. Our results make clear that prestige is very important, but volatility results to be a very important social parameter as well. For example, comparing Figure 2.5 and Figure 2.7 one can observe that when an option disappears, this happens much faster in the high volatility regime ($a < 1$) than in the low volatility regime ($a > 1$). Generally speaking, high volatility appears to enhance the coexistence of options of similar prestige. However, when an option is situated in a low prestige position, low volatility of the agents gives larger times before its disappearance. In this last case, the delay in the path to extinction of the less prestigious option is reinforced by the presence of AB-agents (Bilg-model).



In the following Chapters, we go beyond the simple mean field description of the models and the qualitative exploration of their phenomenology we have presented here. We analyze in detail the microscopic dynamics in which discrete and finite size effects, as well as the topology of the network of interaction are taken into account. We consider from fully connected networks and regular lattices, to random, small world networks and networks with community structure.

Regarding two dimensional lattices and beyond the qualitative simulations shown in this Section, in Chapter 3 we study the dynamics of the AB-model in comparison to the voter model by performing an exhaustive numerical analysis. Moreover, in Chapter 6 we derive a macroscopic description based on a continuum field approximation, which makes possible an analytical study of the AS-model and the Bilg-model in the full range of values of the prestige and volatility parameters.

2.5

Analysis of the models. General concepts

In the last part of this Chapter, we present the general concepts used in this work in order to analyze the models presented above: the nature of the numerical simulations, the order parameters used to characterize the ordering dynamics, and the distributions of lifetimes. Other particular concepts and methods needed in specific Chapters will be introduced when necessary.

2.5. ANALYSIS OF THE MODELS. GENERAL CONCEPTS

The main methodological tool we use is the numerical simulation of the models. In the simulations, we use random asynchronous node update: at each iteration or time step a single node is randomly chosen and updated according to the transition probabilities (2.1) and (2.4-2.5) in the case of the AS-model and the Bilg-model; and (2.8) and (2.10-2.11) in the case of the voter* and the AB-model.

We normalize time so that in every unit of time each node has been updated on average once. Therefore, a unit of time includes N iterations. In most of our simulations we start from random initial conditions: in the Bilg-model or the AB-model, random distribution in the network of 1/3 of the population in state A, 1/3 in state B and 1/3 in state AB (in the AS-model or the voter model, 1/2 of the population in state A and 1/2 in state B).

For a quantitative description of the ordering dynamics towards consensus in the A or B state we use as an order parameter the ensemble average interface density $\langle \rho \rangle$. This is defined as the density of links joining nodes in the network which are in different states [120, 129, 136]. The ensemble average, indicated as $\langle \dots \rangle$, denotes average over realizations of the stochastic dynamics starting from different random initial conditions. For our random initial conditions in the Bilg-model or the AB-model, $\langle \rho(t=0) \rangle = 2/3$: a given node has probability 2/3 of being connected to a node in a different state ($\langle \rho(t=0) \rangle = 1/2$ in the AS-model or the voter model). During the time evolution, the decrease of ρ from its initial value describes the ordering dynamics by a coarsening process with growth of spatial domains in which agents are in the same state. The minimum value $\rho = 0$ corresponds to an absorbing state where all the agents have reached consensus in the same state.

Finally, the *lifetime* of a run is defined as the number of time steps it takes for a given ordering dynamics to reach either of the absorbing states. For a detailed analysis of the lifetimes in a given model, we generally analyze the *fraction of alive runs*, that is, the fraction of simulations which still have not reached an absorbing state at time t , $P(t) \equiv 1 - \int_0^t p(t') dt'$, where $p(t)$ is the probability distribution of lifetimes. Naturally, the average time to reach consensus is defined as $\tau \equiv \int_0^\infty t p(t) dt$, and we study its dependence on the parameters of the network of interaction, specially its scaling with system size.

*To be precise, the original voter model dynamics is recovered by neglecting the prefactor 1/2 in Equation (2.8); see Section 2.3.

The AB-model (I): from regular lattices to small world networks

In this Chapter, and within the general framework of dynamics with two non-excluding options described in the Introduction (Section 1.6), we study in detail the *AB-model*, a three-state model which reduces to the voter model when AB agents are not taken into account. We aim to explore possible mechanisms for the stabilization of a coexistence between the two options, possible metastable states, and the role of AB agents and the interaction network in these processes. To this end, we analyze the growth mechanisms of A or B spatial domains, the dynamics at the interfaces, and the scaling laws for the times to reach consensus (dominance/extinction). This is studied in fully connected networks, in regular lattices and in small world networks of interaction, where we study the effect of long range interactions in the dynamics (publication in Ref. [198]).

Generally speaking, we find that allowing for the AB-state (bilinguals) modifies the nature and dynamics of interfaces: agents in the AB-state define thin interfaces and coarsening processes change from voter-like dynamics to curvature driven dynamics. This change of coarsening mechanism is also shown to originate for a class of perturbations of the voter model that we present at the end of the Chapter.

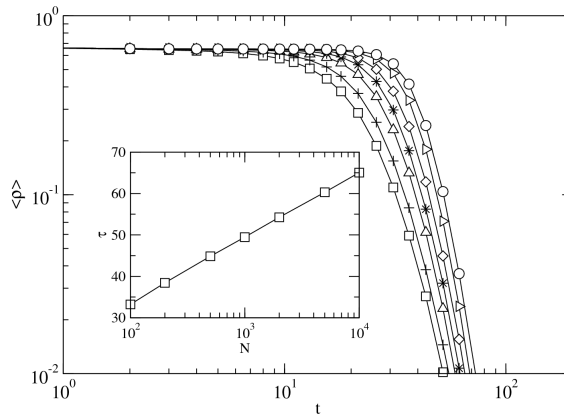


Figure 3.1: Time evolution of the average interface density $\langle \rho \rangle$ for the AB-model in a fully connected network for different system sizes. Random initial conditions. From left to right: $N = 100$ (\square), 200 (+), 500 (\triangle), 1000 (*), 2000 (\diamond), 5000 (\blacktriangleright), 10000 (\circ). Averages are calculated over 10000 realizations. Inset: dependence of the average time to reach an absorbing state τ with the system size: $\tau \sim \ln(N)$.

3.1

Fully connected networks

As a first step, we consider the dynamics of the AB-model in a fully connected network of N individuals, i.e., a network where all agents interact with one another. In this way, we go beyond population dynamics described by ODEs, and we account for the finite size effects of the resulting stochastic dynamics.

Figure 3.1 shows the time evolution of the average interface density (see Section 2.5) in fully connected networks for different system sizes starting from random initial conditions. Consensus in the A or B option is always reached, with equal probability. The average interface density reaches first a plateau, and then approaches exponentially the absorbing state due to finite size fluctuations: $\langle \rho(t) \rangle \sim e^{-kt}$ (the exponent k of the exponential decay is a constant independent of system size). In the inset of this Figure, the average time to reach an absorbing state, τ , is shown to scale logarithmically with the system size as $\tau \sim \ln(N)$.

3.1. FULLY CONNECTED NETWORKS

In the limit of infinite system size, the dynamics is exactly described by the ODEs (2.12)-(2.13). When starting from random initial conditions, the system lies on top of the stable manifold of the saddle point corresponding to coexistence of the three phases (Figure 2.2). Therefore, the system moves until reaching the saddle fixed point and stays there; the stable consensus solution is never reached. When we consider finite size fully connected networks instead, the system moves towards the saddle and fluctuates around this fixed point (stage corresponding to the plateau in Figure 3.1). At a certain point, a finite size fluctuation is large enough to drive the system far enough towards one of the two basins of attraction of the two stable fixed points, so that the system reaches consensus in the A or B option exponentially (stage corresponding to the decay of $\langle \rho(t) \rangle$ in Figure 3.1).

In comparison, the results for the voter model in fully connected networks when starting from random initial conditions are the following (see Section 1.4.2): for a single realization, $\rho(t)$ fluctuates grossly until a finite size fluctuation drives it to the absorbing state. The time evolution of the average interface density, though, is $\langle \rho(t) \rangle \sim e^{-2t/N}$; giving an exponential decay depending on system size. This is related to the fact that the probability that a simulation reaches consensus at time t , $S(t)$, decays as $S(t) \sim e^{-t/N}$ [133]. In addition, the time to reach an absorbing state, τ , scales with the system size as $\tau \sim N$ [131], giving rise to a much slower path to consensus compared to the AB-model ($\tau \sim \ln(N)$).

Moreover, the ensemble average magnetization is conserved in the voter model in networks with an homogeneous degree distribution [127]*. Therefore, the fraction of runs which lead to consensus in the A option are proportional to the fraction of initial agents in the state A. This is not the case in the AB-model, where the average magnetization, defined as $\langle m(t) \rangle \equiv \langle \Sigma_A(t) - \Sigma_B(t) \rangle$, is not conserved:

$$\frac{d \langle m \rangle}{dt} = \frac{1}{2} \langle \Sigma_{AB} \rangle \langle m \rangle \quad (3.1)$$

$\langle \Sigma_{AB} \rangle \geq 0, \forall t$ so that $\text{sign}(\frac{d \langle m \rangle}{dt}) = \text{sign}(\langle m \rangle)$: if there is a bias in the initial conditions towards one of the two options, this option will be the one who will take over the system.

*As reported in the Introduction (Section 1.4.2), in heterogeneous networks only an ensemble average magnetization weighted by the degree of the node is conserved [129].

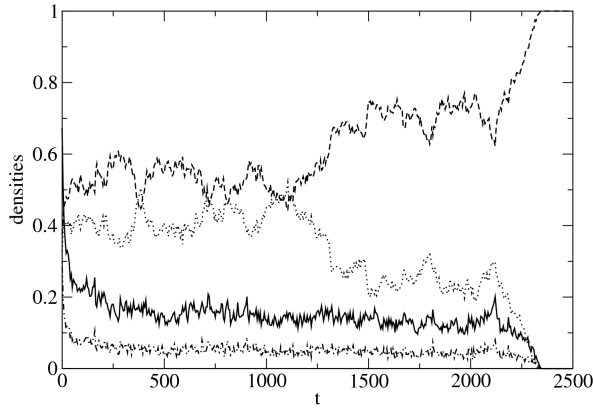


Figure 3.2: Time evolution of the total densities of agents in the three states, Σ_i ($i = A, B, AB$), and the interface density, ρ for the AB-model in a two-dimensional regular lattice. One realization in a population of $N = 400$ agents is shown. From top to bottom: Σ_A (dashed line), Σ_B (dotted line), ρ (solid line), Σ_{AB} (dot-dashed line).

3.2

Two-dimensional lattices

In order to take into account local effects, we consider next the dynamics of the AB-model in a two-dimensional regular lattice with four neighbors per node [198]. In Figure 3.2 we show, for a typical realization, the time evolution of the total densities of agents in state A, Σ_A , in state B, Σ_B , and in state AB, Σ_{AB} ; and the density of interfaces, ρ . State A takes over the system, while the opposite option B disappears. Consensus in either of the two equivalent states A or B is always reached (with equal probability to reach consensus in state A or B). We observe an early very fast decay of the interface density and of the total density of agents in the state AB, Σ_{AB} , followed by a slower decay corresponding to the coarsening dynamical stage. This stage lasts until a finite size fluctuation causes the dominance of one of the states A or B, and the density of AB agents disappears together with the density of agents in the state opposite to the one that becomes dominant.

3.2. TWO-DIMENSIONAL LATTICES

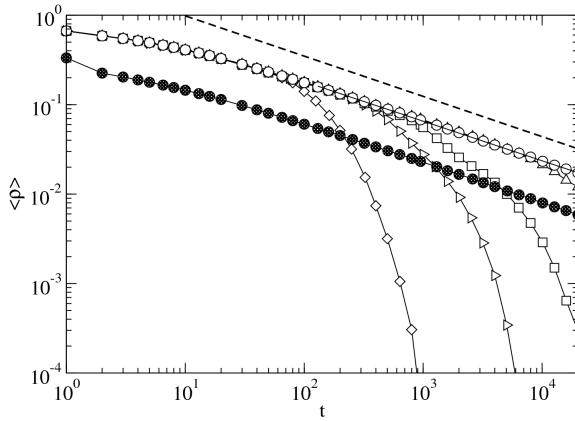


Figure 3.3: Time evolution of the average interface density $\langle \rho \rangle$ for the AB-model in a two-dimensional regular lattice for different system sizes. Empty symbols: from left to right: $N = 10^2$ (\diamond), 20^2 (\triangleright), 30^2 (\square), 100^2 (\triangle), 300^2 (\circ). The average global density of AB agents, $\langle \Sigma_{AB} \rangle$, for $N = 300^2$ agents is also shown (\bullet). Averages are calculated over 100-1000 realizations depending on the system size. Dashed line for reference: $\langle \rho \rangle \sim t^{-0.45}$.

In Figure 3.3 we show the time evolution of the average interface density and of the average total density of AB agents, averaged over different realizations. For the relaxation towards one of the absorbing states (dominance of either A or B) both the average interface density and the average density of AB agents decay following a power law with the same exponent, $\langle \rho \rangle \sim \langle \Sigma_{AB} \rangle \sim t^{-\gamma}$, $\gamma \simeq 0.45$. This indicates that the evolution of the average density of the AB agents is correlated with the interface dynamics. Several systems sizes are shown in order to see the effect of finite size fluctuations. During the coarsening stage described by the power law behavior, A and B spatial domains are formed and grow in size. From the dependence of $\langle \rho \rangle$ with time*, it follows that the typical size of a domain, ξ , grows as $\xi \sim t^\gamma$, $\gamma \simeq 0.45$. Eventually a finite size fluctuation occurs (as the one shown in Figure 3.2) so that the whole system is taken to an absorbing state in which there is consensus in either the A or B option.

*Notice that the average domain size ξ relates to the interface density in the following way: $\xi(t) \sim 1/\rho(t)$. Argument in Section 1.4.2 (regular lattices).

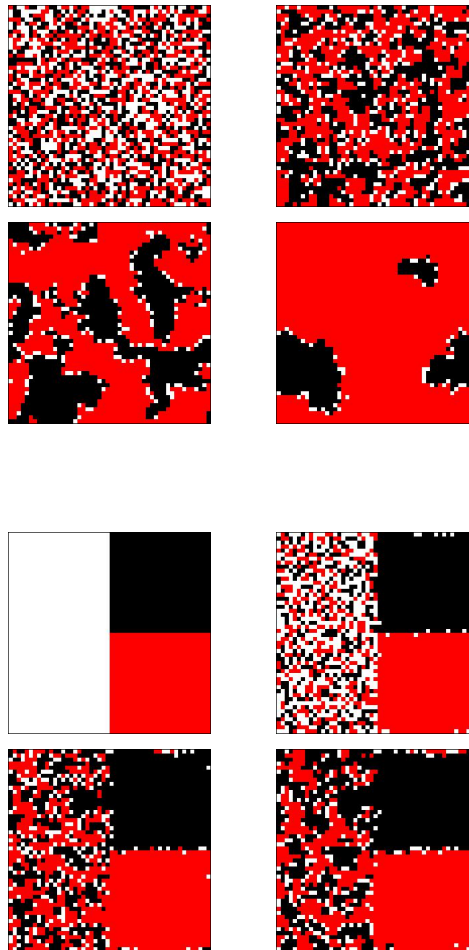


Figure 3.4: AB-model in a regular lattice of $N = 50^2$ individuals. *Top:* Random initial conditions: snapshots of a typical simulation of the dynamics; $t = 0, 8, 80, 800$ from left to right. *Bottom:* Disintegration of an initial AB-domain; $t = 0, 1, 5, 10$ from left to right. Red: option *A*, black: option *B*, white: *AB*-state.

3.2. TWO-DIMENSIONAL LATTICES

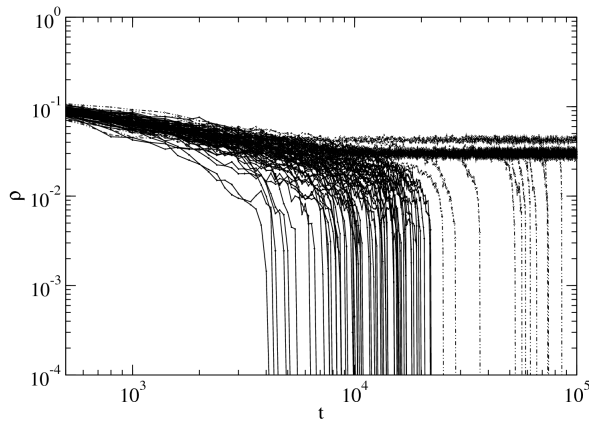


Figure 3.5: The time evolution of the interface density ρ for the AB-model in a two-dimensional regular lattice is shown for 100 realizations. We observe two types of realizations: most of them decay by a finite size fluctuation to an absorbing state after the stage of coarsening (solid lines); however, around 1/3 of them get stuck in trapped metastable states, identified by an essentially constant value of ρ , until they eventually decay (dotted lines).

As we have seen already in Section 2.4, during the coarsening process spatial domains of AB agents are never formed. Rather, during an early fast dynamics AB agents place themselves in the boundaries between A and B growing domains. This explains the finding that the density of AB agents follows the same power law than the average density of interfaces. We can observe in Figure 3.4-Top snapshots of the time evolution of a typical realization of the dynamics: the fast decay of the amount of AB agents, the formation of A and B domains, and the presence of AB agents only at the interfaces between them. We have also checked the intrinsic instability of an AB spatial domain: an initial AB domain disintegrates very fast into smaller A and B domains, with AB agents just placed at the interfaces, as shown in the set of snapshots in Figure 3.4-Bottom.

Our result for the growth law of the characteristic length of A or B domains is compatible with the well known exponent 0.5 associated with domain growth driven by mean curvature and surface tension reduction observed in SFKI models [110]*. However, systematic deviations from 0.5 are observed when mea-

*See Section 1.4.3 for a detailed description of the SFKI model.

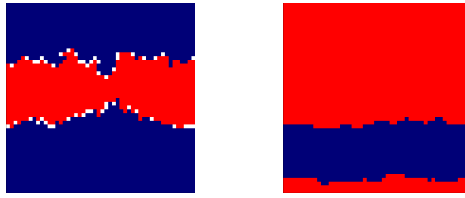


Figure 3.6: Snapshots of simulations which get trapped in stripe-like metastable states. $N = 50^2$ agents. Legend: Red: state A, blue: state B, white: state AB. Left panel: AB-model in a two dimensional regular lattice; 4 neighbors per site. Right panel: ϵ -model ($\epsilon = 1.0$). Two dimensional regular lattice; 8 neighbors per site.

asuring the coarsening exponent γ . These deviations are at least partially due to the fact that on closer inspection there are two type of qualitatively different realizations, which we show in Figure 3.5: while many of them have a coarsening stage followed by a finite size fluctuation which drives the system to an absorbing state, a finite fraction of the realizations (1/3 of them, for large enough systems) gets stuck in long-lived trapped metastable states. These metastable states are reminiscent of the ones found [221] in the analysis of a two states majority rule dynamics based on group interaction [101]*. They correspond to stripe-like configurations for an A or B domain. The boundaries of these stripe-shaped domains are close to flat interfaces but with interfacial noise present (Figure 3.6-Left). Although long-lived, these configurations continue to evolve and in this sense they are different from the stripe-like trapped frozen states with completely flat boundaries found in a zero temperature SFKI model [148][†]. When a realization falls in such trapped metastable states, coarsening stops (the average interface density fluctuates around a fixed value), until eventually a finite size fluctuation makes the two walls collide and takes the system to one of the absorbing states (see Figure 3.5).

If the realizations that fall into long-lived metastable states are removed when computing the average interface density, the power law exponent for the decay of $\langle \rho \rangle$ increases, approaching the value $\gamma = 0.5$ characteristic of curvature driven

*Similar stripes have been found in models considering individual learning together with imitation [118].

[†]Notice that in SFKI at $T \neq 0$ and below the critical temperature, these trapped states become metastable, and they finally reach an absorbing state due to thermal fluctuations.

3.2. TWO-DIMENSIONAL LATTICES

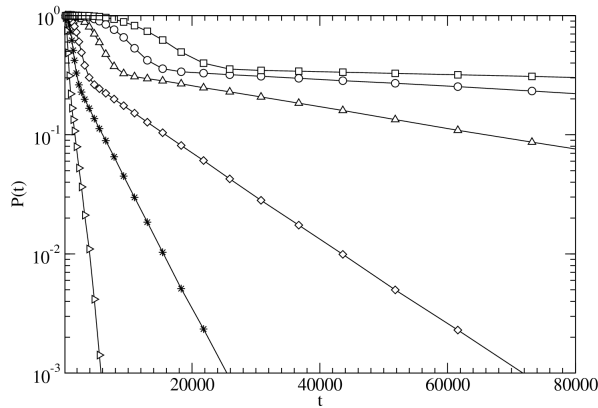


Figure 3.7: Time evolution of the fraction of alive runs, $P(t)$, for the AB-model in a two-dimensional regular lattice for different system sizes. From left to right: $N = 20^2$ (\blacktriangleright), 30^2 ($*$), 40^2 (\diamond), 60^2 (\triangle), 80^2 (\circ), 100^2 (\square). Averages are calculated over 5000-20000 realizations depending on the system size. The exponential tail corresponds to the stripe-like metastable states.

coarsening. Other deviations from the exponent $\gamma = 0.5$ can be due to non trivial logarithmic corrections. In 1 and 3-dimensional lattices, we also find an exponent close to 0.5, which substantiates the claim that curvature reduction is the dominant mechanism at work for the coarsening process in the AB-model.

The existence of two type of realizations gives rise to two different characteristic times. Starting from random initial conditions we consider the distribution of survival times, $p(t)$, i.e., the distribution for the times to reach an absorbing state. From numerical simulations, it has been proven that this distribution displays an exponential tail corresponding to the realizations that involve a trapped metastable state. The characteristic time to reach consensus can be calculated from,

$$\tau \equiv \int_0^{\infty} tp(t) dt = \int_0^T tp_1(t) dt + \int_T^{\infty} tp_2(t) dt$$

where $p_1(t)$ corresponds to the first type of realizations, $p_2(t)$ to the second type, and T is the time where there remain only stripe-like metastable states (1/3 of the realizations, as mentioned above) corresponding to the stage where $p(t)$ becomes exponential.

CHAPTER 3. THE AB-MODEL (I)

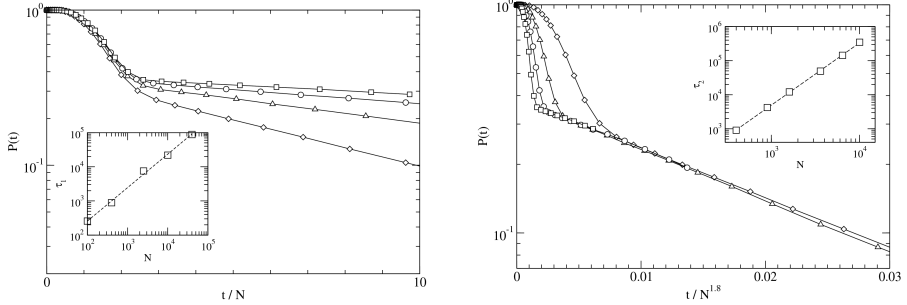


Figure 3.8: Time evolution of the fraction of alive runs, $P(t)$, for the AB-model in a two-dimensional regular lattice for different system sizes. Averages are calculated over 5000-20000 realizations depending on the system size. *Left:* the time has been rescaled by N , in order to observe the scaling for the first type of realizations that approach the absorbing state after the coarsening stage. From bottom to top: 40^2 (\diamond), 60^2 (Δ), 80^2 (\circ), 100^2 (\square). Inset: dependence on the system size of the characteristic time to reach an absorbing state τ_1 for these first type of realizations: $\tau_1 \sim N$. *Right:* the time has been rescaled by $N^{1.8}$, in order to observe the scaling for the second type of realizations that get stuck in stripe-like metastable states. From right to left: 40^2 (\diamond), 60^2 (Δ), 80^2 (\circ), 100^2 (\square). Inset: dependence on the system size of the characteristic time to reach an absorbing state τ_2 for these second type of realizations: $\tau_2 \sim N^{1.8}$.

For the first type of realizations, the ones that do not get trapped in long lived metastable states, the characteristic time to reach an absorbing state can be estimated to scale as $\tau_1 \sim N$ since the coarsening is described by $\langle \rho \rangle \sim t^{-\gamma}$, with $\gamma \simeq 0.5$, and at the time of reaching consensus $\langle \rho \rangle \sim (1/N)^{1/d}$ (d is the dimensionality of the lattice). This has been confirmed by numerical simulations which consider only such kind of realizations. For the second type, $p_2(t) \sim e^{-\alpha(N)t}$, where $\alpha(N)$ is a constant depending on system size N . It is straightforward to show that for large enough systems, the second term scales as $\tau_2 \sim 1/\alpha(N)$. Therefore, to obtain the dependence of τ_2 with system size, we are just interested in the exponent $\alpha(N)$. In order to reduce the fluctuations observed in the tail for the distribution $p(t)$, we analyze instead the fraction of alive runs, i.e., the fraction of simulations which have not reached consensus yet: $P(t) \equiv 1 - \int_0^t p(t') dt'$ (see Section 2.5). As $p_2(t)$ is exponential, we can obtain $\alpha(N)$ from the fraction of

3.2. TWO-DIMENSIONAL LATTICES

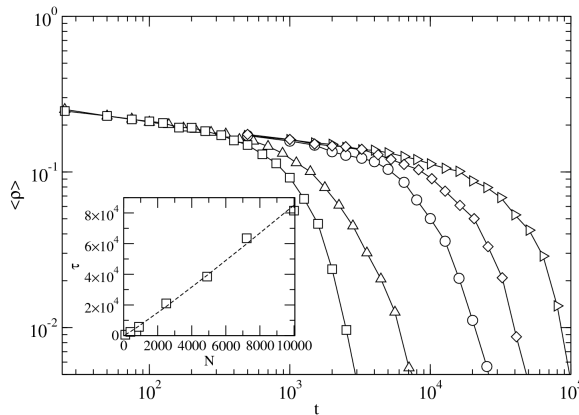


Figure 3.9: Time evolution of the average interface density $\langle \rho \rangle$ for the voter model in a two-dimensional regular lattice for different system sizes. From left to right: $N = 20^2$ (\square), 30^2 (\triangle), 50^2 (\circ), 70^2 (\diamond), 100^2 (\triangleright). Inset: dependence of the characteristic time to reach an absorbing state τ with the system size: $\tau \sim N^{1.08}$; compatible with the theoretical $\tau \sim N \ln(N)$.

alive runs: the tails of $P(t)$ also decay as $P(t) \sim e^{-\alpha(N)t}$. We show in Figure 3.7 the fraction of alive runs for different system sizes. The first fast decay corresponds to the first type of simulations, while the exponential tail describes the approach to the absorbing state for simulations which get trapped in metastable states. Analyzing the exponential tails for different system sizes, i.e., plotting $1/\alpha(N)$, we obtain $\tau_2 \sim N^\alpha$, with $\alpha \simeq 1.8$. The scalings regarding the two types of realizations are shown in Figure 3.8.

When taking into account all realizations, the global characteristic time to reach an absorbing state for large system sizes is dominated by the persistence of the trapped metastable states, so that $\tau \sim N^\alpha$, with $\alpha \simeq 1.8$.

The AB-model analyzed here is a modification of the two-state voter model*. Regarding the times to reach consensus in this model, in Figure 3.9 we can observe that for a finite system the characteristic time to reach an absorbing state scales as $\tau \sim N \ln N$ [123, 180]. Moreover, and as we have shown in Section 1.4.2, for the voter model coarsening in a $d = 2$ square lattice occurs by a different

*See Section 1.4.2 for a detailed description of the voter model.

CHAPTER 3. THE AB-MODEL (I)

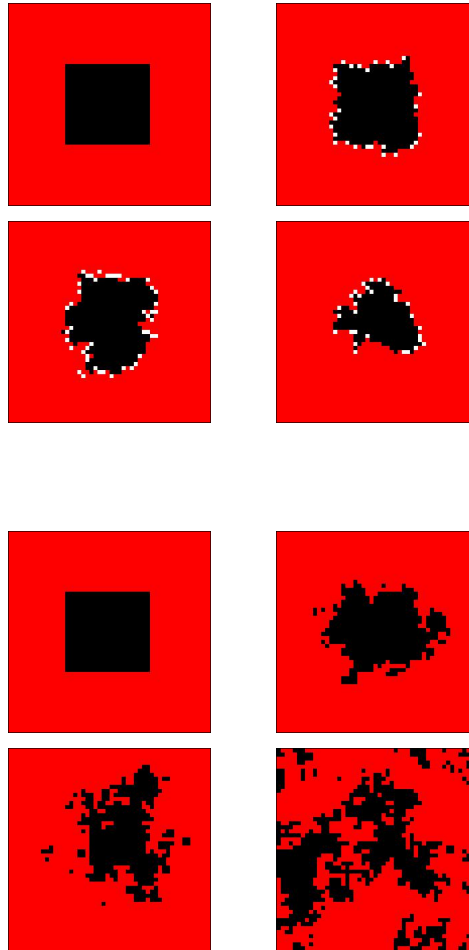


Figure 3.10: Comparison of the interface dynamics (I). Initial conditions with a single-option domain surrounded by a domain in the opposite option. Regular lattice of $N = 50^2$ individuals; $t=0, 40, 200, 1000$ from left to right. *Top:* AB-model. Curvature driven interface dynamics: the closed domain shrinks due to surface tension. *Bottom:* voter model. Noisy interface dynamics: the closed domain diffuses throughout the lattice. Red: option A , black: option B , white: AB -state.

3.2. TWO-DIMENSIONAL LATTICES

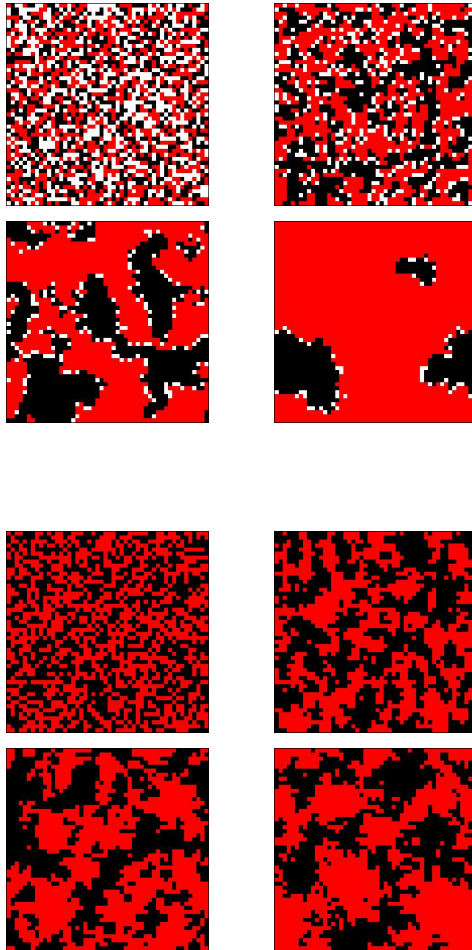


Figure 3.11: Comparison of the interface dynamics (II). Random initial conditions: snapshots of a typical simulation of the dynamics in a regular lattice of $N = 50^2$ individuals; $t=0, 8, 80, 800$ from left to right. *Top:* AB-model. Coarsening leading to the formation of single-option domains that evolve by curvature reduction. *Bottom:* voter model. Slower coarsening leading to non-localized domains evolving by interfacial noise. Red: option A , black: option B , white: AB -state.

CHAPTER 3. THE AB-MODEL (I)

mechanism, interfacial noise, such that $\langle \rho \rangle \sim (\ln t)^{-1}$ [120, 131]. Therefore, the introduction of the AB-state is identified as a mechanism to modify the interface dynamics from interfacial noise to curvature driven dynamics. In spite of the small number of AB agents that survive in the dynamical process, they cause a nontrivial modification of the dynamics. Indeed, in our simulations we observe the formation of well defined interfaces between A and B domains, populated by AB agents, that evolve by a curvature driven mechanism. The different nature of the coarsening process is illustrated comparing Figure 3.10-Top (AB-model) and Figure 3.10-Bottom (voter model), for initial conditions with a closed single-option domain surrounded by a domain in the opposite option; and Figure 3.11-Top (AB-model) and Figure 3.11-Bottom (voter model) for random initial conditions.

On the qualitative side, the inclusion of the AB agents gives rise to a much faster coarsening process, $\langle \xi \rangle \sim t^{1/2}$ (AB-model) VS $\langle \xi \rangle \sim \ln t$ (voter model); but due to the existence of metastable states, on the average it also favors a longer dynamical transient in which domains of the two competing options coexist. When comparing the times to reach consensus for both models, this results in $\frac{\tau_{AB}}{\tau_{voter}} \sim \frac{N^{0.8}}{\ln(N)}$, implying larger lifetimes on average in the AB-model before reaching an absorbing state for large fixed N .

3.3

Small world networks

Up to now, we have considered finite size effects and a regular spatial distribution of the agents. However, and as we have shown in the Introduction (Section 1.2), social networks display complex features like the small world effect: short average path length and high clustering [52]. This is a consequence of the existence in the network of long range social interactions. To study the effect of such interactions in consensus problems with two non-excluding options, we next consider the dynamics of the AB-model on a small world network [198] constructed following the algorithm of Watts & Strogatz (Section 1.2.3; [7]): starting from a two dimensional regular lattice with four neighbors per node, we rewire with probability p each of the links at random, getting in this way for intermediate values of p a partially disordered network with long range interactions throughout it.

In Figure 3.12 we show the evolution of the average interface density for different values of p . As we found in the regular lattice, we also observe here a dynamical stage of coarsening with a power law decrease of $\langle \rho \rangle$ followed by a fast decay to the A or B absorbing states caused by a finite size fluctuation. During the

3.3. SMALL WORLD NETWORKS

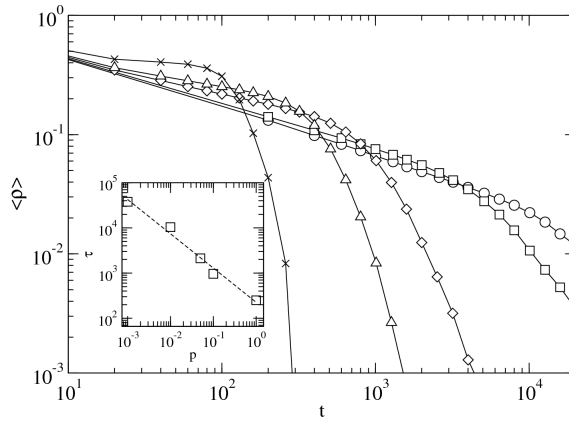


Figure 3.12: Time evolution of the average interface density $\langle \rho \rangle$ for the AB-model in small world networks with different values of the rewiring parameter p . From left to right: $p=1.0$ (\times), 0.1 (Δ), 0.05 (\diamond), 0.01 (\square), 0.0 (\circ). For comparison, the case $p = 0$ for a regular network and the case $p = 1$ corresponding to a random network are also shown. The inset shows the dependence of the characteristic time to reach an absorbing state τ with the rewiring parameter p . The dashed line corresponds to the power law fit $\tau \sim p^{-0.76}$. Population of $N = 100^2$ agents. Averages taken over 500 realizations.

dynamical stage of coarsening, the A and B communities have similar size, while the total density of AB agents is much smaller. In the range of intermediate values of p properly corresponding to a small world network, increasing the rewiring parameter p has two main effects: i) the coarsening process is notably slower; ii) the characteristic time to reach an absorbing state τ , which can be computed here as the time when $\langle \rho \rangle$ sinks below a given small value, drops following a power law (inset of Figure 3.12): $\tau \sim p^{-0.76}$, so that the absorbing state is reached much faster as the network becomes disordered.

To understand the role of the AB-state in the ordering dynamics in a small world network, the results of Figure 3.12 should be compared with the ones in Figure 3.13 for the two-state voter model in the same small world network*. In

*Notice that the small world network considered in [136] is obtained by a rewiring process of a $d = 1$ regular lattice (see Figure 1.12 in the Introduction).

CHAPTER 3. THE AB-MODEL (I)

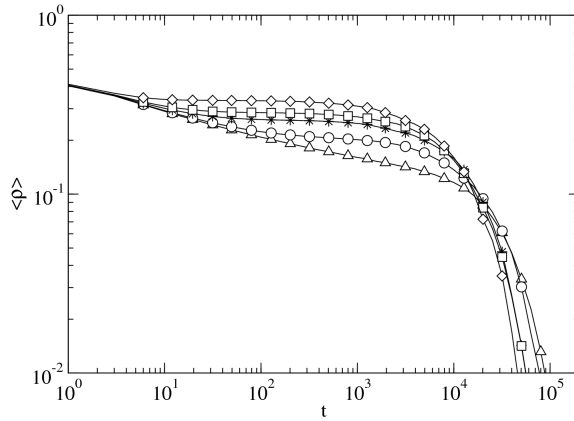


Figure 3.13: Time evolution of the average interface density $\langle \rho \rangle$ for the voter model in a small world network with different values of p . From up to bottom, $p=1.0$ (\diamond), 0.1 (\square), 0.05 ($*$), 0.01 (\circ), 0.0 (\triangle). Population of $N = 100^2$ agents. Averages taken over 900 realizations.

contrast with the AB-model, moderate values of p stop the coarsening process of the voter model leading to metastable states[†] characterized by a plateau regime for the average interface density [136, 138]. The plateau height is larger for increasing p , indicating that the domains become smaller. However, the lifetime of these states is not very sensitive to the value of p , with the characteristic time to reach an absorbing state being just slightly smaller than the one obtained in a regular lattice ($p = 0$). This is a different effect than the strong dependence on p found for the characteristic time to reach an absorbing state when AB agents are included in the dynamics. Comparing the results of Figures 3.12 and 3.13 for a fixed intermediate value of p , we observe that including AB agents in the dynamics on a small world network of interactions allows the coarsening process to take place, and it also produces an earlier decay to the absorbing state. To illustrate qualitatively the different effect of the long range interactions on the two models, we show in Figure 3.14 snapshots of the two dynamics in a small world network with $p = 0.1$. A comparison with the results in a regular

[†]In the AB-model, a metastable state is also reached, but only after the coarsening stage. As we show at the end of this Section, $\tau \sim \ln N$; and therefore, this can only be observed for very large system sizes. For comparison, let us remind that in SFKI at zero temperature these configurations become active trapped states (see Introduction 1.4.3).

3.3. SMALL WORLD NETWORKS

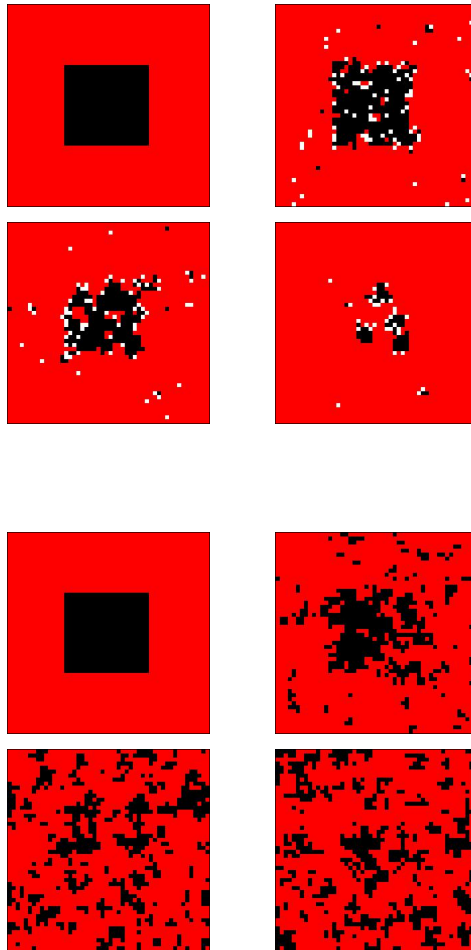


Figure 3.14: Initial conditions with a single-option domain surrounded by a domain in the opposite state: Small world network with $p = 0.1$ projected in two dimensions of $N = 50^2$ individuals; $t=0, 20, 60, 140$ from left to right. *Top:* AB-model: a domain shrinks much faster due to the long range interactions that connect it to the rest of the network, which fragment the initial domain accelerating the approach to consensus. *Bottom:* voter model: long range connections do not make a qualitative different behavior than the one observed in a regular lattice (Figure 3.10). Red: option A , black: option B , white: AB -state.

CHAPTER 3. THE AB-MODEL (I)

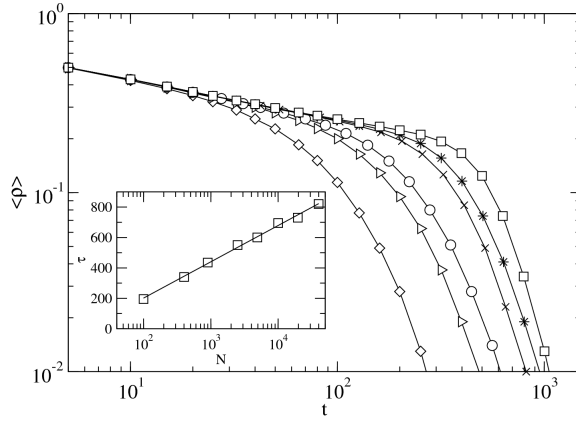


Figure 3.15: Time evolution of the average interface density, $\langle \rho \rangle$, for different values of the population size, N , in a small world network with $p = 0.1$. $N = 10^2$ (\diamond), 20^2 (\triangleright), 30^2 (\circ), 70^2 (\times), 100^2 ($*$), 200^2 (\square); from left to right. Averaged over 1000 realizations in 10 different networks. Inset: dependence of the characteristic time to reach an absorbing state τ with the system size: $\tau \sim \ln N$.

lattice (Figure 3.10) shows that a curvature driven dynamics (AB-model) is very sensitive to long range links, while noisy interface dynamics (voter model) is barely affected by them.

System size dependence for a fixed value of the rewiring parameter p is analyzed in Figure 3.15. We observe that the initial stage of the coarsening process is grossly independent of system size, but the characteristic time to reach an absorbing state scales with the system size N as $\tau \sim \ln(N)$. This results to be the same scaling law obtained in fully connected networks (see Figure 3.1), while for the voter model $\tau \sim N$ [136]. Therefore, the faster decay to the absorbing state caused by the presence of AB agents in a large system interacting through a small world network is measured by the ratio $\frac{\tau_{AB}}{\tau_{voter}}|_{SW} \sim \frac{\ln(N)}{N}$. We note that this faster decay is qualitatively the opposite result than the one found in a regular lattice where $\tau_{AB} \sim N^{1.8} > \tau_{voter} \sim N \ln(N)$. In the case of a regular lattice, on the average, AB agents slow down the decay towards the absorbing state due to the dominance of the metastable states described in the previous Section.

From random imitation to majority rule dynamics: the ϵ -model

In the previous Sections, we have shown how the extension of the voter model dynamics by the introduction of a third AB-state of coexisting options at the individual level (AB-model), leads to a radical change in the interface dynamics. A natural question that these results pose is if the crossover from interfacial noise dynamics of the voter model to curvature driven dynamics is generic for any structural modification of the voter model. In order to interpolate from the voter model dynamics towards the majority model represented by the zero-temperature SFKI model, where the dynamics is curvature driven, we have considered the coarsening process in a two-dimensional lattice in which agents can choose between two excluding options (states A and B) and the dynamic rules are as defined in Chapter 2 but with the transition probabilities (see Figure 3.16) [198]:

$$p_{i,A \rightarrow B} = \sigma_{i,B} - \epsilon \sin(2\pi\sigma_{i,B}), \quad p_{i,B \rightarrow A} = \sigma_{i,A} - \epsilon \sin(2\pi\sigma_{i,A}), \quad \epsilon \leq \frac{1}{2\pi} \quad (3.2)$$

In the following, we call this modification of the voter model the ϵ -model. The parameter ϵ measures the strength of the term that perturbs the interaction rules of the voter model ($\epsilon = 0$). This perturbation of the voter model implies that the probability of changing option is no longer a linear function of the density of neighboring agents in the option to be adopted. With the perturbation term chosen here, there is a nonlinear reinforcing (of order ϵ) of the effect of the local majority: the probability to make the change $A \rightarrow B$ is larger [smaller] than σ_B when $\sigma_B > 1/2$ [$\sigma_B < 1/2$]. In particular, we note that for $\epsilon \neq 0$, the conservation law of the ensemble average magnetization [127, 129], a characteristic symmetry of the voter model, is no longer fulfilled. For later comparison we recall that in the zero-temperature SFKI model the local majority determines, with probability one, the change of option: $p_{A \rightarrow B} = 1$ [0] if $\sigma_B > 1/2$ [$\sigma_B < 1/2$].

Notice that the AS-model (Figure 2.1) defines another modification of the linear transition probabilities of the voter model*, in which the volatility of the agents accounts for a different interaction mechanism: the reinforcing ($a > 1$) or relaxation ($a < 1$) of the inertia to change the current state of the agent[†].

*Other nonlinear modifications of the voter model dynamical rules have been extensively studied in [222].

[†]The AS-model is studied in detail in Chapter 6.

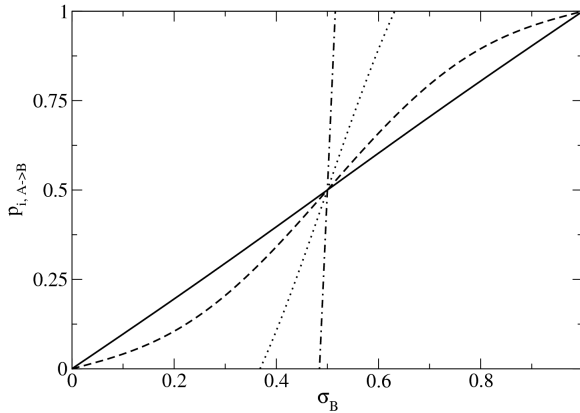


Figure 3.16: Transition probabilities (Equation (3.2)) for the ϵ -model for different values of ϵ . When $\epsilon > 1/(2\pi)$ the transition probability for such a given ϵ is defined as follows: $p_{i,A \rightarrow B}$ as given by Equation (3.2) for values of σ such that $0 \leq p_{i,A \rightarrow B} \leq 1$; $p_{i,A \rightarrow B} = 0[1]$ for values of σ such that Equation (3.2) gives $p_{i,A \rightarrow B} < 0[> 1]$. The limit $\epsilon \rightarrow \infty$, corresponds to the step-function transition probability of the SFKI model at zero temperature. $\epsilon = 0.01$ (solid line), 0.2 (dashed), 1.0 (dotted), 10.0 (dot-dashed).

Our results for the exponent γ in a power law fitting $\langle \rho \rangle \sim t^{-\gamma}$ for the ϵ -model are shown in Figure 3.17 for different values of ϵ . In these simulations we have considered a two-dimensional lattice with eight neighbors per node so that more values are allowed for the perturbation term in Equation (3.2). For very small values of ϵ we observe an exponent $\gamma \simeq 0.1$ compatible with the logarithmic decay ($\langle \rho \rangle \sim (\ln t)^{-1}$) of the voter model, as obtained in [180]. However, for small but significant values of ϵ there is a crossover to a value $\gamma \simeq 0.5$ associated with curvature driven coarsening. With probability around 1/3 (for large enough systems), trapped metastable states analogous to the ones found in the AB-model (Figure 3.6-Right) are also found for values of ϵ for which $\gamma \simeq 0.5$. The fraction of realizations close to 1/3 corresponds to the probability to reach a frozen configuration in the SFKI at zero temperature [147, 148]. The distribution of survival times of these metastable states also displays an exponential tail analogous to the one found in Figure 3.7 for the AB-model. These realizations have been removed to calculate the values of γ in Figure 3.17.

3.5. CONCLUDING REMARKS

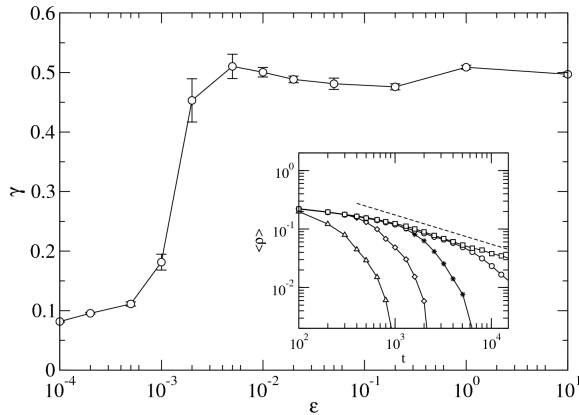


Figure 3.17: Characteristic coarsening exponent γ ($\langle \rho \rangle \sim t^{-\gamma}$) for the ϵ -model as a function of the perturbation parameter ϵ . $N = 400^2$ agents. Averages taken over 75 realizations. Inset: time evolution of the average interface density. From left to right: $N = 20^2$ (Δ), 50^2 (\diamond), 100^2 ($*$), 200^2 (\circ), 400^2 (\square) agents. Averages taken over 100 realizations. Given a value of ϵ ($\epsilon = 0.01$ in the inset), a power law for the average interface density decay is found for large enough system sizes. Dashed line for reference: $\langle \rho \rangle \sim t^{-0.5}$.

We conclude that a small perturbation on the linear transition probabilities of the voter model dynamics, such that there is a nonlinear reinforcing of the effect of the local majority, leads to a new interface dynamics equivalent to the one found for the AB-model by including a third state where options are non-excluding. This illustrates the fact that the voter model dynamics is very sensitive to perturbations of its dynamical rules.

3.5

Concluding remarks

In this Chapter, we have analyzed an extension of the voter model, the AB-model, addressing the effects of introducing a third state of non-excluding options at the individual level (AB-state). For this, we have studied the model in different

CHAPTER 3. THE AB-MODEL (I)

networks, fully connected networks, two-dimensional lattices and small world networks.

The mean field analysis shows that in the thermodynamic limit a global consensus state (A or B) is reached in the AB-model with probability one, except for initial conditions lying on the stable manifold ($\Sigma_A = \Sigma_B$) of the saddle fixed point corresponding to unstable coexistence of the three states. However, when considering a fully connected network to account for the finite size effects, fluctuations drive the system out from the unstable fixed point and consensus is always reached, with an average time to consensus that scales with the system size as $\tau \sim \ln(N)$.

We have analyzed exhaustively the AB-model dynamics in two-dimensional lattices. A domain of agents in the AB-state is not stable and the density of AB agents becomes very small after an initial fast transient, with AB agents placing themselves in the interfaces between single-option domains. In spite of these facts, the AB agents produce an essential modification of the processes of coarsening and domain growth, changing the interfacial noise dynamics of the voter model into a curvature driven interface dynamics characteristic of two-state models with updating rules based on local majorities like SFKI dynamics [110]. In this way, the typical growth of the size of single-option domains, ξ , changes from $\xi(t) \sim \ln(t)$ to $\xi(t) \sim t^\alpha$, with $\alpha \simeq 0.5$. This change in the coarsening mechanism is also found for small perturbations of the random imitation dynamics of the voter model that modify the linear dependence of the transition probabilities on the local densities (ϵ -model). This result indicates that the effect might be generic for small structural modifications of the voter model dynamical rules. We have also shown that in a two dimensional regular lattice, the system reaches stripe-like trapped metastable states with a probability around 1/3 in both the AB-model and the ϵ -model, as observed in the majority rule dynamics based on group interaction [101]. The average time to consensus for the AB-model has been shown to scale with the system size as $\tau \sim N^{1.8}$. This dependence with system size is dominated by the presence of the metastable states mentioned above. Compared to the $\tau \sim N \ln(N)$ for the voter model, the AB agents produce a faster coarsening, but also longer times for extinction due to the presence of these metastable states.

The effect of the topology of interactions such as the role of long range connections throughout the network, has been addressed considering a small world network. While for the original two-state voter model the small world topology results in long lived metastable states in which coarsening has become to a halt [136, 138], the AB agents restore the processes of coarsening and domain

3.5. CONCLUDING REMARKS

growth*. Additionally, they speed-up the decay to the absorbing state by a finite size fluctuation: while in the voter model the times to consensus are essentially not affected by the parameter of rewiring p , in the AB-model we obtain $\tau \sim p^{-0.76}$, indicating a strong dependence of the times to consensus on the parameter of rewiring. Moreover, we obtain a characteristic time to reach an absorbing state that scales with system size as $\tau \sim \ln N$, to be compared with the result $\tau \sim N$ for the voter model: the decay to the absorbing state is much faster in small world networks when AB agents are present. Notice that the effect of the AB agents on the times to consensus depends on the network of interaction: τ increases in two-dimensional lattices due to the existence of trapped metastable states, while it is shown to decrease in small world networks due to the fragmentation of domains and its faster shrinking produced by the presence of long range interactions in the network.

*Notice that in the AB-model, a metastable state is also eventually reached but only after the coarsening stage. As $\tau \sim \ln N$, this can only be observed for very large system sizes.

The AB-model (II): networks with mesoscale structure

A key characteristic of nonequilibrium dynamics of interacting many body systems is the relaxation time. Typically, finite systems starting from generic initial conditions far from equilibrium reach a final stationary state or attractor in a characteristic time. For simple nonequilibrium lattice models [128] the dynamics often leads to an absorbing state. In some cases the system might get stuck in a metastable state, which generally also has a well defined expected lifetime. Frozen trapped configurations that persist indefinitely in the absence of fluctuations are also possible [148]. An intriguing situation occurs when such a characteristic time cannot be defined. In the first part of this Chapter, we show that this is the case for the AB-model in networks with community structure (see Section 1.2.4), in which the system reaches different trapped metastable states with very different lifetimes, leading to a broad distribution of consensus times (publication in Ref. [215]). Trapped metastable states are associated to different topological substructures in the network where the dynamics gets stuck for long but finite times in finite systems (see Section 1.4.1). The class of networks studied [109] accounts for many of the features observed in real social networks, incorporating nontrivial community structure which introduces structural correlations. The results for the AB-model are compared to the voter model dynamics in the same class of networks.

The question of general conditions under which a broad distribution of lifetimes is obtained merits a detailed and systematic study. In the second part of this Chapter and motivated by the results obtained for the AB-model in the class of networks mentioned above, we address this question by investigating the role

of the mesoscale structure of the network and its topological traps in nonequilibrium ordering dynamics with two non-excluding options. We focus on the question of which features of the network topology, such as relatively isolated groups of nodes, the presence of communities, their interconnectivity, or their size distribution, give rise to trapped metastable states. To this end, we study the dynamics of the AB-model in a controlled setting by constructing simple test case networks in which community boundaries are clear (publication in Ref. [216]).

4.1

Anomalous lifetime distributions and topological traps in ordering dynamics

In order to study the effects of networks with mesoscale structure in consensus dynamics with two non-excluding options, in this Section we analyze and compare the voter model and the AB-model in a class of social networks with community structure. With this aim, we explore the time evolution of the average interface density, the nature of the metastable states appearing in the dynamics, and the lifetime distributions in a large sample of networks.

4.1.1 The network model: a class of social networks

Several models have been designed to capture some of the characteristics of social networks, based on mechanisms such as geographical proximity [104], social similarity [103, 107], and local search [105, 106, 109] (see also Section 1.2.4). A combination of random attachment with local search for new contacts has

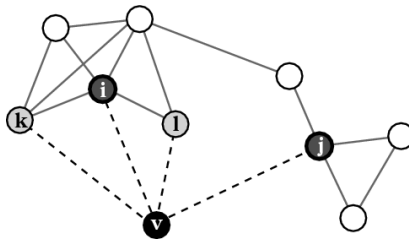


Figure 4.1: Growth process of the network. The new vertex v links to one or more randomly chosen initial contacts (here i, j) and possibly to some of their neighbors (here k, l).

4.1. LIFETIME DISTRIBUTIONS AND TOPOLOGICAL TRAPS

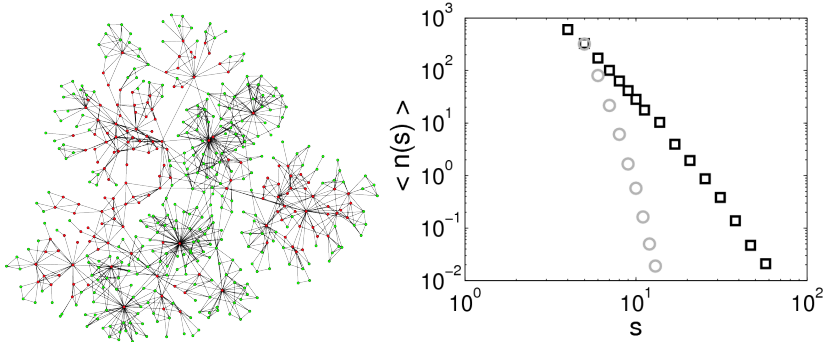


Figure 4.2: Left: A partial view of the network centered on a randomized selected node. Right: Average number $\langle n(s) \rangle$ of k -clique-communities of size s for $k = 4$ (\square) and $k = 5$ (\circ), in networks of size $N = 10\,000$, averaged over 400 realizations.

proved fruitful in generating well-known features of social networks, such as assortativity, broad degree distributions, and community structure [109] (see also [65]). In this way, the community structure leads naturally to high values of the clustering coefficient.

The algorithm to generate this class of networks [109] consists of two growth processes: 1) random attachment, and 2) implicit preferential attachment resulting from following links from the randomly chosen initial contacts. The local nature of the second process gives rise to high clustering, assortativity, broad degree distribution and community structure. Starting from any small connected seed network of N_0 vertices, new nodes are added as follows (see Figure 4.1): i) Pick $n_{init} \geq 1$ random nodes as initial contacts. ii) Pick $n_{sec} \geq 0$ neighbors of each initial contact as secondary contacts. iii) Connect the new node to the initial and secondary contacts. In this Chapter, we use the *standard parameters* [109]: the number of initial contacts is selected according to the probabilities $p(n_{init} = 1) = 0.95$, $p(n_{init} = 2) = 0.05$; and the number of secondary contacts from each initial contact, n_{sec} , is chosen from a uniform probability distribution between 0 and 3. The initial seed contains $N_0 = 10$ nodes.

The degree distributions of the resulting networks are found to decay slower than exponential [109]. Using the k -clique algorithm [86] for detecting communities*, a broad distribution of community sizes is found in the model (Figure 4.2).

*In fact, the algorithm searches for k -clique communities. A k -clique community is defined as a union of all k -cliques (complete subgraphs of size k) that can be reached from each other through a series of adjacent k -cliques (where adjacency means sharing $k - 1$ nodes).

CHAPTER 4. THE AB-MODEL (II)

For reference, we use randomized versions of the same networks, where the degree sequence is kept intact but edges are randomly rewired under the restriction that the network must stay connected [223]. This eliminates degree correlations, and as a consequence, community structure and clustering. The randomized networks are therefore locally treelike.

4.1.2 Trapped metastable states and lifetime distributions

We have considered the transition probabilities (2.8) for the voter model*, and (2.10)-(2.11) for the AB-model in the class of networks described above. We followed the evolution over time of the interface density and of the fraction of runs that had not yet reached consensus at any particular time, $P(t)$ (see Section 2.5). When results for the original and randomized networks differ, we can conclude that structural characteristics other than the degree distribution are responsible for the differences.

Interface density

The average interface density $\langle \rho \rangle$ on the class of networks considered here, and on their randomized counterparts is shown in Figure 4.3. For the voter model (Figure 4.3(a)), the structure of the network does not alter the qualitative behavior. In both classes of networks we observe plateau values of $\langle \rho \rangle$ associated with metastable states. Still, the plateau value for networks with community structure is lower than for the randomized networks, indicating that the typical size of spatial domains where agents are in the same state is larger. We also observe in both cases that finite size fluctuations drive the system to an absorbing state. The characteristic time to reach consensus (mean lifetime of the metastable state) depends on network size but it does not depend sensitively on network structure. The inset in Figure 4.3(a) shows that the time to reach consensus depends linearly on network size for networks with communities and their randomized counterparts[†]. These results support the earlier finding made on networks without mesoscale structure that effective dimensionality dominates voter model behavior [138].

*To be precise, we have considered the original voter model dynamics, neglecting the prefactor 1/2 in Equation (2.8).

[†]The slight deviation from linear scaling is due to the violation of the magnetization conservation law when using node update dynamics on networks with nodes of very different degree (see Section 1.4.2; [129]).

4.1. LIFETIME DISTRIBUTIONS AND TOPOLOGICAL TRAPS

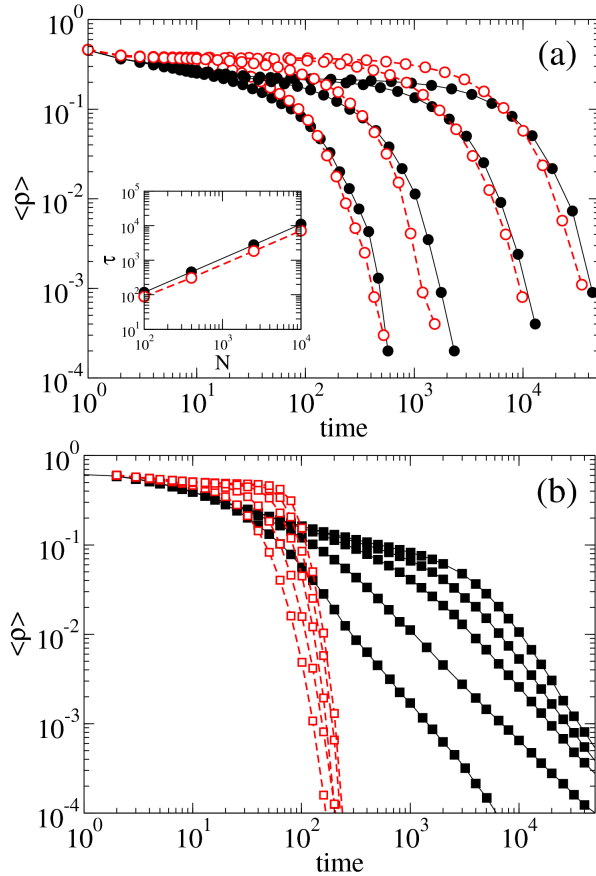


Figure 4.3: Time evolution of the average interface density in networks with community structure (solid symbols) and randomized networks (empty symbols) with the same degree distributions. (a) Voter model. Network sizes increase from left to right: $N = 100, 400, 2500, 10000$. Averages are taken over 100 different realizations of the model network, with 10 runs in each. Inset: the time to reach consensus scales with network size as $\tau \sim N^\gamma$, $\gamma \approx 0.96$ for the randomized and $\gamma \approx 0.98$ for the original networks. (b) AB-model. Network sizes increase from left to right: $N = 100, 400, 2500, 10000, 40000$. Averages taken over 400 – 5000 realizations (depending on system size) of the model network, and with 10 runs in each.

CHAPTER 4. THE AB-MODEL (II)

Figure 4.3(b) shows the average interface density for the AB-model. We observe significant differences between the original and the randomized version networks: a plateau value of $\langle\rho\rangle$ is observed for randomized networks, while a first dynamical stage of coarsening where spatial domains grow in size is found for large networks with community structure. The plateau observed in randomized networks indicates that a metastable state of the class found in the voter model for both types of networks is rapidly reached*. Moreover, in the randomized networks there is a fast decay of $\langle\rho\rangle$ towards an absorbing state with a characteristic time to reach consensus almost independent of system size. On the contrary, for the networks with a community structure we observe two dynamical stages in the time evolution of $\langle\rho\rangle$. After an initial power law associated with coarsening there appears a second power law tail in the approach to the absorbing state. This last power law decay indicates that the mean lifetime to reach consensus for the AB-model does not characterize the dynamics on these networks and that metastable states exist at all time scales, as we discuss below. Additionally, the difference with the randomized networks in several orders of magnitude for the extinction times, which increases with system size, shows that the network with communities slows down the dynamics significantly. All together, these results manifest a sensitivity of the AB-model to the mesoscale network structure which is not found for the voter model.

Fraction of alive runs

The *lifetime* of a run is defined as the number of time steps it takes to reach either of the absorbing states. Figure 4.4 shows the *fraction of alive runs*, that is, the fraction of simulations which still have not reached an absorbing state at time t , $P(t) = 1 - \int_0^t p(t')dt'$, where $p(t)$ is the probability distribution of lifetimes[†] (see Section 2.5). For the voter model, the fraction of alive runs decreases exponentially in both the original and randomized networks (Figure 4.4-inset), giving a characteristic time for the dynamics. This is in agreement with previous results for the voter model in high dimensional complex networks [138]. A rather different result is shown for the AB-model (Figure 4.4), where we find a power law behavior $P(t) \sim t^{-\alpha}$, $\alpha \approx 1.3$, so that a mean lifetime of the realizations of the AB-model does not give a characteristic time scale[‡]. At any time there are alive realizations which have not reached the absorbing state. Different parameterizations of the

*This behavior is similar to the one previously found in a random network obtained with the Watts-Strogatz algorithm ($p = 1.0$); see Figure 3.12.

[†]In our numerical analysis, we use $P(t)$ instead of $p(t)$ in order to reduce the fluctuations in the tails of the distribution.

[‡]This is because for exponents $1 < \alpha < 2$, the mean lifetime is well defined, but the second moment of the probability distribution of lifetimes, $p(t) \sim t^{-(\alpha+1)}$, diverges.

4.1. LIFETIME DISTRIBUTIONS AND TOPOLOGICAL TRAPS

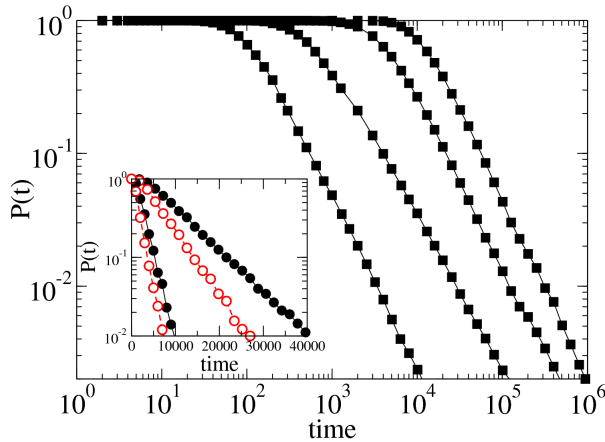


Figure 4.4: Fraction of alive runs in time for networks with communities (solid symbols) and randomized networks (empty symbols). AB-model (double logarithmic plot); system sizes $N = 100, 400, 2500, 10000$ from left to right, with averages taken over different realizations of the network (400 – 5000 depending on system size), with 10 runs in each. Inset: voter model (semilogarithmic plot). System sizes $N = 2500, 10000$. Averages are taken over 100 different realizations of the networks, with 10 runs in each.

network model (not shown) produce the same qualitative phenomenon: we have modified the number of secondary contacts from each initial contact, n_{sec} , using uniform probability distributions between 0 and 1, 2, 4, obtaining also a power law for the distribution of alive runs with an exponent smaller than 2, which indicates the robustness of this result. This behavior is different from the usual exponential decay of the tails of $P(t)$ observed for the AB-model, either in regular, small world and random networks (see Sections 3.2-3.3; [198]), or Barabási-Albert scale-free networks (not shown), and reflects the existence of metastable states at all time scales. This fact indicates that the anomalous lifetime distribution is linked to the structure of the network at a mesoscale level. Such structure seems to give rise to trapped metastable states at all time scales. To substantiate this claim, we next look at some detailed dynamics.

Discussion

Further understanding of the dynamical process can be obtained by considering the measure called overlap of a link, $O(i, j)$ [49]. This characteristic of a link

CHAPTER 4. THE AB-MODEL (II)

between two nodes (i and j) tells us essentially which fraction of their neighbors is shared by the nodes. Within a community, nodes tend to share many neighbors, and thus overlap is high, while edges between communities have low or zero overlap. Considering dynamics of competing options on a network, the overlap can be used to identify spatially homogeneous domains in the network: if the average overlap (O) of the links in the interface between domains is low, we may assume that the domain boundaries follow the community boundaries. On the other hand, if the overlap at the interfaces is high, it indicates that nodes within communities are in different states. For the voter model dynamics, the average overlap of interface links drops to about 80 percent of the average value $\langle O \rangle = 0.27$ of the whole network, while in the AB-model it drops to under 70 percent. This indicates that in both models the interfaces between domains lie preferably in low overlap links, so that domains of the same option follow the community structure, but in the AB-model these domains are correlated with the communities closer.

The difference between the two dynamics is better understood by looking at snapshots of the dynamics (Figure 4.5) which show the characteristic behavior for each of the models starting from random initial conditions. In the voter model (left), the homogeneous domains of nodes with the same option appear to follow the community structure, but a particular community (topological region) may change the option adopted by the community rather quickly ($t = 50, 60, 70$). At variance with this behavior, in the AB-model (right) spatial domains grow and homogenize steadily in a community without much fluctuation. For this dynamics, communities that have adopted a given option, and which are poorly linked to the rest of the network, take a long time to be invaded by a different option, acting therefore as topological traps. As an example, we show two trapped metastable states at $t = 430$ and $t = 1000$, where the interface stayed relatively stable for a prolonged period* (about 100 and 1000 time steps, respectively). These different behaviors reflect in the community structure the two different interfacial dynamics discussed in Section 3.2: interfacial noise driven dynamics for the voter model, and curvature driven dynamics for the AB-model with agents in the AB-state at the interfaces.

Different realizations of the algorithm to construct the network produce different detailed structures of the network. The power-law for the fraction of alive runs in Figure 4.4 is a statistical effect of the average over such realizations. The time evolution of the average interface density on single realizations of the network,

*Notice that a qualitatively similar picture has been obtained by Blondel et al. [46] when analyzing real data from customers of a Belgian mobile phone network (see Figure 1.3). They also find correlations between community structure and the language of the customers.

4.1. LIFETIME DISTRIBUTIONS AND TOPOLOGICAL TRAPS

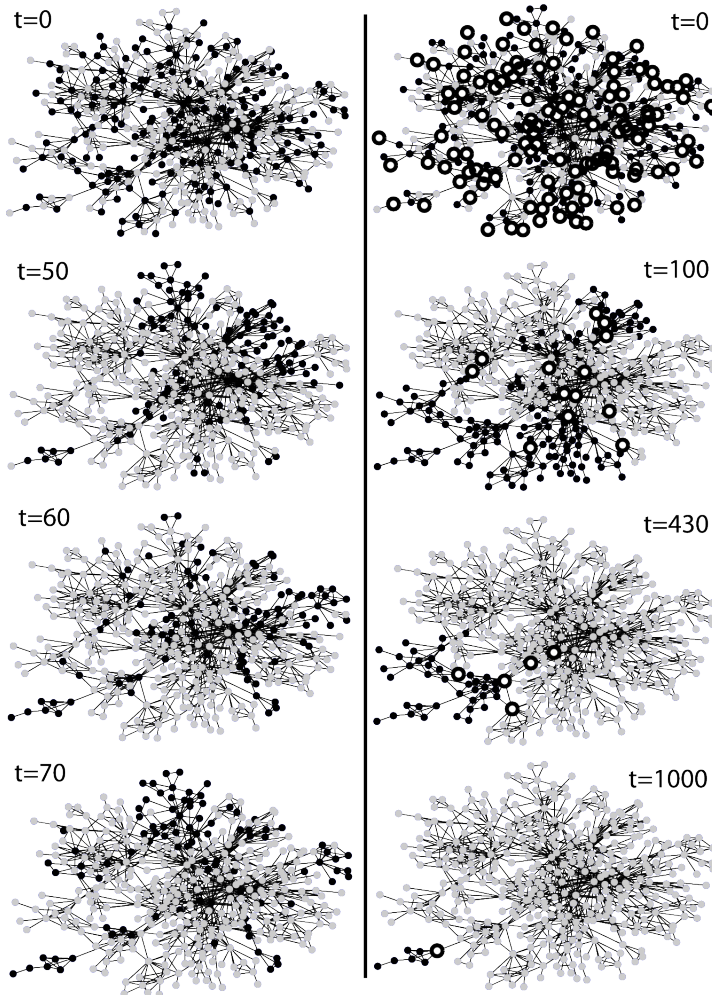


Figure 4.5: Snapshots of the dynamics, with nodes in state A in black, B in gray, and AB in white circled in black. Simulations start from random initial conditions. Left: voter model. Right: AB-model; where we show typical configurations of trapped metastable states ($t = 430$ and $t = 1000$).

CHAPTER 4. THE AB-MODEL (II)

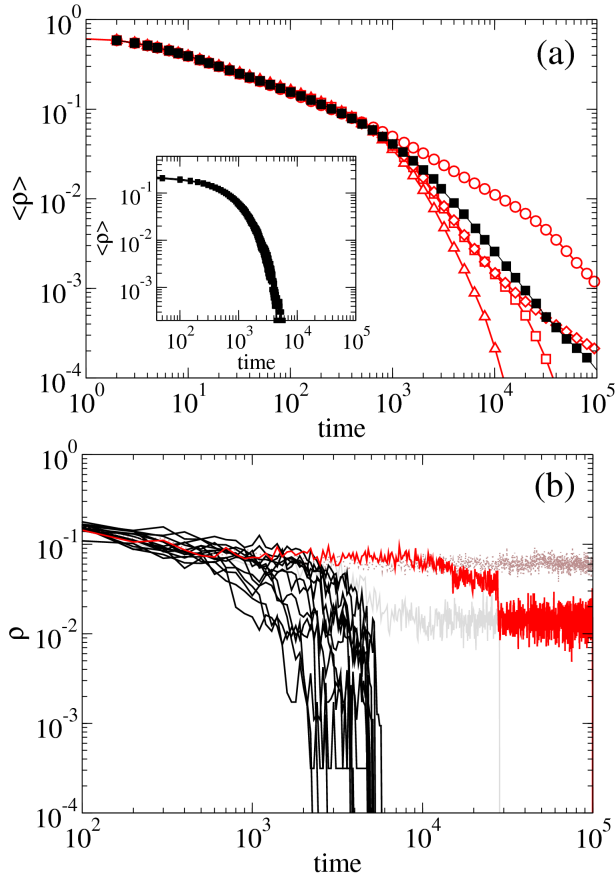


Figure 4.6: (a) Time evolution for the AB-model of the average interface density on different realizations of the network with 2500 agents; 20000 runs on each (empty symbols). The extreme cases were selected as examples of networks where *trapped metastable states* (see text) are found *often* (○); and found *rarely* (△). For comparison, the average over 500 networks (10 runs on each) is also shown (■). Inset: time evolution for the voter model of the average interface density for four realizations of the network model with 2500 agents; 5000 runs on each network. (b) Time evolution of the interface density in single realizations of the AB-model on a network with 2500 agents. A class of realizations decay to the absorbing state after a coarsening stage (solid black lines), while others fall in long-lived trapped metastable states. The latter display several plateaus, indicating hierarchical levels of ordering before reaching the absorbing state, or cascading between several trapped metastable states.

4.1. LIFETIME DISTRIBUTIONS AND TOPOLOGICAL TRAPS

$\langle \rho \rangle$, is shown for the AB-model in Figure 4.6(a). After the coarsening stage, we observe different behaviors in the second stage of the decay of $\langle \rho \rangle$ depending on the specific realization of the network: from broad tails to exponential-like decays, with an intermediate behavior. On the contrary, and in agreement with our previous discussion, the voter model dynamics (Figure 4.6(a), inset) is not sensitive to the details of the network structure. For the AB-model some realizations of the network topology produce particularly long lived metastable states, while in others, corresponding to exponential-like decay of $\langle \rho \rangle$, they are observed rarely*. Plots of the interface density of individual runs on a given network show a class of realizations with different plateaus (ordering levels) where the system gets trapped for a long time (Figure 4.6(b)). These trapped metastable states, analogous to those displayed in Figure 4.5-Right, correspond to the structure in the network. The variety of traps and associated different lifetimes seems to be the mechanism that causes an anomalous power law distribution for the lifetimes.



The main result obtained in this Section concerns the power law distribution for the times to reach consensus in the AB-model, such that its mean lifetime does not give a characteristic time scale for the ordering dynamics. This has been found to be due to the existence of trapped metastable states at any time scale, appearing when the noisy interface dynamics of the voter model becomes curvature driven due to the introduction of the AB-state in the dynamics (AB-model).

Within this context, simpler configurations of community structure should be considered in order to gain a deeper understanding of the microscopic mechanisms underlying the dynamical effects observed for the AB-model. Therefore, in the following Section we study sufficient conditions for the existence of broad consensus time distributions in networks with mesoscale structure.

*We note that although the details of each network realization matter for the occurrence of trapped metastable states, the community size distribution detected by the k -clique-percolation method [86] is the same for all the network realizations that we have considered. The available statistical methods seem not to be sufficient to discern between the network topologies producing many or few trapped metastable states.

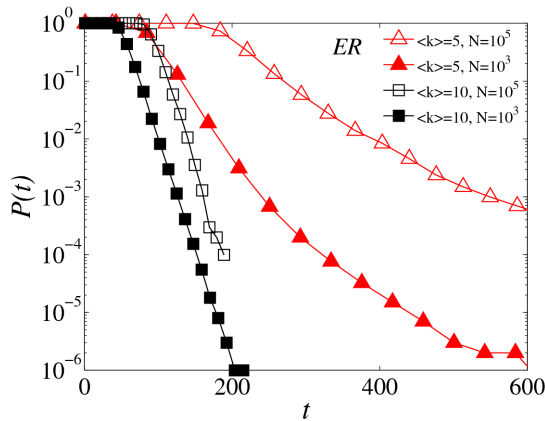


Figure 4.7: Fraction of alive runs at time t , $P(t)$, for Erdős-Rényi networks with different average degrees: $\langle k \rangle = 10$ (\square), $\langle k \rangle = 5$ (\triangle). Solid symbols, network size $N = 10^3$; open symbols, $N = 10^5$. Averaged over 100 network realizations, 100 runs in each (1000 in each for $N = 10^3$).

4.2

Sufficient conditions for broad lifetime distributions in complex networks

In order to gain further understanding on the broad lifetime distributions obtained in the previous Section, in the remainder we focus on the study of the AB-model dynamics in networks with a predesigned mesoscale structure. As a preliminary study, we consider random networks where we already identify substructures causing broad distributions of lifetimes in random networks with low average degree. To explain the observations therein, we introduce the concept of *dynamical robustness* measured by the survival time (i.e., a characteristic relaxation time) of relatively isolated groups of nodes in a state different from the one in the final absorbing state. Then, we study the effect of the presence of communities starting from an underlying random network and communities of equal size, to consider later an exponential distribution for the sizes of different communities.

4.2. BROAD LIFETIME DISTRIBUTIONS IN COMPLEX NETWORKS

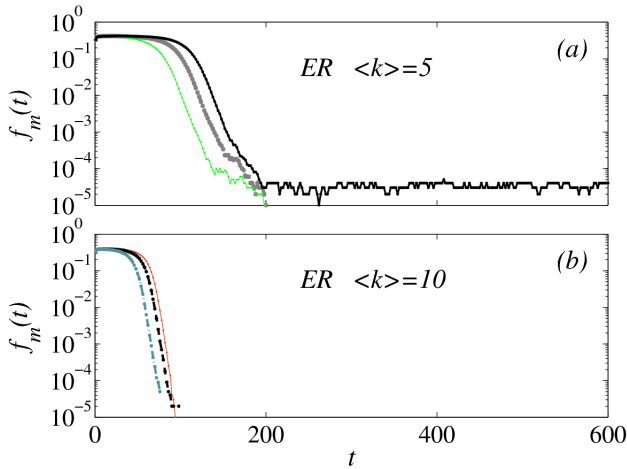


Figure 4.8: Time evolution of the fraction f_m of nodes in the state (A or B) that becomes the minority and finally dies out. We show several individual runs. (a) ER network: $\langle k \rangle = 5$, $N = 10^5$; (b) ER network: $\langle k \rangle = 10$, $N = 10^5$.

4.2.1 Random networks

Erdős-Rényi Networks

We first consider the Erdős-Rényi (ER) random network topology (see Section 1.2.3; [30]), in which each of the possible links between the N nodes is present with probability p (link density). Notice that the network can equivalently be characterized by the average degree $\langle k \rangle = p(N - 1)$. We find that in Erdős-Rényi networks the fraction of alive runs $P(t)$ depends unexpectedly on link density (Figure 4.7), so that, for high link densities up to a fully connected network, $P(t)$ is clearly exponential, but for low link densities it turns out to be broader, indicating the existence of metastable states. The cases of $\langle k \rangle = 10$ and $\langle k \rangle = 5$ are selected to illustrate this difference.

The metastable states are visualized by displaying the fraction f_m of nodes in the minority state* in individual runs (Figure 4.8(a)). Figure 4.8(b) shows that metastable states do not arise for $\langle k \rangle = 10$. The observed metastable states concern only a very small fraction of nodes and further analysis reveals that they

*In fact, notice that the real minority state is the AB-state. However, for convenience we use the term *minority state* to refer to the single-option state (A or B) with less agents in the system and which finally dies out.

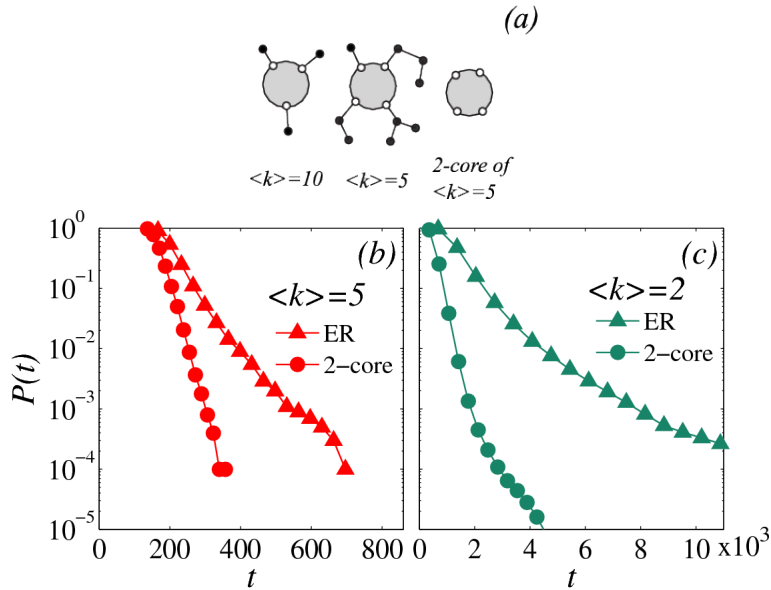


Figure 4.9: (a) Schematic illustration of branches in the different ER networks studied. The root nodes are indicated by open circles. (b) The fraction of alive runs $P(t)$ for ER networks with $\langle k \rangle = 5$ and $N = 10^5$, and their two-cores. (c) ER networks with $\langle k \rangle = 2$ and $N = 2 \times 10^3$, and their two-cores. Averages over 100 network realizations, 100 runs in each (5000 network realizations for two-core of $\langle k \rangle = 2$).

are associated primarily with “branches”. We use the term branch to indicate maximal treelike substructures that are connected to the rest of the network through a node that has degree $k > 2$, which we call the root node of the branch (see Figure 4.9(a) for illustration). Therefore, the metastable states found here are trapped metastable states associated with branches. Branches can be removed from the network (except for the root node) by successively removing nodes of degree $k = 1$ until all the remaining nodes have degree $k \geq 2$, that is, by taking the *two-core* of the network [224]. We call diameter of the branch, the maximal network distance from the root node to any other node in the branch. Figure 4.9(a) displays schematically the difference between the ER networks with $\langle k \rangle = 5$ and 10 with respect to the presence of branches. In the ER networks with $\langle k \rangle = 10$, typically only branches with diameter one are present, while branches with diameter 2 or 3 arise frequently in ER networks with $\langle k \rangle = 5$, often with claw-like bifurcations.

4.2. BROAD LIFETIME DISTRIBUTIONS IN COMPLEX NETWORKS

Taking the two-core of ER networks with $\langle k \rangle = 5$ and running the AB-model in the resulting networks confirms the role of branches in producing a deviation from an exponential distribution in $P(t)$, see Figure 4.9(b). The trapped metastable states disappear and an exponential lifetime distribution is recovered. In very sparse ER networks, illustrated by the case $\langle k \rangle = 2$ in Figure 4.9(c), a slight deviation not explained by branches remains that could be attributed to the largely chainlike structure of the networks*. However, the branches are clearly responsible for the longest-lived trapped metastable states.

Dynamical robustness and survival times

In order to characterize the behavior of relatively isolated groups of nodes that remain in the minority state after most of the network has homogenized in either state A or B, we introduce the concept of *dynamical robustness* against invasion for a given topological structure. It concerns a group of nodes, G , subject to dynamics of competing options. It measures the resistance of G against the outside pressure applied to G by its neighbors, G' (Figure 4.10). We initialize the nodes in G to state B, and fix the nodes in G' permanently to state A. The dynamical robustness of G is then characterized by a survival time, τ , defined as the characteristic time it takes for G to homogenize to state A. The dynamical robustness of G becomes larger with increasing survival time.

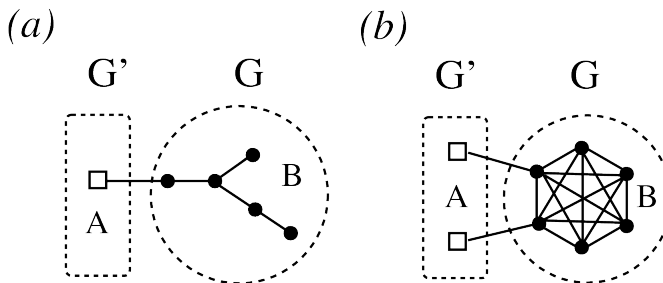


Figure 4.10: Characterization of the dynamical robustness against invasion for a given topological structure G . We show a schematic view for two example cases: (a) branch excluding the root node; (b) clique.

As an example, consider the dynamical robustness of branches with diameters 2 and 3, one of them containing a bifurcation (Figure 4.11). The time it takes for each of these topologies to homogenize to the consensus state appears to

*Notice also that it has been argued that modularity may arise from fluctuations in sparse ER networks [225].

CHAPTER 4. THE AB-MODEL (II)

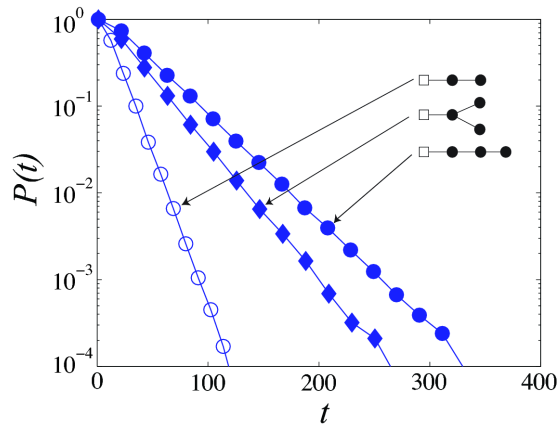


Figure 4.11: Fraction of alive runs $P(t)$ for a chain (a branch with no bifurcations) with diameter 2 (open circles), a branch with diameter 2 with a single bifurcation (diamonds), and a chain with diameter 3 (solid circles), initialized such that the nodes denoted by open squares are permanently set to one state, and the remaining nodes are initially set to the opposing state (as in Figure 4.10(a)). We performed 10 000 runs in each topology.

be distributed exponentially, $P(t) \sim e^{-t/\tau}$ but with a different characteristic time τ , corresponding to different time scales. For a branch with a given diameter, bifurcations increase the survival time. It is noteworthy that, compared to the times it takes for an ER network with no branches to reach consensus (Figure 4.9(b)), the time that a single branch may remain with the minority option is very long.

Each branch of different diameter, and with a different number of bifurcations, produces an exponential lifetime distribution with a different characteristic time τ . The combination of various time scales leads to the observed broader than exponential lifetime distribution in ER networks with low-link-density .

4.2.2 The role of communities

Networks with equally sized cliques

In this Section, we discuss the effect of communities on lifetimes of the system, using simple test networks with equally sized communities. To keep things as clear as possible, we use cliques, i.e., fully connected subgraphs, as communities.

4.2. BROAD LIFETIME DISTRIBUTIONS IN COMPLEX NETWORKS

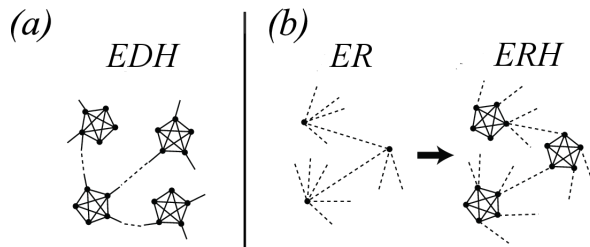


Figure 4.12: Generation of networks with equally sized cliques: (a) EDH and (b) ERH. To obtain an ERH network of size N , we begin with an underlying ER network with N/s nodes, where s is the clique size.

We denote by $k_{c,out}$ the clique out-degree, that is, the number of links connecting each clique to outside nodes (note that the term out-degree here does not refer to directed edges). For a node in a clique of size s , we denote the number of links to the other nodes within the clique by $k_{n,in} = s - 1$, and the average number of links to nodes outside the clique by $\langle k_{n,out} \rangle = k_{c,out}/s$ *

We use two different methods for connecting the cliques. In the first construction, $k_{c,out}$ is equal for all cliques. We label these networks EDH, for Equal out-Degree and Homogeneously sized cliques. The $k_{c,out}$ link ends are assigned to randomly selected nodes in each clique, and then randomly paired, under the condition that two link ends from the same clique are not allowed to be connected (Figure 4.12(a)). In the second construction, we begin with an ER network, with high link-density to avoid branches with diameter larger than one, and replace its nodes with equally sized cliques (Figure 4.12(b)). Each of the ends of the links of the underlying Erdős-Rényi network, which connect two cliques, are again assigned to a randomly selected node in each clique. We label these networks ERH, as they are based on an underlying ER network, and consist of Homogeneously sized cliques. In ERH networks, $k_{c,out}$ is distributed according to the Poisson distribution of the underlying ER network.

We have run the AB-model dynamics in different realizations of the EDH and ERH networks with $\langle k_{c,out} \rangle = 10$ and various clique sizes s , always starting from random initial conditions. Let us first obtain a detailed view of the time evolution of the dynamics by monitoring the fraction of agents in each state within each clique. Note that, because the AB agents do not tend to form AB domains (see Section 3.2; [198]), the densities f_A and f_B of A and B agents within each clique are practically complementary ($f_B \approx 1 - f_A$). Figure 4.13 displays f_A within each clique for a run in an ERH network, where each row corresponds to one

*Notice that we use subindices n and c standing for *node* and *clique*, respectively.

CHAPTER 4. THE AB-MODEL (II)

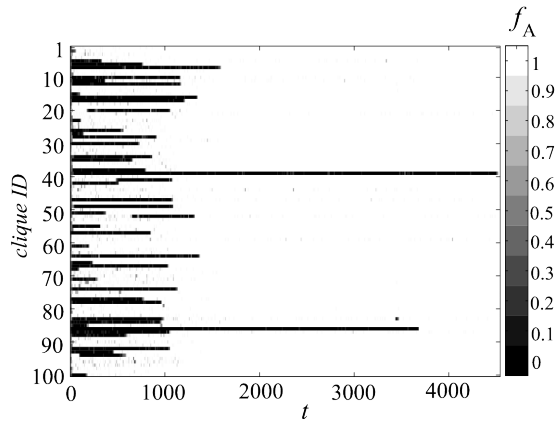


Figure 4.13: Time evolution of the fraction of A agents in each clique, f_A , labeled with IDs from 1 to 100. Gray scale: from white (all A agents) to black (no A agents). Single run in an ERH network with clique size $s = 10$, $N = 1000$, and $\langle k_{c,out} \rangle = 10$. The resolution is 10 time steps.

clique. The randomly initialized cliques very rapidly homogenize to either state A (white) or B (black). The plot shows that cliques remain homogenized to either state A or B during most of the run, and that they do not often flip from one state to the other (this is also true for the EDH networks, not shown). Notice that this was already qualitatively observed in the class of social networks with communities analyzed in the previous Section (see Figure 4.5-Right). Two of the clusters remained in the minority state B for long after the rest of the network was homogenized to the opposing state, indicating a trapped metastable state. These appeared frequently in the ERH networks, in contrast to the EDH networks.

Two typical runs that got stuck in trapped metastable states in the ERH network topologies are presented in Figure 4.14, employing two measures: the number n_m of agents in the minority state (Figure 4.14(a)), and the interface density ρ (Figure 4.14(b)). Run (2) corresponds to the detailed view in Figure 4.13. We observe that n_m decreases in steps of size s , indicative of cliques that are homogenized to the minority state, which are consenting to the majority state one by one. The number of minority agents rarely increases in the ERH networks. A closer inspection of the topology of the network shows that the cliques that remain longest in the minority state have a relatively small number of out-links, although not necessarily only one (in runs (1) and (2) displayed in Figure 4.14, $k_{c,out} = 4$ and 6, respectively).

4.2. BROAD LIFETIME DISTRIBUTIONS IN COMPLEX NETWORKS

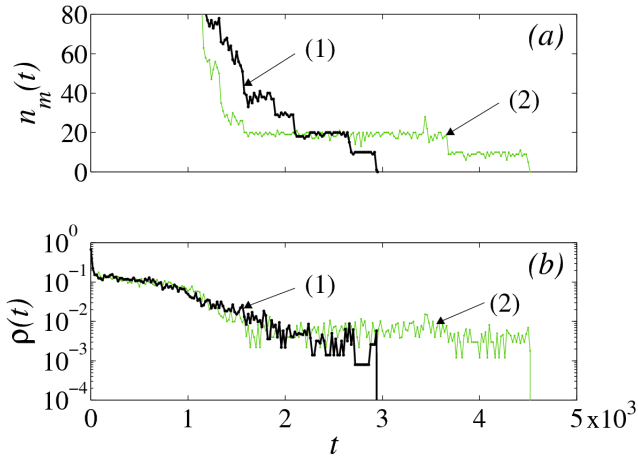


Figure 4.14: Time evolution of (a) the number n_m of agents in the minority state, and (b) interface density ρ , for two typical runs that developed trapped metastable states in an ERH network, $s = 10$, $\langle k_{c,out} \rangle = 10$, $N = 1000$.

In order to shed more light on how cliques with various out-degrees resist changing their state, we study them in a controlled setting. According to our definition of dynamical robustness, we initialize all agents within the clique to the state B, and the links leading out of the clique are connected to nodes permanently in state A (as shown in Figure 4.10(b)). As cliques remain mostly homogenized to one state during the evolution of the dynamics, the resulting lifetime distributions are also relevant for understanding the resistance of communities against changing their state within the network. Figure 4.15(a) displays the observed fraction of alive runs for cliques of various sizes s and out-degrees $k_{c,out}$. The distributions are roughly exponential, $P(t) \sim e^{-t/\tau}$, and it turns out that their survival times τ show a clear trend with the ratio $r = k_{n,in} / \langle k_{n,out} \rangle = s(s-1)/k_{c,out}$, which appears to be an appropriate topological measure of the dynamical robustness for cliques. Figure 4.15(b) displays the relation $\tau(r)$, determined for cliques of fixed size with varying clique out-degree. The time scales associated with the invasion of cliques, and therefore their dynamical robustness, grow rapidly with r .

Finally, let us observe the fraction of alive runs $P(t)$ in networks with equally sized cliques. In EDH networks with clique sizes $s = 6, 8, 9$, and 10 , and clique out-degree $k_{c,out} = 10$, $P(t)$ has an exponential tail (Figure 4.16(a)), indicating that the presence of communities alone is not sufficient for a broad distribution to appear. In these networks, all cliques have equal dynamical robustness. In

CHAPTER 4. THE AB-MODEL (II)

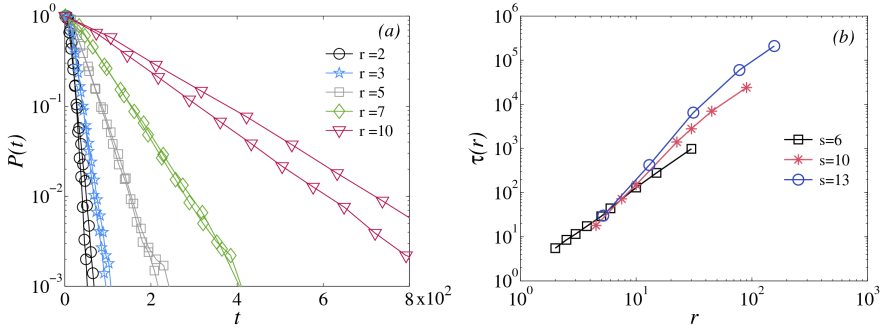


Figure 4.15: Dynamical robustness of cliques (as in Figure 4.10(b), see text). (a) The fraction of alive runs $P(t) \sim e^{-t/\tau}$ shows a trend with $r = s(s-1)/k_{c,out}$. Various ratios r are represented by two pairs of $(s, k_{c,out})$. From left to right: $r = 2$: (6,15) and (3,3); $r = 3$: (6,10) and (4,4); $r = 5$: (6,6) and (5,4); $r = 7$: (8,8) and (7,6); $r = 10$: (6,3) and (10,9). Averages calculated over 10 000 runs in each topology. (b) Dependence $\tau(r)$. Clique sizes $s = 6$ (\square), $s = 10$ ($*$), and $s = 13$ (\circ), and $k_{c,out}$ ranging from 1 to 15, 20, or 30 respectively, leading to the displayed r values.

contrast, in the ERH networks the resulting fractions of alive runs $P(t)$ are clearly broader than exponential, as depicted in Figure 4.16(b) for clique sizes $s = 3, 6$, and 10, and average clique out-degree $\langle k_{c,out} \rangle = 10$. The variance in dynamical robustness caused by the different clique out-degrees seems to play an important role.

We probe the effect of the most isolated node groups in the ERH networks by eliminating the least well connected cliques, i.e., those that are connected to the network by a single link. This is done by taking the two-core of the underlying ER network before replacing its nodes with cliques. We call these networks PERH for “pruned” ERH. Figure 4.16(c) displays $P(t)$ for ERH and PERH networks with $s = 10$ and $\langle k_{c,out} \rangle = 10$. It is seen that pruning the network results in $P(t)$ decaying slightly faster, but remaining broader than exponential. This gives further confirmation that the trapped metastable states with various time scales produced by cliques with different out-degrees are responsible for the broader than exponential lifetimes in the ERH networks.

The fraction of alive runs $P(t)$ in the ERH networks shown in Figure 4.16(b) has broad tails that appear power-law like. Moreover, they appear to broaden with increasing clique size. When approximating these tails by power laws, the exponents are far larger than those observed in the class of networks with community structure studied in the previous Section (4.1), in which the range of

4.2. BROAD LIFETIME DISTRIBUTIONS IN COMPLEX NETWORKS

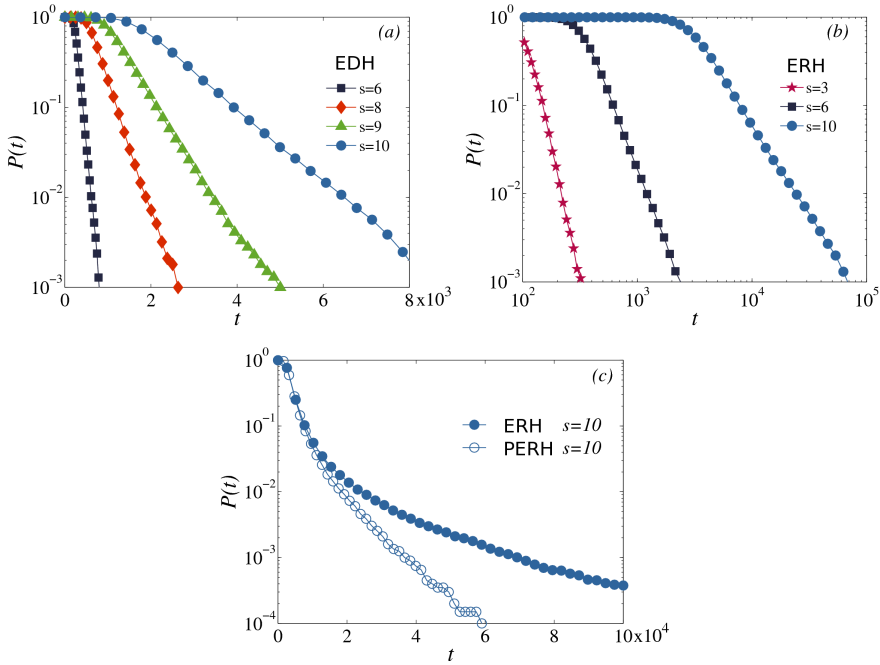


Figure 4.16: Fraction of alive runs in EDH, ERH, and PERH networks with $N \approx 10^3$ and $\langle k_{c,out} \rangle = 10$. (a) EDH with clique sizes $s = 6, 8, 9$, and 10 . (b) ERH networks with clique sizes $s = 3, 6$, and 10 . (c) ERH with $s = 10$ together with the corresponding PERH network. All cases averaged over 100 network realizations (except 10^3 for ERH $s = 6$), with 100 runs in each.

exponents was such that the variance of the lifetimes was not defined. Hence the distributions observed here are fundamentally different from the findings in Section 4.1. In order to obtain broader lifetime distributions, we apparently need a broader distribution in the dynamical robustness of communities, which in the case of cliques can be achieved by increasing variance in r . As it is more practical to obtain large variance in r by varying s than $k_{c,out,r}$, we take this approach in the following Section.

Networks with a broad size distribution of clique sizes

In this Section, we study a network consisting of cliques with equal out-degree $k_{c,out}$ and with an exponential clique size distribution, shifted to obtain a mini-

CHAPTER 4. THE AB-MODEL (II)

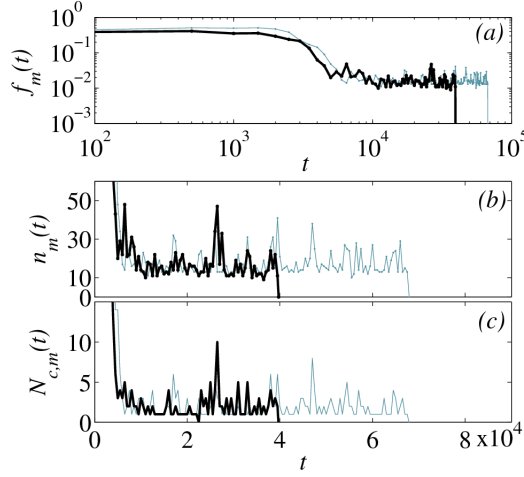


Figure 4.17: Two typical runs that developed trapped metastable states in EDE networks with $k_{c,out} = 3$, $\mu = 1.2$, $s_{min} = 3$, and $N_c = 270$, leading to $N \approx 10^3$. Time evolution of (a) the fraction and (b) the number of agents in the state that becomes the minority, and (c) the number of cliques in which more than 90 percent of the agents are in the minority state.

mum clique size, s_{min} . We construct networks from N_c cliques whose sizes s are obtained as $s = \lfloor x \rfloor + s_{min}$, where $\lfloor \cdot \rfloor$ refers to rounding downwards and x is drawn from the exponential distribution $p(x) = \frac{1}{\mu} e^{-x/\mu}$, leading to $p(s) \sim e^{-(s-s_{min})/\mu}$ for integer values of s starting from s_{min} . As with the EDH networks, the $k_{c,out}$ out-links of each clique are randomly assigned to its nodes, and link ends are randomly paired, except that no two link ends from the same clique are connected. We label these networks as EDE, for Equal out-Degree and Exponential clique size distribution.

We have shown above that the factor $\tau(r)$ of the exponential lifetime distribution of a clique being “invaded”, grows very rapidly with r , which in turn grows approximately as $r \sim s^2$. Therefore, the communities in EDE networks display a large variance in dynamical robustness. Again, cliques remain homogenized to either of the states A or B most of the time (not shown), but it turns out that some of the smaller cliques frequently adopt the state of a larger clique homogenized to the minority state. Figure 4.17(a) displays the fraction f_m of nodes in the minority state in a few typical runs that developed trapped metastable states in the EDE networks. A close-up of the same runs (Figure 4.17(b)) shows that the number n_m of minority nodes fluctuates above a baseline of roughly 11 – 13 nodes. This

4.2. BROAD LIFETIME DISTRIBUTIONS IN COMPLEX NETWORKS

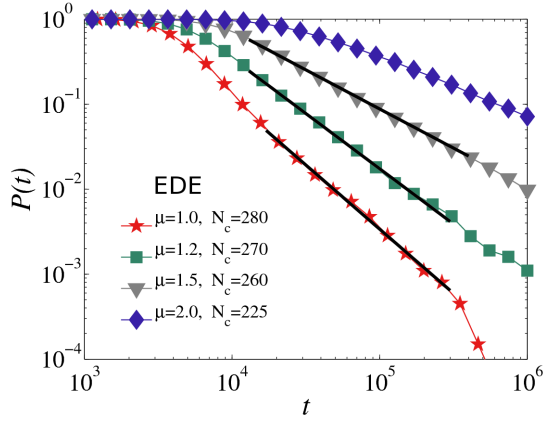


Figure 4.18: Fraction of alive runs $P(t)$ in EDE networks with various factors μ of the clique size distribution $p(s) \sim e^{-(s-s_{min})/\mu}$ with $s_{min} = 3$. From left to right: $\mu = 1.0, 1.2, 1.5, 2.0$ and $N_c = 280, 270, 260, 225$, leading to $N \approx 1000$. Clique out-degree $k_{c,out} = 3$. Results are averaged over 1000 network realizations (2000 for $\mu = 1.0$) with 10 runs in each. The fitted lines are power laws $P(t) \sim t^{-\eta}$ with exponents from left to right: $\eta = 1.51, 1.3, 0.92$.

seems to indicate a relatively large clique homogenized to the minority state that is “converting” its smaller (and hence less dynamically robust) neighboring cliques to the minority state, thereby producing around itself a *buffer* of cliques in the minority state. This assumption is confirmed by closer inspection of the networks, as well as by Figure 4.17(c), which shows the number $N_{c,m}$ of clusters in which more than 90 % of the agents are in the minority state. Most of the time there is only one cluster in the minority state (corresponding to the baseline in Figure 4.17(b)), while it is frequently joined by other, mostly smaller clusters, judging by the combination of n_m and $N_{c,m}$. The buffering effect is an additional ingredient causing trapped metastable states with various time scales, on top of the dynamical robustness that depends on r .

The EDE networks are shown to give rise to very broad lifetime distributions, shown in Figure 4.18 for $s_{min} = 3$, $\mu = 1.0 \dots 2.0$, $k_{c,out} = 3$, and $N \approx 1000$. Approximating the tails of the fraction of alive runs by a power law, $P(t) \sim t^{-\eta}$, the best fits to the cases with $\mu = 1.0$ and $\mu = 1.2$ have exponents $\eta = 1.51$ and $\eta = 1.3$, respectively. Values $1 < \eta < 2$ imply that the variance of the lifetime probability density distribution $p(t)$ is not defined (the second moment of $p(t)$ diverges). In this way, we recover the result found in the previous Section (4.1), where a

characteristic lifetime could not be defined because of the existence of trapped metastable states at any time scale. The best fit to the case with $\mu = 1.5$ has an exponent smaller than unity, $\eta = 0.92$, indicating that a mean lifetime is not defined either. We note that for each network realization, the community sizes are sampled from a distribution, and the observed broad lifetime distribution is a result of averaging over several runs in many network realizations.

Concluding remarks

In the first part of this Chapter (Section 4.1), we have considered the voter and the AB-model in a class of social networks, studying metastable states and the role of community structure in these consensus processes. The voter model dynamics, driven by interfacial noise, is not particularly sensitive to the mesoscale structure of the network: we find that all realizations of the dynamics are of the same class, leading to a type of dynamical metastable states shared by other complex networks of high dimensionality without degree correlations. On the contrary, for the AB-model dynamics, driven by curvature, we find different classes of realizations leading to a power law distribution for the times to reach consensus. This is explained in terms of trapped metastable states associated with the structure of the network. They seem to be a consequence of the curvature interface dynamics in which mechanisms of local majority favor consensus in a given option in each of the communities. Our result implies that a mean lifetime for these states does not give a characteristic time scale of the ordering dynamics. We note that a mean lifetime does not exist either for the zero-temperature kinetic Ising model dynamics on regular [149] or complex networks [152], due to realizations that lead to trapped states (infinite lifetime in finite systems). However, the novelty of our finding is that in the AB-model we observe realizations with any lifetime. For the AB-model in a regular two-dimensional lattice, metastable states with stripe-like configuration have been found, but in that case the distribution of lifetimes is exponential $P(t) \sim e^{-at}$ and the mean lifetime is representative of the dynamics (see Section 3.2; [198]). The power-law distribution for the lifetimes originates here in the multiplicity of different traps that reflects the mesoscale structure of the networks.

In the second part of this Chapter (Section 4.2), we set out to determine minimal network features that would produce broad lifetime distributions for the ordering dynamics described by the AB-model. We have introduced the concept of dynamical robustness against invasion in relation to the dynamics of competing options, in order to describe the resistance against outside influence of topolog-

4.3. CONCLUDING REMARKS

ical substructures that involve relative isolation from the rest of the network. Dynamical robustness is characterized by the survival time of the substructure, i.e., the characteristic time needed for this set of nodes before changing its option towards the one of the surrounding majority. In all of the topologies in which a broader than exponential distribution for the relaxation time of the whole system arises, we have identified substructures that individually have exponential lifetime distributions, implying a well defined survival time for such topologies. The broad distribution appears because of the heterogeneity of these substructures: the network has a variety of different substructures with different survival times; that is, with different dynamical robustness.

In an Erdős-Rényi network, branches were seen to produce exponential lifetime distributions when isolated from the rest of the network. Their dynamical robustness has been proven to be affected by the diameter as well as the number and location of bifurcations. Lifetime distributions also appear to be exponential for isolated cliques, and the ratio $r = k_{n,in} / \langle k_{n,out} \rangle$ has proven an appropriate topological measure to characterize the dynamical robustness of a clique.

In the case of networks with mesoscale structure built up from randomly connected cliques, it has been shown that simply the presence of communities is not a sufficient condition to produce a broader than exponential lifetime distribution. This was demonstrated by networks consisting of cliques with equal size and same out-degree (EDH, for Equal out-Degree and Homogeneously sized cliques), and hence equal dynamical robustness, where the lifetime distribution for the whole network has proven to be exponential. Although the interactions between the cliques in a network may cause clique lifetimes to deviate from those that arise in isolation, the broader than exponential lifetime distributions observed for ERH (for Erdős-Rényi underlying network and Homogeneously sized cliques) and EDE (for Equal out-Degree and Exponential clique size distribution) may in part be explained by the different dynamical robustness against invasion of the cliques forming the network, leading to a combination of exponential processes with various time scales. The most interesting feature is obtained for EDE networks where we have recovered the main results in Section 4.1, i.e. very broad $P(t)$ with a best power law fit such that the second moment of the lifetime distribution is not defined, and therefore there does not exist a characteristic time scale for the dynamics. The results in this Chapter might be generic for a class of models where the dynamics at the interfaces is curvature driven, such as SFKI models.

In summary, complementing studies on the effects of heterogeneous interacting agents (a research line of growing interest [226]), we have seen that heterogeneity at the mesoscale level of the network of interaction results in non-trivial effects in the dynamics of ordering processes. A large variability in the dynamical

CHAPTER 4. THE AB-MODEL (II)

robustness of different topological substructures (communities) appears to be a sufficient mechanism for the absence of a characteristic time for the dynamics. This mechanism causes the existence of trapped metastable states that survive at any time scale.

Comparing models with two non-excluding options

In Chapters 3 and 4 we have studied in detail the AB-model in different networks of interaction. In this Chapter, we are interested in another model with two non-excluding options, which has its roots in semiotic dynamics: the *Naming Game* [116]. This model describes a population of agents playing pairwise interactions in order to *negotiate* conventions, i.e., associations between forms and meanings, and elucidates the mechanisms leading to the emergence of a global consensus among them. For the sake of simplicity the model does not take into account the possibility of homonymy, so that all meanings are independent and one can work with only one of them, without loss of generality. An example of such a game is that of a population that has to reach the consensus on the name (i.e. the form) to assign to an object (i.e. the meaning) exploiting only local interactions. However, it is clear that the model, originally inspired to artificial intelligence experiments [116], is appropriate to address general situations in which negotiation rules a decision process on a set of conventions (i.e. opinion dynamics, etc.). The Naming Game has been studied in fully connected networks [116, 192, 227], regular lattices [193], small world networks [194] and complex networks [195, 196], and it constitutes also the fundamental brick of more complex models in computational cognitive sciences [228]. The final state of the system is always consensus, but coexistence scenarios can be reached introducing a simple confidence/trust parameter [197].

In this Chapter, we analyze and compare the AB-model and the Naming Game restricted to two conventions, that is, the particular case in which only two options compete within the population [197]. We show that even though these

CHAPTER 5. MODELS WITH TWO NON-EXCLUDING OPTIONS

two models are equivalent at the mean field level, their microscopic differences have nontrivial effects. To point them out, we first generalize the AB-model introducing a confidence/trust parameter analogous to the one studied in [197] for the Naming Game. From the point of view of the AB-model, this parameter can be interpreted as a measure of the resistance of the agents to abandon an acquired language, and reconnects to the concept of inertia already introduced in extensions of the voter model [210, 213]. We show that the transition to an asymptotically stable disordered state observed in the Naming Game [197] is absent in the AB-model, and we investigate the microscopic origin of this difference. Then we focus on the interface dynamics in one and two-dimensional lattices for the original models, pointing out that beyond a qualitative analogy of the behaviors observed in the two models, the AB-model rules determine a slower dynamics (publication in Ref. [217]).

5.1

The Naming Game vs the AB-model: generalized models

We present here the two models considered in this Chapter: the generalized Naming Game restricted to two conventions [192, 197] and the AB-model (see Section 2.3), extended in such a way that confidence/inertia is considered. In both models, we consider a set of N interacting agents embedded in a network. At each time step, and starting from a given initial condition, we select randomly an agent and we update its state according to the dynamical rules corresponding to each model.

In the Naming Game, an agent is endowed with an internal inventory in which it can store an a priori unlimited number of conventions. Initially, all inventories are empty. At each time step, a pair of neighboring agents is chosen randomly, one playing as “speaker”, the other as “hearer”, and negotiate according to the following rules:

- the speaker selects randomly one of its conventions and conveys it to the hearer (if the inventory is empty, a new convention is invented by the speaker);
- if the hearer’s inventory contains such a convention, the two agents update their inventories so as to keep only the convention involved in the interaction, that is, they delete all their conventions but the one that has just been transmitted by the speaker (*success*);

5.1. THE NAMING GAME VS THE AB-MODEL: GENERALIZED MODELS

Before game		Convention	Outcome		P(outcome)
Sp	Hr	(Sp \rightarrow Hr)	Sp	Hr	
A	A	A	A	A	1.0
A	B	A	A	AB	1.0
A	AB	A	A	A	β
			A	AB	$1.0 - \beta$
AB	A	A (p=0.5)	A	A	β
			AB	A	$1.0 - \beta$
AB	A	B (p=0.5)	AB	AB	1.0
AB	AB	A (p=0.5)	A	A	β
			AB	AB	$1.0 - \beta$
AB	AB	B (p=0.5)	B	B	β
			AB	AB	$1.0 - \beta$

Table 5.1: Typical interactions in the 2c-Naming Game. Agents are identified by the conventions contained in their inventories, i.e. an agent can be A, B or AB. The speaker (*Sp*) conveys a convention to the hearer (*Hr*). In case it stores both A and B (i.e. it is an AB agent), one of them is randomly selected (with probability $p = 0.5$). After the game, the agents modify their inventories according to the rules described in the text. The post-success rearrangement takes place with a probability depending on β , $P(\text{outcome})$ (the original Naming Game rules correspond to the case $\beta = 1$). Notice that the model is symmetric under the exchange of A and B.

- otherwise, the hearer adds the convention to those already stored in its inventory (*failure*).

Here we are interested in the particular case in which a population deals with only two competing conventions (say A or B) [197]. We therefore assign to each agent one of the two conventions at the beginning of the process, preventing in this way further invention (that can happen only when the speaker's inventory is empty). Moreover, we adopt the generalized Naming Game scheme [197], in which a confidence/trust parameter, β , determines the update rule following a success: with probability β the usual dynamics takes place, while with the complementary probability $1 - \beta$ nothing happens. The original model is thus recovered for $\beta = 1$. For brevity we refer to this setting (generalized Naming Game restricted to two conventions) as the *2c-Naming Game*. In this simplified case (for which typical interactions are shown in Table 5.1), it is easy to see that

CHAPTER 5. MODELS WITH TWO NON-EXCLUDING OPTIONS

the transition probabilities for the agent i are the following [197]:

$$p_{i,A \rightarrow AB} = n_{i,B} + \frac{1}{2}n_{i,AB}, \quad p_{i,B \rightarrow AB} = n_{i,A} + \frac{1}{2}n_{i,AB} \quad (5.1)$$

$$p_{i,AB \rightarrow A} = \frac{3\beta}{2}n_{i,A} + \beta n_{i,AB}, \quad p_{i,AB \rightarrow B} = \frac{3\beta}{2}n_{i,B} + \beta n_{i,AB} \quad (5.2)$$

where $n_{i,l}^*$ ($l=A, B, AB$) are the fraction of neighboring agents storing in their inventory the conventions A, B or both A and B, respectively.

In this Chapter, we extend the original AB-model (see Section 2.3) in analogy to the extension proposed for the Naming Game above. The transition probabilities are the following:

$$p_{i,A \rightarrow AB} = \frac{1}{2}n_{i,B}, \quad p_{i,B \rightarrow AB} = \frac{1}{2}n_{i,A} \quad (5.3)$$

$$p_{i,AB \rightarrow A} = \frac{1}{2}\beta(1 - n_{i,B}), \quad p_{i,AB \rightarrow B} = \frac{1}{2}\beta(1 - n_{i,A}) \quad (5.4)$$

An agent abandons an option or language according to the dynamics of the AB-model (changes from AB to A or B) with a probability β , while with a probability $1 - \beta$ nothing happens. In the context of language competition, the parameter β can be interpreted as a measure of the resistance or inertia to stop using a language, and at the same time, as a reinforcement of the status of being bilingual, which was not taken into account in the original model (recovered by setting $\beta = 1$)[†]. From the point of view of statistical physics, the parameter β in the modified AB-model recalls the concept of inertia defined in recent extensions of the voter model. In this context, assuming for instance that inertia depends on the persistence time of a voter's current opinion leads to a parameter region where an increasing inertia causes a faster consensus [213], while adding memory effects in the form of noise reduction determines the emergence of surface tension [210].

In both models, a unit of time is also defined as N iterations, so that at every unit of time each agent has been updated on average once. In order to describe the dynamics of the system, we also use as an order parameter the interface density, ρ , defined as the fraction of links connecting nodes in different states (see Section 2.5).

*For convenience, we use this notation in this Chapter.

[†]Notice that small β corresponds to large inertia and vice-versa.

Macroscopic description

In the previous Section, we have presented the microscopic description of the 2c-Naming Game and the AB-model, that is, the set of local interactions among the agents. In order to have a macroscopic description of the dynamical evolution of the system as a whole, we derive the mean-field equations for the fraction of agents in each state. For the 2c-Naming Game [197]:

$$\frac{dn_A}{dt} = -n_A n_B + \beta n_{AB}^2 + \frac{3\beta - 1}{2} n_A n_{AB} \quad (5.5)$$

$$\frac{dn_B}{dt} = -n_A n_B + \beta n_{AB}^2 + \frac{3\beta - 1}{2} n_B n_{AB} \quad (5.6)$$

and $n_{AB} = 1 - n_A - n_B$; where n_i ($i=A, B, AB$) are the total fraction of agents storing in their inventory the conventions A, B or both A and B, respectively.

The stability analysis shows that there exist three fixed points [197]: (1) $n_A = 1, n_B = 0, n_{AB} = 0$; (2) $n_A = 0, n_B = 1, n_{AB} = 0$ and (3) $n_A = b(\beta), n_B = b(\beta), n_{AB} = 1 - 2b(\beta)$, with $b(\beta) = \frac{1+5\beta - \sqrt{1+10\beta+17\beta^2}}{4\beta}$ (and $b(0)=0$). An order-disorder transition occurs for a critical value $\beta_c = 1/3$. For $\beta_c > 1/3$ consensus is stable. For $\beta_c < 1/3$ a change of stability gives place to a stationary coexistence of $n_A = n_B$ and a finite density of AB agents n_{AB} , fluctuating around the average values $b(\beta)$ and $1 - 2b(\beta)$. In the Naming Game with invention, in fact, the one observed at $\beta_c = 1/3$ is the first of a series of transitions yielding the asymptotic survival of a diverging (in the thermodynamic limit) number of conventions as $\beta \rightarrow 0$ [197].

For the AB-model:

$$\frac{dn_A}{dt} = \frac{1}{2}(-n_A n_B + \beta n_{AB}^2 + \beta n_A n_{AB}) \quad (5.7)$$

$$\frac{dn_B}{dt} = \frac{1}{2}(-n_A n_B + \beta n_{AB}^2 + \beta n_B n_{AB}) \quad (5.8)$$

and $n_{AB} = 1 - n_A - n_B$.

These equations have three fixed points: (1) $n_A = 1, n_B = 0, n_{AB} = 0$; (2) $n_A = 0, n_B = 1, n_{AB} = 0$ and (3) $n_A = f(\beta), n_B = f(\beta), n_{AB} = 1 - 2f(\beta)$ with $f(\beta) = \frac{3\beta - \sqrt{\beta(\beta+4)}}{2(2\beta-1)}$. Their stability is addressed in the next Section.

Notice that in both models, at $\beta = 0$ the third fixed point becomes a stable absorbing state in which the system reaches consensus in the AB-state.

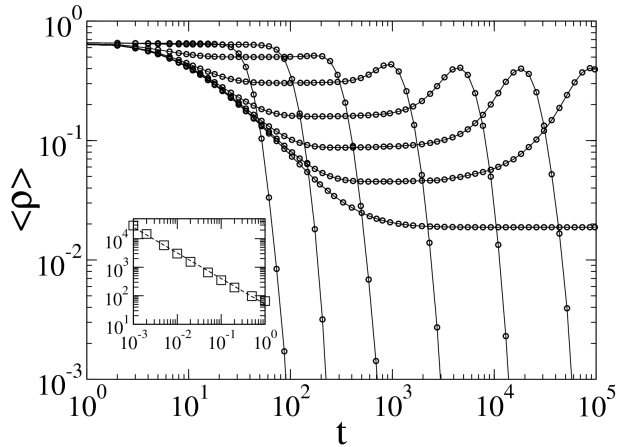


Figure 5.1: AB-model: time evolution of the average interface density, $\langle \rho \rangle$, in a fully connected network of $N = 10000$ agents for different values of β . From left to right: $\beta = 1.0, 0.2, 0.05, 0.01, 0.002, 0.0005, 0.0001, 0.0$. Averages over 1000 runs. *Inset:* Scaling of the average time to reach consensus with β for $N = 10000$: $\tau \sim \beta^{-1}$. Averages over 200-800 runs depending on the value of β .

Surprisingly, the two original models ($\beta = 1$) are equivalent in the mean-field approximation. There is just a different time scale coming from the prefactor $1/2$ in the AB-model (Equations (5.7) and (5.8)). The mean-field approximation is exact in the thermodynamic limit, and valid for large systems in fully connected networks. However, the two models differ at their local interactions (see Equations (5.1-5.4) for $\beta = 1$). To explore the effects of these differences at the microscopic level, in Section 5.3 we investigate, in a fully connected network, the role of the parameter β as described in Equations (5.5-5.8), while in Section 5.4 we focus on the interface motion in regular lattices for the original models ($\beta = 1$).

5.3

Order-disorder transition

Here we consider the extension of the AB-model presented above in a fully connected network, with the aim to explore a possible order-disorder transition in β similar to the one found in the 2c-Naming Game. In Figure 5.1 we show

5.3. ORDER-DISORDER TRANSITION

the time evolution of the average interface density, $\langle \rho \rangle$, for different values of the parameter β . For large values of β , $\langle \rho \rangle$ reaches a plateau followed by a finite size fluctuation that drives the system to an absorbing state. However, for $\beta \lesssim 0.01$ we observe a non-monotonic* time evolution for $\langle \rho \rangle$: after $\langle \rho \rangle$ reaches the plateau, it increases again, reaching a maximum value after which a finite size fluctuation drives the system to consensus. In finite systems and for $\beta = 0$, the system reaches a constant value of $\langle \rho \rangle$, a frozen state corresponding to almost consensus in the AB-state, except for a small fraction of agents (less than 1% on average for $N = 10000$). This fraction decreases as N increases, and complete consensus in the AB-state is reached in the thermodynamic limit (see stability analysis in the previous Section). For $\beta = 0$, $p_{AB \rightarrow A} = p_{AB \rightarrow B} = 0$, so the only possible evolution is that A and B agents move towards the AB-state. At the last stage of the dynamics, when n_A and n_B approach to zero, as soon as one of the two single-option densities, n_i , vanishes, n_j remains constant ($i, j = A, B, i \neq j$) because $p_{j \rightarrow AB} \sim n_i$, giving rise to the small fraction of agents in the state j present in the frozen state. The average time to reach consensus scales with beta as $\tau \sim \beta^{-1}$ (Inset in Figure 5.1), as observed for the 2c-Naming Game for $\beta > \beta_c$ ($\tau \sim (\beta - \beta_c)^{-1}$) [197][†].

Contrary to the order-disorder transition described in Section 5.2 obtained in the 2c-Naming Game, there is no order-disorder transition in the AB-model: at $\beta = 0$, the system reaches trivially a frozen state (dominance of the AB-state, with complete consensus in the thermodynamic limit); while for $\beta > 0$ the final absorbing state is, as usual, consensus in the A or B option. Even though the two original models are equivalent in the mean-field approximation (case $\beta = 1$), we observe two different behaviors when the parameter β is taken into account. This can be shown formally by looking at the time evolution of the magnetization, $m \equiv n_A - n_B$. For the 2c-Naming Game and the AB-model, we have respectively:

$$\frac{dm}{dt} = \frac{3\beta - 1}{2} n_{AB} m \quad (5.9)$$

$$\frac{dm}{dt} = \frac{1}{2} \beta n_{AB} m \quad (5.10)$$

In Equation (5.9), we can observe the origin of the order-disorder transition described in Section 5.2 for the 2c-Naming Game. The time derivative of the magnetization, $\frac{dm}{dt}$, vanishes at the critical point $\beta_c = 1/3$. For $\beta_c > 1/3$, $\text{sign}(\frac{dm}{dt}) = \text{sign}(m)$, and therefore $|m| \rightarrow 1$: the system is driven to an absorbing state of

*A non-monotonic time evolution for $\langle \rho \rangle$ of different nature has also been observed in the Axelrod Model [201, 229].

[†]Notice that since the two models are equivalent in the mean field for $\beta = 1$, the time to reach consensus scales with the system size in both models as $\tau \sim \ln N$, indicating that τ increases slowly with N (see Figure 3.1 for the AB-model and [227] for the Naming Game).

CHAPTER 5. MODELS WITH TWO NON-EXCLUDING OPTIONS

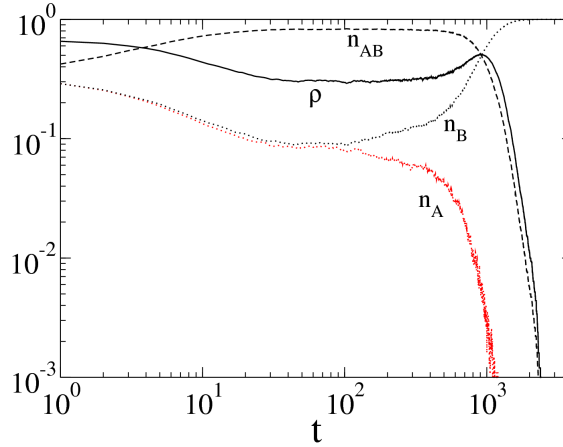


Figure 5.2: AB-model: time evolution for a typical realization of the density of agents in state A, n_A (dotted red), in state B, n_B (dotted black), and in state AB, n_{AB} (dashed); and of the interface density, ρ (solid line). In the plateau, $n_A \sim n_B \simeq 0.1$, while the majority of agents are in the AB-state. Fully connected network, $\beta = 0.01$ and $N = 10000$ agents.

consensus in the A or B option. For $\beta_c < 1/3$, $\text{sign}(\frac{dm}{dt}) = -\text{sign}(m)$ and $|m| \rightarrow 0$, giving rise to the stationary coexistence of the three phases, with $n_A = n_B$ and a finite density of AB agents. For the AB-model, instead, we can see in Equation (5.10) that for $\beta > 0$, $\text{sign}(\frac{dm}{dt}) = \text{sign}(m)$ so that consensus in the A or B option is always reached. The time derivative of the magnetization, $\frac{dm}{dt}$, vanishes at $\beta = 0$, where the dynamics gets stuck in an absorbing state corresponding to consensus in the AB-state in the thermodynamic limit. Therefore, the order-disorder transition observed in the 2c-Naming Game does not exist.

The reason for the different behavior shown above has to be found in the differences that the original models have at the microscopic level, which give rise to different mean field equations for $\beta \neq 1$ when this parameter is introduced in the $AB \rightarrow A$ and $AB \rightarrow B$ transition probabilities (Equations (5.2) for the 2c-Naming Game and (5.4) for the AB-model). The fact that in the AB-model, A and B agents do not feel the influence of AB agents is the key point which explains the absence of a transition for this model. For the case $\beta = 1$, in the 2c-Naming Game the second term in Equation (5.1) (influence of AB agents on the A or B agents) and the first term in Equation (5.2) (influence of the A or B agents on the AB agents) combine in such a way that the mean-field equations are equivalent to the ones in

5.4. INTERFACE DYNAMICS: 1-D AND 2-D LATTICES

the AB-model. However, when $\beta < 1$ the combination of these terms originates the order-disorder transition from an absorbing final state towards a dynamical stationary state of coexistence, as found in [197].

To understand the non-monotonic time evolution of the average interface density $\langle \rho \rangle$ shown in Figure 5.1 for $\beta \lesssim 0.01$, we show in Figure 5.2 the time evolution of ρ and the densities of agents in each state, n_A , n_B and n_{AB} , for a typical realization of the dynamics and a given small β . Because of the inertia of the AB agents to move away from their state (small β), at the beginning we observe an increase of n_{AB} together with the corresponding decrease of n_A , n_B and ρ . Then, ρ and the three densities reach a plateau. Most of the agents are in the AB-state, while a competition between options A and B takes place, with $n_A \approx n_B < n_{AB}$. This configuration lasts longer as we increase the system size. At a certain point, however, a system size fluctuation drives the density of one of the two states (A in the Figure) to zero, while the other (B in the Figure) starts gaining ground. Since there are less and less agents in the state becoming extinct, and agents having one option do feel only the presence of agents in the opposite state, agents in the dominant state become more and more stable, until, when the other state disappears, they become totally stable. During this process, the interface density increases as n_{AB} decreases. The peak of ρ corresponds to the point where $n_{AB} = n_i$ (being i the state which takes over the whole system, B in the Figure). When one of the states has vanished (A in the Figure), the AB agents slowly move towards the remaining state (B in the Figure) and the system reaches consensus.

5.4

Interface dynamics: 1-d and 2-d lattices

In this Section, we study and compare the interface dynamics in regular lattices with periodic boundary conditions for the two original models ($\beta = 1$). The 2c-Naming Game has been shown to exhibit a diffusive interface motion in a one-dimensional lattice, with a diffusion coefficient $D = 401/1816 \approx 0.221$ [193]. We therefore focus on the AB-model and, to analyze the interface dynamics in a one-dimensional lattice with N agents, we consider a single interface between two linear clusters of agents. In each of the clusters, all the agents are in the same state. We consider a cluster of agents in the state A on the left and another cluster of agents in the state B on the right. We call C_m an interface of m agents in state C (for clarity, here C labels an AB agent). Due to the dynamical rules, the only two possible interface widths are C_0 , corresponding to a two directly connected clusters $\cdots AAABBB \cdots$, or C_1 , corresponding to an interface of width one, $\cdots AAACBBB \cdots$. It is straightforward to compute the probability $p_{0,1} = 1/2N$

CHAPTER 5. MODELS WITH TWO NON-EXCLUDING OPTIONS

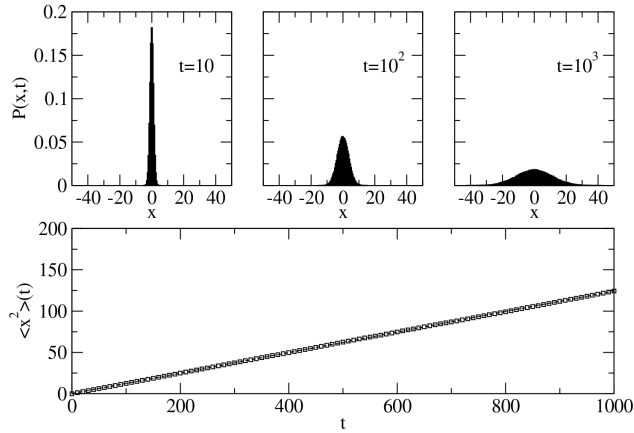


Figure 5.3: AB-model: evolution of the position of an interface in a one-dimensional regular lattice. *Top:* time evolution of the distribution $P(x, t)$. *Bottom:* time evolution of the mean square displacement $\langle x^2(t) \rangle = 2D_{exp}t$. The value $D_{exp} = 0.06205$ obtained from the fitting is in perfect agreement with the theoretical prediction $D = 1/16 = 0.0625$.

that a C_0 interface becomes a C_1 in a single time step. Otherwise, it stays in C_0 . In the same way, $p_{1,0} = 1/2N$. We are now interested in determining the stationary probabilities of the Markov chain defined by the transition matrix:

$$M = \begin{pmatrix} 1 - \frac{1}{2N} & \frac{1}{2N} \\ \frac{1}{2N} & 1 - \frac{1}{2N} \end{pmatrix} \quad (5.11)$$

in which the basis is $\{C_0, C_1\}$. The stationary probability vector, $\mathbf{P} = \{P_0, P_1\}$ is computed by imposing $\mathbf{P}(t+1) - \mathbf{P}(t) = 0$, i.e., $(M^T - I)\mathbf{P} = 0$. We obtain $P_0 = 1/2, P_1 = 1/2$. Since the interface has a bounded width, we assume that it can be modeled as a point-like object localized at position $x = (x_l + x_r)/2$, where x_l is the position of the rightmost site of cluster A, and x_r the position of the leftmost site of cluster B. An interaction $C_m \rightarrow C_{m'}$ corresponds to a set of possible movements for the central position x . We denote by $W(x \rightarrow x \pm \delta)$ the transition probability that an interface centered in x moves to the position $x \pm \delta$. The only possible transitions are: $W(x \rightarrow x \pm \frac{1}{2}) = \frac{1}{4N}P_0 + \frac{1}{4N}P_1$. Using the results obtained for the stationary probability vector we get $W(x \rightarrow x \pm \frac{1}{2}) = \frac{1}{4N}$. We are now able to write the master equation for the probability $P(x, t)$ to find the interface in position x at time t . In the limit of continuous time and space:

5.4. INTERFACE DYNAMICS: 1-D AND 2-D LATTICES

$$P(x, t + 1) \approx P(x, t) + \delta t \frac{\partial P(x, t)}{\partial t}, \quad (5.12)$$

$$P(x + \delta x, t) \approx P(x, t) + \delta x \frac{\partial P(x, t)}{\partial x} + \frac{1}{2} (\delta x)^2 \frac{\partial^2 P(x, t)}{\partial x^2} \quad (5.13)$$

In this limit, the master equation reads:

$$\frac{\partial P(x, t)}{\partial t} = \frac{D}{N} \frac{\partial^2 P(x, t)}{\partial x^2} \quad (5.14)$$

where the diffusion coefficient is $D = 1/16 = 0.0625$ (in the appropriate dimensional units $(\delta x)^2/\delta t$). These analytical results are confirmed by numerical simulations. In Figure 5.3 we show the time evolution of $P(x, t)$, which displays a clear diffusive behavior. The mean-square distance follows a diffusion law $\langle x^2 \rangle = 2D_{exp}t$, where $D_{exp} = 0.06205$ is the diffusion coefficient obtained numerically.

Therefore, the AB-model and the 2c-Naming Game display the same diffusive interface motion in one-dimensional lattices, but they differ in about one order of magnitude in the diffusion coefficient, indicating that in the AB-model interfaces diffuse much slower. It can also be shown that the growth of the typical size of the clusters, ξ , is $\xi(t) \sim t^\alpha$, with $\alpha \simeq 0.5$, leading to the well known coarsening process found also in SFKI models [110].

Regarding two-dimensional lattices, it has been shown that starting from random initially distributed options among the agents, both models present a coarsening $\xi(t) \sim t^\alpha$, $\alpha \simeq 0.5$, corresponding to a curvature driven interface dynamics (see Section 3.2 and [198] for the AB-model; see [193] for the Naming Game) with AB agents placing themselves at the interfaces between single-option domains. In Figure 5.4 we show snapshots comparing the two dynamics, starting from initial conditions where we have half of the lattice in state A, and the other half in state B. Given that the interface dynamics is curvature driven, flat boundaries are very stable. In both models these stripe-like configurations give rise to trapped metastable states, already found in Section 3.2 for the AB-model: dynamical evolution of interfaces close to flat boundaries but with interfacial noise present. These configurations evolve by diffusion of the two walls (average interface density fluctuating around a fixed value) until they meet and the system is driven to an absorbing state. In the AB-model, also when starting from options randomly distributed through the lattice, 1/3 of the realizations end up in such

CHAPTER 5. MODELS WITH TWO NON-EXCLUDING OPTIONS

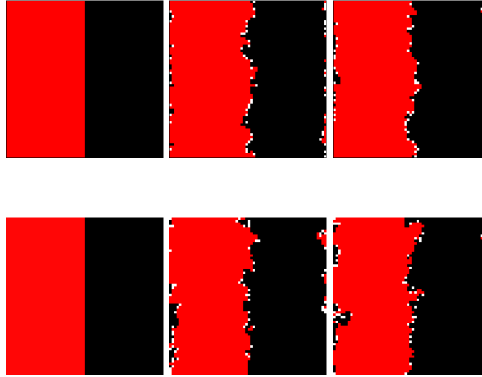


Figure 5.4: Stripe-like trapped metastable states: initial conditions with one half of the lattice in state A, and the other half in state B. $N = 64^2$. *Top:* AB-model: $t=0, 100, 200$, from left to right. *Bottom:* 2c-Naming Game: $t=0, 50, 100$, from left to right. Snapshots are selected taking into account the different time scale coming from the prefactor $1/2$ in the mean field Equations (5.7) and (5.8). Color code: black (A), red (B), white (AB).

stripe-like metastable states (see Section 3.2; [198]). We checked that the same turns out to be true also for the 2c-Naming Game. In the usual Naming Game with invention, instead, stripes are better avoided since in that case the state with only two options at play is usually reached when one cluster is already considerably larger than the other.

We show in Figure 5.5 the distribution of survival times for the two models, i.e., the time needed for a stripe-like configuration to reach an absorbing state. Both distributions display an exponential tail, $p(t) \sim e^{-t/\tau_i}$ with a characteristic time τ_i , where i is a label accounting for the AB-model (AB) or the Naming Game (NG). The characteristic time for the AB-model is however larger than the one for the 2c-Naming Game ($\tau_{AB} > \tau_{NG}$), confirming that the AB-model interface dynamics slows down the diffusion of configurations such as stripes in two dimensional lattices, or walls in one dimensional lattices. Notice that in both cases, the differences found are beyond the trivial different time scale corresponding to the prefactor $1/2$ in the mean field equations for the AB-model (Equations (5.7) and (5.8)).

5.5. CONCLUDING REMARKS

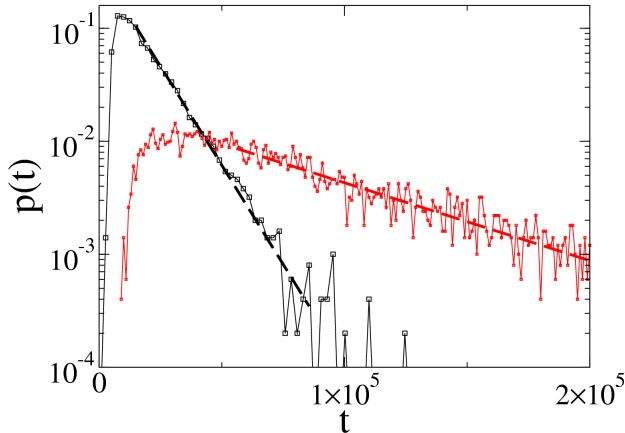


Figure 5.5: Probability distribution for the time to reach consensus, starting from stripe-like configurations. Two-dimensional regular lattice, $N = 64^2$. Black: 2c-Naming Game, $\tau_{NG} \approx 1.2 \cdot 10^4$; red: AB-model, $\tau_{AB} \approx 6.3 \cdot 10^4$. Averages are over 5000 runs.

5.5

Concluding remarks

We have analyzed and compared the 2c-Naming Game and the AB-model, originally defined in the context of language emergence and competition, respectively. We have shown that although these two models are equivalent in mean-field, their microscopic differences give rise to different behaviors. In particular, we have focused on (1) the extension of the models by introducing the parameter β , describing the inertia of the agents to abandon an acquired option, and (2) the interface dynamics in one and two-dimensional lattices.

As for the extension of the models incorporating the parameter β , even though the original models are equivalent in the mean field approximation for $\beta = 1$, an important difference concerns the existence of an order-disorder transition. While the 2c-Naming Game features an order-disorder transition between consensus and stationary coexistence of the three phases present in the system, in the AB-model such a transition does not exist. Instead, the model features a trivial frozen state for $\beta = 0$ (dominance of the AB-state, with complete consensus in the thermodynamic limit), and the usual consensus in the A or B state, for $0 < \beta \leq 1$. In this perspective, it is interesting to note that a different order-disorder transi-

CHAPTER 5. MODELS WITH TWO NON-EXCLUDING OPTIONS

tion between consensus and coexistence has also been found in a two-parameter family of models which interpolates between the voter model and the Naming Game [214]. Moreover, and contrary to the original AB-model ($\beta = 1$), where the AB agents are systematically the minority state in the system, it is worth to note that for β small enough, AB agents become the majority during the transient stage before one of the options takes advantage and the system finally reaches an absorbing state. In addition, when a single-option dies out (also in the case of small β) this option still remains in the system through the AB agents, which disappear much later.

As for the interface dynamics, we have shown in one-dimensional lattices that the AB-model has a diffusive interface motion analogous to the one already found in the 2c-Naming Game, but with a diffusion coefficient nearly one order of magnitude smaller. In two-dimensional lattices, we have studied the time evolution of stripe-like configurations, which correspond to trapped metastable states in both models but have a larger lifetime in the AB-model. Both results indicate that in comparison to the 2c-Naming Game, the AB-model interface dynamics slows down the diffusion of these configurations (walls in $d = 1$ and stripes in $d = 2$).

Macroscopic descriptions and order-disorder transitions

In the previous Chapters, our study has focused on theoretical and numerical analyses of the consensus models for the case of symmetrical prestige ($s = 0.5$) and neutral volatility ($a = 1$). For these parameter values, the microscopic Abrams-Strogatz model coincides with the voter model, while the Bilinguals model reduces to the AB-model (see Chapter 2). The emphasis has been in describing the effects of the third AB-state in the consensus dynamics with two non-excluding options as compared with the reference case provided by the voter model. This includes the characterization of the different processes of domain growth (Chapter 3; [198]), and the role of the network topology, like small world networks (Chapter 3; [198]) and networks with mesoscopic community structure (Chapter 4; [215, 216]). The AB-model has also been studied in comparison to other models with two non-excluding options like the Naming Game (Chapter 5; [217]).

However, we have not yet considered the study of the AS-model and the Bilg-model in the volatility-prestige parameter space. Beyond the qualitative description of the phenomenology of these models presented in Section 2.4, in this Chapter we present a detailed analysis of the role of these parameters in the general dynamical properties of the models. Notice that for the voter model, macroscopic field theory descriptions [212, 230] as well as macroscopic and analytical solutions in different complex networks [133] have been reported, but there is still a lack of useful macroscopic descriptions of these models for arbitrary values of the prestige and volatility parameters. The general aim of this Chapter is then to study the behavior of these models for a wide range of these param-

CHAPTER 6. MACROSCOPIC DESCRIPTIONS

eters values, and to derive appropriate macroscopic descriptions (mean field, pair approximation and field description; depending on the network structure) that account for the observed order-disorder transitions (consensus-coexistence) in the volatility-prestige parameter space. In particular, we analyze how the introduction of an intermediate AB-state affects the scenario of coexistence, by comparing the regions of consensus and coexistence of the AS-model and the Bilg-model in the parameter space. In addition, we study how these regions are modified, within the same models, when the dynamics takes place on networks with different topologies: fully connected networks, complex random networks and two-dimensional lattices (publication in Ref. [218]).

6.1

Abrams-Strogatz model

We study in this Section the AS-model, the two-state model introduced in Chapter 2 which was originally developed to account for the competition between two languages [13] (see Section 2.1 for a detailed description).

In order to perform an analytical and numerical study of the evolution of the system, and in an analogy to spin models, in this Chapter we consider A and B agents as spin particles in states $s = -1$ (spin down) and $s = +1$ (spin up) respectively. Therefore, the state of the system in a given time can be characterized by two macroscopic quantities: the global magnetization, $m \equiv \frac{1}{N} \sum_{i=1}^N s_i$, where s_i with $i = 1, \dots, N$ is the state of agent i in a population of size N ; and the interface density, $\rho \equiv \frac{1}{2N_l} \sum_{\langle ij \rangle} (1 - s_i s_j)/2$, where N_l is the number of links in the network and the sum is over all pairs of neighbors. It corresponds to the density of neighboring nodes in an opposite state (see also Section 2.5). The magnetization measures the balance in the fractions of A and B agents ($m = 0$ corresponding to the perfectly balanced case), whereas ρ measures the degree of disorder in the system. The case $|m| = 1$ and $\rho = 0$ corresponds to the totally ordered situation, with all agents in the same state, while $|m| < 1$ and $\rho > 0$ indicates that the system is disordered, that is, composed by both types of agents.

Our aim in this Section is to obtain differential equations for the time evolution of the average values of m and ρ , as these equations are useful in the study of the properties of the system from an analytical point of view. In particular we concentrate in their stability analysis, in order to explain the observed order-disorder transitions (consensus-coexistence) in the volatility-prestige parameter space. We start by deriving these equations in the case of a fully connected network, that corresponds to the simplified assumption of a “well mixed” popu-

6.1. ABRAMS-STROGATZ MODEL

lation, widely used in population dynamics. We then obtain the equations when the topology of interactions between the agents is a complex random network. We shall see that the results depend on the particular properties of the network under consideration, reflected in the moments of the degree distribution.

6.1.1 Fully connected networks

We consider a fully connected network, that is, a network composed by N nodes in which each node has a connection to any other node. In a time step $\delta t = 1/N$, a node i with state s ($s = \pm 1$) is randomly chosen. Then, according to the transition probabilities (2.1) introduced in Chapter 2, i switches its state with probability

$$P(s \rightarrow -s) = \frac{1}{2}(1 - sv)(\sigma_{-s})^a, \quad (6.1)$$

where σ_{-s} is the density of neighbors of i with state $-s$, that in a fully connected network is equal to the global density of $-s$ nodes. Given that the total number of agents is conserved we have that $\sigma_- + \sigma_+ = 1$. For convenience, we define the bias $v \equiv 1 - 2S$ ($-1 < v < 1$) as a measure of the preference for one of the two states (where S is the prestige parameter*), with $v > 0$ ($v < 0$) favoring the $s = 1$ ($s = -1$) state. In the case that the switch occurs, the density σ_s is reduced by $1/N$, for which the magnetization $m = \sigma_+ - \sigma_-$ changes by $-2s/N$. Then, the average change in the magnetization can be written as[†]

$$\frac{dm(t)}{dt} = \frac{1}{1/N} \left[\sigma_- P(- \rightarrow +) \frac{2}{N} - \sigma_+ P(+ \rightarrow -) \frac{2}{N} \right]. \quad (6.2)$$

Using Eq. (6.1) and expressing the global densities σ_{\pm} in terms of the magnetization, $\sigma_{\pm} = (1 \pm m)/2$, we arrive to

$$\frac{dm(t)}{dt} = 2^{-(a+1)}(1 - m^2) \left[(1 + v)(1 + m)^{a-1} - (1 - v)(1 - m)^{a-1} \right]. \quad (6.3)$$

Equation (6.3) describes the evolution of a very large system ($N \gg 1$) at the macroscopic level, neglecting finite size fluctuations. This equation for the magnetization is enough to describe the system, given that the interface density ρ can be indirectly obtained through the relation

$$\rho(t) = 2\sigma_+(t)\sigma_-(t) = \frac{[1 - m^2(t)]}{2}. \quad (6.4)$$

*For convenience, in this Chapter the prestige parameter is labeled as S to avoid confusion with the spin state s .

[†]Notice that in Section 2.1 we have introduced an ordinary differential equation for the total density of agents in state A (Eq. (2.2)), but for symmetry arguments, we use throughout this Chapter the magnetization instead.

CHAPTER 6. MACROSCOPIC DESCRIPTIONS

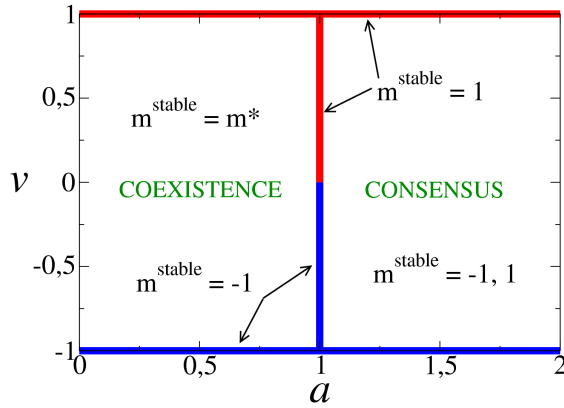


Figure 6.1: Coexistence and consensus regions of the Abrams-Strogatz model in a fully connected network. For values of the volatility parameter $a > 1$, the stable solutions are those of consensus, i.e., all agents in state A ($m_s = -1$) or all in state B ($m_s = 1$), whereas for $a < 1$ both options coexist, with a relative fraction of agents that depends on a and the relative prestige, measured by the bias v . In the extreme case $v = -1$ ($v = 1$), only transitions towards A (B) are allowed, and thus only one consensus state is stable, independent on a .

Stability

Equation (6.3) has three stationary solutions

$$m_- = -1, \quad m^* = \frac{(1-v)^{\frac{1}{a-1}} - (1+v)^{\frac{1}{a-1}}}{(1-v)^{\frac{1}{a-1}} + (1+v)^{\frac{1}{a-1}}} \quad \text{and} \quad m_+ = 1. \quad (6.5)$$

The stability of each of the solutions depends on the values of the parameters a and v . A simple stability analysis can be done by considering a small perturbation ϵ around a stationary solution m_s . For $m_s = m_{\pm}$, we replace m in Eq. (6.3) by $m = \pm 1 \mp \epsilon$ (with $\epsilon > 0$), and expand to first order in ϵ to obtain

$$\frac{d\epsilon}{dt} = 2^{-a} \left[(1 \mp v) \epsilon^{a-1} - 2^{a-1} (1 \pm v) \right] \epsilon. \quad (6.6)$$

When $a < 1$, $\epsilon^{a-1} \rightarrow \infty$ as $\epsilon \rightarrow 0$, thus both solutions m_{\pm} are unstable, whereas for $a > 1$, $\epsilon^{a-1} \rightarrow 0$ as $\epsilon \rightarrow 0$, thus m_{\pm} are stable. In the line $a = 1$, m_+ is unstable (stable) for $v < 0$ ($v > 0$), and vice-versa for m_- . The same analysis for the

6.1. ABRAMS-STROGATZ MODEL

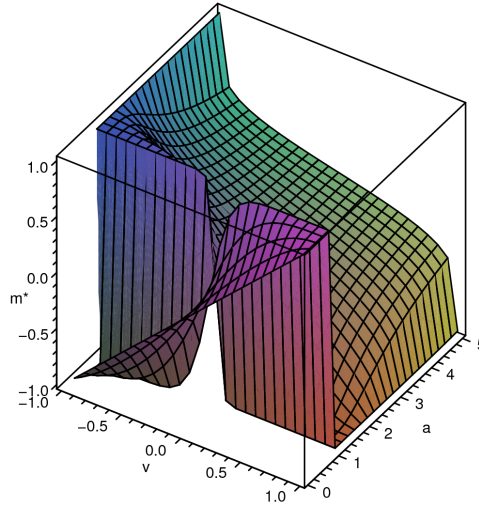


Figure 6.2: Stationary solution $m^*(a, v)$ for the Abrams-Strogatz model (vertical axis) as a function of the two parameters of the model, a and v (horizontal-plane). See Expression (6.5). Notice how m^* approaches the values of the two trivial stationary solutions, $m_- = -1$ and $m_+ = +1$ when $a \rightarrow 1$: for $v > 0$, $\lim_{a \rightarrow 1^+}(m^*) = \mp 1$. The opposite holds for $v < 0$. The non-trivial stationary solution, m^* , is effectively not defined at $a = 1$, and in this case the system has only two stationary states, m_- and m_+ . The Figure illustrates the change of stability of m^* at $a_c = 1$. Notice that the voter model corresponds to $(a = 1, v = 0)$.

intermediate solution m^* leads to

$$\frac{d\epsilon}{dt} = 2^{-(a+1)}(a-1)(1-m^{*2})\left[(1+v)(1+m^*)^{a-2} + (1-v)(1-m^*)^{a-2}\right]\epsilon. \quad (6.7)$$

Then, m^* is unstable (stable) for $a > 1$ ($a < 1$). In Figure 6.1, we show the regions of stability and instability of the stationary solutions on the (a, v) plane obtained from the above analysis. We observe a region of coexistence (m^* stable) and one of bistable consensus (m_+ and m_- stable).

The non-trivial stationary solution, m^* , is shown in Figure 6.2 as a function of the parameters a and v . For the coexistence regime ($a < 1$), the absolute value

CHAPTER 6. MACROSCOPIC DESCRIPTIONS

of the stable stationary magnetization $|m^*|$ increases with both, $|v|$ and a . When $v \neq 0$ the coexistence solution includes a majority of agents in the state with higher prestige, and the rest of the agents in the one with lower prestige. On the contrary, for the consensus regime ($a > 1$) $|m^*|$ decreases with a and increases with $|v|$.

In order to account for possible finite size effects neglected in Eq. (6.3) we have run numerical simulations in a fully connected network. We first notice that the solutions $m = \pm 1$ correspond to the totally ordered *absorbing* configurations, that is, once the system reaches those configurations it never escapes from them. This is because, from the transition probabilities Eq. (6.1), a node never flips when it has the same state as all its neighbors. Thus, to study the stability of these solutions we have followed a standard approach [128] that consists of adding a defect (seed) to the initial absorbing state and let the system evolve (*spreading experiment*). If, in average, the defect spreads over the entire system, then the absorbing state is unstable; otherwise, if the defect quickly dies out, the absorbing state is stable. For instance, to study the stability of $m = -1$, we started from a configuration composed by $N - 1$ down spins and 1 up spin (seed), that corresponds to a magnetization $m = -1 + 2/N \gtrsim -1$, and we let the system evolve until an absorbing configuration is reached. Whether $m = -1$ is stable or not depends on the values of v and a . If $m = -1$ is unstable, then the seed creates many up spins and spreads over the system. If $m = -1$ is stable, then the initial perturbation dies out, and the system ends in the $m = -1$ absorbing state. The theory of criticality predicts that the survival probability $P(t)$, i.e, the fraction of simulations which still have not reached an absorbing state at time t (see Section 2.5), follows a power-law at the critical point [128], where the stability of the absorbing solution changes. Figure 6.3 shows that for a fixed value of the bias $v = 0$, $P(t)$ decreases exponentially fast to zero for values of $a > 1$, while it reaches a constant value for $a < 1$. For $a_c \simeq 1.0$, $P(t)$ decays as $P(t) \sim t^{-\delta}$, with $\delta \simeq 0.95$, indicating the transition line from an unstable to a stable solution $m = -1$ as a is increased, in agreement with the previous stability analysis.

Following the same procedure, we also run spreading experiments to check the stability transition for different values of the bias. For $v = -0.02$ and $v = -0.2$, and a system of size $N = 10^5$, we find the transitions at $a \simeq 1.007$ and $a \simeq 1.052$, respectively. These values are slightly different from the analytical value $a_c = 1.0$, but we have checked that as N is increased, the values become closer to 1.0, in agreement with the stability analysis on infinite large systems.

An alternative and more visual way of studying stability in the mean field limit, is by writing Eq. (6.3) in the form of a time-dependent Ginzburg-Landau equation

$$\frac{dm(t)}{dt} = -\frac{\partial V_{a,v}(m)}{\partial m}, \quad (6.8)$$

6.1. ABRAMS-STROGATZ MODEL

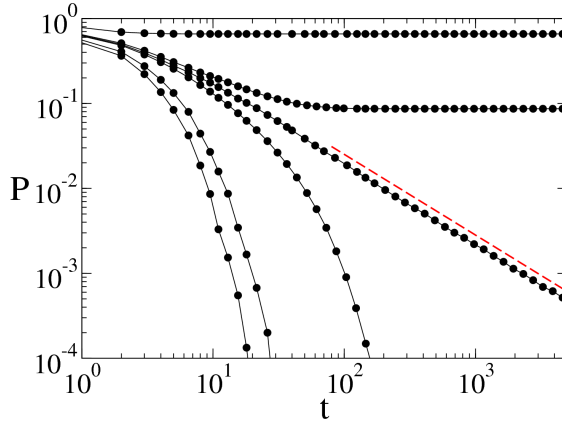


Figure 6.3: Probability $P(t)$ that the system is still alive at time t , when it starts from a configuration composed by an up spin in a sea of $10^5 - 1$ down spins, endowed with the Abrams-Strogatz dynamics with equivalent options (bias $v = 0$), on a fully connected network. Different curves correspond to the values $a = 0.90, 0.99, 1.00, 1.01, 1.10$ and 2.0 (from top to bottom). At $a_c \simeq 1.0$, $P(t)$ follows a power law decay with exponent $\delta \simeq 0.95$, indicated by the dashed line.

with potential

$$\begin{aligned}
 V_{a,v}(m) \equiv & 2^{-a} \left\{ -vm - \frac{1}{2}(a-1)m^2 + \frac{v}{6} [2 - (a-1)(a-2)] m^3 \right. \\
 & + \frac{1}{24}(a-1) [6 - (a-2)(a-3)] m^4 + \frac{v}{10}(a-1)(a-2)m^5 \\
 & \left. + \frac{1}{36}(a-1)(a-2)(a-3)m^6 \right\}. \quad (6.9)
 \end{aligned}$$

$V_{a,v}$ is obtained by Taylor expanding the term in square brackets of Eq. (6.3) up to third order in m , and integrating once over m . We assume that higher order terms in the expansion are irrelevant, and the dynamics is well described by an m^6 -potential.

Within this framework, the state of the system, represented by a point $m(t)$ in the magnetization one-dimensional space $-1 \leq m \leq 1$, moves “down the potential hill”, trying to reach a local minimum. Therefore, a minimum of $V_{a,v}$ at some point m_s represents a stable stationary solution, given that if the system is

CHAPTER 6. MACROSCOPIC DESCRIPTIONS

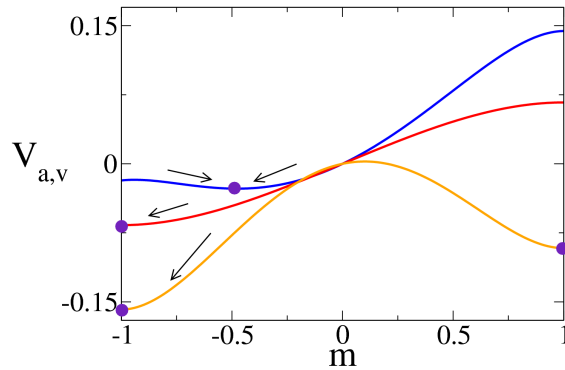


Figure 6.4: Ginzburg-Landau potential from Eq. (6.9) for the Abrams-Strogatz model with bias $v = -0.1$ and values of volatility $a = 0.8, 1.0$ and 2.0 (from top to bottom). Arrows show the direction of the system's magnetization towards the stationary solution (solid circles). For $a = 0.8$ the minimum is around $m \approx -0.5$, indicating that the system relaxes towards a partially ordered stationary state, while for $a = 1.0$ and 2.0 , it reaches the complete ordered state $m = -1$.

moved apart from m_s and then released, it immediately goes back to m_s , whereas a maximum of $V_{a,v}$ represents an unstable stationary solution. As Figure 6.4 shows, for $a < 1$ and all values of v , the single-well potential has a minimum at $|m_s| < 1$ indicating that the system reaches a partially ordered stable state (in the Figure, $m_s \approx -0.5$ for $a = 0.8$ and $v = -0.1$, with fractions 0.75 and 0.25 of down and up spins, respectively, and an interface density $\rho \approx 0.375$). For $a > 1$, the double-well potential has a minimum at $m = \pm 1$, thus depending on the initial magnetization, the system is driven to one of the stationary solutions $m = \pm 1$, corresponding to the totally ordered configurations in which $\rho = 0$.

This description works well in infinite large systems, where there are no finite size fluctuations. But in finite systems, the absorbing solutions $m = \pm 1$ are the only "truly stationary states", given that fluctuations ultimately take the system to one of those states. Even for the case $a < 1$, where the minimum is at $|m_s| < 1$, the magnetization fluctuates around m_s for a very long time until after a large fluctuation it reaches an absorbing state $|m| = 1$.

6.1. ABRAMS-STROGATZ MODEL

The biased voter model (case $a = 1$)

For $a = 1$ the AS-model becomes equivalent to the voter model with bias (the original voter model is trivially recovered fixing $v = 0$). Notice once more that a switching probability proportional to the local density of neighbors in the opposite state is statistically equivalent to adopt the state of a randomly chosen neighbor. In this limit of neutral volatility, $a = 1$, Eq. (6.3) becomes

$$\frac{dm}{dt} = \frac{v}{2}(1 - m^2), \quad (6.10)$$

whose solution is

$$m(t) = \frac{(1 + m_0)e^{vt} - (1 - m_0)}{(1 + m_0)e^{vt} + (1 - m_0)}, \quad (6.11)$$

with $m_0 = m(t = 0)$. For random initial conditions, $m_0 = 0$. Thus

$$m(t) = \tanh(vt/2), \quad (6.12)$$

and

$$\rho(t) = \frac{1}{2} \left[1 - \tanh^2(vt/2) \right]. \quad (6.13)$$

In Figure 6.5, we observe that the analytical solutions from Eqs. (6.12) and (6.13) agree very well with the results from numerical simulations of the model for large enough systems. They also reproduce the Monte Carlo results found in [180]. This is so, because finite-size fluctuations effects are negligible compare to bias effects, even for a small bias.

When the bias is exactly zero (voter model), one recovers the known result that in an infinite large network $dm/dt = 0$, thus m and ρ are conserved (see Section 1.4.2). However, in a finite network fluctuations always lead the system to one of the absorbing states [180]. To find how the system relaxes to the final state, one needs to calculate the evolution of the second moment $\langle m^2 \rangle$ of the magnetization, related to the fluctuations in m , where the symbol $\langle \dots \rangle$ represents an average over many realizations. This leads to a decay of the average interface density of the form (see Section 1.4.2; [133])

$$\langle \rho(t) \rangle = \frac{1}{2} \left[1 - \langle m^2(t) \rangle \right] = \langle \rho(0) \rangle e^{-2t/N}. \quad (6.14)$$

In terms of the potential description of Eq. (6.8), we observe that when $v \neq 0$, $V_{a,v}$ has only one minimum (see Figure 6.4), thus the system has a preference for one of the absorbing states only, whereas if $v = 0$, then $V_{a,v} = 0$, and the magnetization is conserved ($m(t) = m(0) = \text{constant}$). In finite systems, even though the average magnetization over many realizations is conserved, the system still orders in individual realizations by finite size fluctuations.

CHAPTER 6. MACROSCOPIC DESCRIPTIONS

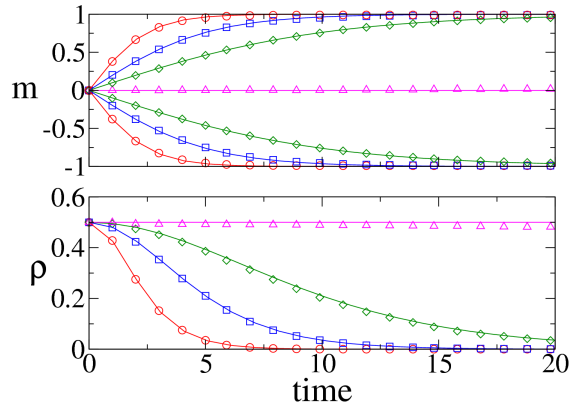


Figure 6.5: Abrams-Strogatz model on a fully connected network of $N = 1000$ nodes with volatility $a = 1$. Top: Average magnetization m vs time for values of the bias $v = 0.8, 0.4, 0.2, 0.0, -0.2, -0.4$ and -0.8 (from top to bottom). Bottom: Average interface density ρ vs time for $v = 0.0, 0.2, 0.4$ and 0.8 (top to bottom). Open symbols are the results from numerical simulations, while solid lines in the upper and lower panels correspond to the solutions from Eqs. (6.12) and (6.13) respectively. Averages are over 100 independent realizations starting from a configuration with a random distribution of spins ($m(0) = 0$).

6.1.2 Complex networks

We consider next a network of N nodes with a given degree distribution P_k , representing the fraction of agents connected to k neighbors, such that $\sum_k P_k = 1$. In order to develop a mathematical approach that is analytically tractable, we assume that the network has no degree correlations, as it happens for instance in Erdős-Renyi networks [30]. It turns out that dynamical correlations between the states of second nearest-neighbors are negligible in voter models on uncorrelated networks [133, 231]. Therefore, taking into account only correlations between first nearest-neighbors allows us to use an approach, called *pair approximation*, that leads to analytical results in good agreement with simulations. In this Section, we use this approximation to build equations for the magnetization and the average interface density.

In a time step $\delta t = 1/N$, a node i with degree k and state s is chosen with probability $P_k \sigma_s$. Here we assume that the density of nodes in state s within the subgroup of nodes with degree k is independent on k and equal to the global

6.1. ABRAMS-STROGATZ MODEL

density σ_s . Then, according to the transition probabilities (2.1) introduced in Chapter 2, i switches its state with probability

$$P(s \rightarrow -s) = \frac{1}{2}(1 - sv) (n_{-s}/k)^a, \quad (6.15)$$

where we denote by n_{-s} the number of neighbors of i in the opposite state $-s$ ($0 \leq n_{-s} \leq k$) and the bias v is defined as in the previous Section. If the switch occurs, the density σ_s is reduced by $1/N$, for which the magnetization $m = \sigma_+ - \sigma_-$ changes by $-2s/N$, while the density ρ changes by $2(k - 2n_{-s})/\mu N$, where $\mu \equiv \sum_k k P_k$ is the average degree of the network. Thus, in analogy to Section 6.1.1, but now plugging the transition probabilities from Eq. (6.15) into Eq. (6.2), we write the average change in the magnetization as

$$\begin{aligned} \frac{dm(t)}{dt} &= \sum_k \frac{P_k \sigma_-}{1/N} \sum_{n_+=0}^k B(n_+, k) \frac{(1+v)}{2} \left(\frac{n_+}{k}\right)^a \frac{2}{N} \\ &\quad - \sum_k \frac{P_k \sigma_+}{1/N} \sum_{n_-=0}^k B(n_-, k) \frac{(1-v)}{2} \left(\frac{n_-}{k}\right)^a \frac{2}{N}, \end{aligned} \quad (6.16)$$

and similarly, the change in the interface density as

$$\begin{aligned} \frac{d\rho(t)}{dt} &= \sum_k \frac{P_k \sigma_-}{1/N} \sum_{n_+=0}^k B(n_+, k) \frac{(1+v)}{2} \left(\frac{n_+}{k}\right)^a \frac{2(k - 2n_+)}{\mu N} \\ &\quad + \sum_k \frac{P_k \sigma_+}{1/N} \sum_{n_-=0}^k B(n_-, k) \frac{(1-v)}{2} \left(\frac{n_-}{k}\right)^a \frac{2(k - 2n_-)}{\mu N}. \end{aligned} \quad (6.17)$$

We denote by $B(n_s, k)$, the probability that a node of degree k and state $-s$ has n_s neighbors in the opposite state s . Defining the a -th moment of $B(n_s, k)$ as

$$\langle n_s^a \rangle_k \equiv \sum_{n_s=0}^k B(n_s, k) n_s^a,$$

we arrive to the equations

$$\frac{dm(t)}{dt} = \sum_k \frac{P_k}{2k^a} [(1+v)(1-m)\langle n_+^a \rangle_k - (1-v)(1+m)\langle n_-^a \rangle_k], \quad (6.18)$$

$$\begin{aligned} \frac{d\rho(t)}{dt} &= \sum_k \frac{P_k}{2\mu k^a} \left\{ (1+v)(1-m) \left[k\langle n_+^a \rangle_k - 2\langle n_+^{(1+a)} \rangle_k \right] \right. \\ &\quad \left. + (1-v)(1+m) \left[k\langle n_-^a \rangle_k - 2\langle n_-^{(1+a)} \rangle_k \right] \right\}. \end{aligned} \quad (6.19)$$

CHAPTER 6. MACROSCOPIC DESCRIPTIONS

The biased voter model (case $a = 1$)

In order to develop an intuition about the temporal evolution of m and ρ from Eqs. (6.18) and (6.19), we first analyze the simplest and non-trivial case $a = 1$, that corresponds to the voter model on complex networks. A rather complete analysis of the time evolution and consensus times of this model on uncorrelated networks, for the symmetric case $v = 0$, can be found in [133]. Following a similar approach, here we study the general situation in which the bias v takes any value. To obtain closed expressions for m and ρ , we consider that the system is “well mixed”, in the sense that the different types of links are uniformly distributed over the network. Therefore, we assume that the probability that a link picked at random is of type $+-$ is equal to the global density of $+-$ links ρ . Then, $B(n_{-s}, k)$ becomes the binomial distribution with

$$P(-s|s) = \rho/2\sigma_s \quad (6.20)$$

as the single event probability that a first nearest-neighbor of a node with state s has state $-s$. Here, we use the fact that in uncorrelated networks dynamical correlations between the states of second nearest-neighbors vanish (pair approximation). $P(-s|s)$ is calculated as the ratio between the total number of links $\rho\mu N/2$ from nodes in state s to nodes in state $-s$, and the total number of links $N\sigma_s\mu$ coming out from nodes in state s . Taking $a = 1$ in Eqs. (6.18) and (6.19), and replacing the first and second moments of $B(n_{-s}, k)$ by

$$\begin{aligned} \langle n_{-s} \rangle &= P(-s|s)k, \\ \langle n_{-s}^2 \rangle &= P(-s|s)k + P(-s|s)^2k(k-1), \end{aligned}$$

leads to the following two coupled closed equations for m and ρ

$$\frac{dm(t)}{dt} = v\rho \quad (6.21)$$

$$\frac{d\rho(t)}{dt} = \frac{\rho}{\mu} \left\{ \mu - 2 - \frac{2(\mu-1)(1+vm)\rho}{(1-m^2)} \right\}. \quad (6.22)$$

For $v = 0$, the above expressions agree with the ones of the symmetric voter model [133]. For the asymmetric case $v \neq 0$, we have checked numerically that the only stationary solutions are $(m = 1, \rho = 0)$ for $v > 0$ and $(m = -1, \rho = 0)$ for $v < 0$, that correspond to the fully ordered states, as we were expecting. Even though an exact analytical solution of Eqs. (6.21) and (6.22) is hard to obtain, we can still find a solution in the long time limit, assuming that ρ decays to zero as

$$\rho = A e^{-t/2\tau(v)}, \quad \text{for } t \gg 1, \quad (6.23)$$

6.1. ABRAMS-STROGATZ MODEL

where A is a constant given by the initial state and $\tau(v)$ is another constant that depends on v , and quantifies the rate of decay towards the solutions $m = 1$ or $m = -1$. To calculate the value of τ , we first replace the ansatz from Eq. (6.23) into Eq. (6.21), and solve for m with the boundary conditions $m(\rho = 0) = 1$ and -1 , for $v > 0$ and $v < 0$, respectively. We obtain

$$m = \begin{cases} 1 - 2v\tau\rho & \text{if } v > 0; \\ -1 - 2v\tau\rho & \text{if } v < 0. \end{cases} \quad (6.24)$$

Then, to first order in ρ we find

$$(1 - m^2) = \begin{cases} 4v\tau\rho & \text{if } v > 0; \\ -4v\tau\rho & \text{if } v < 0. \end{cases} \quad (6.25)$$

Replacing the above expressions for m and $(1 - m^2)$ into Eq. (6.22), and keeping only the leading order terms, we arrive to the following expression for τ

$$\tau(v) = \begin{cases} \frac{\mu-1-v}{2v(\mu-2)} & \text{if } v > 0; \\ \frac{1-\mu-v}{2v(\mu-2)} & \text{if } v < 0. \end{cases} \quad (6.26)$$

Finally, the magnetization for long times behaves as

$$m = \begin{cases} 1 - \frac{(\mu-1-v)A}{\mu-2} \exp\left[-\frac{v(\mu-2)}{\mu-1-v}t\right] & \text{if } v > 0; \\ -1 + \frac{(\mu-1+v)A}{\mu-2} \exp\left[\frac{v(\mu-2)}{\mu-1+v}t\right] & \text{if } v < 0, \end{cases} \quad (6.27)$$

whereas the interface density decays as

$$\rho = A \exp\left[-\frac{|v|(\mu-2)}{\mu-1-|v|}t\right]. \quad (6.28)$$

Using the expression for $\tau(v)$ from Eq. (6.26) in Eq. (6.25), and taking the limit $v \rightarrow 0$, we find that $\rho(t) = \frac{(\mu-2)}{2(\mu-1)} [1 - m(t)^2]$, in agreement with previous results of the voter model on uncorrelated networks [133]. By taking $\mu = N - 1 \gg 1$ in Eqs. (6.27) and (6.28), we recover the expressions for m and ρ on fully connected networks (Eqs. (6.12) and (6.13), respectively), in the long time limit. This result means that the evolution of m and ρ in the biased voter model on uncorrelated networks in the long time limit is very similar to the mean-field case, with the time rescaled by the constant τ that depends on the topology of the network, expressed by the average connectivity μ . From the above equations we observe that the system reaches the absorbing state $\rho = 0$ in a time of order τ . For the special case $v = 0$, τ diverges, thus Eqs. (6.27) and (6.28) predict that both

CHAPTER 6. MACROSCOPIC DESCRIPTIONS

m and ρ stay constant over time. However, as mentioned in Section 6.1.1, finite-size fluctuations drive the system to the absorbing state ($\rho = 0, |m| = 1$). Taking fluctuations into account, one finds that the approach to the final state is described by the decay of the average density ρ (Section 1.4.2; [133])

$$\langle \rho(t) \rangle = \frac{(\mu - 2)}{2(\mu - 1)} e^{-2t/T}, \quad (6.29)$$

where $T \equiv \frac{(\mu-1)\mu^2 N}{(\mu-2)\mu_2}$, depends on the system size N , and the first and second moments of the network, μ and μ_2 respectively.

Stability analysis

As in fully connected networks, we assume that Eq. (6.18) for the magnetization has three stationary solutions. Indeed, we have numerically verified that for different types of networks there is, apart from the trivial solutions $m = 1, -1$, an extra non-trivial stationary solution $m = m^*$. Due to the rather complicated form of Eq. (6.18), we try to study the stability of the solutions in an approximate way, in order to find a qualitative picture of the stability diagram in the (a, v) plane. For the general case in which a and v take any values, we assume, as in the voter model case, that $B(n_{-s}, k)$ is a binomial probability distribution with single event probabilities given by Eq. (6.20). Then, the explicit form for the a -th moment of $B(n, k)$ is

$$\langle n_s^a \rangle = \sum_{n_s=0}^k n_s^a C_{n_s}^k \left(\frac{\rho}{2\sigma_{-s}} \right)^{n_s} \left(1 - \frac{\rho}{2\sigma_{-s}} \right)^{k-n_s}. \quad (6.30)$$

We also assume that, as it happens for the voter model case $a = 1$ [see Eq. (6.25)], ρ and m are related by $\rho(t) \simeq \frac{q}{2} [1 - m^2(t)]$, where q is a constant that depends on a and v . We note that this relation satisfies the fully-ordered-state condition $\rho = 0$ when $|m| = 1$. We shall see that the exact functional form of $q = q(a, v)$ is irrelevant for the stability results, as long as $q > 0$. To simplify calculations even more, we consider that the network is a degree-regular random graph with degree distribution $P_k = \delta_{k,\mu}$, that is, all nodes have exactly μ neighbors chosen at random (see Section 1.2.3). Then, replacing the above expression for the moments into Eq. (6.18), and substituting ρ by the approximate value $\frac{q}{2} [1 - m^2]$, we arrive to the following closed equation for m

$$\begin{aligned} \frac{dm}{dt} &= \frac{(1 - m^2)}{2\mu^a} \sum_{n=0}^{\mu} C_n^{\mu} n^a \left(\frac{q}{2} \right)^n \left\{ (1 + v)(1 + m)^{n-1} [1 - q(1 + m)]^{\mu-n} \right. \\ &\quad \left. - (1 - v)(1 - m)^{n-1} [1 - q(1 - m)]^{\mu-n} \right\}, \end{aligned} \quad (6.31)$$

6.1. ABRAMS-STROGATZ MODEL

where mute indices n_- and n_+ were replaced by the index n . To check the stability of $m = 1$, we take $m = 1 - \epsilon$ in Eq. (6.31), and expand it to first order in ϵ . We obtain after some algebra

$$\frac{d\epsilon}{dt} = \frac{\mu^{-a}}{2} (\langle n \rangle_q + \langle n^a \rangle_q) [\mathcal{V}_1(a) - v] \epsilon, \quad (6.32)$$

where the symbols $\langle \cdot \rangle_q$ represent the moments of a Binomial distribution with probability q , and the bias function $\mathcal{V}_1(a)$ is defined as

$$\mathcal{V}_1(a) = \frac{\langle n \rangle_q - \langle n^a \rangle_q}{\langle n \rangle_q + \langle n^a \rangle_q}. \quad (6.33)$$

Then, for a fixed value of a the solution $m = 1$ is stable (unstable), when v is larger (smaller) than $\mathcal{V}_1(a)$. The shape of the function $\mathcal{V}_1(a)$ can be guessed using that for a larger (smaller) than 1, the moment $\langle n^a \rangle$ is larger (smaller) than $\langle n \rangle$. Then $\mathcal{V}_1(a)$ goes to $(\langle n \rangle - 1)/(\langle n \rangle + 1) \lesssim 1$ and -1 as a approaches to 0 and ∞ , respectively. Also $\mathcal{V}_1(a) = 0$, for $a = 1$. With a similar stability analysis we obtained that $m = -1$ is stable (unstable) for the points (a, v) below (above) the transition line $\mathcal{V}_{-1}(a) = -\mathcal{V}_1(a)$, while $m = m^*$ is stable in the region where both $m = -1$ and $m = 1$ are unstable. In Figure 6.6 we show a picture that summarizes the stability regions defined by the transition lines $\mathcal{V}_1(a)$ and $\mathcal{V}_{-1}(a)$. These lines were obtained by integrating numerically the two coupled Eqs. (6.18) and (6.19), with the moments defined in Eq. (6.30), and finding the points (a, v) where the stationary solutions $m = 1, -1$ became unstable. We considered two degree-regular random graphs with degrees $\mu = 3$ (solid lines $\mathcal{V}_1^3(a)$ and $\mathcal{V}_{-1}^3(a)$) and $\mu = 10$ (dashed-lines $\mathcal{V}_1^{10}(a)$ and $\mathcal{V}_{-1}^{10}(a)$), thus we took $P_k = \delta_{k,\mu}$ in the equations. For clarity, only the stable solutions are labeled in the picture. We observe that as the degree of the network increases, the coexistence region expands and approaches to the corresponding region $a < 1$ on fully connected networks.

In order to give numerical evidence, from Monte Carlo simulations, of the different phases and transition lines predicted in Figure 6.6, we run spreading experiments as explained in Section 6.1.1, for a degree-regular random graph (DRRG) with degree $\mu = 3$ and $N = 10^5$ nodes, and test the stability of the homogeneous solutions $m = \pm 1$. We first set the bias in $v = 0$ and, by varying a , we obtained a transition at $a_c \simeq 1.0$ from consensus to coexistence, as a is decreased: in the consensus region the survival probability $P(t)$ decays exponentially fast to zero, indicating that $m = 1$ is stable, while in the coexistence region $P(t)$ reaches a constant value larger than zero, showing that $m = 1$ is unstable (not shown). This transition is the same as the one in fully connected networks (FCN); see Figure 6.3. We then repeat the experiment with $v = -0.2$, whose results are summarized in Figure 6.7, where we show $P(t)$ for different values of a . Increasing

CHAPTER 6. MACROSCOPIC DESCRIPTIONS

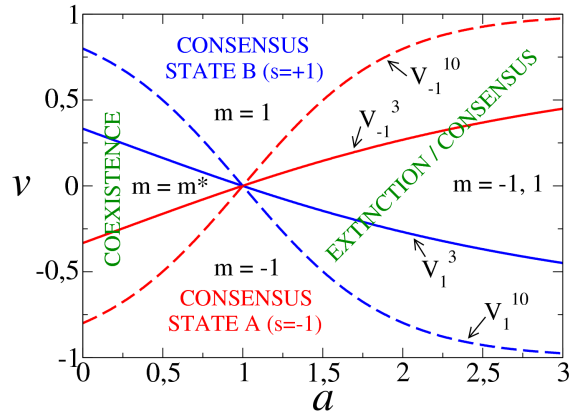


Figure 6.6: Stability diagram for the Abrams-Strogatz model in a degree-regular random graph, obtained by numerical integration of Eqs. (6.18), (6.19), using Eq. (6.30). The solution $m = 1$ is stable above the line \mathcal{V}_1 , while the solution $m = -1$ is stable below the line \mathcal{V}_{-1} . Solid and dashed lines correspond to graphs with degrees $\mu = 3$ and $\mu = 10$ respectively. In the coexistence region, where the stable solution is m^* , the system is composed by both type of agents, while in the consensus region, agents in either one or the other option prevail, depending on the initial conditions. We observe that the region of coexistence is reduced, compared to the model on fully connected networks (Figure 6.1), due to the emergence of two monostable-consensus regions, where always the same option dominates.

a from 0, which corresponds to the coexistence regime ($m = \pm 1$ are unstable solutions, and m^* is stable), we show in Figure 6.7(a) how in a DRRG $m = -1$ changes from unstable to stable at a value $0.25 < a < 0.3$, as $P(t)$ starts to decay to zero. This corresponds to crossing the line \mathcal{V}_{-1}^3 in the horizontal direction (see Figure 6.6), and entering the *monostable-consensus region* where there exist only two solutions, $m = -1$ stable, and $m = +1$ unstable (m^* becomes equal to -1 along the transition line \mathcal{V}_{-1}^3). In Figure 6.7(b), we observe how in a DRRG $m = +1$ becomes stable at a value $1.80 < a < 1.85$. This corresponds to crossing the line \mathcal{V}_1^3 (see Figure 6.6) and entering to the consensus region, where both $m = \pm 1$ are stable. Notice that for $a = 1.80$, $P(t)$ first curves up and then it quickly decays to zero at a time $t \simeq 4000$. This means that a finite fraction of realizations starting from a system with a single down spin took, in average, a mean time $t \simeq 4000$ to end up in a configuration with all down spins, showing that $m = -1$ is a stable solution. This supports our claim that in the monostable-consensus region there exist only two solutions, $m = -1$ stable, and $m = +1$ unstable. These

6.1. ABRAMS-STROGATZ MODEL

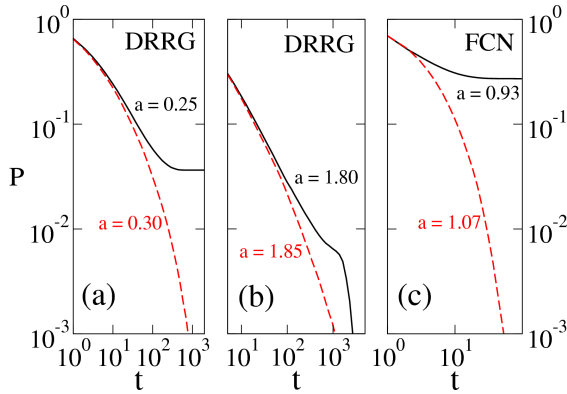


Figure 6.7: Spreading experiments: probability $P(t)$ that the system is still alive at time t in the Abrams-Strogatz model with bias $v = -0, 2$ and various values of volatility a , showing the stability of the solutions $m = 1, -1$. Dashed curves decay quickly to zero, indicating that the solution is stable, while solid curves represent unstable solutions. (a) Degree-regular random graph (DRRG, $\mu = 3$). Stability of the solution $m = -1$: $a = 0.25$ (solid curve), $a = 0.30$ (dashed curve). (b) Degree-regular random graph (DRRG, $\mu = 3$). Stability of the solution $m = +1$: $a = 1.80$ (solid curve), $a = 1.85$ (dashed curve). (c) Fully connected network (FCN). Stability of the solutions $m = \pm 1$: $a = 0.93$ (solid curve), $a = 1.07$ (dashed curve). All curves correspond to an average over 10^5 independent realizations on networks with $N = 10^5$ nodes.

results confirm the existence of a quite broad monostable-consensus region in DRRG ($0.30 \lesssim a \lesssim 1.85$ for $v = -0.2$ and $\mu = 3$), in agreement with the stability diagram obtained in Figure 6.6, while this region seems to be absent in FCN. Indeed, Figure 6.7(c) shows how this unstable-stable transition happens in a FCN at a value $0.93 < a < 1.07$, in agreement with the transition line $a_c \simeq 1.0$ in FCN. Here, both $m = \pm 1$ gain stability at the same point, and the system enters to the consensus region (see Figure 6.1).

In summary, we find that, compared to the fully connected case, the region of coexistence is shrunk for $v \neq 0$, as there appear two regions where only one solution is stable. These regions also reduce part of the consensus region, where both solutions $m = \pm 1$ are stable. The effect of the bias is shown to be more important in DRRGs with low connectivity μ and, as a general result, coexistence becomes harder to achieve in sparse networks.

Bilinguals model

We study in this Section the Bilg-model, the extension of the AS-model to account for bilingual agents introduced in Chapter 2 (see Section 2.2 for a detailed description). As in the AS-model, it is convenient to consider A and B agents, as particles with opposite spins -1 and 1 respectively. AB agents are considered as spin-0 particles because they share both states at the same time (-1 and 1). Given that the model is invariant under the interchange of -1 and 1 particles, the system is better described using the global magnetization $m \equiv \sigma_+ - \sigma_-$ and the density of AB agents σ_0 , where σ_- , σ_0 , σ_+ , are the global densities of nodes in states -1 , 0 and 1 , respectively. Another alternative could be the use of the interface density $\rho \equiv 2\sigma_- \sigma_+ + 2\sigma_- \sigma_0 + 2\sigma_+ \sigma_0$, but numerical simulations show that ρ and σ_0 are proportional*. We now study the evolution of the system on fully connected and complex networks, by deriving equations for m and σ_0 .

6.2.1 Fully connected networks

In the fully connected case, the local densities of neighbors in the different states agree with the global densities σ_- , σ_0 , σ_+ . Thus, using the transition probabilities (2.4)-(2.5) introduced in Chapter 2, the rate equations for σ_- and σ_+ can be written as

$$\frac{d\sigma_-}{dt} = \frac{(1-v)}{2}\sigma_0(1-\sigma_+)^a - \frac{(1+v)}{2}\sigma_- \sigma_+^a, \quad (6.34)$$

$$\frac{d\sigma_+}{dt} = \frac{(1+v)}{2}\sigma_0(1-\sigma_-)^a - \frac{(1-v)}{2}\sigma_+ \sigma_-^a, \quad (6.35)$$

where $v \equiv 1 - 2S$ is the bias. The rate equations for $m = \sigma_+ - \sigma_-$ and $\sigma_0 = 1 - \sigma_+ - \sigma_-$ can be derived from the above two equations, and by making the substitutions $\sigma_s = (1 - \sigma_0 + s m)/2$, with $s = \pm 1$. We obtain

$$\begin{aligned} \frac{dm}{dt} &= 2^{-(2+a)} \left\{ 2\sigma_0 [(1+v)(1+\sigma_0+m)^a - (1-v)(1+\sigma_0-m)^a] \right. \\ &\quad \left. + (1+v)(1-\sigma_0-m)(1-\sigma_0+m)^a - (1-v)(1-\sigma_0+m)(1-\sigma_0-m)^a \right\} \end{aligned} \quad (6.36)$$

and

$$\begin{aligned} \frac{d\sigma_0}{dt} &= 2^{-(2+a)} \left\{ -2\sigma_0 [(1+v)(1+\sigma_0+m)^a + (1-v)(1+\sigma_0-m)^a] \right. \\ &\quad \left. + (1+v)(1-\sigma_0-m)(1-\sigma_0+m)^a + (1-v)(1-\sigma_0+m)(1-\sigma_0-m)^a \right\}. \end{aligned} \quad (6.37)$$

*Notice that this result has already been shown for regular lattices in Section 3.2.

6.2. BILINGUALS MODEL

Equations (6.36) and (6.37) are difficult to integrate analytically, but an insight on its qualitatively behavior can be obtained by studying the stability of the stationary solutions with a and v . As in the AS-model, we expect that, for a given v , an order-disorder transition appears at some value a_c of the volatility parameter, where the stability of the stationary solutions changes. If a is small, then flipping rates are high, thus we expect the system to remain in an active disordered state, while for large enough values of a , spins tend to be aligned, thus the system should ultimately reach full order. In the following, we calculate the transition point for the symmetric case $v = 0$, and we find an approximate solution for the linear case $a = 1$.

Transition point for $v = 0$

In the symmetric case $v = 0$, one can easily verify that the points $(m = \pm 1, \sigma_0 = 0)$ in the (m, σ_0) plane are two stationary solutions of Eqs. (6.36) and (6.37). But there is also a third non-trivial stationary solution, that for the symmetric case $v = 0$ is $(m = 0, \sigma_0 = \sigma_0^*)$, where σ_0^* satisfies

$$2\sigma_0^*(1 + \sigma_0^*)^a - (1 - \sigma_0^*)^{(1+a)} = 0. \quad (6.38)$$

By doing a small perturbation around $(0, \sigma_0^*)$ in the σ_0 direction, one finds from Eq. (6.37) that the point $(0, \sigma_0^*)$ is stable for all values of a . Instead, the stability in the m direction changes at some value a_{fc} (fc stands for *fully connected network*). Replacing m by $\epsilon \ll 1$ and σ_0 by σ_0^* in Eq. (6.36), one arrives to the following relation that σ_0^* and a hold when the stability changes

$$2a_{fc}\sigma_0^*(1 + \sigma_0^*)^{(a_{fc}-1)} + (a_{fc} - 1)(1 - \sigma_0^*)^{a_{fc}} = 0. \quad (6.39)$$

Combining Eqs. (6.38) and (6.39), one arrives to the following closed equation for a_{fc}

$$a_{fc} \ln \left(\frac{1 - a_{fc}}{a_{fc}} \right) = \ln \left(\frac{2a_{fc} - 1}{1 - a_{fc}} \right), \quad (6.40)$$

whose solution is $a_{fc} \approx 0.63$. Then, assuming that the transition point does not depend on v for FCN, as it happens in the AS-model, we find that the (a, v) plane is divided into two regions. In the region $a < a_{fc}$, the stable solution is $(0, \sigma_0^*)$, representing a stable coexistence of the three kinds of agents, while in the region $a > a_{fc}$, the stable solutions $(\pm 1, 0)$ indicate the ultimate dominance of one of the states. By performing spreading experiments we estimated that the transition point for a network of $N = 10^5$ nodes is around 0.62 (see Figure 6.8), and we observed that this value approaches to the analytical one 0.63 as N increases. We have also checked numerically the transition point when there is a bias

CHAPTER 6. MACROSCOPIC DESCRIPTIONS

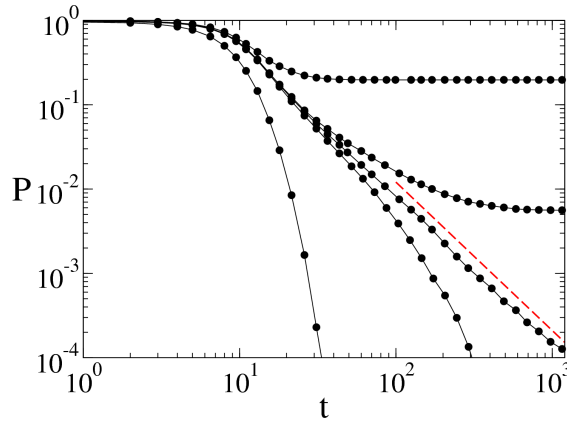


Figure 6.8: Spreading experiments: probability $P(t)$ that the system is still alive at time t in the Bilinguals model on a fully connected network, obtained from the same spreading experiments and parameters ($v = 0$, $N = 10^5$) as described in Figure 6.3 for the Abrams-Strogatz model. The curves correspond to volatilities $a = 0.600, 0.618, 0.620, 0.622$ and 0.700 , (top to bottom). $P(t)$ decays as $t^{-\delta}$ at the transition point 0.620 (close to the theoretical value $a_{fc} \simeq 0.63$), with $\delta \simeq 1.76$, indicated by the dashed line.

($v \neq 0$), that is, when the two options are not equivalent. In this case, we find a value around 0.675 for a bias $v = -0.2$ and $N = 10^5$ nodes, what represents a small deviation from the analytical value. However, this difference is similar to the one found for the AS-model in Section 6.1.1 with the same system size. Therefore, we assume that this discrepancy is again due to finite size effects. In the thermodynamic limit, though, the value $a_{fc} \simeq 0.63$ should be independent of v .

We note that the transition point $a_{fc} \simeq 0.63$ is smaller than the value $a_c \simeq 1.0$ for the transition in the Abrams-Strogatz model, thus the region for coexistence is reduced when AB agents are considered.

AB-model: Neutral volatility ($a = 1$) and symmetric options ($v = 0$)

For $a = 1$ and $v = 0$, the Bilg-model reduces to the AB-model. In this case, Equations (6.36) and (6.37) become

$$\frac{dm}{dt} = \frac{1}{2}\sigma_0 m, \quad (6.41)$$

6.2. BILINGUALS MODEL

$$\frac{d\sigma_0}{dt} = \frac{1}{4}(1 - m^2 - 4\sigma_0 - \sigma_0^2). \quad (6.42)$$

The three stationary solutions are $(m, \sigma_0) = (-1, 0); (1, 0)$ and $(0, \sqrt{5} - 2)^*$. Given that the above equations are difficult to integrate analytically, we try an approximate solution by assuming that the density of AB agents is proportional to the interface density ρ , something observed in our simulations, and already found for the AB-model (Section 3.2; [198]). Indeed, AB agents are found to be at the interface between single-option domains, for all the networks studied. Therefore, we write $\sigma_0 \simeq \alpha\rho$, with $\rho = 2\sigma_-\sigma_+ + 2\sigma_0(\sigma_- + \sigma_+) = \frac{1}{2}[(1 - \sigma_0)^2 - m^2] + 2\sigma_0(1 - \sigma_0)$, from where we obtain that m can be expressed in terms of σ_0 as $m^2 = (1 - \sigma_0)^2 + 4\sigma_0(1 - \sigma_0) - 2\sigma_0/\alpha$. Replacing this expression for m^2 into Eq. (6.42), we obtain the following equation for σ_0

$$\frac{d\sigma_0}{dt} = \frac{\sigma_0}{2}(-3 + \frac{1}{\alpha} + \sigma_0). \quad (6.43)$$

We have checked by numerical simulations that $\alpha > 1/3$, then the solution of the above equation in the long time limit is $\sigma_0 \sim e^{(-3+1/\alpha)t/2}$. Thus, σ_0 and $|m|$ approach to 0 and 1, respectively, and the system reaches full order exponentially fast[†].

6.2.2 Complex networks

We now consider the model on complex networks. Following the same approach as in Section 6.1.2, it is possible to write down a set of nine coupled differential equations: three for the densities σ_- , σ_0 and σ_+ of node states, and six for the densities $\rho_{--}, \rho_{-0}, \rho_{+0}, \rho_{+-}, \rho_{+0}$ and ρ_{++} of different types of links. However, due to the complexity of these equations, we limit our study here to the investigation of the stability regions through Monte Carlo simulations. We find that in a degree-regular random graph with mean degree $\mu = 3$, the stability diagram is qualitatively similar to the one in Figure 6.6 for the AS-model, where the coexistence region corresponds to stationary states with a mix of the three types of agents. However, the coexistence-dominance transition point for $v = 0$ is shifted to $a_{cn} \simeq 0.3$ (cn stands for *complex networks*). For $v = -0.02$, a monostable region appears for $0.2 \lesssim a \lesssim 0.4$, while this region becomes wider for $v = -0.2$ ($0 \lesssim a \lesssim 1.4$). We have also observed that the coexistence region disappears for $|v| \geq 0.2$. Therefore, in the Bilg-model, the region for coexistence also shrinks as

*Notice that in Section 2.3 we have derived these stationary solutions as a function of the state global densities.

[†]An exponential decay to the absorbing state of $\langle \rho(t) \rangle$ for the AB-model in fully connected networks has already been numerically observed in Section 3.1, Figure 3.1.

CHAPTER 6. MACROSCOPIC DESCRIPTIONS

the connectivity of the network decreases (going from fully connected to complex networks with low degree). But on top of that, for $v = 0$ there exists a shift of the critical value from $a_{fc} \simeq 0.63$ (fully connected networks) to $a_{cn} \simeq 0.3$ (degree-regular random graphs) which results in a translation of the whole stability diagram to smaller values of the volatility parameter. In a few words, compared to the AS-model, the overall effect of the inclusion of the AB agents is that of a large reduction of the region of coexistence.

6.3

Two-dimensional lattices

Dynamical properties of the AS-model and the Bilg-model in two-dimensional lattices can be explored for different initial conditions, system sizes, and values of the prestige and volatility parameters, through a simulation applet available online (see Section 2.4; [220]). It turns out that the behavior of these models in square lattices is very different to their behavior in fully connected or complex networks. On the one hand, the mean distance between two sites in the lattice grows linearly with the length of the lattice side L , thus a spin only “feels” the spins that are in its near neighborhood, and therefore the mean-field approach that works well in fully connected networks gives poor results in lattices. On the other hand, correlations between second, third and higher order nearest-neighbors are important in lattices, what causes the formation of same-spin domains, unlike in random networks where correlations to second nearest-neighbors are already negligible. Therefore, pair approximation does not provide a good enough description of the dynamics in lattices either, and one is forced to implement higher order approximations (triplets, quadruplets, etc), that lead to a coupled system of many equations, impossible to solve analytically. Due to the fact that the mean-field and pair approximations, that use global quantities such as the magnetization and the interface density to describe the system, do not give good results in lattices, we follow here a different approach to obtain a macroscopic description. This approach, also developed in [212] for general nonequilibrium spin models, consists in deriving a macroscopic equation for the evolution of a continuous space dependent spin field. Within this approach it is possible to describe coarsening processes, that is, processes of formation and growth of local domains caused by interface motion (see Section 1.4.1). In particular, one can explain whether the system orders or not, or if the ordering is curvature or noise driven.

We focus here on the AS-model, but this macroscopic description can also be applied for systems with three states, as the Bilg-model (see [211]). Given that

6.3. TWO-DIMENSIONAL LATTICES

neighboring spins tend to be aligned (due to the ferromagnetic nature of the interactions), together with the fact that correlations between spins reinforce the alignment between far neighbors, the dynamics is characterized by the formation of same-spin domains. Starting from a well-mixed system with up and down spins randomly distributed over the lattice, after a small transient, if we look at the lattice from far we observe domains growing and shrinking slowly with time, and we can interpret this dynamics at the coarse-grained level as the evolution of a continuous *spin field* ϕ over space and time. Then, we define $\phi_{\mathbf{r}}(t)$ as the spin field at site \mathbf{r} at time t , which is a continuous representation of the spin at that site ($-1 < \phi < 1$), also interpreted as the average value of the spin over many realizations of the dynamics. Thus, we assume that there are Ω spin particles at each site of the lattice, and we replace $\phi_{\mathbf{r}}(t)$ by the average spin value $\phi_{\mathbf{r}}(t) \rightarrow \frac{1}{\Omega} \sum_{j=1}^{\Omega} S_{\mathbf{r}}^j$, where $S_{\mathbf{r}}^j$ is the spin of the j -th particle inside site \mathbf{r} [211]. Within this formulation, the dynamics is the following. In a time step of length $\delta t = 1/\Omega$, a site \mathbf{r} and a particle from that site are chosen at random. The probability that the chosen particle has spin $s = \pm 1$ is equal to the fraction of \pm spins in that site $(1 \pm \phi_{\mathbf{r}})/2$. Then the spin flips with probability

$$P(s \rightarrow -s) = \frac{1}{2}(1 - sv) \left(\frac{1 - s\psi_{\mathbf{r}}}{2} \right)^a, \quad (6.44)$$

where $\psi_{\mathbf{r}} \rightarrow \frac{1}{4} \sum_{\mathbf{r}'/\mathbf{r}} \phi_{\mathbf{r}'}(t)$ is the average neighboring field of site \mathbf{r} , and the sum is over the 4 first nearest-neighbors sites \mathbf{r}' of site \mathbf{r} . If the flip happens, $\phi_{\mathbf{r}}$ changes by $-2s/\Omega$, thus its average change in time is given by the rate equation

$$\frac{\partial \phi_{\mathbf{r}}(t)}{\partial t} = [1 - \phi_{\mathbf{r}}(t)]P(- \rightarrow +) - [1 + \phi_{\mathbf{r}}(t)]P(+ \rightarrow -), \quad (6.45)$$

where the first (second) term corresponds to a $- \rightarrow +$ ($+ \rightarrow -$) flip event. In order to obtain a closed equation for ϕ (see Appendix A for details), we substitute the expression for the transition probabilities Eq. (6.44) into Eq. (6.45), we then expand around $\psi_{\mathbf{r}} = 0$, and replace the neighboring field $\psi_{\mathbf{r}}$ by $\phi_{\mathbf{r}} + \Delta\phi_{\mathbf{r}}$, where Δ is defined as the standard Laplacian operator, $\Delta\phi_{\mathbf{r}} \equiv \frac{1}{4} \sum_{\mathbf{r}'/\mathbf{r}} (\phi_{\mathbf{r}'} - \phi_{\mathbf{r}}) = \psi_{\mathbf{r}} - \phi_{\mathbf{r}}$. Keeping the expansion up to first order in $\Delta\phi_{\mathbf{r}}$, results in the following equation for the spin field

$$\begin{aligned} \frac{\partial \phi_{\mathbf{r}}(t)}{\partial t} &= 2^{-a} (1 - \phi_{\mathbf{r}}^2) \left[v + (a-1)\phi_{\mathbf{r}} + \frac{v}{2}(a-1)(a-2)\phi_{\mathbf{r}}^2 \right. \\ &\quad \left. + \frac{1}{6}(a-1)(a-2)(a-3)\phi_{\mathbf{r}}^3 \right] \\ &\quad + 2^{-a} a \left[1 + v(a-2)\phi_{\mathbf{r}} + \frac{1}{2}(a-1)(a-4)\phi_{\mathbf{r}}^2 \right] \Delta\phi_{\mathbf{r}}. \end{aligned} \quad (6.46)$$

CHAPTER 6. MACROSCOPIC DESCRIPTIONS

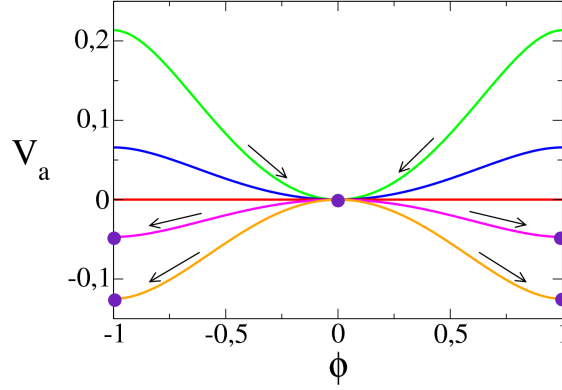


Figure 6.9: Two-dimensional lattice: Ginzburg-Landau potential Eq. (6.50) for the symmetric case $v = 0$ of the Abrams-Strogatz model, with volatility values $a = 0.5, 0.8, 1.0, 1.2$ and 2.0 (from top to bottom). For $a = 0.5$ and 0.8 , the system relaxes to an active state with the same fraction of up and down spins uniformly distributed over space, corresponding to the minimum of the potential at $\phi = 0$; while for $a = 1.2$ and 2.0 it reaches full order, described by the field $|\phi| = 1$.

Equation (6.46) can be written in the form of a time dependent Ginzburg-Landau equation

$$\frac{\partial \phi_{\mathbf{r}}(t)}{\partial t} = D(\phi_{\mathbf{r}}) \Delta \phi_{\mathbf{r}} - \frac{\partial V_{a,v}(\phi_{\mathbf{r}})}{\partial \phi_{\mathbf{r}}}, \quad (6.47)$$

with diffusion coefficient

$$D(\phi_{\mathbf{r}}) \equiv 2^{-a} a \left[1 + v(a-2)\phi_{\mathbf{r}} + \frac{1}{2}(a-1)(a-4)\phi_{\mathbf{r}}^2 \right] \quad (6.48)$$

and potential

$$\begin{aligned} V_{a,v}(\phi_{\mathbf{r}}) \equiv & 2^{-a} \left\{ -v\phi_{\mathbf{r}} - \frac{1}{2}(a-1)\phi_{\mathbf{r}}^2 + \frac{v}{6} [2 - (a-1)(a-2)] \phi_{\mathbf{r}}^3 \right. \\ & + \frac{1}{24}(a-1) [6 - (a-2)(a-3)] \phi_{\mathbf{r}}^4 + \frac{v}{10}(a-1)(a-2)\phi_{\mathbf{r}}^5 \\ & \left. + \frac{1}{36}(a-1)(a-2)(a-3)\phi_{\mathbf{r}}^6 \right\}, \quad (6.49) \end{aligned}$$

which is analogous to the potential for the global magnetization m in the fully connected network case (Figure 6.4). As we already discussed in section 6.1.1,

6.3. TWO-DIMENSIONAL LATTICES

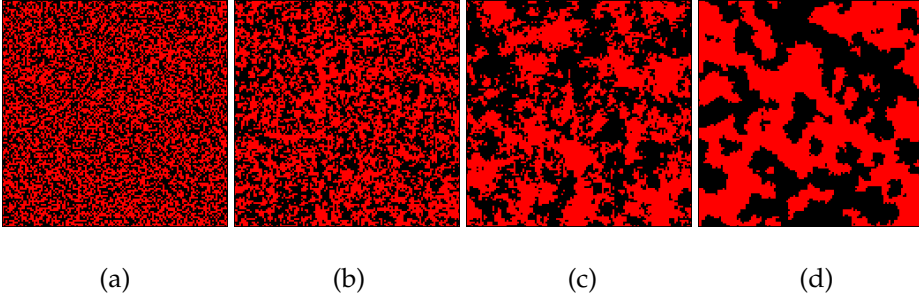


Figure 6.10: Snapshots of the Abrams-Strogatz model with bias $v = 0$ on a two-dimensional lattice. $N = 128^2$. (a) Random initial conditions: each site is occupied with a spin $+1$ or -1 with the same probability $1/2$. (b) $a = 0.5$: the system reaches an active disordered stationary state, with a global magnetization that fluctuates around zero. (c) $a = 1.0$: the system displays coarsening driven by noise, characterized by domains with noisy boundaries. (d) $a = 2.0$: there is also coarsening but driven by surface tension, generating domains with more rounded boundaries.

for the asymmetric case $v \neq 0$ the ordering dynamics is strongly determined by v . When $a > 1$, $V_{a,v}$ has the shape of a double-well potential with minima at $\phi = \pm 1$, and with a well deeper than the other, thus the system is quickly driven by the bias towards the lowest minimum, reaching full order in a rather short time. For $a < 1$ there is a minimum at $|\phi| < 1$, thus the system relaxes to a partially ordered state of coexistence composed by a well mixed population with different proportions of agents in the two states (depending on v).

Specially interesting is the analysis of the symmetric case $v = 0$, for which the potential is (see Figure 6.9)

$$V_a(\phi_{\mathbf{r}}) = 2^{-a}(a-1) \left\{ -\frac{\phi_{\mathbf{r}}^2}{2} + [6 - (a-2)(a-3)] \frac{\phi_{\mathbf{r}}^4}{24} + (a-2)(a-3) \frac{\phi_{\mathbf{r}}^6}{36} \right\}. \quad (6.50)$$

In this bias-free case, when $a < 1$ the minimum is at $\phi = 0$, thus the average magnetization in a small region around a given point \mathbf{r} is zero, indicating that the system remains disordered (coexistence). This can be seen in Figure 6.10(b), where we show a snapshot of the lattice for the model with $v = 0$ and $a = 0.5$,

CHAPTER 6. MACROSCOPIC DESCRIPTIONS

after it has reached a stationary configuration*. For $a > 1$ the potential has two wells with minima at $\phi = \pm 1$, but with the same depth, thus there is no preference for any of the two states, and the system orders in either of the two states by spontaneous symmetry breaking. Complete ordering for $a > 1$ is achieved through domain coarsening driven by surface tension [110]. That is, as the system evolves, same-spin domains are formed, small domains tend to shrink and disappear while large domains tend to grow. Figure 6.10(d) shows a snapshot of the lattice for the evolution of the model with $a = 2$. We observe that domains have rounded boundaries given that the dynamics tends to reduce their curvature, leading to an average domain length that grows with time as $\xi \sim t^{1/2}$ [198, 211]. For the special case $a = 1$ (voter model; see Chapter 3) the potential is $V_a = 0$. There is still coarsening but without surface tension, meaning that domain boundaries are driven by noise, as seen in Figure 6.10(c). As a consequence of this, the average length of domains grows very slowly with time, as $\xi \sim \ln t$ [123, 131, 132].

The order-disorder nonequilibrium transition at $a = 1$ is reminiscent of the well known Ising model transition, but with the volatility parameter a playing the role of temperature: high volatility ($a < 1$) corresponds to the high temperature paramagnetic phase and low volatility ($a > 1$) to the low temperature phase. An important difference is that the transition is here first order, since the low volatility stable states $\phi = \pm 1$ appear discontinuously at $a = 1$. In addition, while in the low temperature phase of the Ising model, spins flip in the bulk of ordered domains by thermal fluctuations, here, spin flips in the low volatility regime only occur at the interfaces (domain boundaries).

In order to compare the behavior of the AS-model and the Bilg-model in fully connected and complex networks with their behavior in two-dimensional lattices, we have numerically explored the stability regions in the (a, v) plane for these models in square lattices. The coexistence-consensus transition in the AS-model for $v = 0$ is at $a_c = 1.0$, as in fully connected and complex networks, whereas the region for coexistence is found to be much more narrow than the ones observed in complex networks with low degree, like the one depicted in Figure 6.6 for $\mu = 3$. Using the simulation applet (see Section 2.4; [220]) one can check that for a given value of $v \neq 0$, the disordered stationary state that characterizes coexistence is harder to maintain in square lattices than in random networks: in order to have an equivalent situation, a smaller value of a is needed in the former case.

*We have already seen in Section 2.4 the different qualitative behavior of the model for $a < 1$, $a = 1$ and $a > 1$. Here, for the case $v = 0$ we study the coarsening processes depending on the volatility parameter a through the analysis of the potential V_a .

6.3. TWO-DIMENSIONAL LATTICES

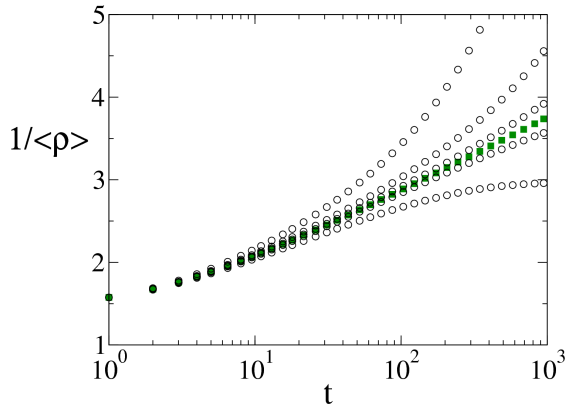


Figure 6.11: Inverse of the average interface density $\langle \rho \rangle$ vs time, on a log-linear scale, for the Bilinguals model in a two-dimensional lattice of side $L = 400$. From top to bottom: $a = 0.30, 0.20, 0.17, 0.16, 0.15$ and 0.10 . Averages are done over 10^3 independent realizations. $\langle \rho \rangle$ decays as $1/\ln(t)$ at the transition point $a_{sl} \approx 0.16$ (in green), corresponding to the behavior of a Generalized voter transition in two dimensions.

In the Bilg-model, apart from the narrowing of the coexistence region, we also find that the transition point for $v = 0$ is shifted to an even smaller value of the volatility a than in complex networks. To see this, in Figure 6.11 we show the time evolution of the inverse of the average interface density $\langle \rho \rangle$ * for various values of a , on a square lattice of size $N = 400^2$. We observe that $\langle \rho \rangle$ decays to zero for values of $a > 0.16$, indicating that the system orders (consensus), while $\langle \rho \rangle$ approaches a constant value larger than zero for $a < 0.16$, thus the system remains disordered (coexistence). At the transition point $a_{sl} \approx 0.16$ (sl stands for *square lattice*) we have that $\langle \rho \rangle \sim 1/\ln(t)$, indicating that the transition belongs to the Generalized Voter class, a typical transition observed in spin systems with two symmetric absorbing states [120, 212, 230, 232].

In the Bilg-model, the fact that $a_{sl} \approx 0.16$ is smaller than the corresponding transition points $a_{fc} \approx 0.63$ and $a_{cn} \approx 0.3$, together with the narrowing effect mentioned above, leads to the result that the region for coexistence is largely reduced in two-dimensional lattices, compared to fully connected and complex networks.

*The $\langle \dots \rangle$ indicates average over independent realizations of the dynamics with different random initial conditions.

Concluding remarks

We have discussed the order-disorder transitions that occur in the volatility-bias parameter space for the Abrams-Strogatz model and its extension to account for bilingualism: the Bilinguals model. We have analyzed their microscopic dynamics on fully connected, complex random networks and two-dimensional lattices and constructed macroscopic descriptions of these dynamics accounting for the observed transitions. At a general level, we have found that both models share the same qualitative behavior, showing a transition from coexistence to consensus of one of the two equivalent states at a critical value of the volatility parameter a_c . The fact that agents are highly volatile ($a < a_c$), i.e, loosely attached to its current option, leads to the enhancement of the scenario of coexistence. On the contrary, in a low volatility regime ($a > a_c$), the final state is one of consensus.

A more detailed comparison of both models shows important differences: in the mean field description for fully connected networks, and for the AS-model, a scenario of coexistence is obtained for $a < 1$. This is independent of the relative prestige between the two options v , but the stationary fraction of agents in the more prestigious option increases with a higher prestige. However, when AB agents are introduced (Bilg-model), the scenario of coexistence becomes the parameter space area corresponding to $a < 0.63$. That is, the area of coexistence is reduced: agents with a higher volatility (smaller a) are needed in order to obtain a coexistence regime.

Network topology and local effects have been addressed through pair approximations for degree uncorrelated networks. For the AS-model on degree-regular random networks we find that the decrease of the network connectivity leads to a reduction, in the parameter space (a, v) , of the area of coexistence and the area of bistable consensus, while monostable-consensus regions emerge, in which only the state of consensus in the more prestigious option is stable. To gain intuition on this result, we first notice that in the fully connected network, the area of coexistence ($a < 1$) corresponds to a situation in which the majority of the agents are in the more prestigious option. The fact that all agents are interconnected, translates to a situation in which agents in the less prestigious option (minority) are in contact with every other agent in the network. In this situation, high volatility (agents switching their state easily) is effective in order to achieve a steady state situation with agents continuously changing their option and making coexistence possible. In contrast, when considering a degree-regular random network, that is, when limiting the number of neighbors in the network, the existence of a bias ($v \neq 0$) opens the possibility for agents in the majority option

6.4. CONCLUDING REMARKS

to be placed in domains without contact with the minority option. For a region of the parameter space where there is coexistence in a fully connected network, these domains can grow in size in a random network until they occupy the entire system. This gives rise to the monostable region of consensus in the more prestigious option found in complex networks with low connectivity. Compared to the fully connected case, a higher volatility is needed in order to overcome this topological effect, leading to a reduction of the area of coexistence. In two dimensional regular lattices, the coexistence is shown to be even more difficult to achieve, probably due to the fact that correlations with second neighbors make the coarsening process of formation and growth of domains easier. The macroscopic field description introduced for two-dimensional lattices accounts for the different coarsening processes observed for large and small volatility.

The network effects described above for the AS-model are also qualitatively valid for the Bilg-model. On top of that though, the reduction of the area of coexistence is more important when considering AB agents. We find a shift of the critical value with the topology for $v = 0$: $a_{fc} \simeq 0.63$ in fully connected networks, $a_{cn} \simeq 0.3$ in complex uncorrelated networks, and $a_{sl} \simeq 0.16$ in two dimensional lattices, with the corresponding translation of the whole stability diagram to smaller values of the volatility parameter.

Conclusions

7.1

General conclusions

In the global context of consensus dynamics and motivated by studies of language competition, we have studied different microscopic models of social interaction: the Abrams-Strogatz two-state model (AS-model) for the competition between two languages, and the Bilinguals model (Bilg-model), a three-state model which is an extension of the AS-model accounting for bilingualism. In particular, we have analyzed in detail the special cases of socially equivalent languages ($s = 0.5$) and neutral volatility ($a = 1$), which correspond to the prototypical voter model and the AB-model respectively. Even though these models have been presented in the context of language competition, their study belongs to the more general problem of consensus dynamics in which there exists the possibility of a third mixed state of coexistence of two options at the individual level, represented by the *AB agents* (bilingual individuals in a sociolinguistic context); that is, the general problem of consensus dynamics with two non-excluding options*.

The general aim of the thesis has been to analyze the asymptotic behavior and the nonequilibrium transient dynamics to the absorbing state for these two-state models (AS-model, voter model), in comparison to the three-state models with two non-excluding options (Bilg-model, AB-model). We have studied the role played by the AB agents in the dynamics, the effects of the network structure, and

*Other examples of these social dynamics beyond language competition processes are the adoption of competing new technologies by a population [209], competing seeds in agriculture, the spread of hobbies in a society, etc.

CHAPTER 7. CONCLUSIONS

the role of the parameters of the models (prestige and volatility). In each Chapter, we have already presented in detail the corresponding concluding remarks, which we also summarize in the following Section 7.2. Here, we wish to stress the most relevant and general conclusions, which concern (i) the interface dynamics and coarsening processes of the models, (ii) the order-disorder transitions and the mechanisms leading to scenarios of consensus or coexistence, and (iii) the trapped metastable states associated to topological properties of the network structure and their dynamical effects. In the last part of the conclusions, we also briefly present the sociolinguistic implications of our work for the dynamics of language competition.

In the first place (i), we have shown that there exist different mechanisms which change the noisy interface dynamics characteristic of the voter model towards curvature driven dynamics. In this way, the typical growth of the size of single-option domains, ξ , changes from $\xi \sim \ln(t)$ to $\xi \sim t^\alpha$, with $\alpha \simeq 0.5$. These mechanisms are: (a) the extension of the voter model allowing for the intermediate AB-state (AB-model; see Chapter 3), (b) the perturbation on the transition probabilities of the voter model, which introduces a reinforcement of the influence of the local majority surrounding an agent (ϵ -model; see Chapter 3), and (c) the low volatility regime in the AS-model (and in the Bilg-model), where agents have a tendency to remain in its current state (see Chapter 6). This change in the interface dynamics, shown in the study of the models in two-dimensional regular lattices, has further implications in both the order-disorder transitions and the metastability observed in the models, as we discuss below.

Secondly (ii), we have explored the whole parameter space in the AS-model, developing macroscopic analytical descriptions in order to study the order-disorder (consensus-coexistence) transitions we have found in the model (see Chapter 6). Due to the complexity of the macroscopic equations in the Bilg-model, we have obtained results for this model only with Monte Carlo simulations. In fully connected networks, we have shown that the AS-model and the Bilg-model have a qualitatively alike behavior in the asymptotic states: they reach consensus for large values of $a > a_c$ (low volatility regime), while the system reaches a scenario of coexistence for small values of $a < a_c$ (high volatility regime). Therefore, high volatility (small a) is shown to generally favor coexistence. This is independent of the prestige in the thermodynamic limit. However, these order-disorder transitions are affected by both, the network structure and the existence of AB agents.

On the one hand, when considering non-equivalent options ($s \neq 0.5$) and in comparison to fully connected networks, coexistence has been shown to be reduced in complex random networks with small average degree. The reason has to be found in the emergence of a new area in the parameter space of dominance of

7.1. GENERAL CONCLUSIONS

the most prestigious option. This effect is enhanced in two-dimensional lattices, where second neighbor correlations enhance the tendency towards consensus. On the other hand, the presence of AB agents reduces further the area of coexistence because they decrease the *effective volatility* of the dynamics. In other words, one needs a higher volatility of the agents (smaller a) to recover the situation without AB agents. This is illustrated when comparing the voter model and the AB-model in the parameter space: the voter model (AS-model in the case of $a = 1$ and $s = 0.5$) corresponds to the critical point between consensus and coexistence ($a_c = 1$), while the AB-model (Bilg-model in the case of $a = 1$ and $s = 0.5$) lies on the area of consensus. In fully connected networks, the volatility needs to be decreased until $a_{fc} \simeq 0.63$ in order to recover the critical point in the Bilg-model. This has important consequences: the area $0.63 < a < 1$ corresponds to coexistence in the voter model, while it corresponds to consensus in the AB-model. Moreover, on top of the network effects described above for $s \neq 0.5$, the critical value for the order-disorder transition in the Bilg-model is shown to be dependent on the network structure and to shift to smaller values of a . For $s = 0.5$, the critical value is shown to be $a_{cn} \simeq 0.3$ in complex networks, and $a_{sl} \simeq 0.16$ in square lattices*, with the corresponding translation of the whole stability diagram to smaller values of the volatility parameter.

Notice that the analysis of the parameter space complements the understanding of the behavior of the AB-model in comparison to the voter model. In particular, it allows us to reinterpret, from a complementary point of view, the result concerning the change in the interface dynamics (see Chapter 3): the addition of the AB-state can be interpreted as an effective shift in the parameter space from a critical point (corresponding to the noisy interface dynamics of the voter model) to the region of consensus (corresponding to the curvature driven interface dynamics of the AB-model).

Therefore, regarding the asymptotic states, volatility generally enhances coexistence while the presence of AB agents hinders it. In the AS-model, the role of the prestige parameter is entwined with that of the network structure: in complex random networks and two-dimensional lattices, the existence of a bias in the relative prestige between the options (non-equivalent states) reduces the scenario of coexistence in favor of new dominance regions for the most prestigious option. When AB agents are considered (Bilg-model), this effect is amplified and coexistence is even reduced in the case of socially equivalent options.

In the third place (iii), and beyond the study of asymptotic states (consensus or coexistence), we have analyzed the nonequilibrium transient dynamics to the absorbing state in the case of neutral volatility ($a = 1$) and equivalent options

*Subindices stand for *fn* (fully connected), *cn* (complex networks) and *sl* (square lattices).

CHAPTER 7. CONCLUSIONS

($s = 0.5$). For this, we have studied the AB-model in comparison to the voter model in networks of increasing complexity: from two-dimensional lattices, to small world networks and networks with community structure (see Chapter 3 and 4). We have been specially interested in the existence of metastable states, which correspond to long-lived coexistence states with a finite lifetime in finite systems. In particular, we have studied in detail trapped metastable states, which are related to the topology of the network. The general mechanism leading to trapped metastable states appears to be a combination of curvature driven interface dynamics (property of the model) and topological traps in the network (property of the structure of the network). Therefore, trapped metastable states appear in the AB-model, while they have shown to be absent in the voter model, which is driven by interfacial noise*.

In two-dimensional lattices, we have found for the AB-model stripe-like trapped metastable states, which appear in 1/3 of the realizations (see Chapter 3). These configurations define a second characteristic time for the dynamics, beyond the one corresponding to the rest of realizations which reach consensus directly. The most interesting trapped metastable states though, have been obtained in networks with mesoscale structure (see Chapter 4). In a class of complex networks with community structure, we have obtained trapped metastable states at any time scale, which lead to broad power law lifetime distributions, such that a characteristic time for the dynamics is not defined[†]. These metastable states have been shown to be related to the dynamics stuck between communities, in which curvature interface dynamics (local majority) favors consensus in a given option in each of the communities, with AB agents placed at the interfaces between them. Next, we have shown through a simple class of networks with community structure built up from connected cliques, that the sufficient condition for these broad lifetime distributions to appear is heterogeneity at the mesoscale level, that is, a large variability in the dynamical robustness of the communities (cliques) in the network.

In this way, while AB agents have been shown to facilitate consensus in small world networks (see Chapter 3), they make possible, at the same time, the existence of trapped metastable states at any time scale in networks with mesoscale structure, which results in a long-lived, although segregated, coexistence of the two options.

Finally, we want to stress that most of the results presented in this thesis can be general for models which develop curvature driven dynamics, like SFKI models

*Notice that we refer to trapped metastable states. In the voter model, there exist metastable states, but they are not *trapped* (see Section 1.4.1).

[†]In the voter model instead, trapped metastable states are not found and the lifetime distribution is shown to be exponential.

7.1. GENERAL CONCLUSIONS

[110]. Indeed, we notice that the order-disorder nonequilibrium transitions we have obtained in the AS-model and the Bilg-model are reminiscent of the well known Ising model transition, but with volatility playing the role of temperature: high volatility ($a < a_c$) corresponds to the high temperature paramagnetic phase and low volatility ($a > a_c$) to the low temperature phase. However, there are two important differences: first, the transition is here first order, since the low volatility stable states appear discontinuously at a_c . Second, while in the low temperature phase of the Ising model, spins flip in the bulk of ordered domains by thermal fluctuations, here, spin flips in the low volatility regime only occur at the interfaces (domain boundaries). In this way, all the detailed results presented for the AB-model, which belongs to the low volatility regime in the Bilg-model, might be compatible with the SFKI in the low temperature phase.

In summary, in this thesis we have contributed to the understanding of the mechanisms underlying in consensus problems in which the options at play can be non-excluding. Motivated by language competition problems, we have analyzed and compared two-state models in which two options compete among the agents, with the corresponding extensions where a third AB-state of coexisting options at the individual level is considered. Taking into account the effects of different network topologies, we have studied the asymptotic behavior and order-disorder transitions of the models, together with their ordering dynamics and coarsening processes in order to characterize the nonequilibrium transient dynamics to the absorbing states.

Implications for the dynamics of language competition

From the point of view of dynamics of language competition, and within the assumptions and limitations of our models, our work has several implications which we briefly comment on here. Several of these implications have already been presented in publications during the development of this thesis (publications in Refs. [233–236]).

On the one hand and regarding the parameters of the models, our results support the common idea that the prestige of a language is very important, as it creates a preference of the agents towards the most prestigious language*. Nevertheless, the volatility of the agents has been shown to be a very crucial social parameter in language competition as well. Generally speaking, high volatility agents, i.e., agents which are less attached to the language they are currently using,

*The situation close to extinction of old Catalan in Alghero in its competition with modern Italian is a representative example of this situation. Also Quechua in its competition with Spanish in Peru was in an endangered situation because of a low prestige, but policies in favor of enhancing it seem to be leading to its recovery in recent times.

CHAPTER 7. CONCLUSIONS

favor language coexistence, while low volatility agents develop scenarios of dominance of one of the languages in the long run. In social networks though, a difference in the prestige of the languages originates scenarios of dominance of the most prestigious language. In this situation, when the parameters are such that the system belongs to a dominance region, extinction happens much faster in the high volatility regime than in the low volatility regime. In a few words, high volatility is then good for the coexistence of languages of similar prestige, because it leads to scenarios of coexistence; but it speeds up the extinction of endangered languages (low prestige languages)*.

On the other hand, bilingual agents in use[†] (AB agents) generally reduce the scenario of coexistence between two competing languages. This has been obtained in different networks: fully connected networks, complex random networks and two-dimensional regular lattices; with an increasing reduction of coexistence in this same order. In addition, bilingual agents together with long range interactions (small world network) have been shown to accelerate the approach to absorbing monolingual states; in other words, the extinction of one of the languages. However, in the range of volatility values close to one[‡] ($a = 1$ corresponds to the AB-model) the results are quite different when considering social networks with community structure, which has been found to be a crucial feature of real social networks. In these topologies, bilingual agents make possible long-lived scenarios of coexistence, in which different communities speak different languages (linguistic segregation). We stress that qualitatively our results are compatible with those obtained by Blondel et al. [46] in the analysis of real data of the language used by the customers of a Belgian mobile phone network, where they also find correlations between community structure and the language of the customers[§]. In addition, although in the AB-model finally one of the languages disappears, there does not exist a characteristic time for extinction of a language, but coexisting languages can be found at any time scale.

We have also studied a modification of the AB-model where the effective status of being bilingual has been reinforced, as the agents have certain resistance to abandon the use of an acquired language (see Chapter 5). Contrary to the original model, AB agents become the majority during most of the competition

*An example of this situation can be the competition between Galician-Spanish in Galicia, where there are reasons to think that the low volatility of the Galician speakers prevented Galician from endangerment in the past [237].

[†]We remind here that we have studied models of language use rather than competence.

[‡]Notice that Abrams and Strogatz obtained a value $a = 1.31 \pm 0.25$ when fitting to real data regarding the competition between Quechua-Spanish, Scottish Gaelic-English and Welsh-English [13]. To our knowledge, this is the only comparison to real data of the models studied here.

[§]Notice that their data are for a fixed time. Dynamical real data analysis in this direction would be very interesting to enhance the knowledge of the evolution of language use in real social networks, and compare it to the models we have studied.

7.1. GENERAL CONCLUSIONS

process, and the extinction of a language takes place then in two steps. At first, monolingual speakers of the endangered language disappear, but the language does not, as it is still spoken in the society by the bilingual agents. Finally, bilingual agents also disappear, which leads to the ultimate extinction of the language. This framework models a mechanism which supports the idea that, in societies with two languages, the disappearance of a monolingual community using a language as its only way of communication could represent the first step in the extinction of that language. The other language would finally become the only spoken one, as the bilingual agents would eventually end up using only the language spoken by the remaining monolingual community.

Finally, we mention here the work on the viability and resilience of two languages in competition using the Abrams-Strogatz model (see Appendix B; [219]). Within the framework of viability theory [238], which provides theoretical concepts and practical tools in order to maintain a dynamical system inside a given set of a priori desired states, the maintenance of two competing languages is shown to be possible by introducing the prestige of a language as a control variable, that is, assuming that public action can modify the prestige of a language in order to avoid language extinction.

The studies of language competition from the point of view of statistical physics and complex systems give a new perspective and formalism to sociolinguistic problems. These models, although still limited, together with an increasing collaboration with linguists, might help to face the challenging question of the mechanisms involved in processes of language contact.

Specific conclusions

In this Section, we summarize the particular results and conclusions obtained in this work, which have already been carefully presented in the concluding remarks at the end of each Chapter of this thesis.

Chapter 3

In this Chapter, we have studied the AB-model in comparison to the voter model in fully connected networks, two-dimensional regular lattices and small world networks. The main results have been the following:

- In the AB-model, the mean field analysis shows that in the thermodynamic limit a global consensus state (A or B) is reached with probability one, except for initial conditions lying on the stable manifold ($\Sigma_A = \Sigma_B$) of the saddle fixed point corresponding to unstable coexistence of the three states. In the voter model, instead, any given initial distribution of states of the agents would persist indefinitely.
- In the AB-model and in finite fully connected networks, the system reaches the absorbing state by finite size fluctuations, with an average time to reach consensus scaling with the system size as $\tau \sim \ln(N)$. In the voter model instead, $\rho(t)$ fluctuates grossly until a finite size fluctuation drives it to the absorbing state. The average time to reach an absorbing state scales with the system size as $\tau \sim N$, giving rise to a much slower path to consensus compared to the AB-model.

In two dimensional lattices, and for the AB-model:

- A domain of agents in the AB-state is not stable and the density of AB agents becomes very small after an initial fast transient, with AB agents placing themselves in the interfaces between single-option domains.
- AB agents produce an essential modification of the processes of coarsening and domain growth, changing the interfacial noise dynamics of the voter model into a curvature driven interface dynamics: the typical growth of the size of single-option domains, ξ , changes from $\xi \sim \ln(t)$ to $\xi \sim t^\alpha$, with $\alpha \simeq 0.5$. This change in the coarsening mechanism is also found in the ϵ -model, a modification of the voter model in which there exists a reinforcement of the influence of the local majority surrounding an agent.

7.2. SPECIFIC CONCLUSIONS

- The system reaches stripe-like trapped metastable states with a probability around 1/3 (also in the ϵ -model). The average time to consensus has been shown to scale with the system size as $\tau \sim N^{1.8}$ (to compare with the voter model, where $\tau \sim N \ln(N)$).

In small world networks, and for the AB-model:

- In comparison to the voter model, where the dynamics reaches a metastable state, AB agents restore the processes of coarsening and domain growth and they speed-up the decay to the absorbing state by a finite size fluctuation. We obtain a characteristic time to reach an absorbing state scaling with the rewiring parameter as $\tau \sim p^{-0.76}$.
- The characteristic time to reach an absorbing state scales with system size as $\tau \sim \ln N$ (to be compared with the result $\tau \sim N$ for the voter model).

Chapter 4

In the first part of this Chapter, we have studied the AB-model in comparison to the voter model in a class of networks with community structure. In the second part, we have studied sufficient conditions under which a broad distribution of lifetimes appears, analyzing the AB-model in a controlled setting by constructing simple test case networks with mesoscopic structure.

In the first part, the main results have been the following:

- The voter model dynamics, driven by interfacial noise, is not particularly sensitive to the mesoscale structure of the network. We obtain similar type of dynamical metastable states shared by other complex networks of high dimensionality without degree correlations.
- In the AB-model instead, we find different classes of realizations leading to a power law distribution for the times to reach consensus, with exponents such that a mean lifetime for these states does not give a characteristic time scale of the ordering dynamics (the fraction of alive runs scaling as $P(t) \sim t^{-\alpha}$, $\alpha \approx 1.3$). As a result, we find realizations with any lifetime. This is explained in terms of trapped metastable states associated with the community structure of the network.
- The results above seem to be a consequence of a curvature interface dynamics, in which mechanisms of local majority favor consensus in a given option in each of the communities.

CHAPTER 7. CONCLUSIONS

In the second part, the main results have been the following (AB-model):

- We define the *dynamical robustness* of a given topological substructure, which is characterized by the survival time of the substructure, i.e., the characteristic time needed for this set of nodes before changing its option towards the one of the surrounding majority. For isolated cliques, the ratio $r = k_{n,in} / \langle k_{n,out} \rangle$ has proven an appropriate topological measure to characterize their dynamical robustness.
- In EDH networks (for Equal out-Degree and Homogeneously sized cliques), we have shown that the mere presence of communities is not a sufficient condition to produce a lifetime distribution broader than exponential.
- In EDE networks (for Equal out-Degree and Exponential clique size distribution), we have recovered the main results obtained in the first part of the Chapter: very broad $P(t)$ with a best power law fit such that the second moment of the distribution is not defined, and therefore, there does not exist a characteristic time scale for the dynamics.
- A large heterogeneity in the dynamical robustness of different topological substructures (communities) appears to be a sufficient mechanism for the absence of a characteristic time for the dynamics. This mechanism causes the existence of trapped metastable states that survive at any time scale.

Chapter 5

In this Chapter, we have analyzed and compared the AB-model and the Naming Game restricted to two conventions (2c-Naming Game). The main results have been the following:

- We have shown that although these two models are equivalent in mean-field, their microscopic differences give rise to different behaviors.
- In fully connected networks, we have studied the extension of the models incorporating the parameter β , which is a measure of the inertia of the agents to abandon one of the options, and at the same time, a reinforcement of the status of the AB-state. We have shown that, while the 2c-Naming Game features an order-disorder transition for a critical value of β between consensus and stationary coexistence of the three phases present in the system, this is absent in the AB-model.
- Contrary to the original AB-model ($\beta = 1$), where the AB agents are systematically the minority state in the system, for β small enough, AB agents

7.2. SPECIFIC CONCLUSIONS

become the majority during the transient stage before one of the options takes advantage and the system eventually reaches an absorbing state.

- In comparison to the 2c-Naming Game, the AB-model interface dynamics in regular lattices, although qualitatively similar, slows down the diffusion of metastable configurations such as walls in one dimension and stripe-like configurations in two dimensions.

Chapter 6

In this Chapter, we have analyzed the microscopic dynamics of the AS-model and the Bilg-model on fully connected, complex random networks and two-dimensional square lattices, and constructed macroscopic descriptions of these dynamics accounting for the observed order-disorder transitions. The main results have been the following:

In fully connected networks:

- The stability analysis in mean field for the AS-model shows a transition from coexistence ($a < 1$) to dominance ($a > 1$) of one of the two equivalent states. The critical value $a_c = 1$ is independent of the relative prestige between the two options. In the region of coexistence though, the fraction of agents in the more prestigious option increases with a higher prestige.
- In the Bilg-model instead, the scenario of coexistence is reduced to $a < 0.63$. That is, agents with a higher level of volatility (smaller a) are needed in order to obtain a coexistence regime.
- At a general level, the fact that agents are highly volatile ($a < a_c$), i.e. loosely attached to its current option, leads to the enhancement of the scenario of coexistence. On the contrary, in a low volatility regime ($a > a_c$), the final state is one of dominance/extinction.

In degree-regular random networks:

- For the AS-model, we derive a macroscopic description of the dynamics using a pair approximation. Due to the complexity of the macroscopic equations in the Bilg-model, we have obtained results for this model only with Monte Carlo simulations.
- In the AS-model, we find analytically and numerically that the decrease of the network connectivity leads to a reduction, in the parameter space (a, v) ,

CHAPTER 7. CONCLUSIONS

of the area of coexistence and the area of bistable dominance, while monostable dominance regions emerge, in which only the state of dominance of the more prestigious option is stable.

- The network effects described above for the AS-model are also qualitatively valid for the Bilg-model, but the reduction is even more important. In addition, we find a shift of the critical value for $v = 0$ to $a_{cn} \simeq 0.3$, with the corresponding translation of the whole stability diagram to smaller values of the volatility parameter.

In two-dimensional regular lattices:

- For the AS-model, we derive a macroscopic equation for the evolution of a continuous space dependent spin field.
- The macroscopic description accounts for the different coarsening processes observed for large (curvature driven) and small volatility (no ordering). In the transition, we find the noisy interface dynamics characteristic of the voter model.
- Compared to degree-regular random networks, the coexistence is shown to be even more difficult to achieve, probably due to the fact that correlations with second neighbors make the coarsening process of formation and growth of domains easier.
- The network effects described above for the AS-model are also qualitatively valid for the Bilg-model, but the reduction is even more important. In addition, we find a shift of the critical value for $v = 0$ to $a_{cn} \simeq 0.16$, with the corresponding translation of the whole stability diagram to smaller values of the volatility parameter.



Viability and resilience. Appendix B

In this Appendix, we have studied the viability and resilience of two languages in competition using the Abrams-Strogatz model within a population dynamics approach. The main results have been the following:

7.2. SPECIFIC CONCLUSIONS

- The maintenance of two competing languages is shown to be possible by introducing the prestige of a language as a control variable, that is, assuming that public action can modify the prestige of a language in order to avoid language extinction.
- We compute viable policies of action on the prestige variable to keep language coexistence within a given constraint set (set of a priori desired states; in our case, coexistence with no endangered languages). For this, we compute the viability kernel of the system, i.e. the set of states, given some possible control actions on the prestige variable, for which the system can be maintained inside the constraint set.
- The viability kernel shrinks as the volatility parameter increases, due to the fact that agents become less likely to change their language.
- We define the resilience of the system in the formalism of viability theory: the system is resilient to a perturbation if, after a perturbation that places the system outside the viability kernel, there exists an action policy driving back the system to the viability kernel. In this way, we determine the action policies that minimize the cost to drive an endangered language to a scenario of safe coexistence (i.e. to the viability kernel of the system).
- In the case that not only the prestige, but also the volatility of the agents could be a control parameter, the results in Section 2.4 indicate possible interesting policies in the case of endangered languages (low prestige) and low volatility of the agents. Notice that when the volatility of the agents is low, it gives larger times before the extinction of the low-prestigious language, and in this way, enough time to try to enhance its prestige. At the eventual point in which social prestige equivalence is achieved, if the volatility is increased, a situation of coexistence for both languages becomes viable and can be maintained indefinitely.

Outlook and final remarks

In this last Section, we wish to describe further research lines that can be considered as next steps in the analysis of the dynamics of the models studied in this thesis, in order to achieve a better understanding of consensus problems, and in particular, of language competition processes. The aim is to move beyond some of the assumptions we have made during our study, which concern essentially the modeling of both the dynamics of interaction and the network structure.

The main research lines are the following:

- Heterogeneous interacting agents

In the present work, all the agents are *homogeneous* in the sense that the parameters of the model are the same for all the agents (although in non-regular topologies, a source of diversity is implicit through their position in the network). Non-trivial effects arise when considering *diversity* in the parameters of the system [226, 239]. In our models, the idea is to allow the prestige parameter s and the volatility parameter a to be assigned to each agent from given distributions, which would tune the diversity introduced; or to use non-random initial conditions according to the different parameter values of the agents. We expect new behavior to emerge, in particular regarding the scenarios of consensus-coexistence, which might be modified in a non-trivial manner.

- Metastability in the Abrams-Strogatz model and the Bilinguals model

The study of the nonequilibrium transient dynamics to the absorbing state in networks with community structure has only been studied for the cases of neutral volatility ($a = 1$) and equivalent options ($s = 0.5$), that is, for the voter and the AB-model. An obvious extension of this study is to analyze how the appearance of trapped metastable states observed in the AB-model, which give rise to broad lifetime distributions, is affected when considering the whole parameter space. The idea is to check the robustness of the result concerning the absence of a characteristic time scale for the dynamics (AB-model), which we expect to hold for large values of the volatility parameter (which correspond to curvature driven coarsening).

- Coevolving networks of interaction

The networks we have considered in this thesis are unweighted, undirected and static. Open lines of research concern the addition of more complex network structures, in which to consider weights and directed

7.3. OUTLOOK AND FINAL REMARKS

interactions. Moreover, social networks of interaction generally evolve in time. Indeed, coevolving networks, i.e., networks in which the characteristic time corresponding to the dynamics is of the same order than the one corresponding to the dynamical evolution of the network, are gaining a special attention these last years [64]. Considering the Abrams-Strogatz model and the Bilinguals model in coevolving networks is a promising line of research.

- Dependence on initial conditions

In this work, we have essentially focused on studying random initial conditions for the distribution of the states of the agents. A systematic study of the role of initial conditions in consensus dynamics is often lacking, and could be an interesting line of research to follow regarding the models studied in this thesis. In fact, the role of initial conditions in the SFKI dynamics has been recently studied in different complex networks [240]. It has been shown how, when the nodes in the minority state are placed according to centrality measures (degree, betweenness, clustering), the minority state can remarkably take over the system. In this way, while generally random initial conditions are assumed by default, the initial conditions might be in some cases as relevant as the network structure to determine the evolution of the system.

Concerning specifically language competition, the main research lines are:

- Language use as a property of the social interaction

In this work we have considered language use as a state of the agents (monolingual A, monolingual B, or bilingual AB). One line of research we are considering concerns the idea of modeling language use as a property of the social interaction (link), instead of a property of the agents (node). In this way, links can be of type A or type B, depending on the language (A or B) used between the two agents connected by a given link. The state of a given node is then inferred from the distribution of the states of its links. Instead of assuming a third node-state AB (as we did in the present thesis), bilingual agents in use with different degrees of bilingualism emerge then naturally.

In this way, we move towards *consensus dynamics based on links*, opening a new class of phenomena to be addressed beyond language competition, in the direction of social balance theories for the dynamics of friendship [241].

CHAPTER 7. CONCLUSIONS

- Language *competence* and language *use*: towards a “complete” model of language competition

In this work, we have considered language use rather than competence. Building upon the consensus dynamics based on links we have presented above, an interesting line of research concerns the coupling between the dynamics of language use (in the links) and a dynamics of language competence (in the nodes) in which one considers learning mechanisms. In this framework, an agent could use only the languages in which it is competent with.

- Emergence of new languages

A different line of research we are considering concerns the emergence of new languages in situations of language contact. In the models we have studied in this thesis, languages are defined *a priori* and do not evolve. The idea is then to explore dynamics which would allow for the emergence of a new language during processes of language contact such as code-switching or creolization [160].

- Modeling diglossia

An extension of the concept of network of interactions which could model different contexts of language use could be appropriate to take into account the phenomenon of diglossia, which is a central one in situations of language contact. This happens when in a situation of two languages in contact, the high-prestige language is the one used in formal situations (institutions, media, education, etc.) while the low-prestige language is essentially used only in familiar and friendly contexts.

- Data

Due to the theoretical perspective of this work and the general difficulties in getting accurate real data in social dynamics problems (see Introduction, Section 1.1), the real data regarding language competition we have referred to during this thesis is rather limited. In fact, it consists of (i) the population data gathered by Abrams and Strogatz [13], concerning Quechua (in competition with Spanish), and Scottish Gaelic and Welsh (both in competition with English); and (ii) the analysis of the language (French-Dutch) of customers in a Belgian mobile phone network by Blondel et al. [46]. Although this last data set allowed us to compare qualitatively some of our results concerning the effect of networks with communities, we did not find data to compare with the general qualitative outputs of our models. Of course, the class of data we are interested in lie beyond the aggregated population data (i), and might come from studies in the line of data (ii), where

7.3. OUTLOOK AND FINAL REMARKS

the new technologies (mobile phone calls, e-mailing, on-line communities) can be used to obtain large networks of social interaction, hopefully including data regarding language use. The step forward should be moving from getting snapshots towards dynamical data. This might help us, for instance, to set the time scale corresponding to a Monte Carlo step in our models.

As a final remark, we think that beginning with very complicated models that tend to consider all the factors involved in a social problem, leads easily to a partial analysis and few understanding of the mechanisms involved in the dynamics. Instead, following the final remarks and outlook presented above, we believe that the understanding of mechanisms of social interaction might come from a deep analysis of simple models like the ones we have presented in this thesis, which can be explored and understood, to later move bottom up towards models of increasing complexity which are built upon a solid background.

We expect that, may be through some of the lines presented above, the work presented in this thesis triggers further research in order to gain an increasing understanding of the mechanisms involved in consensus dynamics, and in particular, within the open research field of dynamics of language competition.

List of publications

Publications related to this thesis:

- F. Vazquez, X. Castelló and M. San Miguel; *"Agent Based Models of Language Competition: Macroscopic descriptions and Order-Disorder transitions"*, Journal of Statistical Mechanics (*in press*; version available at arXiv:1002.1251) (2010).
- L. Chapel, X. Castelló, C. Bernard, G. Deffuant, V. M. Eguíluz, S. Martin and M. San Miguel; *"Viability and Resilience of Languages in Competition"*, PlosOne, **5**(1), pp. e8681 (2010).
- X. Castelló, A. Baronchelli and V. Loreto; *"Consensus and ordering in language dynamics"*, European Physical Journal B, **71**, pp. 557-564 (2009).
- R. Toivonen, X. Castelló, V. M. Eguíluz, J. Saramäki, K. Kaski and M. San Miguel; *"Broad lifetime distributions for ordering dynamics in complex networks"*, Physical Review E, **79**, pp.016109 (1-8) (2009).
- X. Castelló, R. Toivonen, V. M. Eguíluz, J. Saramäki, K. Kaski and M. San Miguel; *"Anomalous lifetime distributions and topological traps in ordering dynamics"*, Europhysics Letters, **79**, pp.66006 (1-6) (2007).
- D. Stauffer, X. Castelló, V. M. Eguíluz and M. San Miguel; *"Microscopic Abrams-Strogatz model of language competition"*, Physica A, **374**, pp. 835-842 (2007).
- X. Castelló, V. M. Eguíluz and M. San Miguel; *"Ordering dynamics with two non-excluding options: bilingualism in language competition"*, New Journal of Physics **8**, pp. 308-322 (2006).

CHAPTER 8. LIST OF PUBLICATIONS

Book chapters:

- X. Castelló, F. Vazquez, L. Chapel, V. M. Eguíluz, L. Loureiro-Porto, G. Deffuant and M. San Miguel; *“Macroscopic descriptions, viability and resilience in the dynamics of language competition”*, Pattern Resilience. Eds. N. Gilbert, G. Deffuant. Springer-Verlag; *to be published* (2010).

Publications in proceedings:

- X. Castelló, R. Toivonen, V. M. Eguíluz, L. Loureiro-Porto, J. Saramäki, K. Kaski and M. San Miguel; *“Modeling language competition: bilingualism and complex social networks”*, The evolution of language; Proceedings of the 7th International Conference (EVOLANG7), Barcelona 2008. Eds. A.D.M. Smith, K. Smith, R. Ferrer-Cancho. World Scientific Publishing Co.; pp. 59-66 (2008).
- X. Castelló, R. Toivonen, V. M. Eguíluz and M. San Miguel; *“Modeling bilingualism in language competition: the effects of complex social structure”*, Proceedings of the 4th Conference of the European Social Simulation Association ESSA 2007. IRIT Editions, pp. 581-584 (2007).
- X. Castelló, L. Loureiro-Porto, V. M. Eguíluz and M. San Miguel; *“The fate of bilingualism in a model of language competition”*, Advancing Social Simulation: The First World Congress. Eds. S. Takahashi, D. Sallach, J. Rouchier. Springer-Verlag, pp. 83-94 (2007).

Appendices

Equation for the spin field $\phi_{\mathbf{r}}$ in the Abrams-Strogatz model

In this Section we derive an equation for the spin field $\phi_{\mathbf{r}}$. We start by substituting the expression for the transition probabilities Eq. (6.44) into Eq. (6.45) and by writing it in the more convenient form

$$\frac{\partial \phi}{\partial t} = \frac{(1+v)}{2^{a+1}}(1-\phi)(1+\psi)(1+\psi)^{a-1} - \frac{(1-v)}{2^{a+1}}(1+\phi)(1-\psi)(1-\psi)^{a-1}, \quad (\text{A.1})$$

where ϕ and ψ are abbreviated forms of $\phi_{\mathbf{r}}$ and $\psi_{\mathbf{r}}$ respectively. We now replace the neighboring field ψ in the terms $(1+\psi)$ and $(1-\psi)$ of Eq. (A.1) by $\psi \equiv \phi + \Delta\phi$, where Δ is defined as the standard Laplacian operator $\Delta\phi_{\mathbf{r}} \equiv \frac{1}{4} \sum_{\mathbf{r}'/\mathbf{r}} (\phi_{\mathbf{r}'} - \phi_{\mathbf{r}}) = \psi_{\mathbf{r}} - \phi_{\mathbf{r}}$, and we obtain

$$\begin{aligned} \frac{\partial \phi}{\partial t} &= 2^{-(a+1)}(1-\phi^2) \left[(1+v)(1+\psi)^{a-1} - (1-v)(1-\psi)^{a-1} \right] \\ &+ 2^{-(a+1)} \left[(1+v)(1-\phi)(1+\psi)^{a-1} + (1-v)(1+\phi)(1-\psi)^{a-1} \right] \Delta\phi. \end{aligned} \quad (\text{A.2})$$

Because our idea is to obtain a Ginzburg-Landau equation with a ϕ^6 -potential, the right hand side of Eq. (A.2) must be proportional to ϕ^5 , and therefore we use the Taylor series expansions around $\psi = 0$

$$\begin{aligned} (1+\psi)^{a-1} &= 1 + (a-1)\psi + \frac{1}{2}(a-1)(a-2)\psi^2 + \frac{1}{6}(a-1)(a-2)(a-3)\psi^3 \quad \text{and} \\ (1-\psi)^{a-1} &= 1 - (a-1)\psi + \frac{1}{2}(a-1)(a-2)\psi^2 - \frac{1}{6}(a-1)(a-2)(a-3)\psi^3 \end{aligned}$$

APPENDIX A. EQUATION FOR THE SPIN FIELD $\phi_{\mathbf{R}}$

into Eq. (A.2), to obtain

$$\begin{aligned}
 \frac{\partial \phi}{\partial t} &= 2^{-a}(1 - \phi^2) \left[v + (a - 1)\psi + \frac{v}{2}(a - 1)(a - 2)\psi^2 + \frac{1}{6}(a - 1)(a - 2)(a - 3)\psi^3 \right] \\
 &+ 2^{-a} \left\{ (1 - v\phi) \left[1 + \frac{1}{2}(a - 1)(a - 2)\psi^2 \right] \right. \\
 &\left. + (v - \phi) \left[(a - 1)\psi + \frac{1}{6}(a - 1)(a - 2)(a - 3)\psi^3 \right] \right\} \Delta \phi. \tag{A.3}
 \end{aligned}$$

We then replace ψ by $\phi + \Delta\phi$ in Eq. (A.3) and expand to first order in $\Delta\phi$, assuming that the field ϕ is smooth, so that $\Delta\phi \ll \phi$. Finally, neglecting ϕ^3 and higher order terms in the diffusion coefficient that multiplies the Laplacian, we arrive to the expression for the spin field quoted in Eq. (6.46).

Viability and Resilience of Languages in Competition

This Appendix corresponds to the work on viability and resilience of two competing languages, which has led to the publication we attach here (publication in Ref. [219]).

Abstract

We study the viability and resilience of languages, using a simple dynamical model of two languages in competition. Assuming that public action can modify the prestige of a language in order to avoid language extinction, we analyze two cases: (i) the prestige can only take two values, (ii) it can take any value but its change at each time step is bounded. In both cases, we determine the viability kernel, that is, the set of states for which there exists an action policy maintaining the coexistence of the two languages, and we define such policies. We also study the resilience of the languages and identify configurations from where the system can return to the viability kernel (finite resilience), or where one of the languages is lead to disappear (zero resilience). Within our current framework, the maintenance of a bilingual society is shown to be possible by introducing the prestige of a language as a control variable.

Introduction

The study of language dynamics using computer simulations has become a research field of increasing interest in the scientific community. Models studying language dynamics range from social impact theory applied to language competition [191] to genetic approaches for the evolution of universal grammar [189]. We are here interested in the problem of language competition, i.e., the dynamics of language use among a population of interacting agents speaking different languages. Around 50% of the 6000 languages spoken today are in danger and will disappear during the current century according to the recent studies in language contact [157]. Beyond Weinreich's *Languages in contact* [164], several studies in sociolinguistics have addressed questions regarding the level of endangerment of specific languages [165] and the challenge to find a common pattern that might relate language choice to ethnicity, community identity or the like [166]. Lately, the need to provide a quantitative analysis in the field of sociolinguistics is getting an increasing attention [169]. This fact has triggered an effort in order to model and understand the mechanisms within scenarios of language competition: some models study the competition between many languages in order to reproduce the distribution of language sizes in the world in terms of the number of speakers [176, 177]; while others focus on the case of language contact between few languages (for a review see Refs [178, 179]). In particular, Abrams and Strogatz [13] proposed a simple mathematical model of competition between two languages. The model describes the system by aggregated variables that represent the fraction of speakers of each language, where a higher local density of speakers and a higher prestige, the relative status of a language, tend to increase the density of speakers of a language. The analytical study of the model and the fitting to real data from the competition between Quechua-Spanish, Scottish Gaelic-English and Welsh-English, predict that the coexistence of two languages is unstable, irrespective of the prestige of the languages and their initial density of speakers in the model, in contrast to the evidence that bilingual societies exist today. The paper finished with the following remarks:

Contrary to the model's stark prediction, bilingual societies do, in fact, exist. [...] The example of Quebec French demonstrates that language decline can be slowed by strategies such as policy-making, education and advertising, in essence increasing an endangered language's status. An extension to [the model] that incorporates such control on s through active feedback does indeed show stabilization of a bilingual fixed point.

Several modifications and extensions of this model of language competition have investigated deeper this problem: (i) developing agent-based models in order to study the behavior of the model in regular networks [180], in which the path to a final scenario of extinction of one of the languages is analyzed in finite size systems; (ii) introducing geographical dependencies in terms of a reaction-diffusion equation, which allow the survival of the two languages, with speakers of different languages mostly located in different geographical areas [172, 174]; (iii) implementing Lotka-Volterra type modifications to the original model which can lead to a scenario of coexistence of the two languages in the same geographical area [175]; (iv) introducing bilingualism in the model: individuals can use both languages [173, 182]. In this last extension [182], and in the same parameter setting studied by Abrams and Strogatz, introducing bilingualism keeps the coexistence of both languages unstable. This extension of the model has been extensively studied and compared to the seminal model of Abrams and Strogatz for the case of socially equivalent languages and linear dependence on the density of speakers [198]. The analysis has been done in agent based models in finite systems where social structure has been taken into account using complex social networks. The models have been studied in two-dimensional regular lattices and small-world networks [198], as well as in networks with community structure [215, 216].

The prestige of a language has been considered as one of the main factors affecting language competition since Labov's *Sociolinguistic Patterns* [170]. It measures the status associated to a language due to individual and social advantages related to the use of that language, being higher according to its presence in education, religion, administration and the media. Minett and Wang [183] defined simple strategies for modifying the prestige to maintain the coexistence of the two languages, following the remarks of the seminal work quoted above [13]. Beyond this initial effort in proposing simple strategies to foster language coexistence, the aim of this work is to provide a more general approach to determine the actions on the prestige to maintain the coexistence of both languages.

We adopt a viability theory perspective: viability theory [238] provides theoretical concepts and practical tools, in order to maintain a dynamical system inside a given set of a priori desired states, called the *viability constraint set*. This set represents the "good health" of a system beyond which its safe existence would be jeopardized; in the context of language maintenance, it characterizes the safe coexistence of both languages. The goal of viability theory is to determine policies (viable policies) that always keep the system inside the viability constraint set, rather than to optimize some criterion. The main concept is the *viability kernel*: the set of states, given some possible control actions on the system, for which the system can be maintained inside the viability constraint set. It provides the

APPENDIX B. VIABILITY AND RESILIENCE OF LANGUAGES

actual constraints of the system: inside the viability kernel, there is at least one control policy which maintains the system indefinitely inside the constraint set; outside the viability kernel, the system will break the constraint set, irrespective of the policy applied. Moreover, viability theory provides a particularly appropriate framework to define rigorously the concept of *resilience* [242], the capacity of a system to undergo some exogenous disturbances and to maintain some of its dynamical properties. Resilience is often defined within the dynamic systems theory: it can be measured as a function of the time needed to return to equilibrium after a perturbation [243], or as a function of the distance to bifurcation points [244], where these are defined as points where the stability of a fixed point changes. In the viability framework, the desired properties can be defined by viability constraints, and resilience, which refers to viable states, becomes the capacity to drive the system inside its viability kernel when a perturbation pulls it off. It focuses on the ways by which the system can recover from such a perturbation by providing control policies (if any) that will drive back the system to a safe coexistence scenario with a minimal cost of restoration. Applying viability theory to the Abrams-Strogatz model, We identify the configurations for which an indefinite coexistence can be insured, and provide the corresponding action policies on the prestige. Following Ref [242]'s approach, we study the resilience of the model by identifying configurations from where the system can return to a state of coexistence (finite resilience) and other configurations from where one of the languages faces extinction irrespective of the policy applied (zero resilience).

This paper is organized as follows: first, we introduce the Abrams-Strogatz model, briefly describing the model and the stability analysis depending on the parameters; we then study the viability of the languages by defining action policies that maintain the system within its viability kernel; finally, we compute the resilience of the two languages using two different criteria. We finally discuss the results and draw some conclusions.

Language Dynamics: the Abrams-Strogatz Model

To study the competition between languages in a given population, Abrams and Strogatz proposed a simple model to represent a population with two languages (A and B) in competition for speakers. Let Σ be the fraction of A -speakers and $1 - \Sigma$ the fraction of B -speakers. A B -speaker can become an A -speaker with the probability $P_{BA}(\Sigma)$, and the inverse event happens with the probability $P_{AB}(\Sigma)$.

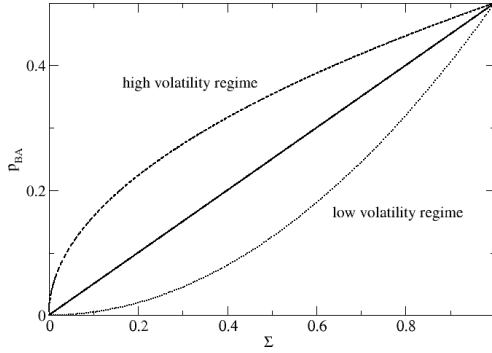


Figure B.1: Dependence on the volatility parameter a for the transition probability to change from state B to state A , P_{BA} . Case of socially equivalent languages ($s = 0.5$). Marginal volatility ($a = 1$, solid line), high volatility regime ($a < 1$, dashed line), and low volatility regime ($a > 1$, dotted line).

In this way, the time evolution for Σ is:

$$\frac{d\Sigma}{dt} = (1 - \Sigma)P_{BA}(\Sigma) - \Sigma P_{AB}(\Sigma). \quad (\text{B.1})$$

Speakers change their language according to the attractiveness of the other language, which depends on the fraction of speakers and on two parameters: the prestige of the language, s , and the volatility, a . The probability for B -speakers to become A -speakers reads:

$$P_{BA}(\Sigma) = \Sigma^a s. \quad (\text{B.2})$$

The prestige of language A is modeled as a scalar, $s \in [0, 1]$ (the prestige of language B is $1 - s$), which aggregates the multiple factors affecting the prestige of a language. Notice that the case $s = 0.5$ corresponds to the case of socially equivalent languages. The functional form of $P_{BA}(\Sigma)$ is shaped by the parameter a , which we define as volatility (see Figure B.1). For the case $a = 1$, we have the special case of linear transition probabilities (marginal volatility); a high volatility regime is obtained for $a < 1$, where the transition probabilities are larger than linear (agents are likely to change language); while a low volatility regime is obtained for $a > 1$ where happens the opposite (agents more rarely change their

APPENDIX B. VIABILITY AND RESILIENCE OF LANGUAGES

language). Similarly, the probability for A -speakers to become B -speakers is:

$$P_{AB}(\Sigma) = (1 - \Sigma)^a(1 - s). \quad (\text{B.3})$$

Equations B.2 and B.3 incorporate the assumption that if a language has no speakers or has zero prestige, the probability for a speaker to change for this extinct language is zero.

Introducing Eqns B.2 and B.3 in Eqn B.1, the Abrams-Strogatz model results in the following population dynamics

$$\frac{d\Sigma}{dt} = (1 - \Sigma)\Sigma[\Sigma^{a-1}s - (1 - \Sigma)^{a-1}(1 - s)]. \quad (\text{B.4})$$

We focus now on a brief stability analysis of the model. When $a \neq 1$, the stability analysis shows that there are three fixed points: $\Sigma^* = 1$ and $\Sigma^* = 0$ which correspond to consensus in the state A or B , respectively; and the other one corresponds to coexistence:

$$\Sigma^* = \left(\left(\frac{s}{1-s} \right)^{\frac{1}{a-1}} + 1 \right)^{-1}. \quad (\text{B.5})$$

- For $a > 1$, the two first fixed points are stable, and the third one is unstable, leading to a scenario of dominance of one of the languages and extinction of the other.
- For $a < 1$ instead, the stability of the fixed points changes: consensus becomes unstable giving rise to the coexistence of the two languages. A change in the status does not change the stability of the fixed points, but changes its value; the higher the difference in the relative prestige, the higher the difference in densities between the two languages in the third fixed point. Notice that the case $s = 0.5$ corresponds to the case of socially equivalent languages, and for this case, the transition probabilities (Eqns B.2 and B.3) become symmetric and the third solution is $\Sigma^* = 0.5$ independently of a .
- For $a = 1$, and $s \neq 0.5$, Eqn B.4 becomes the logistic-Verhulst equation [180]:

$$\frac{d\Sigma}{dt} = (2s - 1)\Sigma(1 - \Sigma). \quad (\text{B.6})$$

In this case, there exist just two fixed points: (i) $\Sigma^* = 0$ and (ii) $\Sigma^* = 1$. For $s < 0.5$, (i) is stable and (ii) unstable while for $s > 0.5$ it happens the opposite. For the case $s = 0.5$, we obtain $d\Sigma/dt = 0$ with a degeneracy of fixed

points: any initial condition is a fixed point of the dynamics. This special case of socially equivalent languages and linear transition probabilities corresponds to the voter model dynamics, extensively studied in complex networks [27, 129, 133, 136].

Language Viability

In this work, we are interested in how active policies in favor of an endangered language might lead to a coexistence of the two languages in competition. Abrams and Strogatz already suggested that [13]:

An extension to Eqn B.4 that incorporates such control on s through active feedback does indeed show stabilization of a bilingual fixed point.

We now give evidence of this remark by studying the Abrams-Strogatz model in a viability theory framework. We consider three values of the volatility parameter: $a = 0.2, 1$ and 2 . Note that in the case $a = 0.2$ (in general for $a < 1$), the fixed point corresponding to coexistence of the two languages is stable, and thus no control parameter on s needs to be included to stabilize a bilingual fixed point. However, when the difference in the prestige of the two languages is very large, the fixed point might lay outside the constraint set.

Stating the Viability Problem

Viability theory [238] focuses on how to maintain a dynamical system inside a viability constraint set. The system is composed by state variables, that describe the system, and by control variables that allow one to act on it. The *viability constraint set* defines a state set outside which the system escapes from an a priori desired setting. A state is called viable if there exists at least one control function that maintains indefinitely the system inside the viability constraint set; the set of all these viable states is called the *viability kernel*. The viability problem is thus to define a control function that keeps the system viable. On the contrary, for states located outside the viability kernel, all possible evolutions break the constraints in finite time. As shown below, the viability kernel is essential in order to define action policies that maintain viability and the main task in order to solve a viability problem is thus to determine its viability kernel.

APPENDIX B. VIABILITY AND RESILIENCE OF LANGUAGES

When defining the viability constraint set in the case of language competition, in general, in order to characterize a language as endangered, the fraction of people speaking it is not enough: other crucial aspects include the point at which children no longer learn the language as their mother tongue; as well as the increase of the average age of speakers (in an endangered language, eventually only older generations speak the language) [163]. However, these factors are out of the scope of the current approach, and we will assume in this work, as a first approximation, that a fraction of speakers below a critical value becomes an endangered situation. Building up from this point, in the Abrams-Strogatz model, we want to determine all the couples of density of speakers and language prestige which let the coexistence of the two languages. The viability constraint set is defined by setting minimal and maximal thresholds on the density of speakers. Below the minimal threshold, $\underline{\Sigma}$, or above the maximal threshold, $\bar{\Sigma}$, we consider that language A , or B respectively, is endangered, meaning that the system is not viable. We set $\bar{\Sigma} = 1 - \underline{\Sigma}$ such that there is no need to consider explicitly language B : if Σ is outside the constraint set, so does $1 - \Sigma$.

As it is advocated in Ref [13], we introduce prestige s as the control variable. The enhancement of the prestige of an endangered language can be triggered by political actions such as the increase of the prestige, wealth and legitimate power of its speakers within the dominant community, the strong presence of the language in the educational system, the possibility that the speakers can write their language down, and the use of electronic technology by its speakers [157]. The computation of the viability kernel for the Abrams-Strogatz model will allow us to answer questions like: for a given density of speakers, are there action policies performed in favor of the endangered language that will keep the coexistence of the two languages? If the answer is yes, which are convenient policies? To answer this question, Minett and Wang [183] proposed strategies in a simple framework (only two control values are considered). The main advantage of using viability theory is that it provides general tools and methods to determine the set of initial density of speakers for which it is possible to control the system such that the coexistence is ensured.

First Case: Two Prestige Values

Following the idea of Minett and Wang [183], we consider first a setting where the control u is the prestige s of language A , and we restrict the possible values of the control to only two discrete values u_1 and u_2 . We consider the following viability problem: Find the action policies (a function defining the action in

time), such that the dynamical system

$$\begin{cases} \frac{d\Sigma}{dt} = (1 - \Sigma)\Sigma \left(\Sigma^{a-1}s - (1 - \Sigma)^{a-1}(1 - s) \right) \\ s = u ; u \in \{u_1, u_2\} \end{cases} \quad (\text{B.7})$$

remains in the viability constraint set K :

$$K = [\underline{\Sigma}, \bar{\Sigma}]. \quad (\text{B.8})$$

Our aim is to find the set of values of Σ for which there exists at least one control function that keeps the states of the system defined by Eqn B.7 always inside the viability constraint set (Eqn B.8). The set of all the values of Σ satisfying Eqns B.7 and B.8 constitutes the viability kernel associated to the model with such control settings, and is denoted $Viab_{(1)}(K)$.

Computation of the viability kernel. We will assume that the critical threshold of the density of speakers is 20% of the size of the whole population. Thus we set $\bar{\Sigma} = 0.8$ and $\underline{\Sigma} = 1 - \bar{\Sigma} = 0.2$, the viability constraint being $K = [0.2, 0.8]$. We also suppose that some action can switch the prestige of language A at any time from $u_1 = 0.4$ to $u_2 = 0.6$. The theoretical boundaries of the viability kernel can be determined analytically. Table B.1 gives the boundaries of viability kernels for three values of the volatility a : $a = 0.2, 1$ and 2 . The details and proofs are given in Appendix B.1.

Table B.1: Boundaries of the viability kernel for the dynamics associated to system (B.7) and (B.8).

	Lower Bound	Upper Bound
a = 0.2	0.2	0.8
a = 1	0.2	0.8
a = 2	0.4	0.6

For $a \leq 1$, the viability kernel is the whole constraint set. This means that it is possible to maintain language coexistence between $0.2 \leq \Sigma \leq 0.8$, irrespective of the initial density of speakers A and the initial value of the prestige (given that the initial state belongs to the constraint set, K). For $a > 1$, the maintenance is only possible for initial densities of speakers A between 0.4 and 0.6. When a state $\Sigma \notin Viab_{(1)}(K)$, the system will leave the viability constraint set, irrespective of the actions applied.

Determining heavy viable trajectories. We are interested now in how frequently policy actions must be performed. We use the heavy control principle, which specifies to change the control only when viability is at stake. The principle of the heavy control algorithm is as follows:

APPENDIX B. VIABILITY AND RESILIENCE OF LANGUAGES

- consider an initial state Σ located inside the viability kernel and an initial control u_0 ;
- anticipate the state of the system at the next time step, keeping the same control;
- if the obtained state is inside the viability kernel, then the control does not change;
- on the contrary, if it is outside the viability kernel, then change the control.

Viability theory guarantees that this procedure maintains language coexistence. However, there may be many action policies that ensure coexistence: the only requirement is that the chosen controls never lead outside the viability kernel. Figure B.2 displays viability kernels and control policies. For $a < 1$, there exists a stable fixed point and the trajectory leads to equilibrium. Starting from any initial density of A -speakers and prestige, there is no need to apply any control policy; the equilibrium is naturally reached. For $a \geq 1$, there are no stable fixed points inside the viability constraint set. The control procedure is then applied at each time step: the control is changed only when it leads to a point located outside the viability kernel.

Second Case: Prestige Chosen in a Continuous Interval

In this section, instead of taking only two values, we suppose that the prestige can take any value $s \in [0, 1]$ but the action on the prestige is not immediate: the time variation of the prestige $\frac{ds}{dt}$ is bounded by a constant denoted c . This bound reflects that changes in prestige take time: to reach a prestige value s_1 starting from an initial prestige $s_0 < s_1$, the stakeholder will have to anticipate at least $\frac{s_1 - s_0}{c\Delta t}$ time steps, where c is the maximum change per unit time Δt . We consider the viability problem to define a function u of time, which maintains the dynamical system:

$$\left\{ \begin{array}{l} \frac{d\Sigma}{dt} = (1 - \Sigma)\Sigma \left(\Sigma^{a-1}s - (1 - \Sigma)^{a-1}(1 - s) \right) \\ \frac{ds}{dt} = u \\ u \in [-c, +c] ; c \in [0, 1] \end{array} \right. \quad (\text{B.9})$$

inside the viability constraint set K :

$$K = [\underline{\Sigma}, \bar{\Sigma}] \times [0, 1]. \quad (\text{B.10})$$

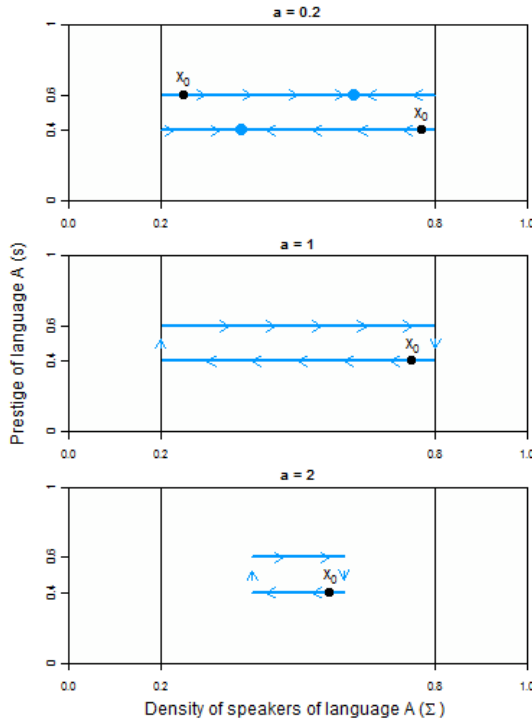


Figure B.2: Viability kernels and trajectories that maintain the system viable for $a = 0.2, 1$ and 2 . The viability kernels are represented in blue and stable attractors (if any) by dots. Arrows represent the field direction and the controls to choose. For $a = 0.2$, any control is convenient because they lead the system to a stable fixed point. For $a = 1$ and 2 , when trajectory lead to a point located outside the viability kernel, the control value must be changed in order to ensure coexistence.

The first step is to determine the viability kernel $Viab_{(2)}(K)$, defined by all couples (Σ, s) that are solution of the system, Eqn B.9, for which there exists at least one control function keeping the system indefinitely inside the viability constraint set defined by Eqn B.10.

Computation of the viability kernel. We still assume again that the critical threshold of the density of speakers is 20% of the size of the whole population. Therefore, the viability constraint set is $K = [0.2, 0.8] \times [0, 1]$. The theoretical boundaries of the viability kernel can be computed analytically (Appendix B.2).

APPENDIX B. VIABILITY AND RESILIENCE OF LANGUAGES

In general, there exists no explicit formula to define the viability kernel boundaries and algorithms have been proposed to approximate them. In this paper and in addition to the theoretical boundaries, we approximate the viability kernel using the algorithm described in Ref [245], that considers the dynamics in discrete time Δt . The obtained approximation enables us to use a simpler heavy control procedure. Figure B.3 shows the analytical and approximated viability kernels of the system for $a = 0.2, 1, \text{ and } 2$. The thick gray lines corresponding to the fixed points of the dynamics has been obtained using Eqn B.5. We set $c = 0.1$, which means that the time variation of the prestige cannot be higher than 10%. The figure shows how for states with a low A or B -speakers density, the prestige associated to this language must be strong enough to maintain viability. In situations where the density of one language is high, smaller values of its associated prestige also give raise to viable situations. On the contrary, non-viable states correspond to situations where the density of one language and its associated prestige are low at the same time. In this case, if the actions in favor of this language come too late, its density of speakers will get below the critical threshold 20% while the other will spread through the majority of the population (above 80%). As a increases, the viability kernel shrinks. Indeed, the higher the parameter a , the more rarely agents change their language (low volatility regime). The impact of the change on the prestige is then lower as a increases, which means that when a language is close to the boundary of the viability kernel, even with the maximal government action, the effect on the density of speakers will be too slow to avoid leaving the viability constraint set. On the contrary, as a decreases, agents are likely to change their language (high volatility regime) and to restore coexistence. Note that for $a = 0.2$, the viability kernel is not the whole constraint set: non-viable states reach a stable fixed point located outside K .

Determining heavy viable trajectories. The control procedure models an action to enhance the prestige of an endangered language, and we assume that such an action is costly. Therefore, if among different possible action policies to maintain language coexistence, doing nothing keeps the system in a viable situation, we assume that this strategy will be chosen in order to reduce costs. In other words, we suppose that, if several situations with $-c \leq u \leq c$ lead to viable situations, the best choice is $u = 0$. The principle of the control algorithm is roughly as follows:

- consider an initial state (Σ, s) located inside the viability kernel;
- anticipate the trajectory in the next time steps, by considering $u = 0$;
- if the obtained state is located inside the viability kernel, do not change the control;

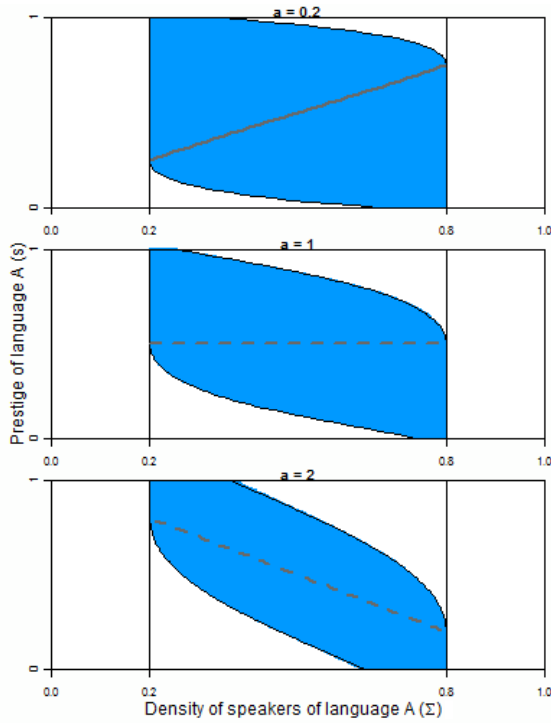


Figure B.3: Viability kernel for the Abrams-Strogatz model, with $c = 0.1$ and $\Delta t = 0.05$. The continuous black lines represent the theoretical curves of the viability kernel, and the area in blue the approximation. The continuous gray line represents stable fixed points and the dotted gray lines unstable fixed points.

- otherwise, choose a control that brings the system away from the viability kernel's boundary as much as possible.

This control procedure is described in more details in Ref [245]. We use here the viability kernel approximation boundary instead of the analytical one because it makes easier to check if the anticipation of the trajectory leads to a point outside the kernel and to approximate the distance to the viability kernel boundary. Figure B.4 presents some examples of trajectories for three different values of a , and the time evolution of the control ($c = 0.1$), during 750 time steps. For $a < 1$, there exist stable fixed points corresponding to coexistence of the two

APPENDIX B. VIABILITY AND RESILIENCE OF LANGUAGES

languages and the dynamics settles there, keeping $u = 0$ along the trajectory. For $a \geq 1$ instead, there are no stable fixed points inside the viability kernel, and the control procedure must be applied at each time step. As long as the trajectory is far away from the kernel's boundary, the control is kept to zero; when it approaches the boundary, the control that brings the system away from the boundary corresponds to the maximum value of the control with the appropriate sign, $\pm c$.

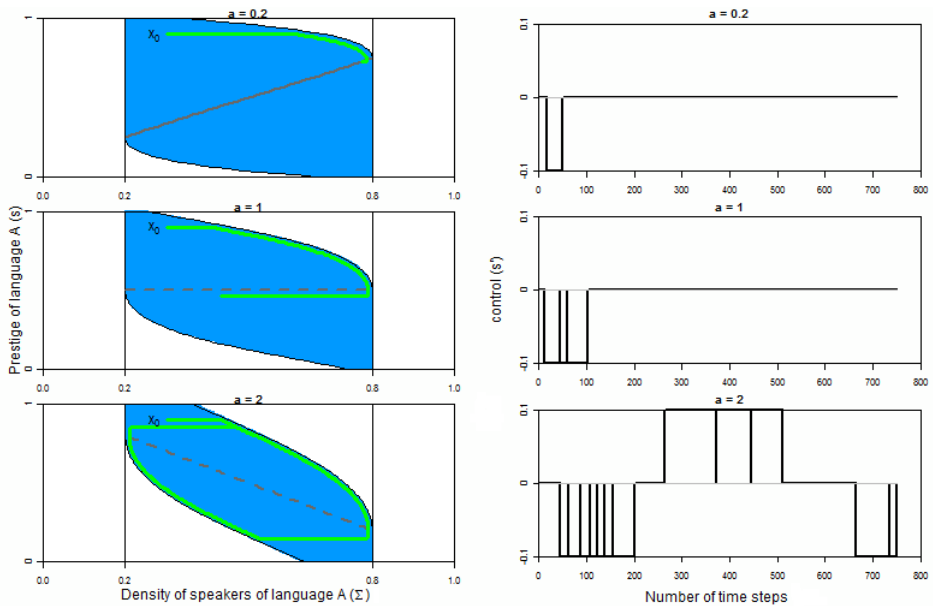


Figure B.4: (Left panel) Examples of trajectories (in green) starting from an initial state x_0 for three values of a ($a = 0.2, 1$ and 2), and (right panel) evolution of the control, with $c = 0.1$. The continuous gray line represents stable fixed points and the dotted gray line unstable fixed points.

Language Resilience

In the previous section, we studied the viability of the language model, supposing that one language is endangered when its density of speakers goes below a critical value. However, being endangered does not necessarily mean that the language will disappear. In this section, we are interested in how to maintain or restore coexistence of the two languages when the system is in danger, meaning that a disturbance pulls it outside the viability constraint set. We deal only with the second case, where the prestige is chosen on a continuous interval.

As we pointed out in the introduction, resilience is the capacity of a system to restore its properties of interest, lost after disturbances. In this section, we define resilience of system Eqns B.9 and B.10 by considering its capacity to return into its viability kernel when a perturbation pulls it out from it, following Ref [242] definition of resilience.

Stating the Resilience Problem

We are interested in situations of crisis, which take place when the system leaves the viability constraint set. We distinguish two types of states located outside the viability kernel:

- States for which there exists at least one evolution driving back the system to the viability kernel after leaving the constraint set, are called resilient. The system is resilient to a perturbation which leads it into a resilient state;
- States for which irrespective of the control policy applied, the system remains outside the viability kernel, are called non-resilient. The system is not resilient to perturbations leading the system into a non-resilient state.

For states located inside the viability kernel, the resilience is infinite. Reference [242] also introduces the notion of cost of restoration in its resilience definition. This cost measures the distance between the evolution of the state of the system and the property of interest (i.e. being inside the viability kernel). Its definition must fulfill three conditions. First, the cost of an action which keeps the property of interest indefinitely is zero: maintaining this property may lead to some action update, but they are not taken into account in the cost computation. Second, when the property of interest can not be restored, the cost of restoration is infinite. Third, when the property can be restored, the cost is finite. It is

APPENDIX B. VIABILITY AND RESILIENCE OF LANGUAGES

often defined by the minimum time the system is outside the viability kernel or the minimal deficit accumulated along the trajectory. Then, the resilience is the inverse of the restoration cost of the properties of interest lost after disturbances. The trajectory starting from (Σ, s) with a minimal cost defines the sequence of “best” action policies to perform, and thus defines the resilience value. Resilience values can be approximated numerically using Ref [246]’s algorithm, which is based on the Ref [245]’s viability kernel approximation algorithm. In the context of language competition, the use of viability theory provides a measure of the cost associated to a policy action which will favor an endangered language.

Determining the Resilient and Non-Resilient States

All the states can undergo a disturbance. For instance, immigration: people speaking language A exile to another country, hence the density of A -speakers reduces dramatically in the home country, and increases in the destination country. Another perturbation to the system can be due to an abrupt change in the prestige of a language because of political actions such as invasion, occupation, etc. The states resulting from disturbances might bring the system outside the constraint set, leading to situations where the density of speakers is lower than the minimal threshold or higher than the maximal threshold. Thus, we consider now the set of all the possible situations $H = [0, 1] \times [0, 1]$, where the first dimension represent the density of speakers of language A and the second the prestige of language A , and we study the resilience of the system in H .

First, we determine the set of states of infinite resilience, that are the states located inside the viability kernel of the system defined by Eqn (B.9) associated to constraint set defined by Eqn B.10. It corresponds to the dark blue area on Figure B.5. Then, we look for all the states for which at least one evolution drives the system back to the viability kernel after spending a finite time in the critical area $H \setminus K$ (where $E \setminus F$ is the complementary set of the set F in the set E). These are the resilient states, in colored light blue in Figure B.5. Note that states located in $K \setminus Viab_{(2)}(K)$ can have a finite resilience: when coming back towards $Viab_{(2)}(K)$, the trajectory leaves the constraint set and reaches $Viab_{(2)}(K)$ after spending time in the critical area. The states that, irrespective of the applied policy, remain outside the viability kernel are in the white zone. For these states, the desired level of language coexistence is impossible and resilience is zero (given the assumed value of c , which limits the effect of action).

In Figure B.5, we show the resilient and non-resilient states for $a = 0.2, 1$, and 2 . For a small value of a , all the states are resilient, except $\Sigma = 0$ and $\Sigma = 1$, irrespective of the value of s . As we pointed out previously, the fixed point

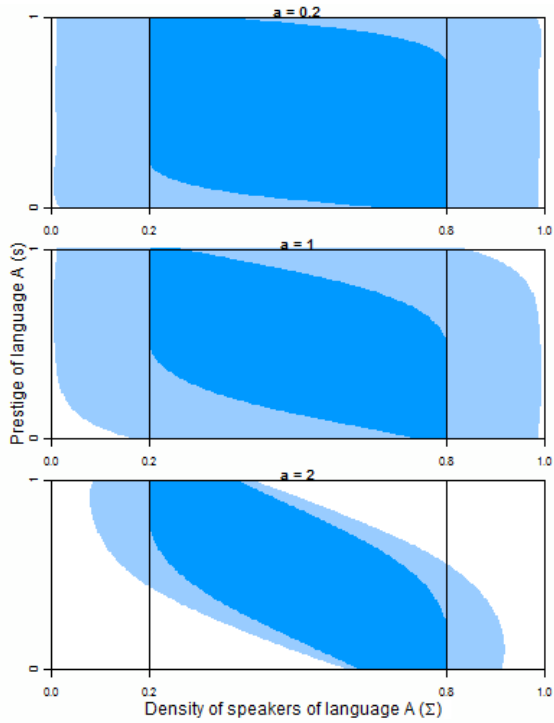


Figure B.5: Resilient (blue) and non resilient states (in white) in the model associated to dynamics Eqn B.9 with constraint set Eqn B.10, for three values of a : $a = 0.2$, $a = 1$, $a = 2$. Viability kernel is in dark blue.

corresponding to coexistence is stable for $a < 1$. Therefore, the desired level of coexistence for the two languages is ensured or can be reached, irrespective of their initial density of speakers and their prestige, except when a perturbation leads to a situation where one language is already extinct. For $a = 1$, nearly for all the initial density of speakers and prestige, reaching the desired level of languages coexistence is possible, except if the initial state represents a large density of speakers of language A associated with high prestige (language B becomes extinct, irrespective of the action applied) or vice versa. For $a > 1$, the set of resilient states becomes smaller as it can be seen in Figure B.5. The larger the value of a , the smaller the set of resilient states is. Indeed, as mentioned before for the shrinking of the viability kernel, a high value of a means that

APPENDIX B. VIABILITY AND RESILIENCE OF LANGUAGES

agents rarely change their language and the effects of increasing or decreasing the prestige of a language become less effective.

Computing Resilience Values

As we pointed out previously, the resilience value is then defined as the inverse of its restoration cost. There exist several ways of defining a cost of restoration, depending on the situations and the point of view. We studied two possibilities for the cost: on the one hand, we considered that the time needed to restore viability is the only ingredient under consideration, the cost value is then the time the system is outside the viability kernel. The cost function C_1 that associates to a state x the minimal cost of restoration among all the trajectories starting from x is defined by:

$$C_1(x) = \min_{x(\cdot)} \left(\int_0^{+\infty} \chi_V(x(t)) dt \right) \quad (\text{B.11})$$

and $\chi_V(x(t)) = 1$ when $x(t) \notin \text{Viab}_{(2)}(K)$ and 0 otherwise,

where x represents the state (Σ, s) , $x(t)$ is the state at time t and $x(\cdot)$ is the trajectory starting from this state. Hence the cost value is zero when the system is inside the viability kernel. On the other hand, we considered a more complete cost function composed of two terms: the first one that accounts for the time the system is not viable, and the second one, representing the distance to the viability constraint set. This cost function, denoted C_2 , thus associates the time of restoration and the measure of the density of speakers above or below the thresholds of the viability constraint set:

$$C_2(x) = \min_{x(\cdot)} \left(\int_0^{+\infty} \chi_V(x(t)) dt + c_2 \chi_K(x(t)) dt \right) \quad (\text{B.12})$$

and $\chi_K(x(t)) = d(x(t), K)$ when $x(t) \notin K$ and 0 otherwise,

where $d(x(t), K) = \max(\underline{\Sigma} - \Sigma(t), \Sigma(t) - \bar{\Sigma})$ measures the distance between the density $\Sigma(t)$ at time t and the density thresholds. Equation B.12 takes into account that the cost of restoration of a state near extinction is more costly than the one for states located near the boundary of K . Parameter c_2 reflects the relative weight of each cost, fixing the cost of being far from K relatively to the time spent outside the viability kernel.

Figure B.6 compares resilience values for the Abrams-Strogatz model for different values of a , and for the two cost functions defined (with an arbitrary cost parameter $c_2 = 20$ for the second cost function). The difference of cost between two iso-cost curves is 4.8, and therefore the difference in resilience is $\frac{1}{4.8} \approx 0.2$ (the 4.8 value is arbitrary and is linked to the parametrization of the algorithm

in Ref [246]). The darker the line, the higher the cost value is. In the white area, cost is infinite, meaning that restoring coexistence of both languages is impossible. For $a = 0.2$, the maximal cost of restoration is equal to 4.8 for cost function C_1 defined by Eqn B.11 and 19.2 for the cost C_2 defined by Eqn B.12. The cost associated to the function defined by Eqn B.12 is bigger than the one associated with Eqn B.11 because it introduces an additional part (the distance to viability) on the final cost. For $a = 1$, the maximal cost of restoration is more important (14.4 for Eqn B.11 and 62.4 for Eqn B.12). For $a = 2$, the resilient zone is smaller and the costs of restoration are larger (24 for Eqn B.11 and 67.2 for Eqn B.12). This means that for higher values of a , where the resilient set is smaller, the cost of restoration is larger: there are less resilient situations and the action policies to perform in order to restore viability are the most costly.

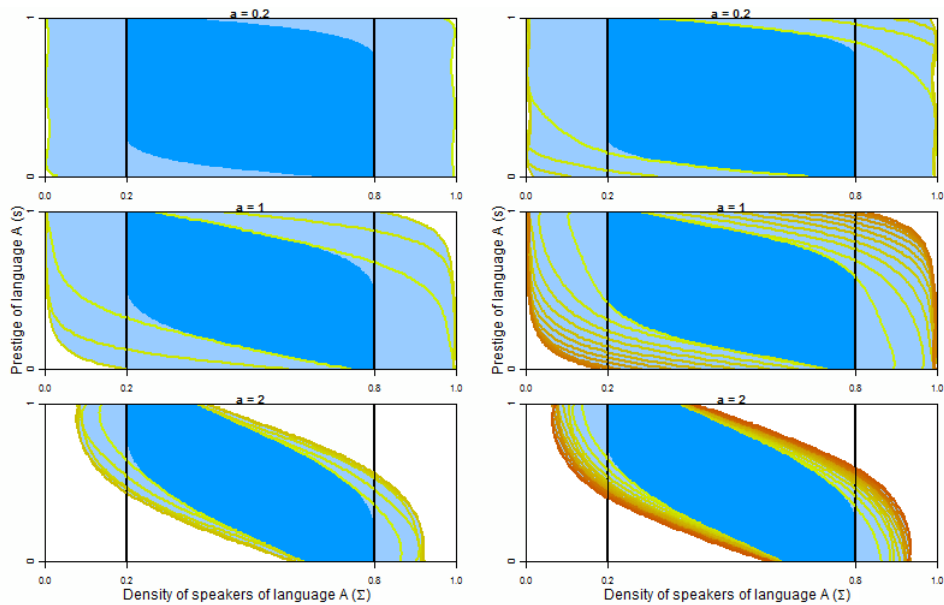


Figure B.6: Resilience values of the Abrams-Strogatz model. In dark blue, the viability kernel; between the level lines (light blue area), the cost of restoration is finite (one level line corresponds to a cost of 4.8 and the darker the line, the higher the cost); in the white area, the cost is infinite and the resilience is zero. (Left panel) Cost function C_1 (Eqn B.11); (Right panel) cost function C_2 (Eqn B.12).

Determining Action Policies to Restore Viability at Minimum Cost

Computing resilience values is instrumental to define action policies that drive back the system inside the viability kernel. Here, we use an optimal controller instead of a heavy controller: we do not look for one action policy that keeps the system in a resilient state, but we define a sequence of actions that allows the system to return to the viability kernel at the lowest cost of restoration. It can be shown (see Ref [246]) that choosing the action that decreases the cost at each step (or increases the resilience), minimizes the whole cost of restoration. Hence, theoretically this approach also provides a means to compute resilient policies, which minimizes the cost of restoration along the trajectory. The procedure is roughly as follows:

- consider an initial state (Σ, s) for which resilience is finite;
- choose the action policy that decreases the cost at maximum at each time step, until the trajectory reaches the viability kernel;
- once the state is viable, use the heavy control procedure described previously to ensure the indefinite maintenance of the system.

Figure B.7 displays some trajectories starting from resilient states for $a = 0.2, 1$ and 2 . Considering the cost C_2 of Eqn B.12, the controller produces a trajectory that avoids situations where the density of speakers is too small or too large, because these are the most costly. Notice that for $a = 0.2$, the trajectory first reaches the equilibrium line outside K , but in order to bring the system inside the viability kernel, the control function is chosen such that it does not get stuck on this fixed point. The procedure leads the system to a second fixed point, located this time inside the viability kernel. Even if the starting point is located inside K but outside the viability kernel (see for example case $a = 1$), the trajectory crosses the viability constraint set before going back to $Viab_{(2)}(K)$, as it is not possible by definition for these states to directly reach the viability kernel.

Conclusion

In this paper, we provide general means for determining action policies to maintain the coexistence of two languages in competition within the Abrams-Strogatz

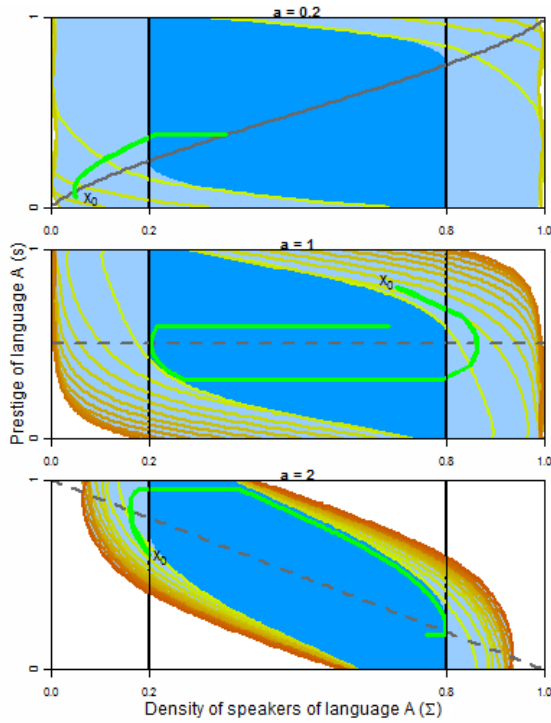


Figure B.7: Examples of trajectories (in green) starting from a point x_0 during 750 time steps, that allow the system to restore its viability at the minimal cost of restoration, using cost function Eqn B.12. The continuous gray line represents stable fixed points and the dotted gray line unstable fixed points. Note that for an initial state x_0 located inside K but outside $Viab_{(2)}(K)$, the trajectory crosses the viability constraint set boundaries before reaching $Viab_{(2)}(K)$.

model [13] by using the framework of viability theory. We compute viable policies of action on the prestige variable to keep language coexistence within a given constraint set, computing the viability kernel of the system. We thus give evidence of the Abrams and Strogatz remark: language coexistence is unstable if we consider a fixed prestige, but introducing the prestige as a control variable of the model enables the maintenance of a bilingual society, where both languages have a density above a critical value. We also define the resilience of the system in the formalism of viability theory: the system is resilient to a perturbation if,

APPENDIX B. VIABILITY AND RESILIENCE OF LANGUAGES

after the perturbation, there exists an action policy driving back the system to its viability kernel. In this way, we determine the action policies that minimize the cost to drive an endangered language to coexistence (i.e. to the viability kernel of the system). In the paper, we have analyzed the role played by the two parameters of the model: the prestige of the language, s , and the volatility, a . The prestige has been considered as the control variable of the system; we have shown how the viability kernel shrinks as the volatility parameter increases, due to the fact that agents become less likely to change their language.

The whole approach illustrates the new definition of resilience proposed in Ref [242], which enlarges previous definitions of resilience, yet with a precise mathematical meaning. In particular, we don't need to define the resilience relatively to the attractors of the dynamics, whereas the presence of such attractors is generally required in previous mathematical views of resilience [243, 244]. In the future, it will be interesting to consider the extension of the Abrams-Strogatz model that includes bilingual speakers [183, 198], and compare the results with the ones presented in this paper in order to illustrate which is the role of bilingual agents in the dynamics of language competition from the viability theory perspective.

Acknowledgments

This work has been supported by European contract PATtern RESilience (FP6 NEST n° 043268) and project FISICOS (Spain). X. Castelló also acknowledges financial support from a PhD fellowship of the Govern de les Illes Balears (Spain). The funders had no role in study design, data collection and analysis, decision to publish, or preparation of the manuscript. We thank Lucía Loureiro-Porto for fruitful discussions and comments.

B.1

Theoretical bounds of the Abrams-Strogatz model (I)

In this appendix, we derive the theoretical bounds of the Abrams-Strogatz model (system Eqn B.7) associated with the viability constraint set Eqn B.8.

B.1. THEORETICAL BOUNDS OF THE ABRAMS-STROGATZ MODEL (I)

Case 1: $a = 1$

In this case, we have $Viab_{(1)}(K) = K$

PROOF.

Equation $\begin{cases} \frac{d\Sigma}{dt} = (1 - \Sigma)\Sigma(\Sigma^{a-1}s - (1 - \Sigma)^{a-1}(1 - s)) \\ s = u ; u \in \{-c, +c\} \end{cases}$ can be rewritten as:

$$\frac{d\Sigma}{dt} = (2u - 1)\Sigma(1 - \Sigma). \quad (\text{B.13})$$

For $0.2 \leq \Sigma \leq 0.8$, we have $\Sigma(1 - \Sigma) > 0$. Thus, with $u = 0.4$, we have $\frac{d\Sigma}{dt} < 0$ and with $u = 0.6$, we have $\frac{d\Sigma}{dt} > 0$.

Then, for all the states $\Sigma \in K$, there exists at least one control function that maintains the system inside K , and all the states are viable.

Case 2: $a \neq 1$

For $\Sigma \in K$, $\frac{d\Sigma}{dt} = 0 \Leftrightarrow \Sigma = \left(\left(\frac{u}{1-u} \right)^{\frac{1}{a-1}} + 1 \right)^{-1} = E_u$, with $u = s$.

Case 2.1: $a < 1$

In this case, we have $Viab_{(1)}(K) = K$.

PROOF.

For $0.2 \leq \Sigma \leq 0.8$, $\forall u \in \{0.4, 0.6\}$, the equilibria are stable (see section Analytical Study of the Model). In addition, it can be easily shown that, for $u \in \{0.4, 0.6\}$, $E_u \in K$. Thus, $\forall u$, the dynamics leads to a stable fixed point $E_u \in K$.

Case 2.1: $a > 1$

In this case, we have $Viab_{(1)}(K) = \{\Sigma \in K \text{ such that } E_{0.6} \leq \Sigma \leq E_{0.4}\}$.

PROOF.

- For all the points located inside the viability kernel, there exists one control that allows the system to stay inside the viability kernel.
For $\Sigma \in Viab_{(1)}(K)$, we have $\frac{d\Sigma}{dt} < 0$ for $u = 0.4$ and $\frac{d\Sigma}{dt} > 0$ for $u = 0.6$.

APPENDIX B. VIABILITY AND RESILIENCE OF LANGUAGES

- For all the points located outside the viability kernel, there is no control that allows the system to return to the viability kernel.

For $\Sigma < E_{0.6}$, we have $\frac{d\Sigma}{dt} < 0$ for $u = 0.4$ and $\frac{d\Sigma}{dt} < 0$ for $u = 0.6$ ($\Sigma \rightarrow 0$).

For $\Sigma > E_{0.4}$, we have $\frac{d\Sigma}{dt} > 0$ for $u = 0.4$ and $\frac{d\Sigma}{dt} > 0$ for $u = 0.6$ ($\Sigma \rightarrow 1$).

B.2

Theoretical bounds of the Abrams-Strogatz model (II)

In this appendix, we derive the theoretical bounds of the Abrams-Strogatz model (system Eqn B.9) associated with the viability constraint set Eqn B.10.

We remind that the dynamics $\left(\frac{d\Sigma}{dt}, \frac{ds}{dt}\right) = F(\Sigma, s, u)$ are defined by:

$$\begin{cases} \frac{d\Sigma}{dt} = F(\Sigma, s, u) = (1 - \Sigma)\Sigma \left(\Sigma^{a-1}s - (1 - \Sigma)^{a-1}(1 - s) \right) \\ \frac{ds}{dt} = u \\ u \in [-0.1, 0.1] \end{cases} \quad (\text{B.14})$$

and that $K = [\underline{\Sigma}, \bar{\Sigma}] \times [0, 1]$ is the viability constraint set.

We aim at finding explicit formulas for $Viab_F(K)$, the viability kernel under the dynamics F . We first introduce two functions f_1 and f_2 and then prove that these functions enable us to define a set which is $Viab_F(K)$.

Definition of f_1 and f_2

- Let $C_1 = \{(\Sigma(t), s(t)), t \in [0; +\infty []$ satisfying

$$\begin{cases} \frac{d\Sigma(t)}{dt} = -(1 - \Sigma(t))\Sigma(t) \left(\Sigma^{a-1}(t)s(t) - (1 - \Sigma(t))^{a-1}(1 - s(t)) \right) \\ \frac{ds(t)}{dt} = 0.1 \\ \Sigma_1 = 0.8 \text{ and } s_1(0) = s_1 = \frac{0.2^{a-1}}{0.8^{a-1} + 0.2^{a-1}} \end{cases} \quad (\text{B.15})$$

where $\Sigma(t)$ is the density of A -speakers at time t and $s(t)$ the prestige at time t .

B.2. THEORETICAL BOUNDS OF THE ABRAMS-STROGATZ MODEL (II)

We have $C_1 = \{(\Sigma, s) \in \mathbb{R}^2 | \Sigma = f_1(s), s \geq s_1\}$ with:

$$f_1(s) = \Sigma_1 + \int_{s_1}^s -(1 - f_1(\bar{s}))f_1(\bar{s})(f_1(\bar{s})^{a-1}\bar{s} - (1 - f_1(\bar{s}))^{a-1}(1 - \bar{s}))d\bar{s}. \quad (\text{B.16})$$

Note that $f_1'(s_1) = 0$ and that $f_1''(s) < 0$ when $f_1(s) \in [0.2, 0.8]$ and $f_1'(s) = 0$. Consequently, $f_1'(s) < 0$ when $s > s_1$ and $f_1(s) \in [0.2, 0.8]$.

- Let $C_2 = \{(\Sigma(t), s(t)), t \in [0; +\infty []\}$ satisfying:

$$\begin{cases} \frac{d\Sigma(t)}{dt} = -(1 - \Sigma(t))\Sigma(t) \left(\Sigma^{a-1}(t)s(t) - (1 - \Sigma(t))^{a-1}(1 - s(t)) \right) \\ \frac{ds(t)}{dt} = -0.1 \\ \Sigma_2 = 0.2 \text{ and } s_2(0) = s_2 = \frac{0.8^{a-1}}{0.2^{a-1} + 0.8^{a-1}} \end{cases} \quad (\text{B.17})$$

We have $C_2 = \{(\Sigma, s) \in \mathbb{R}^2 | \Sigma = f_2(s), s \leq s_2\}$ with:

$$f_2(s) = \Sigma_2 - \frac{1}{0.1} \int_{s_2}^s -(1 - f_2(\bar{s}))f_2(\bar{s})(f_2(\bar{s})^{a-1}\bar{s} - (1 - f_2(\bar{s}))^{a-1}(1 - \bar{s}))d\bar{s}. \quad (\text{B.18})$$

Note that $f_2'(s_2) = 0$ and that $f_2''(s) > 0$ when $f_2(s) \in [0.2, 0.8]$ and $f_2'(s) = 0$. Consequently, $f_2'(s) < 0$ when $s < s_2$ and $f_2(s) \in [0.2, 0.8]$.

Definition of $Viab_F(K)$ and proofs

THEOREM.

Let $E \subset K$ the subset defined by:

$$\left\{ (\Sigma, s) \in K \mid \begin{array}{l} \Sigma \leq f_1(s) \text{ if } s \geq s_1(0) \\ \Sigma \geq f_2(s) \text{ if } s \leq s_2(0) \end{array} \right\} \quad (\text{B.19})$$

then we have $E = Viab_F(K)$.

PROOF PART 1: E is a viability domain: all the points inside E are viable.

We have to prove that for all $(\Sigma, s) \in \partial E$ (where ∂E is the boundary of the subset E), there exists at least one control u such that $F(\Sigma, s, u)$ belongs to the tangent cone of E at the point (Σ, s) , denoted $T_E(\Sigma, s)$.

Let $(\Sigma, s) \in \partial E$,

- if $\Sigma = 0.2$, as $f_2'(s) < 0$ when $s < s_2$ and $f_2(s) \in [0.2, 0.8]$, necessarily $s \geq s_2$. Moreover, $s \leq \min(1, f_1^{-1}(0.2))$. If $s = s_2$, $F(\Sigma, s, 0) = 0 \in T_E(\Sigma, s)$, if $s_2 < s < \min(1, f_1^{-1}(0.2))$, $F(\Sigma, s, u) \in T_E(\Sigma, s)$ for all $u \in [-0.1, 0.1]$.

APPENDIX B. VIABILITY AND RESILIENCE OF LANGUAGES

- if $s = 1$, or if $(\Sigma, s) \in C_1, \Sigma < 0.8, F(\Sigma, s, -0.1) \in T_E(\Sigma, s)$.
- if $\Sigma = 0.8$, as $f_1'(s) < 0$ when $s > s_1$ and $f_1(s) \in [0.2, 0.8]$, necessarily $s \leq s_1$. Moreover, $s \geq \max(1, f_2^{-1}(0.8))$. If $s = s_1, F(\Sigma, s, 0) = 0 \in T_E(\Sigma, s)$, if $\max(1, f_2^{-1}(0.8)) < s < s_1, F(\Sigma, s, u) \in T_E(\Sigma, s)$ for all $u \in [-0.1, 0.1]$.
- if $s = 0$, or if $(\Sigma, s) \in C_2, \Sigma > 0.2, F(\Sigma, s, +0.1) \in T_E(\Sigma, s)$.

PROOF PART 2: E is the largest viability domain.

Let's first introduce some notations:

- Let $(\bar{\Sigma}, \bar{s}) \in K \setminus E$. We can suppose $\bar{s} > f_1^{-1}(\bar{\Sigma})$. The argument is the same if $\bar{s} > f_2^{-1}(\bar{\Sigma})$.
- Let $(\bar{\Sigma}(t), \bar{s}(t)), t \in [0; +\infty[$ an evolution starting from $(\bar{\Sigma}, \bar{s})$ and satisfying equation (B.14).
- Let $(\Sigma^*(t), s^*(t)), t \in [0; +\infty[$ defined by:

$$\begin{cases} \frac{d\Sigma^*(t)}{dt} = (1 - \Sigma^*(t))\Sigma^*(t) \left(\Sigma^{*a-1}(t)s^*(t) - (1 - \Sigma^*(t))^{a-1}(1 - s^*(t)) \right) \\ \frac{ds^*(t)}{dt} = -0.1 \\ \Sigma^*(0) = \bar{\Sigma} \text{ and } s^*(0) = f_1^{-1}(\bar{\Sigma}) \end{cases} \quad (\text{B.20})$$

Then, $(\Sigma^*(0), s^*(0)) \in C_1$ and there exists T such that $(\Sigma^*(T), s^*(T)) = (\Sigma_1, s_1)$ and $(\Sigma^*(t), s^*(t)) \in C_1, \forall t \in [0; T]$.

We have $\bar{s}(0) > s^*(0)$ and as $s^{*\prime}(t) = -0.1$ and $\bar{s}'(t) = u \in [-0.1, 0.1], \forall t \in [0; T], \bar{s}(t) > s^*(t)$. Furthermore, $\bar{\Sigma}(0) = \Sigma^*(0)$ and $\frac{d\bar{\Sigma}}{dt}(0) = F(\bar{\Sigma}(0), \bar{s}(0)) > F(\Sigma^*(0), s^*(0)) = \frac{d\Sigma^*}{dt}(0)$ so there exists $\hat{t} > 0$ such that $\bar{\Sigma}_A(t) > \Sigma_A^*(t)$ for all $t \in]0, \hat{t}]$.

Assume that there exists $\tilde{t} \in]\hat{t}, T]$ such that $\bar{\Sigma}_A(t) > \Sigma_A^*(t)$ for all $t \in]\tilde{t}, \tilde{t}]$ and $\bar{\Sigma}_A(\tilde{t}) > \Sigma_A^*(\tilde{t})$. Then $\frac{d\bar{\Sigma}_A}{d}(\tilde{t}) \leq \frac{d\Sigma_A^*}{d}(\tilde{t})$ but $\frac{d\bar{\Sigma}_A}{d}(\tilde{t}) = F(\bar{\Sigma}_A(\tilde{t}), \bar{s}(\tilde{t})) > F(\Sigma_A^*(\tilde{t}), s^*(\tilde{t})) = \frac{d\Sigma_A^*}{d}(\tilde{t})$ since $\bar{\Sigma}_A(\tilde{t}) = \Sigma_A^*(\tilde{t})$ and $\bar{s}(\tilde{t}) > s^*(\tilde{t})$. Hence the contradiction, so $\forall t \in [0, T], \bar{\Sigma}_A(t) > \Sigma_A^*(t)$.

Consequently, $(\bar{\Sigma}_A(T), \bar{s}(T)) \notin K$ and $(\bar{\Sigma}_A(T), \bar{s}(T)) \notin \text{Viab}_F(K)$.

List of Tables

5.1	Typical interactions in the 2c-Naming Game	119
B.1	Boundaries of the viability kernel for the dynamics associated to system (B.7) and (B.8).	193

List of Figures

1.1	Illustration of the Konigsberg bridge problem	7
1.2	The network of runaways constructed by Moreno	8
1.3	Network with community structure extracted from a Belgian mobile phone network of about 2 million customers	10
1.4	The Watts-Strogatz random rewiring procedure for small world networks	17
1.5	Characteristic path length $l(p)$ and clustering coefficient $C(p)$ for the Watts-Strogatz model	18
1.6	Degree distributions in the BA-network	20
1.7	Examples of networks with community structure	22
1.8	Basic mechanisms of social interaction: imitation (voter model) and social pressure (SFKI model)	26
1.9	Illustration of the domain growth in the $d = 2$ voter model	31
1.10	Typical metastable state in the voter model	32
1.11	Average interface density $\langle \rho(t) \rangle$ in different topologies: BA, EN and ER networks	34
1.12	Time evolution for the average interface density. Voter model in small world network	36
1.13	Coarsening in the SFKI model on a square lattice	39

LIST OF FIGURES

1.14	Typical trapped state on a cubic regular lattice	40
1.15	Survival probability for SFKI dynamics on an Erdős-Rényi random network	42
1.16	Active trapped states in a one-dimensional SW network	43
2.1	Volatility parameter, a : neutral case ($a = 1$), high volatility regime ($a < 1$) and low volatility regime ($a > 1$)	54
2.2	Phase portrait: trajectories in the (Σ_A, Σ_B) space for the AB-model	59
2.3	Snapshots showing the formation of domains in the voter model and the AB-model ($a = 1, s = 0.5$)	60
2.4	Snapshots showing the formation of domains in the AS-model and the Bilg-model ($a = 3, s = 0.5$)	60
2.5	Snapshots of the AS-model and the Bilg-model ($a = 3, s = 0.6$) . .	62
2.6	Snapshots showing the coexistence regime in the AS-model and the Bilg-model ($a = 0.1, s = 0.5$)	63
2.7	Snapshots of the AS-model and the Bilg-model ($a = 0.1, s = 0.6$) .	63
3.1	Time evolution of the average interface density $\langle \rho \rangle$ for the AB-model in a fully connected network	68
3.2	Time evolution of the densities of agents, Σ_i ($i = A, B, AB$), and the interface density, ρ for the AB-model in a two-dimensional lattice	70
3.3	Time evolution of the average interface density $\langle \rho \rangle$ for the AB-model in a two-dimensional regular lattice	71
3.4	AB-model in a regular lattice: snapshots of a typical simulation of the dynamics	72
3.5	Time evolution of the interface density ρ for the AB-model in a two-dimensional regular lattice	73
3.6	Snapshots of simulations which get trapped in stripe-like metastable states (regular lattice). AB-model and ϵ -model	74
3.7	Time evolution of the fraction of alive runs, $P(t)$, for the AB-model in a two-dimensional regular lattice	75
3.8	Rescalings with system size of the time evolution of the fraction of alive runs, $P(t)$, for the AB-model in a two-dimensional lattice .	76

LIST OF FIGURES

3.9	Time evolution of the average interface density $\langle \rho \rangle$ for the voter model in a two-dimensional regular lattice	77
3.10	Comparison of the interface dynamics (I): snapshots for the AB-model and the voter model	78
3.11	Comparison of the interface dynamics (II): snapshots for the AB-model and the voter model	79
3.12	Time evolution of the average interface density $\langle \rho \rangle$ for the AB-model in small world networks with different values of p	81
3.13	Time evolution of the average interface density $\langle \rho \rangle$ for the voter model in small world networks with different values of p	82
3.14	Snapshots for the AB-model and the voter model in a small world network with $p = 0.1$	83
3.15	Time evolution of the average interface density, $\langle \rho \rangle$ for the AB-model. Small world networks with different system sizes	84
3.16	Transition probabilities for the ϵ -model for different values of ϵ	86
3.17	Characteristic coarsening exponent γ ($\langle \rho \rangle \sim t^{-\gamma}$) for the ϵ -model as a function of ϵ	87
4.1	Growth process of the class of network with community structure	92
4.2	Partial view of the network centered on a randomized selected node. Average number of k -clique-communities of size s	93
4.3	Average interface density in networks with community structure and randomized networks. Voter model and AB-model	95
4.4	AB-model: fraction of alive runs in time for networks with communities and randomized networks	97
4.5	Snapshots of the dynamics for the voter model the AB-model. Typical configurations of trapped metastable states	99
4.6	Time evolution for the AB-model of the average interface density on different realizations of the network	100
4.7	Fraction of alive runs at time t , $P(t)$, for Erdős-Rényi networks with different average degrees	102
4.8	Time evolution of the fraction f_m of nodes in the state (A or B) that becomes the minority state for an Erdős-Rényi network	103

LIST OF FIGURES

4.9	Illustration of branches and time evolution of the fraction of alive runs $P(t)$ in different ER networks	104
4.10	Characterization of the dynamical robustness against invasion for a given topological structure G	105
4.11	Fraction of alive runs $P(t)$ for different topological substructures . .	106
4.12	Generation of networks with equally sized cliques: EDH and ERH	107
4.13	Time evolution of the fraction of A agents in each clique f_A in an ERH network	108
4.14	Time evolution of the number n_m of agents in the minority state, and of the interface density ρ in an ERH	109
4.15	Dynamical robustness of cliques	110
4.16	Fraction of alive runs in EDH, ERH, and PERH networks	111
4.17	Two typical runs that developed trapped metastable states in EDE networks	112
4.18	Fraction of alive runs $P(t)$ in EDE networks with various factors μ of the clique size distribution $p(s) \sim e^{-(s-s_{min})/\mu}$	113
5.1	AB-model: time evolution of the average interface density $\langle \rho \rangle$ in a fully connected network for different values of β	122
5.2	AB-model: time evolution of the density of agents in state A, n_A , in state B, n_B , and in state AB, n_{AB} ; and of the interface density, ρ .	124
5.3	AB-model: evolution of the position of an interface in a one-dimensional regular lattice	126
5.4	Stripe-like trapped metastable states for the AB-model and the 2c-Naming Game in a two-dimensional regular lattice	128
5.5	2c-Naming Game and AB-model: probability distribution for the time to reach consensus, starting from stripe-like configurations .	129
6.1	Stability diagram for the Abrams-Strogatz model in a fully connected network	134
6.2	Stationary solution $m^*(a, v)$ for the Abrams-Strogatz model as a function of the two parameters of the model, a and v	135

LIST OF FIGURES

6.3	Spreading experiments: probability $P(t)$ that the system is still alive at time t in the Abrams-Strogatz model ($v = 0$)	137
6.4	Ginzburg-Landau potential for the Abrams-Strogatz model with bias $v = -0.1$	138
6.5	Average magnetization m and average interface density ρ for the Abrams-Strogatz model in a fully connected network ($a = 1$) . . .	140
6.6	Stability diagram for the Abrams-Strogatz model in a degree-regular random graph	146
6.7	Spreading experiments: probability $P(t)$ that the system is still alive at time t in the Abrams-Strogatz model with bias $v = -0,2$.	147
6.8	Spreading experiments: probability $P(t)$ that the system is still alive at time t in the Bilinguals model ($v = 0$)	150
6.9	Two-dimensional lattice: Ginzburg-Landau potential for the symmetric case $v = 0$ of the Abrams-Strogatz model	154
6.10	Snapshots of the Abrams-Strogatz model with bias $v = 0$ on a two-dimensional lattice. Coarsening processes	155
6.11	Inverse of the average interface density $\langle \rho \rangle$ for the Bilinguals model in a two-dimensional regular lattice	157
B.1	Dependence on the volatility parameter a for the transition probability to change from state B to state A , $P_{BA}(s = 0.5)$	189
B.2	Viability kernels and trajectories that maintain the system viable for $a = 0.2, 1$ and 2	195
B.3	Viability kernel for the Abrams-Strogatz model, with $c = 0.1$ and $\Delta t = 0.05$	197
B.4	Examples of trajectories starting from an initial state x_0 for $a = 0.2, 1$ and 2 , and evolution of the control, with $c = 0.1$	198
B.5	Resilient and non resilient states in the model	201
B.6	Resilience values of the Abrams-Strogatz model	203
B.7	Examples of trajectories that allow the system to restore its viability at the minimal cost of restoration	205

BIBLIOGRAPHY

Bibliography

- [1] T. C. Schelling, *Micromotives and Macrobehavior*, Norton, New York, 1978.
- [2] T. C. Schelling *Journal of Mathematical Sociology* **1**, p. 143, 1971.
- [3] D. J. Watts *Nature* **445**, p. 489, 2003.
- [4] P. L. Garrido, J. Marro, and M. A. Muñoz, *Eight Granada Lectures on Modeling cooperative behavior in the Social Sciences; AIP Conference proceedings 779*, AIP, Melville, New York, 2005.
- [5] C. Castellano, S. Fortunato, and V. Loreto *Rev. Mod. Phys.* **81**, p. 591, 2009.
- [6] R. Albert and A. L. Barabási *Rev. Mod. Phys.* **74**, p. 47, 2002.
- [7] D. J. Watts and S. H. Strogatz *Nature* **393**, p. 440, 1998.
- [8] A. L. Barabási and R. Albert *Science* **286**, p. 509, 1999.
- [9] G. Deffuant, D. Neau, F. Amblard, and G. Weisbuch *Advances in Complex Systems* **3**, p. 87, 2000.
- [10] R. Axelrod, *The Complexity of Cooperation*, Princeton University Press, Princeton, New Jersey, 1997.
- [11] R. Axelrod *The Journal of Conflict Resolution* **41**, p. 203, 1997.
- [12] O. Diekmann and J. Heesterbeek, *Mathematical epidemiology of infectious disease, Model Building, Analysis and Interpretation*, Wiley, New York, 2000.
- [13] D. M. Abrams and S. H. Strogatz *Nature* **424**, p. 900, 2003.
- [14] R. N. Mantegna and H. E. Stanley, *An introduction to econophysics: correlations and complexity in finance*, Cambridge University Press, New York, 2000.
- [15] G. Hardin *Science* **162**, p. 1243, 1968.
- [16] R. Axelrod, *Handbook of Computational Economics Vol. 2: Agent-Based Computational Economics*, ch. Agent-based modeling as a bridge between disciplines. North Holland/Elsevier, Amsterdam, 2006.
- [17] P. Ball, *Critical mass : how one thing leads to another*, Heinemann, London, 2004.

BIBLIOGRAPHY

- [18] A. Quételet, *On Man and the Development of Human Facilities, An Essay on Social Physics*, Bachelier, Paris, 1835.
- [19] A. Comte, *Course in Positivist Philosophy*, 1830.
- [20] A. Rosenberg, *Philosophy of social science*, Oxford University Press, Oxford, 1988.
- [21] P. L. Berger, *Invitation to Sociology: A Humanistic Perspective*, Anchor Books, New York, 1963.
- [22] B. Latané *American Psychologist* **36**, p. 343, 1981.
- [23] M. S. Granovetter *The American Journal of Sociology* **78**, p. 1360, 1973.
- [24] J. S. Sichman, R. Conte, and N. Gilbert, *Multi-agent systems and agent-based simulation*, Springer, Berlin, 1998.
- [25] F. Vega-Redondo, *Economics and the Theory of Games*, Cambridge University Press, Cambridge, 2003.
- [26] M. San Miguel, V. M. Eguíluz, R. Toral, and K. Klemm *Computing in Science and Engineering* **7**, p. 67, 2005.
- [27] R. Holley and T. Liggett *Annals of Probability* **3**, p. 643, 1975.
- [28] R. J. Glauber *Journal of Mathematical Physics* **4**, p. 294, 1963.
- [29] S. Mufwene, *Language evolution. Contact, competition and change*, Continuum International Publishing Group, London/New York, 2008.
- [30] P. Erdős and A. Rényi *Publicationes Mathematicae* **6**, p. 290, 1959.
- [31] S. Fortunato *Phys. Rep.* **486**, p. 75, 2010.
- [32] S. N. Dorogovtsev and J. F. F. Mendes *Adv. Phys.* **51**, p. 1079, 2002.
- [33] M. E. J. Newman *SIAM Review* **45**, p. 167, 2003.
- [34] S. Boccaletti, V. Latora, Y. Moreno, M. Chavez, and D. Hwang *Phys. Rep.* **424**, p. 175, 2006.
- [35] S. N. Dorogovtsev, A. V. Goltsev, and J. F. F. Mendes *Rev. Mod. Phys.* **80**, p. 1275, 2008.
- [36] B. Bollobás, *Random Graphs*, Academic Press, London, 1985.

BIBLIOGRAPHY

- [37] S. P. Borgatti, A. Mehra, D. J. Brass, and G. Labianca *Science* **323**, p. 892, 2009.
- [38] J. L. Moreno, *Who shall survive?*, Mental Disease Publishing Company, Washington DC, 1934.
- [39] J. Travers and S. Milgram *Sociometry* **32**, p. 425, 1969.
- [40] D. J. Watts *American Journal of Sociology* **105**, p. 493, 1999.
- [41] P. S. Dodds, R. Muhamad, and D. J. Watts *Science* **301**, p. 827, 2003.
- [42] S. Wasserman and K. Faust, *Social Network Analysis: Methods and Applications*, Cambridge University Press, Cambridge, 1994.
- [43] J. Scott, *Social network analysis: A Handbook, 2nd ed.*, Sage, London, 2000.
- [44] D. J. Watts, *Six Degrees: The Science of a Connected Age*, Norton, New York, 2003.
- [45] A. L. Barabási, *Linked: How Everything Is Connected to Everything Else and What It Means*, Plume, New York, 2003.
- [46] V. D. Blondel, J.-L. Guillaume, R. Lambiotte, and E. Lefebvre *J. Stat. Mech.* **P10008**, 2008.
- [47] R. Pastor-Satorras and A. Vespignani, *Evolution and Structure of the Internet: A Statistical Physics Approach*, Cambridge University Press, New York, 2004.
- [48] S. Boccaletti, *Handbook on biological networks*, World Scientific, Singapore, 2010.
- [49] J. P. Onnela, J. Saramaki, J. Hyvonen, G. Szabo, D. Lazer, K. Kaski, J. Kertesz, and A. L. Barabasi *Proc. Natl. Acad. Sci. USA* **104**, p. 7332, 2007.
- [50] W. W. Zachary *Journal of Anthropological Research* **33**, p. 452, 1977.
- [51] L. A. Amaral, A. Scala, M. Barthélemy, and H. E. Stanley *Proc. Natl. Acad. Sci. USA* **97**, p. 11149, 2000.
- [52] D. J. Watts, *Small-worlds: The Dynamics of Networks between Order and Randomness*, Princeton University Press, Princeton, New Jersey, 1999.
- [53] H. R. Bernard, P. D. Kilworth, M. J. Evans, C. McCarty, and G. A. Selley *Ethnology* **27**, p. 155, 1988.
- [54] T. J. Fararo and M. H. Sunshine, *A Study of a Biased Friendship Net*, Syracuse University Press, Syracuse, New York, 1964.

BIBLIOGRAPHY

- [55] M. E. J. Newman *Proc. Natl. Acad. Sci. USA* **98**, p. 404, 2001.
- [56] F. Liljeros, C. R. Edling, L. A. N. Amaral, H. E. Stanley, and Y. Aaberg *Nature* **411**, p. 907, 2001.
- [57] M. E. J. Newman *Phys. Rev. E* **74**, p. 036104, 2006.
- [58] M. Faloutsos, R. Pankaj, and K. C. Sevcik, "Multicasting in directed graphs," in *18th Biennial Symposium on Communications*, p. 2, 1996.
- [59] N. Schwartz, R. Cohen, D. Ben-Avraham, A. L. Barabási, and S. Havlin *Phys. Rev. E* **66**, p. 015104, 2002.
- [60] M. E. J. Newman *Phys. Rev. E* **64**, p. 016132, 2001.
- [61] M. A. Serrano, M. Boguña, and A. Vespignani *Proc. Natl. Acad. Sci. USA* **106**, p. 6483, 2009.
- [62] M. Marsili, F. Vega-Redondo, and F. Slanina *Proc. Natl. Acad. Sci. USA* **101**, p. 1439, 2004.
- [63] V. M. Eguíluz, M. G. Zimmermann, C. J. Cela-Conde, and M. San Miguel *American Journal of Sociology* **110**, p. 977, 2005.
- [64] T. Gross and B. Blasius *Journal of the Royal Society Interface* **5**, p. 259, 2008.
- [65] M. O. Jackson and B. W. Rogers *American Economic Review* **97**, p. 890, 2007.
- [66] M. E. J. Newman *Phys. Rev. Lett.* **89**, p. 208701, 2002.
- [67] D. Stauffer, *Introduction to Percolation Theory*, Taylor & Francis, London, 1985.
- [68] B. Bollobás *European Journal of Combinatorics* **1**, p. 311, 1980.
- [69] M. E. J. Newman, S. H. Strogatz, and D. J. Watts *Phys. Rev. E* **64**, p. 026118, 2001.
- [70] M. E. J. Newman and D. J. Watts *Phys. Lett. A* **263**, p. 341, 1999.
- [71] M. A. de Menezes, C. F. Moukarzel, and T. J. P. Penna *Europhys. Lett.* **50**, p. 574, 2000.
- [72] A. L. Barabási, R. Albert, and H. Jeong *Physica A* **272**, p. 173, 1999.
- [73] S. N. Dorogovtsev, J. F. F. Mendes, and A. N. Samukhin *Phys. Rev. Lett.* **85**, p. 4633, 2000.

BIBLIOGRAPHY

- [74] P. L. Krapivsky, S. Redner, and F. Leyvraz *Phys. Rev. Lett.* **85**, p. 4629, 2000.
- [75] R. Guimerà, L. Danon, A. Díaz-Guilera, F. Giralt, and A. Arenas *Journal of Economic Behaviour and Organization* **61**, p. 653, 2006.
- [76] M. Girvan and M. E. Newman *Proc. Natl. Acad. Sci. USA* **99**, p. 7821, 2002.
- [77] R. Cohen and S. Havlin *Phys. Rev. Lett.* **90**, p. 058701, 2003.
- [78] B. Bollobás and O. Riordan, *Handbook of Graphs and Networks*. Wiley-VCH, Berlin, 2002.
- [79] P. L. Krapivsky and S. Redner *Phys. Rev. E* **63**, p. 066123, 2001.
- [80] K. Klemm and V. M. Eguíluz *Phys. Rev. E* **65**, p. 057102, 2002.
- [81] G. C. Homans, *The human groups*, Harcourt, Brace & Co., New York, 1950.
- [82] R. S. Weiss and E. Jacobson *American Sociological Review* **20**, p. 661, 1955.
- [83] M. Newman *Eur. Phys. J. B* **38**, p. 321, 2004.
- [84] F. Radicchi, C. Castellano, F. Cecconi, V. Loreto, and D. Parisi *Proc. Natl. Acad. Sci. USA* **101**, p. 2658, 2004.
- [85] A. Arenas, L. Danon, A. Díaz-Guilera, P. Gleiser, and R. Guimerà *Eur. Phys. J. B* **38**, p. 373, 2004.
- [86] G. Palla, I. Derenyi, I. Farkas, and T. Vicsek *Nature* **435**, p. 814, 2005.
- [87] G. Palla, A.-L. Barabási, and T. Vicsek *Nature* **446**, p. 664, 2007.
- [88] L. Danon, J. Duch, A. Arenas, and A. Díaz-Guilera, "Community structure identification," in *Large Scale Structure and Dynamics of Complex Networks: From Information Technology to Finance and Natural Science*, pp. 93–113, World Scientific, Singapore, 2007.
- [89] M. Rosvall and C. T. Bergstrom *Proc. Natl. Acad. Sci. USA* **105**, p. 1118, 2008.
- [90] T. S. Evans and R. Lambiotte *Phys. Rev. E* **80**, p. 016105, 2009.
- [91] M. E. J. Newman and M. Girvan *Phys. Rev. E* **69**, p. 026113, 2004.
- [92] A. Lancichinetti and S. Fortunato *Phys. Rev. E* **80**, p. 016118, 2009.
- [93] L. Danon, A. Díaz-Guilera, J. Duch, and A. Arenas *J. Stat. Mech.* **P09008**, 2005.

BIBLIOGRAPHY

- [94] Y. M. Vega, M. Vázquez-Prada, and A. F. Pacheco *Physica A* **343**, p. 279, 2004.
- [95] A. Arenas and A. Díaz-Guilera *Eur. Phys. J. B* **143**, p. 19, 2007.
- [96] A. Arenas, A. Díaz-Guilera, and C. Pérez-Vicente *Phys. Rev. Lett.* **96**, p. 114102, 2006.
- [97] E. Oh, K. Rho, H. Hong, and B. Kahng *Phys. Rev. E* **72**, p. 047101, 2005.
- [98] T. Zhou, M. Zhao, G. Chen, G. Yan, and B.-H. Wang *Phys. Lett. A* **368**, p. 431, 2007.
- [99] A. Arenas, A. Díaz-Guilera, J. Kurths, Y. Moreno, and C. Zhou *Phys. Rep.* **469**, p. 93, 2008.
- [100] S. Lozano, A. Arenas, and A. Sánchez *Plos One* **3**, p. e1892, 2008.
- [101] P. L. Krapivsky and S. Redner *Phys. Rev. Lett.* **90**, p. 238701, 2003.
- [102] R. Lambiotte, M. Ausloos, and J. Holyst *Phys. Rev. E* **75**, p. 030101, 2007.
- [103] M. Boguñá, R. Pastor-Satorras, A. Díaz-Guilera, and A. Arenas *Phys. Rev. E* **70**, p. 056122, 2004.
- [104] L. H. Wong, P. Pattison, and G. Robins *Physica A* **360**, p. 99, 2006.
- [105] E. M. Jin, M. Girvan, and M. E. J. Newman *Phys. Rev. E* **64**, p. 046132, 2001.
- [106] J. Davidsen, H. Ebel, and S. Bornholdt *Phys. Rev. Lett.* **88**, p. 128701, 2002.
- [107] A. Grönlund and P. Holme *Phys. Rev. E* **70**, p. 036108, 2004.
- [108] J. Kumpula, J.-P. Onnela, J. Saramäki, K. Kaski, and J. Kertész *Phys. Rev. Lett.* **99**, p. 228701, 2007.
- [109] R. Toivonen, J.-P. Onnela, J. Saramäki, J. Hyvönen, J. Kertész, and K. Kaski *Physica A* **371**, p. 851, 2006.
- [110] J. D. Gunton, M. San Miguel, and P. Sahní, *Phase Transitions and Critical Phenomena*, vol. 8, ch. The dynamics of first order phase transitions, pp. 269–446. Academic Press, London, 1983.
- [111] L. Festinger, S. Schachter, and K. Back, *Social Pressures in Informal Groups: A Study of Human Factors in Housing*, Harper, New York, 1950.
- [112] H. E. Stanley, *Introduction to Phase Transitions and Critical Phenomena*, Oxford University Press, New York and Oxford, 1971.

BIBLIOGRAPHY

- [113] K. S. Weron and J. Sznajd *Int. J. Mod. Phys. C* **11**, p. 1157, 2000.
- [114] M. Granovetter *American Journal of Sociology* **83**, p. 1420, 1978.
- [115] D. Centola and M. Macy *American Journal of Sociology* **113**, p. 702, 2007.
- [116] L. Steels *Artificial Life* **2**, p. 319, 1995.
- [117] S. Galam *Eur. Phys. J. B* **25**, p. 403, 2002.
- [118] M. Nakamaru and S. A. Levin *Journal of Theoretical Biology* **230**, p. 57, 2004.
- [119] R. Durrett and S. A. Levin *Journal of Economic Behavior & Organization* **57**, p. 267, 2005.
- [120] I. Dornic, H. Chaté, J. Chave, and H. Hinrichsen *Phys. Rev. Lett.* **87**, p. 045701, 2001.
- [121] C. Castellano, V. Loreto, A. Barrat, F. Cecconi, and D. Parisi *Phys. Rev. E* **71**, p. 066107, 2005.
- [122] P. Clifford and A. Sudbury *Biometrika* **60**, p. 581, 1973.
- [123] P. L. Krapivsky *Phys. Rev. A* **45**, p. 1067, 1992.
- [124] R. Durrett and S. A. Levin *Journal of Theoretical Biology* **179**, p. 119, 1996.
- [125] J. Chave and E. Leigh *Theoretical Population Biology* **62**, p. 153, 2002.
- [126] P. G. de Prado Salas and J.C.González-Avella, "Applet for the voter model in complex networks." from IFISC website: <http://www.ifisc.uib-csic.es/research/socio/Voteraplet/applet.html>, 2008.
- [127] T. M. Liggett, *Interacting Particle Systems*, Springer, New York, 1985.
- [128] J. Marro and R. Dickman, *Nonequilibrium Phase Transitions in Lattice Models*, Cambridge University Press, Cambridge, UK, 1999.
- [129] K. Suchecki, V. M. Eguíluz, and M. San Miguel *Europhys. Lett.* **69**, p. 228, 2005.
- [130] T. M. Liggett, *Stochastic Interacting Systems: Contact, Voter and Exclusion Processes*, Springer, New York, 1999.
- [131] L. Frachebourg and P. L. Krapivsky *Phys. Rev. E* **53**, p. R3009, 1996.
- [132] S. Redner, *A Guide to First-Passage Processes*, Cambridge University Press, New York, 2001.

BIBLIOGRAPHY

- [133] F. Vazquez and V. M. Eguíluz *New J. Phys.* **10**, p. 063011, 2008.
- [134] F. Vazquez, J. C. González-Avella, V. M. Eguíluz, and M. San Miguel, *Applications of Nonlinear Dynamics. Model and Design of Complex Systems*, vol. XII, ch. Collective Phenomena in Complex Social Networks, pp. 189–200. Springer Verlag, Berlin-Heidelberg, 2009.
- [135] V. Sood and S. Redner *Phys. Rev. Lett.* **94**, p. 178701, 2005.
- [136] C. Castellano, D. Vilone, and A. Vespignani *Europhys. Lett.* **63**, p. 153, 2003.
- [137] M. Barthélemy and L. A. N. Amaral *Phys. Rev. Lett.* **82**, p. 3180, 1999.
- [138] K. Suchecki, V. M. Eguíluz, and M. San Miguel *Phys. Rev. E* **72**, p. 036132, 2005.
- [139] V. M. Eguíluz, E. Hernández-García, O. Piro, and K. Klemm *Phys. Rev. E* **68**, p. 055102, 2003.
- [140] F. Vazquez, V. M. Eguíluz, and M. San Miguel *Phys. Rev. Lett.* **100**, p. 108702, 2008.
- [141] M. A. Serrano, K. Klemm, F. Vazquez, V. M. Eguíluz, and M. San Miguel *J. Stat. Mech.* **P10024**, 2009.
- [142] A. V. M. Leone, A. Vázquez and R. Zecchina *Eur. Phys. J. B* **28**, p. 191, 2002.
- [143] J. Viana Lopes, Y. G. Pogorelov, J. M. B. Lopes dos Santos, and R. Toral *Phys. Rev. E* **70**, p. 026112, 2004.
- [144] A. D. Sánchez, J. M. López, and M. A. Rodríguez *Phys. Rev. Lett.* **88**, p. 048701, 2002.
- [145] C. Tessone, “Applet for the ising model in a two dimensional lattice.” From IFISC website: http://ifisc.uib-csic.es/research/applet_complex/bidimensional/JIsing.php, 2003.
- [146] C. Tessone, R. Toral, P. Amengual, H. Wio, and M. San Miguel *Eur. Phys. J. B* **39**, p. 535, 2004.
- [147] K. Barros, P. L. Krapivsky, and S. Redner *Phys. Rev. E* **80**, p. 040101, 2009.
- [148] V. Spirin, P. L. Krapivsky, and S. Redner *Phys. Rev. E* **63**, p. 036118, 2001.
- [149] V. Spirin, P. Krapivsky, and S. Redner *Phys. Rev. E* **65**, p. 016119, 2001.
- [150] C. Godreche and J. M. Luck *J. Phys. Cond. Matt* **17**, p. S2573, 2005.

BIBLIOGRAPHY

- [151] O. Häggström *Physica A* **310**, p. 275, 2002.
- [152] C. Castellano and R. Pastor-Satorras *J. Stat. Mech.* **P05001**, 2006.
- [153] H. Zhou and R. Lipowsky *Proc. Natl. Acad. Sci. USA* **102**, p. 10052, 2005.
- [154] D. Boyer and O. Miramontes *Phys. Rev. E* **67**, p. 035102, 2003.
- [155] C. P. Herrero *J. Phys. A: Math. Theor.* **42**, p. 415102, 2009.
- [156] M. Krauss *Language* **68**, p. 4, 1992.
- [157] D. Crystal, *Language death*, Cambridge University Press, Cambridge, 2000.
- [158] J. F. Hamers and M. H. A. Blanc, *Bilinguality and bilingualism*, Cambridge University Press, Cambridge, 1989.
- [159] D. Nettle and S. Romaine, *Vanishing Voices. The extinction of the world's languages*, Oxford University Press, Oxford, 2000.
- [160] S. Mufwene, *The ecology of language evolution*, Cambridge University Press, Cambridge, 2001.
- [161] S. Mufwene *Annual Review of Anthropology* **33**, p. 201, 2004.
- [162] UNESCO, *Language Vitality and Language Endangerment*, UNESCO (Ad Hoc Expert Group on Endangered Languages), 2003.
- [163] S. A. Wurm, "Atlas of the world's languages in danger of disappearing," tech. rep., Unesco Publishing, 2001.
- [164] U. Weinreich, *Languages in Contact*, Linguistic Circle of New York, New York, 1953.
- [165] T. Tsunoda, *Language endangerment and language revitalisation*, Mouton de Gruyter, Berlin and New York, 2005.
- [166] J. O' Driscoll *Multilingua* **20**, p. 245, 2001.
- [167] J. A. Fishman, *Reversing Language Shift: Theoretical and Empirical Foundations of Assistance to Threatened Languages*, Multilingual Matters, Clevedon, 1991.
- [168] K. de Bot and S. Stoessel, eds., *International Journal of the Sociology of Language: Language change and social networks*, vol. 153, Mouton de Gruyter, Berlin and New York, 2002.
- [169] K. de Bot and S. Stoessel *International Journal of the Sociology of Language* **153**, p. 1, 2002.

BIBLIOGRAPHY

- [170] W. Labov, *Sociolinguistic Patterns*, University of Pennsylvania Press, Philadelphia, 1972.
- [171] P. Trudgill, *The dialects of England*, Blackwell, Oxford, 1990.
- [172] M. Patriarca and T. Leppanen *Physica A* **338**, p. 296, 2004.
- [173] J. Mira and A. Paredes *Europhys. Lett.* **69**, p. 1031, 2005.
- [174] M. Patriarca and E. Heinsalu *Physica A* **388**, p. 174, 2009.
- [175] J. Pinasco and L. Romanelli *Physica A* **361**, p. 355, 2006.
- [176] C. Schulze and D. Stauffer *Int. J. Mod. Phys. C* **16**, p. 781, 2005.
- [177] V. M. de Oliveira, M. Gomes, and I. Tsang *Physica A* **361**, p. 361, 2006.
- [178] C. Schulze and D. Stauffer *Computing in Science and Engineering* **8**, p. 60, 2006.
- [179] C. Schulze, D. Stauffer, and S. Wichmann *Communications in Computational Physics* **3**, p. 271, 2008.
- [180] D. Stauffer, X. Castelló, V. M. Eguíluz, and M. San Miguel *Physica A* **374**, p. 835, 2007.
- [181] R. Appel and P. Muysken, *Language Contact and Bilingualism*, Edward Arnold Publishers, London, 1987.
- [182] W. S.-Y. Wang and J. W. Minett *Trends in Ecology and Evolution* **20**, p. 263, 2005.
- [183] J. W. Minett and W. S.-Y. Wang *Lingua* **118**, p. 19, 2008.
- [184] L. Milroy, *Theories on Maintenance and Loss of Minority Languages*, ch. Bridging the micro-macro gap: social change, social networks and bilingual repertoires, pp. 39–64. Waxmann, Münster and New York, 2001.
- [185] L. Milroy, *Language and Social Networks*, Blackwell, Oxford, 1980.
- [186] S. Stoessel *International Journal of the Sociology of Language* **153**, p. 93, 2002.
- [187] C. Raschka, L. Wei, and S. Lee *International Journal of the Sociology of Language* **153**, p. 9, 2002.
- [188] M. Nowak and D. Krakauer *Proc. Natl. Acad. Sci. USA* **96**, p. 8028, 1999.
- [189] M. A. Nowak, N. L. Komarova, and P. Niyogi *Science* **291**, p. 114, 2001.

BIBLIOGRAPHY

- [190] G. J. Baxter, R. A. Blythe, W. Croft, and A. J. McKane *Phys. Rev. E* **73**, p. 046118, 2006.
- [191] D. Nettle *Lingua* **108**, p. 95, 1999.
- [192] A. Baronchelli, M. Felici, V. Loreto, E. Caglioti, and L. Steels *J. Stat. Mech.* **P06014**, 2006.
- [193] A. Baronchelli, L. Dall'Asta, A. Barrat, and V. Loreto *Phys. Rev. E* **73**, p. 015102, 2006.
- [194] L. Dall'Asta, A. Baronchelli, A. Barrat, and V. Loreto *Europhys. Lett.* **73**, p. 969, 2006.
- [195] L. Dall'Asta, A. Baronchelli, A. Barrat, and V. Loreto *Phys. Rev. E* **74**, p. 036105, 2006.
- [196] L. Dall'Asta and A. Baronchelli *J. Phys. A: Math. Gen.* **39**, p. 14851, 2006.
- [197] A. Baronchelli, L. Dall'Asta, A. Barrat, and V. Loreto *Phys. Rev. E* **76**, p. 051102, 2007.
- [198] X. Castelló, V. M. Eguíluz, and M. San Miguel *New J. Phys.* **8**, p. 308, 2006.
- [199] P. S. Sahní, D. J. Srolovitz, G. S. Grest, M. P. Anderson, and S. A. Safran *Phys. Rev. B* **28**, p. 2705, 1983.
- [200] K. Kaski, M. Grant, and J. D. Gunton *Phys. Rev. B* **31**, p. 3040, 1985.
- [201] C. Castellano, M. Marsili, and A. Vespignani *Phys. Rev. Lett.* **85**, p. 3536, 2000.
- [202] K. Klemm, V. M. Eguíluz, R. Toral, and M. San Miguel *Phys. Rev. E* **67**, p. 026120, 2003.
- [203] J. C. González-Avella, V. M. Eguíluz, M. G. Cosenza, K. Klemm, J. L. Herrera, and M. San Miguel *Phys. Rev. E* **73**, p. 046119, 2006.
- [204] K. Klemm, V. M. Eguíluz, R. Toral, and M. San Miguel *Journal of Economic Dynamics and Control* **29**, p. 321, 2005.
- [205] M. Blume, V. J. Emery, and R. B. Griffiths *Phys. Rev. A* **4**, p. 1071, 1971.
- [206] F. Vazquez, P. L. Krapivsky, and S. Redner *J. Phys. A: Math. Gen.* **36**, p. L61, 2003.
- [207] M. S. de la Lama, J. M. López, and H. S. Wio *Europhys. Lett.* **72**, p. 851, 2005.

BIBLIOGRAPHY

- [208] J. M. Pujol, J. Delgado, R. Sangüesa, and A. Flache, "The role of clustering on the emergence of efficient social conventions," in *International Joint Conferences on Artificial Intelligence*, L. P. Kaelbling and A. Saffiotti, eds., pp. 965–970, Professional Book Center, 2005.
- [209] S. Park *The Review of Economics and Statistics* **86**, p. 937, 2004.
- [210] L. Dall'Asta and C. Castellano *Europhys. Lett.* **77**, p. 60005, 2007.
- [211] L. Dall'Asta and T. Galla *J. Phys. A: Math. Theor.* **41**, p. 435003, 2008.
- [212] F. Vazquez and C. López *Phys. Rev. E* **78**, p. 061127, 2008.
- [213] H.-U. Stark, C. J. Tessone, and F. Schweitzer *Phys. Rev. Lett.* **101**, p. 018701, 2008.
- [214] R. A. Blythe *J. Stat. Mech.* **P02059**, 2009.
- [215] X. Castelló, R. Toivonen, V. M. Eguíluz, J. Saramäki, K. Kaski, and M. San Miguel *Europhys. Lett.* **79**, p. 66006, 2007.
- [216] R. Toivonen, X. Castelló, V. M. Eguíluz, J. Saramäki, K. Kaski, and M. San Miguel *Phys. Rev. E* **79**, p. 016109, 2008.
- [217] X. Castelló, A. Baronchelli, and V. Loreto *Eur. Phys. J. B* **71**, p. 557, 2009.
- [218] F. Vazquez, X. Castelló, and M. San Miguel *J. Stat. Mech. (in press; version available at arXiv:1002.1251)*, 2010.
- [219] L. Chapel, X. Castelló, C. Bernard, G. Deffuant, V. Eguíluz, S. Martin, and M. San Miguel *Plos One* **5**, p. e8681, 2010.
- [220] X. Castelló, "Dynamics of language competition." From IFISC website: http://www.ifisc.uib-csic.es/research/complex/APPLET_LANGDYN.html, 2007.
- [221] P. Chen and S. Redner *Phys. Rev. E* **71**, p. 036101, 2005.
- [222] F. Schweitzer and L. Behera *Eur. Phys. J. B* **67**, p. 301, 2009.
- [223] S. Maslov and K. Sneppen *Science* **296**, p. 910, 2002.
- [224] L. da F. Costa, F. A. Rodrigues, G. Travieso, and P. R. Villas Boas *Adv. Phys.* **56**, p. 167, 2007.
- [225] R. Guimerá, M. Sales-Pardo, and L. A. N. Amaral *Phys. Rev. E* **70**, p. 025101, 2004.

BIBLIOGRAPHY

- [226] C. Tessone, C. Mirasso, R. Toral, and J. Gunton *Phys. Rev. Lett.* **97**, p. 194101, 2006.
- [227] A. Baronchelli, V. Loreto, and L. Steels *Int. J. Mod. Phys. C* **19**, p. 785, 2008.
- [228] A. Puglisi, A. Baronchelli, and V. Loreto *Proc. Natl. Acad. Sci. USA* **105**, p. 7936, 2008.
- [229] F. Vazquez and S. Redner *Europhys. Lett.* **78**, p. 18002, 2007.
- [230] O. Al Hammal, H. Chaté, I. Dornic, and M. A. Muñoz *Phys. Rev. Lett.* **94**, p. 230601, 2005.
- [231] E. Pugliese and C. Castellano *Europhys. Lett.* **88**, p. 58004, 2009.
- [232] M. Droz, A. L. Ferreira, and A. Lipowski *Phys. Rev. E* **67**, p. 056108, 2003.
- [233] X. Castelló, L. Loureiro-Porto, V. M. Eguíluz, and M. San Miguel, *Advancing Social Simulation: The First World Congress*, ch. The fate of bilingualism in a model of language competition, pp. 83–94. Springer, Berlin, 2007.
- [234] X. Castelló, R. Toivonen, V. M. Eguíluz, and M. San Miguel, *Proceedings of the 4th Conference of the European Social Simulation Association*, ch. Modelling bilingualism in language competition: the effects of complex social structure, pp. 581–584. IRIT Editions, 2007.
- [235] X. Castelló, R. Toivonen, V. M. Eguíluz, L. Loureiro-Porto, J. Saramäki, K. Kaski, and M. San Miguel, *The evolution of language; Proceedings of the 7th International Conference (EVOLANG7)*, ch. Modelling language competition: bilingualism and complex social networks, pp. 59–66. World Scientific Publishing Co., Singapore, 2008.
- [236] X. Castelló, F. Vazquez, L. Chapel, V. M. Eguíluz, L. Loureiro-Porto, G. Defuant, and M. San Miguel, *Pattern Resilience*, ch. Macroscopic descriptions, viability and resilience in the dynamics of language competition. Springer-Verlag (to be published), 2010.
- [237] M. Ayestaran Aranaz and A. Justo de la Cueva, *Las familias de la provincia de Pontevedra (Galleguidad y conflicto lingüístico)*, Instituto de Ciencias de la Familia, Sevilla, 1974.
- [238] J. P. Aubin, *Viability Theory*, Birkhauser, Boston, 1991.
- [239] C. Tessone and R. Toral *Eur. Phys. J. B* **71**, p. 549, 2009.
- [240] M. Uchida and S. Shirayama *Phys. Rev. E* **75**, p. 046105, 2007.

- [241] T. Antal, P. L. Krapivsky, and S. Redner *Phys. Rev. E* **72**, p. 036121, 2005.
- [242] S. Martin *Ecology and Society* **9**, p. 8, 2004.
- [243] S. Pimm *Nature* **307**, p. 321, 1984.
- [244] J. Ludwig, B. Walker, and C. Holling *Conservation Ecology* **1**, p. 7, 1997.
- [245] G. Deffuant, L. Chapel, and S. Martin *IEEE transactions on automatic control* **52**, p. 933, 2007.
- [246] L. Chapel, S. Martin, and G. Deffuant, "Lake eutrophication: using resilience evaluation to compute sustainable policies," in *Proceedings of the international conference on environmental systems and technology. Kos Island, Greece.*, p. 204, 2007.

“Nothing is forever except change.” — Siddhārta Gautama

